BUILDINGS UNDER RECURRING NEAR-FIELD EARTHQUAKES

A THESIS SUBMITTED TO
THE GRADUATE SCHOOL OF NATURAL AND APPLIED SCIENCES
OF
MIDDLE EAST TECHNICAL UNIVERSITY

BY

BEYHAN BAYHAN

IN PARTIAL FULFILLMENT OF THE REQUIREMENTS
FOR
THE DEGREE OF DOCTOR OF PHILOSOPHY
IN
CIVIL ENGINEERING

SEPTEMBER 2010

Approval of the thesis:

BUILDINGS UNDER RECURRING NEAR-FIELD EARTHQUAKES

submitted by **BEYHAN BAYHAN** in partial fulfillment of the requirements for the degree of **Doctor of Philosophy in Civil Engineering Department, Middle East Technical University** by,

Prof. Dr. Canan Özgen
Dean, Graduate School of **Natural and Applied Sciences**   _____

Prof. Dr. Güney Özcebe
Head of Department, **Civil Engineering**   _____

Prof. Dr. Polat Gülkan
Supervisor, **Civil Engineering Dept., METU**   _____

Assoc. Prof. Dr. Ahmet Yakut
Co-Supervisor, **Civil Engineering Dept., METU**   _____

Examining Committee Members: _____

Prof. Dr. Güney Özcebe
Civil Engineering Dept., METU   _____

Prof. Dr. Polat Gülkan
Civil Engineering Dept., METU   _____

Prof. Dr. Sinan Altın
Civil Engineering Dept., Gazi University   _____

Prof. Dr. Haluk Sucuoğlu
Civil Engineering Dept., METU   _____

Assoc. Prof. Dr. Barış Binici
Civil Engineering Dept., METU   _____

Date:

I hereby declare that all information in this document has been obtained and presented in accordance with academic rules and ethical conduct. I also declare that, as required by these rules and conduct, I have fully cited and referenced all material and results that are not original to this work.

Name, Last Name: Beyhan Bayhan

Signature   :

ABSTRACT

BUILDINGS UNDER RECURRING NEAR-FIELD EARTHQUAKES

Bayhan, Beyhan

Ph.D., Department of Civil Engineering

Supervisor: Prof. Dr. Polat Gülkan

Co-Supervisor: Assoc. Prof. Dr. Ahmet Yakut

September 2010, 198 pages

Prior to this study, to our best knowledge, no cast-in-place, older-type RC building has ever been subjected to near-field strong ground motions from three major earthquakes. This happened in an indirect way in Turkey over a time span of eleven years. Three identical buildings belonging to Ministry of Public Works and Resettlement (MPWR) that had been built to the same design templates, experienced March 13th 1992 Erzincan earthquake in Erzincan, November 12th 1999 Düzce earthquake in Bolu and May 1st 2003 Bingöl earthquake in Bingöl, respectively. The ground motion sensor stations were fortuitously nearby in an adjacent single-story building in Bolu and Bingöl. The station in Erzincan was in a single-story building about 2 km away from the case study building but we assume that the record applies to the building there. These three data represent

characteristics of near-field ground motions and the distance of the sensor stations to the nearest fault trace was less than 10 km.

The buildings sustained varying degrees of damage during the earthquakes and their damage survey was employed through site investigations. Given that the damage information, input motions, design drawings and material properties of the buildings are all known, this provided an opportunity to predict the structural damage to these buildings by proper modeling using the tools of current computational performance assessment procedures.

In this circumstance, three dimensional (3D) analytical models of the MPWR buildings have been performed. Bi-directional excitations have been applied to the models by nonlinear time history analyses (NTHA). The results illustrate that NTHA are capable of indicating the occurrence of shear failure in captive columns; however, they overestimate the global damage level for all buildings. The overestimation is more significant in Erzincan case where the building sustained a pulse-type motion without significant distress.

Keywords: RC frame building, near-field strong ground motion, 3D model, nonlinear time history analysis, performance assessment

ÖZ

TEKRARLANAN YAKIN MESAFE DEPREM ETKİLERİNE MARUZ KALAN BİNALAR

Beyhan, Bayhan

Doktora, İnşaat Mühendisliği Bölümü

Tez Yöneticisi: Prof. Dr. Polat Gülkan

Ortak Tez Yöneticisi: Doç. Dr. Ahmet Yakut

Bilgimiz dâhilinde, şimdiye kadar, herhangi yerinde dökme, eski tip betonarme bir bina üç büyük deprem sebebiyle yakın mesafe kuvvetli yer hareketine maruz kalmamıştır. Bu durum dolaylı olarak on bir senelik bir süreç dâhilinde ülkemizde gerçekleşmiştir. Aynı uygulama projelerine göre inşaa edilmiş Erzincan Bayındırlık İl Müdürlüğü binası 13 Mart 1992'de Erzincan depremine, Bolu Bayındırlık İl Müdürlüğü binası 12 Kasım 1999'da Düzce depremine, Bingöl Bayındırlık İl Müdürlüğü binası 1 Mayıs 2003'de Bingöl depremine maruz kalmıştır. Bolu ve Bingöl'de yer hareketi ölçüm istasyonları rastlantı sonucu bu binlara komşu bir katlı binalar içerisinde bulunmaktaydı. Erzincan'daki ölçüm cihazı yaklaşık iki kilometre uzaktaki bir katlı binadaydı ancak bu kaydın söz konusu binaya tesir ettiğini kabul ediyoruz. Bu üç kayıt da yakın mesafe yer

hareketi özelliklerini taşımakla birlikte ölçüm istasyonlarının en yakın fay hattına olan uzaklıkları 10 km.'nin altındadır.

Depremler sırasında çeşitli seviyelerde hasara uğrayan bu binaların yerinde incelenmesi ile hasar tespitleri yapılmıştır. Hasar düzeyinin, yer ivme kayıtlarının, uygulama projelerinin ve malzeme özelliklerinin biliniyor olması, uygun modelleme teknikleri ve yürürlükteki performans değerlendirme yöntemlerini kullanarak yapısal hasarın tahminine imkân sağlamıştır.

Bu bağlamda, Bayındırlık İl Müdürlüğü binalarının üç boyutlu analitik modelleri oluşturulmuştur. Yer ivme kayıtları, zaman tanım alanında hesap yöntemiyle, aynı anda iki yönlü olarak modellere etki ettirilmiştir. Analiz sonuçları kısa kolonlardaki kesme göçmesini doğru tahmin ederken genel hasarı mevcuttan fazla öngörmüştür. Bu durum, yakın kaynaklı depreme maruz kalan ancak hafif hasar gören Erzincan binasında oldukça göze çarpmaktadır.

Anahtar Kelimeler: betonarme bina, yakın mesafe kuvvetli yer hareketi, üç boyutlu model, zaman tanım alanında analiz, performans değerlendirmesi

To my family…

ACKNOWLEDGEMENTS

I would like to thank Ertuğ & Filiz Yurdutemiz, Colleen McQuoid, Linda & Keith Cranmer, Shinji Kishida, Gabriel Hurtado, Selim Günay, for their support and making my life more pleasant in Berkeley.

There is one I have to mention especially: Gökhan Özdemir. He means a lot to me for his devotion and his great help. I deeply appreciate both his help and his friendship.

My special thanks goes to "can dostum" Şeref Çaylak who has stood by me in every difficult situation since 1989. His friendship is invaluable.

I dedicate this thesis to Pınar for her confidence in me, for her understanding, support, patience and love.

Last but not the least, I wish to dedicate this dissertation to "Annem" Hayrünnisa Bayhan, "Babam" Taci Bayhan and "Kardeşim" Cevdet Bayhan. Their enduring love, unconditional support and encouragement have been the real inspiration that I always felt during the course of this study.

TABLE OF CONTENTS

LIST OF TABLES

LIST OF FIGURES

FIGURES

xix

CHAPTER 1

INTRODUCTION

1.1   GENERAL

The major confrontation faced by performance-based engineering is to develop simple but accurate enough methods for prediction of seismic performance of the structures considering their inelastic behavior. Another key issue that highly affects the accuracy of the followed simplified methods is the accurate recognition of the seismic hazard. This is particularly crucial for the zones which are in the vicinity of causative faults that are capable of generating large magnitude earthquakes with characteristic near-fault properties such as forward rupture directivity and fling.

Significance of forward directivity in near-fault records was assigned as the main research topic of engineers in the last few decades (Housner and Trifunac, 1967; Boore and Zoback, 1974; Somerville et al., 1997; Iwan et al. 2000; Cuesta et al., 2003; Akkar et al., 2005). Metin (2006) defines the forward directivity as "*fault rupture propagating towards site at high velocities would result a dominant high amplitude pulse in the fault-normal direction*". In the same context, Mavroeidis and Papageorgiou (2004) summarized the characteristics of near-fault ground motions with forward directivity effect as follows: "*most of the elastic energy arrives coherently in a single, intense, relatively long-period pulse at the beginning of the record, representing the cumulative effect of almost all the seismic radiation from the fault*".

Numerous methods have been proposed to define proper analytical models for the simulation of near-fault ground motions (Alavi and Krawinkler, 2001; Menun and Fu, 2002; Mavroeidis and Papageorgiou, 2003). These studies revealed that there is a need to study the detrimental impacts of near-fault motions with directivity effect on structures.

The simplified methods namely, nonlinear static procedures (NSPs) or pushover analysis, are being favorable compared to complex nonlinear time history analysis (NTHA) which is most of the time impractical for professional use.

There are two well-known NSPs used to estimate the performance of structures which is of utmost importance in performance-based seismic engineering. One is the displacement coefficient method (CM) proposed by FEMA-356 (2000) and the other is the capacity spectrum method (CSM) recommended by ATC-40 (1996). What is common for both of the procedures is that the pushover curves of the evaluated structures are needed to be established.

The CM suggested by FEMA-356 is based on the displacement demand of a representative single-degree-of-freedom (SDOF) system of the considered multi-degree-of freedom-system (MDOF) structure which is modified by a series of modification factors. On the other hand, in CSM, which was developed by Freeman (1978), the capacity of the structure under consideration is approximated by intersecting the established pushover curve with the corresponding elastic response spectrum. Nonlinearity in the structure is taken into consideration by modifying the 5%-damped elastic response spectrum. This modification is done in accordance with the calculated equivalent viscous damping which is supposed to be greater than 5%. Since equivalent viscous damping is a function of the deformation demand, CSM is based on an iterative solution initiated with an assumption for the deformation demand of the structure.

1.1.1 Review of Pushover Analysis Development

The use of nonlinear static analysis in estimating the performance of structures for engineering purposes is traced back to the study of Gülkan and Sözen

(1974). They approximated the dynamic response of reinforced concrete (RC) structures by equivalent SDOF representation by means of linear response analysis using reduced stiffness and "substitute damping". The authors related the displacement of the "substitute" system to both reduction in stiffness and change in energy dissipation capacity of the real MDOF system. Gülkan and Sözen (1974) came up with a simplified method for estimating the design base shear where inelastic response is taken into account. Similar approaches have also been followed by Saidii and Sözen (1981) and Fajfar and Fischinger (1988) where authors proposed simplified procedures for predicting performance of MDOF systems. Hence, in fact performing pushover analysis for NSPs is not a recent development. Nevertheless, they are still open to developments for increasing their accuracy in estimating the structural performance. Attempts to improve the accuracy of pushover analysis due date are given chronologically in the following paragraphs.

Shear-beam model of structures where the stiffness of each story was assigned to a nonlinear shear spring was one of the initial works. Aziz (1976) analyzed ten-story frames through shear-beam model and compared the results with those of MDOF models. Pique (1976) proposed an equivalent SDOF system based on the assumption that structures deform through their first mode shapes. Freeman (1978) proposed a procedure for estimating the response of RC structures to severe ground motions. In this procedure, capacity of the structure is determined by combining elastic analysis with bilinear approximations. The demand of ground motion is represented by response spectra at some values of critical damping. The demand and capacity characteristics are plotted on the same graph and their intersection is the maximum response of a structure for a particular earthquake.

Saiidi and Sözen (1981) proposed Q(uick)-model which is a SDOF system composed of a mass, viscous damper, a massless rigid bar and rotational spring. The load-deformation model of the rotational spring was obtained by nonlinear static analysis of the MDOF system. To account for stiffness changes during a ground motion, a simple hysteresis model was developed. The analytical model was verified with eight small-scale ten-story RC test structures. The analytical results

were compared with those of experimental through displacement histories. The model was successful in prediction of response histories.

Another simple nonlinear method-the N2 method where N stands for nonlinear and 2 for two mathematical models: a SDOF and a MDOF model-for seismic analysis of the structures was proposed by Fajfar and Fischinger in 1987 and 1989, respectively. The idea came from the Q-model. This method combined response spectrum with the aforementioned equivalent SDOF model. In 1996, Fajfar and Fischinger developed this method and applied to a test structure where its fundamental period is dominant. Although reasonably accurate results were obtained, this method had a drawback: when the higher mode effects were important, some demand quantities might be underestimated.

In 1996, the method of Freeman (1978) was recommended by ATC-40 as a tool for design and assessment of structures. In this method, capacity of the structure is compared with demand on the structure. The capacity is represented with a pushover curve and the demand is represented with a linear-elastic response spectrum modified with an effective damping value to represent an inelastic response spectrum; however, as early as 1995, Krawinkler had stated two deficiencies of this method. First, it is difficult to decide a value for the effective damping because a stable relationship between the hysteretic energy dissipation and effective damping does not always exist. Second, the period calculated by the intersection of the capacity curve with the highly damped spectrum has a little to do with dynamic response of the inelastic system.

Bracci et al. (1997) extended the CSM to include the effects of mid-story mechanisms by means of adaptive pushover analysis. Seismic demand curves were established at varying levels of inelasticity ranging from initial elastic response to final failure mechanism. The resulting ranges of demand are compared with the inelastic force-deformation capacities for each story level. This comparison enables engineers to provide a quick estimate of the margin of safety against collapse for the selected seismic demand level. The procedure was also verified with a one-third scale, three-story RC test frame at varying levels of seismic excitation on a shaking table. Later, Krawinkler and Seneviratna (1998) indicated the advantages and

4

disadvantages of pushover analysis which is used to obtain capacity curves of the structures in the aforementioned methods. The factors affecting the inelastic displacement demand were discussed. They stated that the topics below need to be investigated.

- Torsional effects and irregularities
- Three-dimensional (3D) Problems
- Use of site specific area
- Higher mode effects

Several methods have been proposed to overcome the weaknesses of the CSM of ATC-40. Chopra and Goel (1999) improved it by using constant-ductility design spectrum in place of the demand diagram.

Fajfar (1999) re-formulated the N2 method in acceleration-displacement format which provided the visual representation of CSM proposed by Freeman.

Aschheim et al. (1998) applied strength and displacement based approaches to assess the performance of a RC moment-resisting-frame (MRF) building damaged in the 1994 Northridge earthquake. They concluded that base shear strength alone was not an adequate measure of seismic performance and performance-based approaches implied greater precision in resolving the comparison of seismic demands and capacities. However, they added that the applicability of various analytical approaches and modeling assumptions require to be more clarified for future applications with confidence.

Gupta and Krawinkler (2000) conducted linear and nonlinear dynamic analyses of nine steel MRFs. The response of those structures was evaluated through 140 ground motions with different hazard levels. They estimated the maximum story drift demands through modification factors applied to the first mode spectral displacement.

Fajfar (2000) used inelastic demand spectra with equivalent damping and period. Although this procedure is convenient for the structures where the fundamental period is dominant, it is not suitable in case of near-fault ground

motions for soft soil sites, for hysteretic loops with significant pinching or significant stiffness degradation and strength deterioration and for systems with low strengths.

Chopra and Goel (2002) developed improved pushover analysis procedure for estimating seismic demands for buildings. First, they developed a modal pushover analysis (MPA) procedure based on structural dynamics theory and then extended it to inelastic buildings. In this method, the seismic demand due to individual terms in the modal expansion of the effective earthquake forces is determined by a pushover analysis using the inertia force distribution for each mode. Then, these modal demands due to the first two or three terms of the expansion are combined according to the square-root-of-sum-of-squares (SRSS) or the complete quadratic combination (CQC) rules to estimate the total inelastic demand. Following this research they recommended structural performance shall be based on story drifts which give more accurate results by pushover analysis.

In displacement CM method of FEMA-356 inelastic displacement spectrum is obtained from the elastic displacement using correction factors based on statistical analyses. The FEMA approach is basically different from the CSM of ATC-40 that in ATC-40 the inelastic behavior of the structure is taken into account by using equivalent damping and period. The capacity curves of the structures are calculated by pushover analyses for both methods; however, in FEMA, as a difference from ATC-40, guidelines for bilinear idealization of load-deformation relation are given.

Browning (2001) proposed a simplified method for design of regular mid-rise RC buildings. This method differs from the aforementioned ones in that the design process is based on the demand defined by linear displacement spectrum that can be modified to include specific site condition effects and a maximum allowable period criterion.

1.1.2 Conventional Pushover Analysis Formulation

In conventional pushover analysis, structural response is basically achieved by solution of $KU = P$ based on the idealized mathematical model of the structure. Here, K is the nonlinear stiffness matrix, U is the displacement vector, and P is the considered load vector. Solution of the expressed equation is performed under step by step increasing (incremental) load pattern. An iterative method is followed at each incremental step and continues until the convergence is achieved and the balanced forces of each step are assigned to reaction vector P^e (Bathe 1982):

$$\Delta U = \left[K_T\right]^{-1} \cdot \left(\lambda \cdot P_0 - P^e\right) \tag{1}$$

In the above equation, ΔU is the displacement increment calculated within iteration; K_T is the instantaneous (tangent) stiffness matrix; λ is the load factor within the corresponding load increment; P_0 is the initial load; and P^e is the converged reaction force of the previous iteration.

Papanikolaou et al. (2005) describe the whole process with the following expressions: "*The procedure continues either until a predefined limit state is reached or until structural collapse is detected. This target limit state may be the deformation expected for the design earthquake in case of designing a new structure, or the drift corresponding to structural collapse for assessment purposes. Generally, this procedure allows tracing the sequence of yielding and failure on the member and structure level, as well as the progress of the overall capacity curve of the structure.*"

1.1.3 Enhancements in Pushover Analysis Methods

In the light of the previous studies discussed, there are some deficiencies of nonlinear static analysis in reflecting the real behavior which is assumed to be the one obtained from NTHA. These deficiencies can be listed as follows:

- The assumption incorporated by pushover analysis that the structural capacity and earthquake demand are separated from each other is

found out to be not convenient by researchers indicating an interconnection between structural capacity and earthquake demand. Furthermore, behavior of the structure highly depends on the load path especially in the nonlinear range and separation between loading input and structural response may not be adequate.

- In pushover analysis, lateral deformation is the only parameter that is used to estimate structural damage. Hence, duration effects and energy dissipation demand are neglected in the process. However, the probable damage observed in a structure is a function of both deformation and energy.

- Pushover analysis also does not consider dynamic effects. Hence, effects of kinetic and viscous damping energy which are mainly associated with dynamic components of forces are neglected. Pushover analysis focuses only on the strain energy (function of deformation) of the structure during a monotonic static push.

- The conventional pushover analysis procedure does not account for the progressive changes in the modal properties during nonlinear yielding and cracking in the structure which leads also to period elongation. This is due to the constant lateral load pattern used, which ignores the potential redistribution of inertia forces, as yielding and cracking governs the nonlinear response of structure.

- It is not in the extent of pushover analysis to incorporate the three-dimensional and cyclic earthquake loading effects.

Due to above listed necessities researchers devoted themselves to develop techniques in order to increase the accuracy of estimations made by NSPs based on pushover analysis. One of the first attempts, which is developed by Sasaki et al. (1998), is to adapt an appropriate load distribution for pushover analysis. In this

method, several pushover analyses are performed for the structure under consideration representing the different modes of the system. Once the solution of each case is established, the overall behavior of the structure is obtained by a combination of each case. Similar adaptive procedures have been proposed by Satyarno et al. (1998), Matsumori et al. (1999), Gupta and Kunnath (2000), Requena and Ayala (2000), Elnashai (2001), Antoniou et al. (2002) and Aydınoğlu (2003). In adaptive pushover analysis, lateral load distribution is instantly updated based on the instantaneous mode shapes of the corresponding inelastic periods of the structure rather than assuming a constant distribution.

In his study, Papanikolau (2000) presented a comparison between conventional pushover analysis where both triangular and uniform load distribution are considered and adaptive pushover analysis based on the dynamic response of structures. It is revealed that the analysis with triangular and uniform load distributions behave as a bounding analysis where they stand for the lower and upper boundaries of the adaptive pushover, respectively. The author also showed that results of adaptive pushover are very close to that of triangular load distribution at lower global drift ratios which was stated as 2%. For drift ratios greater than 2%, results of adaptive pushover get close to that of uniform load distribution.

1.1.4 Research for Evaluation of Nonlinear Static Procedures (NSPs)

There are several studies that evaluated the accuracy of the NSPs. Miranda and Ruiz-Garcia (2002), Goel (2003), Medina and Krawinkler (2005), Goel (2005), Goel and Chadwell (2007) are among these studies. Most of the previous studies compare the performance of an analytical model subjected to recorded or generated earthquakes with the response estimated by NSPs. However, these studies do not consider the behavior of real structures at the site. In this sense, studies conducted by Goel (2003, 2005, 2007) are somehow different from the rest of the previous researches by considering recorded response of real buildings.

In the studies of Goel (2003, 2005), four existing buildings that sustained damage (deformed beyond the yield limit) namely, Van Nuys (7-story), Woodland

Hills (13-story), Sherman Oaks (13-story), Los Angeles (19-story) are evaluated. All of the considered buildings were instrumented to record their response during a probable earthquake which turned out to be 1994 Northridge earthquake. Author developed two dimensional analytical models of the structures. These models were calibrated according to the recorded displacement histories at different story levels. The accuracy of the NSPs was validated by comparing the results from calibrated analytical models. The author revealed that the accuracy of the NSP highly depends on the story height. For example, in Van Nuys building, predictions of NSP lead to 90% underestimation in the drifts of upper stories whereas it yields to 50% overestimation in those of lower stories.

More recently, Goel and Chadwell (2007) evaluated the NSP specified in FEMA-356 (2000), ASCE/SEI-41 (2007), ATC-40 (1996), and FEMA-440 (ATC-55, 2003) based on the recorded behavior of five RC structures ranging from low-rise to high-rise. Hence, the recorded behavior of Imperial County Service Building, Sherman Oaks Commercial Building, North Hollywood Hotel, Watsonville Commercial Building, and Santa Barbara Office Building were considered. The author stated the reason why these buildings were selected as because they were strongly shaken that leads to "*deformation beyond their linear-elastic range*". Goel and Chadwell (2007) stated that the considered NSPs either underestimate or overestimate peak roof displacement. Moreover, ASCE/SEI-41 method which is based on the improved FEMA-356 method according to FEMA-440 document, "*does not necessarily provide a better estimate*" for the roof displacement.

In his studies, Goel (2003, 2005, and 2007) either considered 2D idealization or 3D idealization with unidirectional ground motion excitation. In this sense, the author also implied that to properly capture the observed behavior, bi-directional excitations should be applied to 3D models of the structures. Furthermore, response of RC structures under bi-directional ground motion excitations were studied by Magliulo and Ramasco (2007) indicating a significant amplification in displacement demand and a reduction in shear force distribution along the height of the structure when compared to response quantities under unidirectional excitations.

In this circumstance, the recent research indicates that there is a lack of investigations on prediction of seismic response of the real structures under bi-directional excitations with their 3D models. Furthermore, research on the seismic behavior of real structures subjected to near-field earthquakes is even scarcer. Thus, the emphasis of this study will be on the estimation of the seismic response of in-situ RC buildings under bi-directional near-field excitations with their 3D idealized models. The main challenge in this research will be to understand whether the structural damage observed at the sites after the earthquakes could have been predicted well by the help of these sophisticated nonlinear analysis methods and performance assessment tools if the ground motions were known.

1.2   OBJECT AND SCOPE

Recent and past earthquakes have taught that structural damage and losses are mainly due to inadequate performance of buildings. In light of this concept, many efforts have been made to develop new design and performance evaluation procedures. These procedures have also been implemented in numerous performance-oriented codes and guidelines for seismic design of structures to be built and assessment of the existing ones. Although these procedures are progressive, the uncertainties in parameters (performance limit states and criteria) that are used to quantify the structural performance of the buildings make those methods open to further debate and investigation. Moreover, simplifications made during the modeling and analysis phases-representation of material behavior, geometrical properties, damping etc. accumulate additional unknown parameters to the questions to be solved. Hence, accuracy and reliability of the existing evaluation procedures need to be verified. In this sense, reliably measured ground motion and corresponding observed damage and response data of full-scale structures become very crucial.

In this circumstance, investigating the response of in-situ structures during earthquakes has been a useful tool for improving methodologies for design and analysis of structures. An early example is the study of Mahin et al. (1976) on the

structural performance of a RC building. This study was an extensive field and analytical investigation of the structural performance of the main building of the Olive View Hospital Medical Treatment and Care Facility that sustained severe damage during the 1971 San Fernando earthquake. The observed structural damage was compared with the predictions made through linear and nonlinear dynamic analyses of the mathematical models. A similar investigation (Kreger et al., 1989) was made for the Imperial County Services Building of El Centro city in California that was severely damaged during the 1979 Imperial Valley Earthquake. The measured response of the building was interpreted and a hypothesis was developed for the prediction of the observed column failures.

The Olive View Hospital and the Imperial County Services Building serve only as two samples from a sizable collection of studies in earthquake engineering literature on the interpretation of observed damages in structures. In most of these cases input motions to the buildings are either unknown or can only be surmised with a good deal of guesswork. Data for structures that have experienced repeated earthquake ground motions is even scarcer. Very few research results examining the response of identical RC frame buildings subjected to different strong ground motions have been reported. An exception perhaps is the Van Nuys Hotel Building, a seven story cast-in-place RC moment-frame building in Van Nuys, California that sustained repeated earthquake ground motions and its response was recorded during the earthquakes. The building was slightly damaged in the M6.6 1971 San Fernando earthquake and severely damaged in the M6.7 1994 Northridge earthquake. The building was however different at each of these two earthquakes and was located in an area where near-field effects are not of concern (Krawinkler, 2005), so perhaps the circumstances described in the following paragraph are truly unique.

To the best of our knowledge, hardly any single building has experienced three successive strong ground motions in the near-field. In Turkey this happened in an indirect way when three identical buildings underwent such an experience over a time span of 11 years in three different cities that were hit by major earthquakes. For ease of access and security, the strong motion recording stations, part of the national network are usually located adjacent to these buildings. This fortuitous

coincidence enabled exact input to the buildings to be known in two of the three cases that will be reported below.

The three identical buildings are the typical branch offices of the Ministry of Public Works and Resettlement (MPWR) which were template-designed and constructed in 1970s and 1980s in different regions of Turkey. These buildings are usually a part of building complexes separated from each other by seismic joints. They sustained varying levels of damage during the March 13th, 1992 Erzincan (M6.6, The magnitude values are taken from the Harvard Centroid Moment Tensor catalogue, HRV), November 12th, 1999 Düzce (M7.1) and May 1st, 2003 Bingöl (M6.3) earthquakes. The recording stations were located in a one-story building adjacent to those buildings in Bolu and Bingöl and in a one-story building 2 km away from that building in Erzincan. Thus, three-component strong ground motion data were recorded that represent what motion the building underwent. These ground motions also represent three different types of near-field ground motions such as ordinary near-field motion-Bingöl record, near-field motion with fling effect-Bolu record (Akkar and Gülkan, 2002), and near-field record with forward directivity effect-Erzincan record (Makris and Black, 2004).

3D analytical models of the buildings were performed based on their architectural design templates, measured material properties and field investigations. Then, both horizontal components of the ground motions were applied simultaneously to the models to perform nonlinear analyses. The challenge is to evaluate the seismic performance of these buildings by using current nonlinear procedures that are expressed in the next chapter of this study and to understand whether these nonlinear procedures would estimate beam-column damage well enough with those observed at the sites.

In summary, the concept on which this thesis statement is based was born due to need to fill the voids in the literature briefly expressed below and make a reasoned judgment of the adequacy of procedures that until now have been judged solely on the basis of computational exercises. Thus, a proof of concept is needed to identify the strengths and weaknesses of the analytical procedures that guide engineers in assessing structural systems or planning intervention for retrofit.

- In most of the studies in the literature, input motions to the buildings were unknown or could only be surmised with a good deal of guesswork

- Data for structures that have experienced repeated earthquake ground motions is even scarcer

- No research results examining the response of identical RC frame buildings subjected to different near-field ground motions have been reported

- Surprisingly, there is still insufficient number of research on 3D analysis of RC structures subjected to bi-directional excitations.

- New procedures and recommendations are being implemented in current codes and guidelines through advanced structural analysis and testing procedures. Although these studies allow us to provide a test of the goodness of these concepts in damage estimation in the light of empirical evidence, there are still many uncertainties in determination of performance assessment criteria and limits.

1.3   ORGANIZATION OF THE DISSERTATION

This thesis is composed of six main chapters and several appendices with brief contents given as follows:

Chapter 1:   General information about the thesis and description of previous research related to this study is given

Chapter 2:   Performance assessment procedures considered in this study are reviewed

Chapter 3:   A benchmark study is performed before the introduction of the main study. A full scale, older-type, 3D RC frame building subjected to pseudo dynamic (PsD) test in the laboratory is simulated through a 3D

analytical model to compare the measured and calculated structural damage

Chapter 4: General information about the MPWR buildings, seismic and geological features of the strong ground motions that the buildings underwent and observed structural damage are described

Chapter 5: Analytical models of the MPWR buildings are described in detail. Eigen value, nonlinear dynamic and static analyses results are presented. Following these analyses, performance assessment of the structures at global and member-level is employed according to ATC-40, ASCE/SEI-41 and the Turkish earthquake code. The calculated damage levels are compared with those observed

Chapter 6: Conclusions and recommendations for future studies are given

Appendix A: Tables and drawings of the buildings
Appendix B: Performance assessment results of the first and second story columns
Appendix C: Performance assessment results of the first and second floor beams
Appendix D: Performance assessment results of the hollow clay brick infill walls

CHAPTER 2

REVIEW OF PERFORMANCE ASSESSMENT PROCEDURES

2.1   INTRODUCTION

Estimation of global and local seismic demands is of great concern for evaluating existing structures that have sustained different levels of damage during ground motions. In this framework, preliminary (quick) or more detailed (lengthy) performance assessment procedures have been proposed in recent years. Preliminary performance procedures (FEMA-154 1998; FEMA-310 1998; Hassan and Sözen 1997; Gülkan and Sözen 1999, Sucuoğlu and Yazgan 2003; Yakut, 2004) were conducted with limited data reflecting the general properties of the buildings that aim to determine the priority for further evaluation. Detailed assessment procedures (ATC-40 1996; FEMA-273 1997; FEMA-310 1988; FEMA-356 2000; TEC 2007, ASCE/SEI-41 2007 and ASCE/SEI-41 Supplement-1 2008) require much more complete information about the building and elaborate seismic analyses. In the latter method, force and deformation capacities of the structural members are calculated according to the recommended values by the standards and guidelines first and then those capacities are compared with the seismic demands determined from the seismic analysis representing a presumed earthquake intensity level. In this study, three of the aforementioned documents are considered. These are;   (i) ATC-40,

(ii) ASCE/SEI-41and Supplement 1

(iii) The Turkish Earthquake Code (TEC)

ATC-40 is one of the initiating documents in performance-based seismic evaluation of existing RC buildings that was published in 1996 by Applied Technology Council (ATC). It originated from a need to develop guidelines for seismic rehabilitation of the buildings and provides detailed and in depth look at different perspectives in performance-based design and evaluation of RC structures

ASCE/SEI-41 was mainly developed from FEMA-356-Prestandard and Commentary for the Seismic Rehabilitation of Buildings (2000) that was based on the ATC-33 project in the early 1990's and published as FEMA-273 (1997). ASCE/SEI-41 is the latest generation of performance-based seismic rehabilitation methodology that began with FEMA-273. It is a much larger effort than ATC-40 that does not only cover RC buildings but also steel, masonry, wood, isolated structures and the structures with energy dissipating devices.

The Turkish Earthquake Code (2007) with added chapter of "Assessment and Strengthening of Existing Buildings" is very similar with the preceding FEMA-356 standard through the approaches that are used in adopting performance-based assessment methodologies for existing buildings (Sucuoğlu, 2006).

In addition to the aforementioned documents, FEMA-440-"*Improvement of Nonlinear Static Seismic Analysis Procedures*" (2005) is of concern, here as a supportive document while applying the coefficient method (CM) of ASCE/SEI-41. FEMA-440 is a guideline for inelastic analysis procedures in which improvements and recommendations to the methods of FEMA-356 such as new limitations and coefficients were developed. This will be described in the following sections.

In this thesis, the emphasis will be on the nonlinear analysis of the structures that are subjected to PsD and dynamic loading and determination of their performance levels considering the different acceptance criteria and limits given in the aforementioned documents. Linear procedures are out of interest here.

In this circumstance, the performance level definitions and global building acceptability limits of ATC-40 are presented, first. Second, nonlinear procedures of ASCE/SEI-41 and corresponding acceptance criteria for these procedures are discussed. As a last step, TEC is examined.

2.2   PERFORMANCE LEVEL DEFINITIONS OF ATC-40 AND CORRESPONDING ACCEPTABILITY LIMITS: GLOBAL PERFORMANCE CHECK

ATC-40 classifies the performance level of any structure according to the observed damage level. Basic concepts are threat to the life safety of people and serviceability of the building after the ground motion. The performance levels of the structures under consideration are defined in four groups:

- Immediate Occupancy (IO)
- Damage Control (DC)
- Life Safety (LS)
- Structural Stability (SS)

These four performance levels are applicable to both ductile and non-ductile structures. The descriptions of those four damage levels used to evaluate the condition of the structures are explained as follows:

Immediate Occupancy (IO):
- Very limited structural damage has occurred
- The vertical and lateral force resisting systems of the building retain nearly all of their pre-earthquake characteristics and capacities
- No life-threatening injury
- Building is safe for occupancy

Damage Control (DC):
- Not a specific level
- Provides a placeholder for many situations where it may be desirable to limit structural damage beyond the life safety level
- Occupancy is not the issue
- Includes protection of significant architectural damage,

Life Safety (LS):
- Significant damage occurred
- Injuries may occur during the earthquake but the risk of life-threatening injury from structural damage is very low
- Extensive structural repairs will likely be necessary prior to reoccupation of the building although the damage may not be always economically repairable

Structural Stability (SS):
- The building's structural system is on the verge of experiencing partial or total collapse
- Significant degradation in the stiffness and deterioration in the strength of the lateral force resisting system
- The gravity load resisting system continue to carry the gravity demands
- Significant risk of injury

The damage levels for the structural elements such as columns and beams are given in Table 2.1. This table contains two types of information. One is the absolute statements that the gravity load capacity of the building remains substantially intact and the other is the qualitative/quantitative statements regarding the magnitude of observed damage to the components. Qualitative descriptions are based on damage observed in prior earthquakes.

2.2.1 Global Building Acceptability Limits: Gravity loads

ATC-40 assures that the load carrying capacity of any structure under gravity loads must remain unchanged at any level. The main cause leading to collapse of the structures is the loss of gravity load carrying capacity in columns, beam-column joints and slab-column connections. Thus, any analysis should consider the probable reduction in vertical load carrying capacity and redistribution of the loads to the other components of the structural system.

Table 2.1. Deformation limits for the structural components, ATC-40 (1996)

	Immediate Occupancy	**Damage Control**	**Life Safety**	**Structural Stability**
Columns	- Very limited flexural and shear cracking with no spalling - No permanent horizontal offset - Gravity capacity maintained	- Limited flexural and shear cracking with little or no spalling - No permanent horizontal offset - Gravity capacity maintained	- Hinges have formed in the lower portions of the building, causing spalling above and below beam-column joints - Permanent horizontal offset approaching 2% inter-story drift with small areas marginally higher - Gravity capacity maintained	- Hinges have formed in the lower portions of the building causing significant spalling above and below beam-column joints and pulverizing of concrete within the core - Permanent horizontal offset approaching 3.5% inter-story drift with small areas marginally higher - Gravity capacity maintained throughout nearly all of the structure
Beams	- Very limited spalling around beam-column joint - Very limited flexural cracking in hinge region - No permanent deflection - Gravity capacity maintained	- Limited spalling around beam-column joint - Limited flexural cracking in hinge region - No permanent deflection - Gravity capacity maintained	- Spalling around the hinge region and beam-column joint - Flexural and shear cracking in hinge region progressing into the beam-column joint - Elongation of shear stirrups adjacent to joint - Permanent vertical deflection approaching $L/175$ - Gravity capacity maintained	- Extensive spalling around hinge region and beam-column joint - Extensive flexural and shear cracking in hinge region, progressing into beam-column joint - Rupture of shear stirrups - Permanent vertical deflection approaching $L/75$ - Gravity capacity maintained

2.2.2 Global Building Acceptability Limits: Lateral Loads

As in the nature of dynamic loading, structural components are subjected to cyclic loading and this may result in degradation in stiffness. If this degradation occurs in a significant number of structural members, there may be a distinct reduction in lateral force resistance of the structure. What ATC-40 requires is that

the lateral load resistance should not degrade by more than 20 percent including the effects of gravity loads on lateral displacements. Thus, it is recommended that the effect of gravity loads acting through lateral displacements be considered in the analytical model and if the resistance degrades by more than 20 percent of maximum resistance, nonlinear dynamic analysis methods should be used to assess earthquake demands.

2.2.3 Global Building Acceptability Limits: Lateral Deformations

Evaluation of lateral deformations in structures according to ATC-40 is based on comparison of the displacements at the performance point with the deformation limits at predefined performance levels. ATC-40 employs a limitation for maximum total drift, which is equal to inter-story drift ratio at performance point. The maximum total drift should be less than 0.33V/P at any story level where V is the lateral shear force and P is the total gravity load at that story. Lateral deformation limits are given in Table 2.2. These limitations are based on laboratory test results for components.

Table 2.2. Lateral deformation limits of ATC-40 (1996)

Inter-story drift limit	Performance Level			
	IO	**DC**	**LS**	**SS**
Maximum total drift (%)	1	1-2	2	$0.33V_i / P_i$

2.3 NONLINEAR PROCEDURES OF ASCE/SEI-41 AND CORRESPONDING ACCEPTABILITY LIMITS: PERFORMANCE CHECK AT MEMBER LEVEL

Two nonlinear procedures of ASCE/SEI-41 that are termed as nonlinear static and nonlinear dynamic procedures (NDPs) are examined here. The NSP of ASCE/SEI-41 is composed of coefficient method (CM) of FEMA-356 with improvements suggested in FEMA-440. The NDP basically consists of response

history analysis and evaluation of structure through comparison of this analysis results with the acceptance limits.

2.3.1 Nonlinear Static Procedure (NSP) of ASCE/SEI-41

In this procedure a structural model, in which all elements of the structural system are idealized by appropriate nonlinear force-deformation relations, is subjected to monotonically increasing lateral loads. These lateral loads represent the actual earthquake forces due to inertia of the structure. Incremental increase in lateral load continues until the target displacement is achieved. Selected target displacement stands for the maximum displacement that may be experienced during the earthquake.

NSP is composed of three consecutive steps:
(i)   selection of control node
(ii)   selection of lateral load patterns and
(iii)   determination of fundamental period of the structure

2.3.1.1 Selection of Control Node

The node which is located at the center of mass at the roof level of a building is assigned as the control node. In case where buildings have a penthouse, floor of the penthouse is considered as the level of the control node.

2.3.1.2 Selection of Lateral Load Pattern

Recent research (FEMA-440, 2005) has shown that multiple load patterns do little to improve the accuracy of NSPs and that a single pattern based on the fundamental mode shape is recommended.

Lateral loads are applied at each floor level and distribution of forces through the height of the structure should be in such a way that they are proportional to inertia forces in the plane of each floor diaphragm. The vertical distribution of these forces shall be proportional to the shape of the fundamental mode in the direction under consideration.

2.3.1.3 *Idealized Force-Deformation Curve and Determination of Effective Fundamental Period*

Fundamental period of the structure is calculated considering the idealized bilinear force-deformation relation obtained from base shear and displacement of control node. Idealization is performed such that the areas above and below the curves are approximately equal (Figure 2.1).
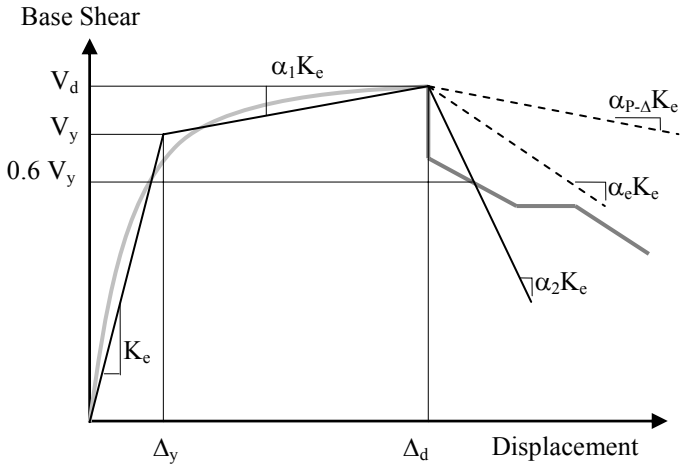
Figure 2.1 Idealized force-deformation curve (ASCE/SEI-41)

Idealized relation is used to get the effective lateral stiffness K_e and effective yield strength V_y of the building. K_e is equal to the secant stiffness calculated at a base shear force equal to 60% of the effective yield strength of the structure (Figure 2.1). Then, the effective stiffness K_e is inserted in Equation (2.8) and used to calculate the fundamental effective period T_e:

$$T_e = T_i \sqrt{\frac{K_i}{K_e}} \qquad (2.1)$$

where T_i is elastic fundamental period in the direction under consideration calculated by elastic dynamic analysis. K_i is the elastic lateral stiffness of the building in the direction under consideration. Furthermore, in Figure 2.1, $\alpha_1 K_e$

represents the positive post-yield slope determined by a point (V_d, Δ_d). V_d, Δ_d is a point on the actual force-displacement curve at the calculated target displacement or at the displacement corresponding to maximum base shear, whichever is least. $\alpha_2 K_e$ represents the negative post-yield slope determined by the point (V_d, Δ_d) and the point at which the base shear degrades to 60 percent of the effective yield strength.

2.3.1.4   Determination of Target Displacement

The effective fundamental period, T_e, calculated by means of Equation (2.1) is used to calculate the spectral displacement (S_d) of the equivalent SDOF system as shown in the equation below;

$$S_d = S_a \frac{T_e^2}{4\pi^2} g \tag{2.2}$$

where S_a is the response spectrum acceleration at the effective fundamental period, T_e, and damping ratio of the building. g is the gravitational acceleration. Once S_d is calculated, the target displacement, δ_t can be obtained by the following equation:

$$\delta_t = C_0 C_1 C_2 S_d \tag{2.3}$$

where C_o relates the spectral displacement of the equivalent SDOF system to the roof displacement of the MDOF system and can be calculated using the one of the following procedures;

- The first mode mass participation factor multiplied by the ordinate of the first mode shape at the level of the control node
- The mass participation factor at the level of the control node using a shape vector corresponding to the deflected shape of the building at the target displacement
- The appropriate value from the Table 3-2 of ASCE/SEI-41 (2007)

C_1 is modification factor to relate expected maximum inelastic displacement to displacement calculated for linear elastic response. This coefficient can be

calculated according to the improved equation stated in FEMA- 440 (2005) as
below;

$$C_1 = \begin{bmatrix} 1.0, & T_e > 1.0\,s \\\\ 1 + \dfrac{R-1}{aT_e^2} & 0.2\,s < T_e \leq 1.0\,s \\\\ 1 + \dfrac{R-1}{0.04a} & T_e \leq 0.2\,s \end{bmatrix} \tag{2.4}$$

where a is a constant dependent on the site classes; 130 for site class A and B, 90
for site class C, 60 for site classes D and E. R is the strength ratio of elastic strength
demand to yield strength coefficient as given below;

$$R = \frac{S_a}{V_y/W} C_m \tag{2.5}$$

where, W is the effective seismic weight of the building including the total dead
load and a minimum 25% of the floor live load. C_m is the effective mass factor that
can be taken as 0.9 for RC moment frame buildings with more than 3 stories.
ASCE/SEI-41 imposed a limitation on strength to avoid dynamic instability by
defining a maximum limit on R as given below;

$$R_{max} = \frac{\Delta_d}{\Delta_y} + \frac{|\alpha_e|^{-h}}{4} \tag{2.6}$$

$$\alpha_e = \alpha_{P-\Delta} + \lambda(\alpha_2 - \alpha_{P-\Delta}) \tag{2.7}$$

where h=1+0.15ln (T_e); α_2 is negative slope ratio defined in Figure 2.1 that includes
P-Δ effects and cyclic degradation; $\alpha_{P-\Delta}$ is the negative slope ratio caused by P-Δ
effects; λ is near-field factor and equal to 0.8 if $S_1 \geq 0.6$, 0.2 if $S_1 < 0.6$; S_1 is the

25

spectral response acceleration parameter at a one second period, obtained from response acceleration maps.

C_2 is modification factor to represent the effects of pinched hysteresis shape, stiffness degradation, and strength deterioration on maximum displacement response as given below;

$$C_2 = 1 + \frac{1}{800}\left(\frac{R-1}{T_e}\right)^2 \qquad (2.8)$$

2.3.2 Nonlinear Dynamic Procedure (NDP) of ASCE/SEI-41

Hysteretic behavior of each component is assigned to each member using the properties verified by experimental evidence. Component strengths are determined considering potential failure in flexure, axial load, shear, torsion, development and other actions along the length of the component under the actions of gravity and earthquake load combinations. Calculated demand is compared with the acceptance criteria as specified in the following section.

2.3.3 Acceptance Criteria for Nonlinear Procedures

The generalized deformation for the beams and columns controlled by flexure is rotation in the flexural plastic hinge zone. For the columns controlled by shear, the permissible deformation was the deformation at which shear strength was calculated to be reached according to ASCE/SEI-41 (2007). However, in the supplementary document (2008), it is stated that unless it is demonstrated by experimental evidence and analysis, the actions shall be defined as force-controlled for shear-critical members.

In Table 2.3, modeling parameters and numerical acceptance criteria for nonlinear procedures corresponding to RC beams are given. Those values of ASCE/SEI-41 (2008) are the same with the previous document (ASCE/SEI-41, 2007).

Table 2.3 Modeling parameters and numerical acceptance criteria for nonlinear procedures–RC beams (adapted from ASCE/SEI-41, Supplement 1, 2008)

Condition: Beam controlled by flexure			Acceptance Criteria		
			Plastic Rotation Angle, radians		
$\dfrac{\rho - \rho'}{\rho_{bal}}$	*Transverse Reinforcement*	$\dfrac{V}{b_w d\sqrt{f_c'}}$	**Performance Level**		
			IO	**LS**	**CP**
≤ 0.0	C	≤ 0.25	0.010	0.020	0.025
≤ 0.0	C	≥ 0.50	0.005	0.010	0.020
≥ 0.5	C	≤ 0.25	0.005	0.010	0.020
≥ 0.5	C	≥ 0.50	0.005	0.005	0.015
≤ 0.0	NC	≤ 0.25	0.005	0.010	0.020
≤ 0.0	NC	≥ 0.50	0.0015	0.005	0.010
≥ 0.5	NC	≤ 0.25	0.005	0.010	0.010
≥ 0.5	NC	≥ 0.50	0.0015	0.005	0.005

Table 2.4 shows the current acceptance limits (ASCE/SEI-41, Supplement-1, 2008) regarding the RC columns. In this supplementary document, acceptance limit values of the old version have been modified.

Table 2.4 Current modeling parameters and numerical acceptance criteria for nonlinear procedures–RC columns (adapted from ASCE/SEI-41, Supplement-1, 2008)

Condition: Columns controlled by flexure			Acceptance Criteria		
			Plastic Rotation Angle, radians		
$\dfrac{\rho - \rho'}{\rho_{bal}}$	$\rho = \dfrac{A_v}{b_w s}$	$\dfrac{V}{b_w d\sqrt{f_c'}}$	**Performance Level**		
			IO	**LS**	**CP**
≤ 0.1	≥ 0.006	≤ 0.25	0.005	0.024	0.0320
≤ 0.1	≥ 0.006	≥ 0.50	0.005	0.019	0.025
≥ 0.4	≥ 0.006	≤ 0.25	0.003	0.008	0.009
≥ 0.4	≥ 0.006	≥ 0.50	0.003	0.006	0.007
≤ 0.1	≤ 0.0005	≤ 0.25	0.005	0.009	0.010
≤ 0.1	≤ 0.0005	≥ 0.50	0.004	0.005	0.005
≥ 0.4	≤ 0.0005	≤ 0.25	0.002	0.003	0.003
≥ 0.4	≤ 0.0005	≥ 0.50	0.000	0.000	0.000

2.4   NONLINEAR PROCEDURE OF THE TURKISH EARTHQUAKE CODE (TEC) AND PERFORMANCE CHECK FOR DUCTILE MEMBERS

The current (2007) seismic design code of Turkey involves seismic performance assessment procedures that are based on linear and nonlinear analyses, either static or dynamic. Here, the nonlinear dynamic assessment procedure will be described.

The nonlinear dynamic procedure of TEC 2007 briefly consists of:

(i)   determination of the deformation capacities of the members and introduction of these to the analytical model

(ii)   nonlinear dynamic analysis

(iii)   comparison of each structural member demand with the allowable limits

(iv)   global performance check.

A schematic introduction of the procedure is depicted in detail in Figure 2.2.

In TEC, damage limits which are used to determine the performance of members have been expressed in a similar way with those of ASCE/SEI-41. These damage levels are,

- Minimum damage limit (IO limit-Initiation of the nonlinear behavior)
- Safety limit (LS limit-Section capacity is still safe enough to carry load)
- Collapse limit (CP limit)

These definitions are valid only for ductile members that are based on plastic deformation demands as discussed in the following section. The members defined as "brittle" according to the code are out of this classification. The brittle members are evaluated according to their force demand and capacity values. Evaluation of the brittle members according to TEC is out of interest in this study.
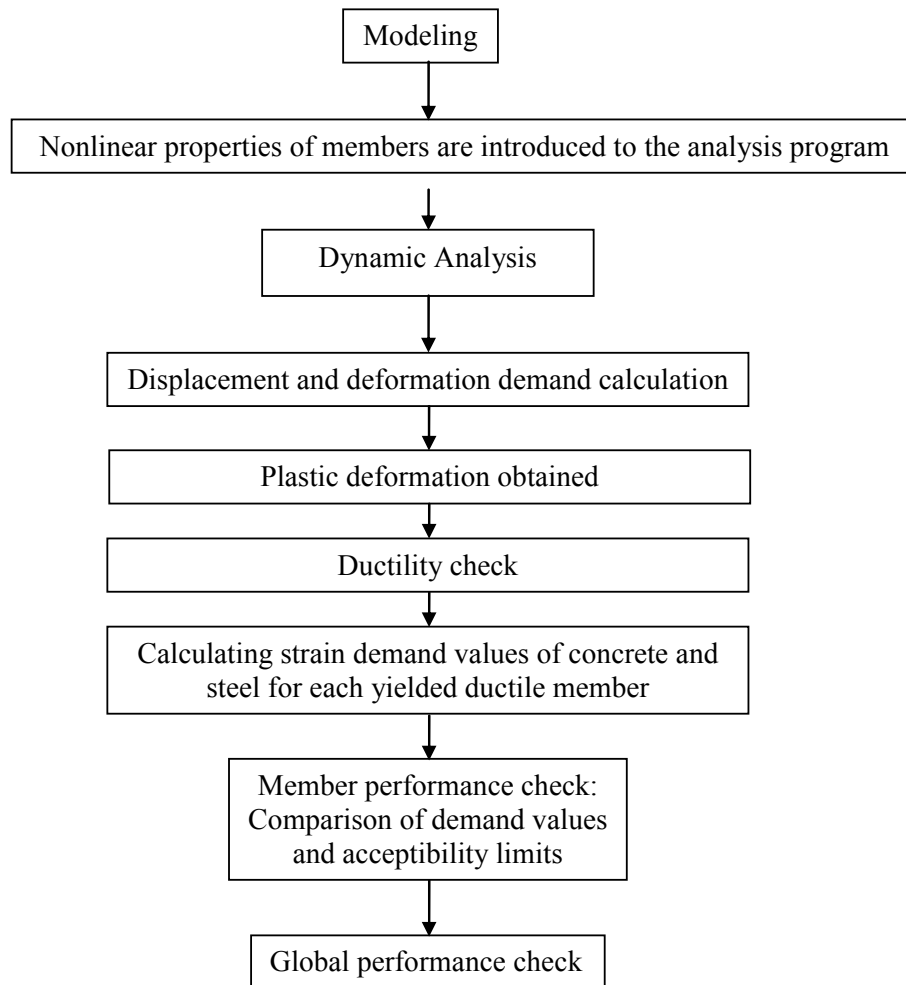
Figure 2.2 Nonlinear dynamic assessment procedure of TEC 2007

2.4.1 Evaluation of Ductile Members and Acceptance Limits of Nonlinear Procedures

For ductile members where plastic deformation occurs, strain limits are defined for three aforementioned performance levels. During NTHA, maximum strain values obtained in the concrete and steel fibers are compared with acceptability limits of the code. Thus, performance check of each member is done. The strain limits to be checked are calculated according to the equations given below;

(i) IO Limit: Strain limits in the concrete extreme fiber (ε_{cu}) and steel reinforcement (ε_s):

$$(\varepsilon_{cu})_{IO}=0.0035 \qquad\qquad (\varepsilon_s)_{IO}=0.01 \qquad (2.9)$$

(ii) LS Limit Strain limits in the confined concrete extreme fiber (ε_{cu}) and steel reinforcement (ε_s):

$$(\varepsilon_{cu})_{LS}=0.0035+0.01(\rho_s/\,\rho_{sm}) \le 0.0135 \qquad (\varepsilon_s)_{LS}=0.04 \qquad (2.10)$$

(iii) CP Limit: Strain limits in the confined concrete extreme fiber (ε_{cu}) and steel reinforcement (ε_s):

$$(\varepsilon_{cu})_{CP}=0.004+0.014(\rho_s/\,\rho_{sm}) \le 0.018 \qquad (\varepsilon_s)_{CP}=0.06 \qquad (2.11)$$

where ρ_s is volumetric ratio of transverse reinforcement and ρ_{sm} is minimum design volumetric ratio of transverse reinforcement

After the performance check of each member by means of strain values for the ductile members is done, global performance assessment of the whole structure is employed. Damage levels considered in three categories are described below.

- IO Performance Level

At any story of the building, in the direction considered, at most 10% of the beams are allowed to go beyond IO Limit. All the other members should be below IO limit.

- LS Performance Level

At any story, in the considered direction, at most 30% of the beams are allowed to go beyond LS performance limit. Columns in CP level should carry at most 20% of the total story shear. At the top story, columns in CP level are allowed to carry 40% of the total story shear. All other members should be in IO or LS

levels. However, columns that exceed IO limit should carry at most 30% of the total shear.

- CP Performance Level

At any story, in the considered direction, at most 20% of the beams are allowed to go beyond CP limit. All other members should be in IO, LS or CP level. However, columns that exceed IO limit should carry at most 30%of total story shear

2.5   CONCLUDING REMARKS

In this chapter, the nonlinear procedures of performance assessment methods that will be used in this study have been reviewed. First, performance level definitions and acceptability limits of ATC-40 were described. The inter-story drift ratio (ISDR) limits and corresponding performance levels are of concern. Second, CM method of FEMA (ASCE/SEI-41, 2007) was introduced. The calculation of target displacement, acceptability limits and criteria regarding the beam and column members are of interest. Lastly, TEC (2007) was introduced; its acceptability limits and criteria regarding the dynamic procedure were described. Only the ductile members were taken into account.

In the following chapters, these procedures will be used to determine the performance levels of the case-study buildings that are subjected to PsD or dynamic excitations. A comparative evaluation will be conducted.

CHAPTER 3

BENCHMARK STUDY

3.1   INTRODUCTION

In this chapter, nonlinear analysis methods and performance assessment procedures described in the previous chapter is verified through a well documented RC test structure before embarking upon investigation of three in-situ case-study buildings which constitutes the main objective of this study. The test structure is a full scale, three-story, plan-wise irregular RC frame test building referenced as SPEAR. This frame structure was constructed and tested in the European Laboratory for Structural Assessment (ELSA) of the Joint Research Center (JRC) of the European Commission under the auspices of the European Union project named Seismic Performance Assessment and Rehabilitation (SPEAR). The SPEAR building was constructed to simulate an actual three-story building that represents older constructions in southern European Countries, such as Greece, without specific provisions for earthquake resistance. Bi-directional pseudo-dynamic (PsD) testing was carried out in ELSA (Jeong and Elnashai 2004; Mola et al. 2004).

PsD and shaking table tests on full scale RC frame structures are very limited due to their high cost and extensive time demand. Having the following features, the SPEAR test building turns out to be a good candidate for verification of the analytical model and tools employed in this dissertation:

- A representative of older type, full scale, 3D, RC frame,
- Subjected to bi-directional PsD test in the laboratory
- Detailed test data is available

First, description of the test structure, analytical model and applied ground motions are provided. Then, the analytical model is assessed at member behavior level through current methods using the NTHA results.

3.2   DESCRIPTION OF THE TEST STRUCTURE

The SPEAR test structure in Figure 3.1 was built by considering the construction practice and materials present in the early 1970s in Greece. For concrete, a nominal strength of f_c=25 MPa was assumed in design. Smooth rebar steel with characteristic yield strength of about 450 MPa was used as the reinforcement. Due to scarcity of current production, steel representing older construction with yield strength of 250 MPa was not used.
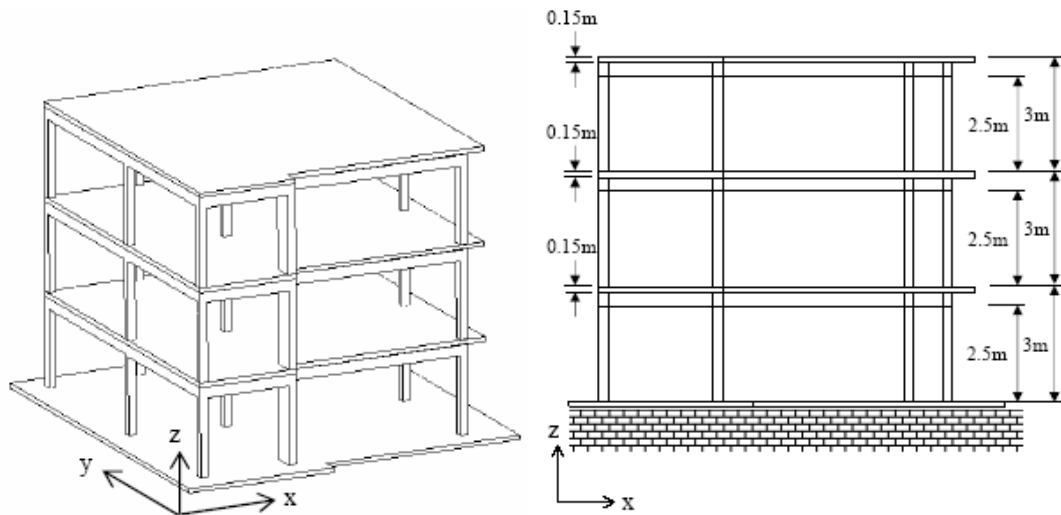
Figure 3.1 3D and elevation view of the SPEAR test building (Adapted from Jeong and Elnashai, 2004)

Beam cross-sections are 250 mm wide and 500 mm deep, bars with 12 and 20 mm diameter were used as the longitudinal reinforcement, which are both straight and bent at 45 degrees angles, representative of old practice in Greece. 8 mm smooth bars with 200 mm spacing were used as transverse reinforcement of the beams, which did not provide sufficient confinement. Eight out of the nine columns (Figure 3.2) has a square 250 by 250 mm cross-section; the ninth one,

column C6, as shown in Figure 3.3, has a cross-section of 250 by 750 mm, which provides the building with slightly more stiffness and strength along the Y direction than the X direction. 12 mm longitudinal bars were used for all columns (4 in the corners of the square columns, 10 along the perimeter of the rectangular one). Transverse reinforcement of columns consisted of 8 mm bars at 250 mm providing almost no confinement. Beam-column connections were built without stirrups (Jeong and Elnashai 2004; Mola et al. 2004; Negro et al. 2004).
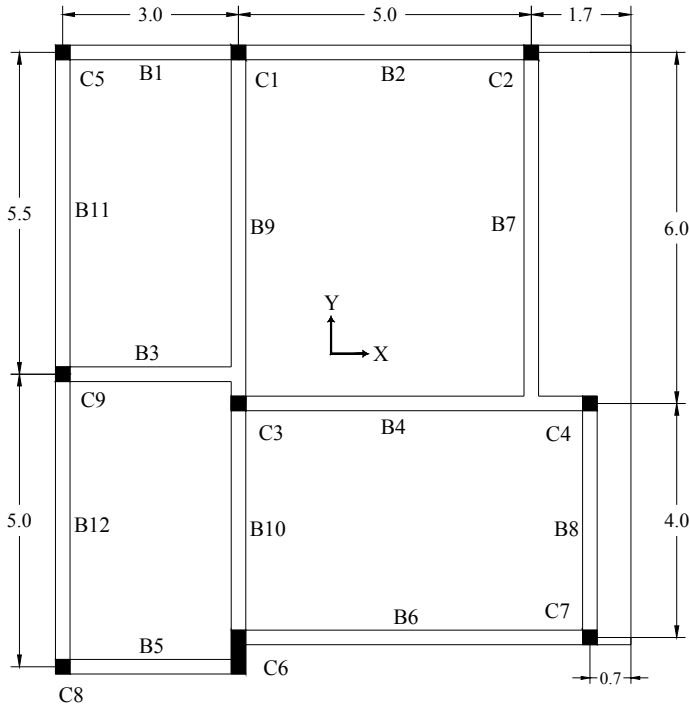
Figure 3.2 Plan of the SPEAR building (units are in m)

In the framing, the columns are weaker than the beams which are typical for older type structures. This is an undesirable condition that causes the plastic hinges form at the end of the columns before the beams resulting in a weak column-strong beam failure mechanism. The plan configuration (Figure 3.2) is not symmetric about either of the orthogonal axes. This plan irregularity is another deficiency of the structure causing additional stresses due to torsion. Height of all stories is 3 m and the frame is regular in elevation (Figure 3.1).
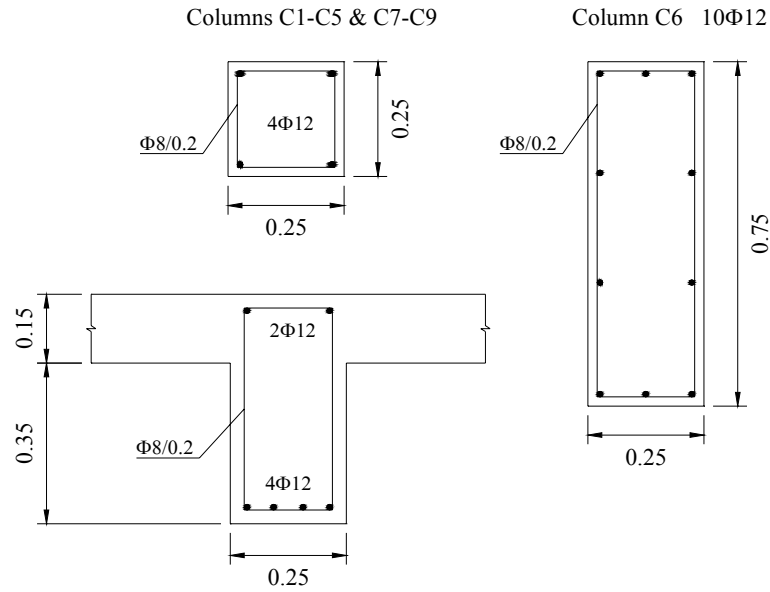
Figure 3.3 Column and beam cross sections (Units are in m)

Gravity loads on the building were determined by summing the self-weight of the structure and 1.1 kN/m^2 additional gravity loads on slabs (0.5 kN/m^2 for finishing and 2 kN/m^2 for live loads) (Jeong and Elnashai 2004).

3.3   APPLIED GROUND MOTIONS

Seismic response of the structure under seven records was analytically investigated. Collapse prevention and obtaining significant damage were the important criteria for selection of the ground motion to provide good response data in the real test. In order tot achieve this goal, Montenegro 1979-Herceg Novi, a semi-artificial record was decided to be used in the laboratory tests (Jeong and Elnashai 2004; Negro et al., 2004).

After selection of the record, the most appropriate direction of application was determined. The purpose was to maximize the torsional effects. As a last step, the levels of peak ground acceleration (PGA) were defined for different phases of the test to obtain the desired damage levels. The aim was to reach a level with significant damage to investigate the behavior of the structure but not severe to be beyond repair (Mola et al. 2004).

Three different intensity level tests were conducted. The initial low-intensity (0.02g PGA) test was carried out to check the functionality of the experimental equipment and to obtain the initial stiffness matrix of the structure in the elastic range. In addition, first mode shape of the structure, along with their frequencies, and modal damping values were obtained. The second test (0.15g PGA) was intended to cause severe damage without going beyond the reparability stage. However, only minor cracking occurred at the end of the test. Since the 0.15g PGA test failed in reproducing significant level of damage, a higher intensity test (0.20g PGA) was carried out (Negro et al. 2004).

Since the observed damage was severe after the third test (0.20g PGA) and the structure had been damaged during the 0.15 PGA test the response estimations were not accurate compared with the second test (0.15g PGA), so the second test is considered in this study. This is in agreement with previous research employed by others (Jeong and Elnashai 2004). The acceleration time histories and response spectra used in this study are shown in Figs. 3.4-3.5.
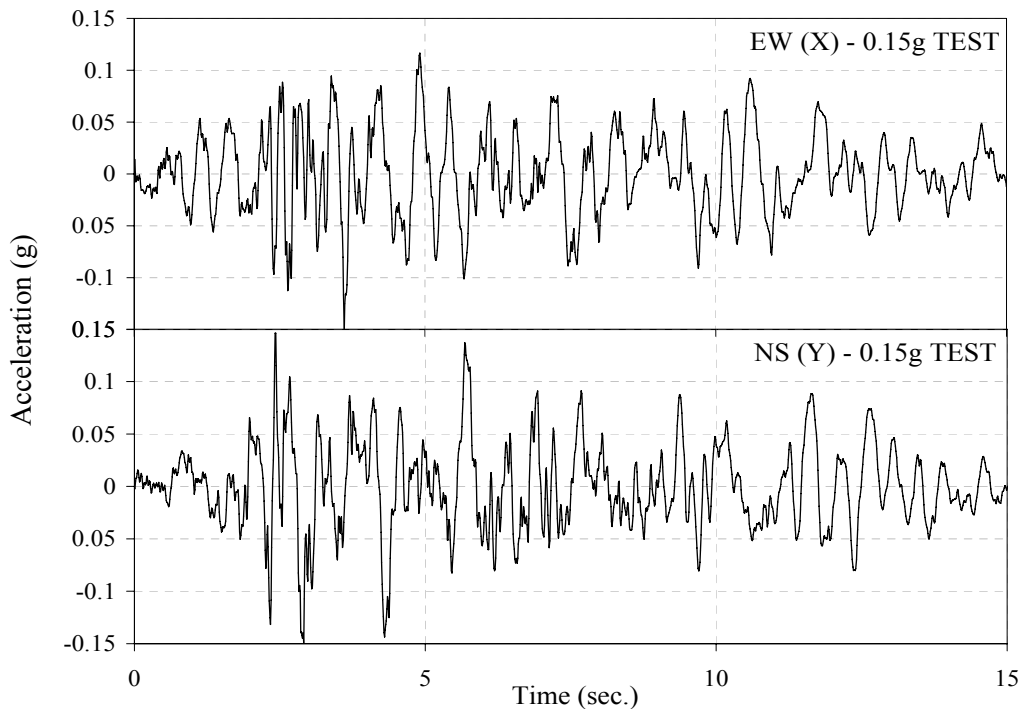
Figure 3.4 Acceleration waveforms applied to the building in the X and Y directions (PGA=0.15g)
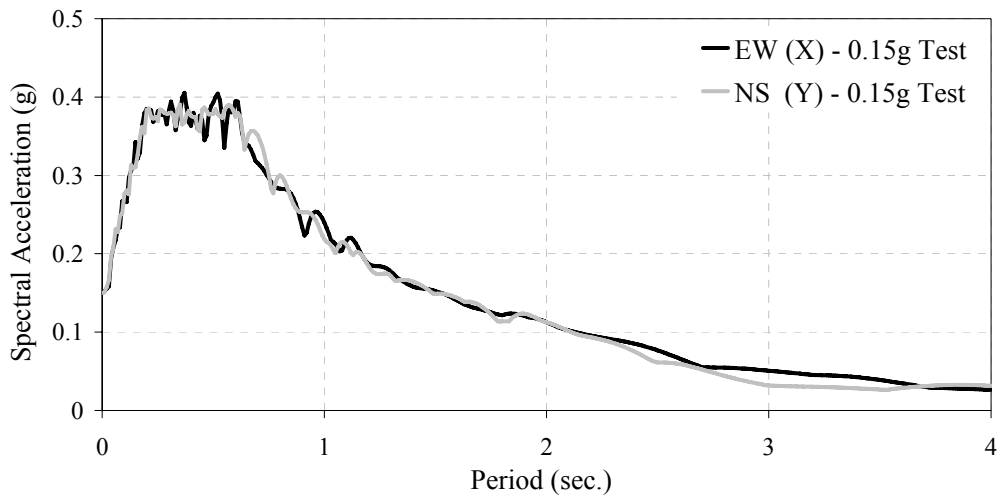
Figure 3.5 Elastic response spectra of the PGA=0.15g records simultaneously applied to the building for both components (5% damping)

3.4   OBSERVED DAMAGE

Damage pattern was identified by visual inspection after the 0.15 PGA test (Figs. 3.6 and 3.7). Only minor damage occurred during the test. It was observed at the top of second story columns. No cracks were observed at the bottom of these members. The beams were undamaged (Jeong and Elnashai, 2004).

(a) C3   (b) C4   (c) C6
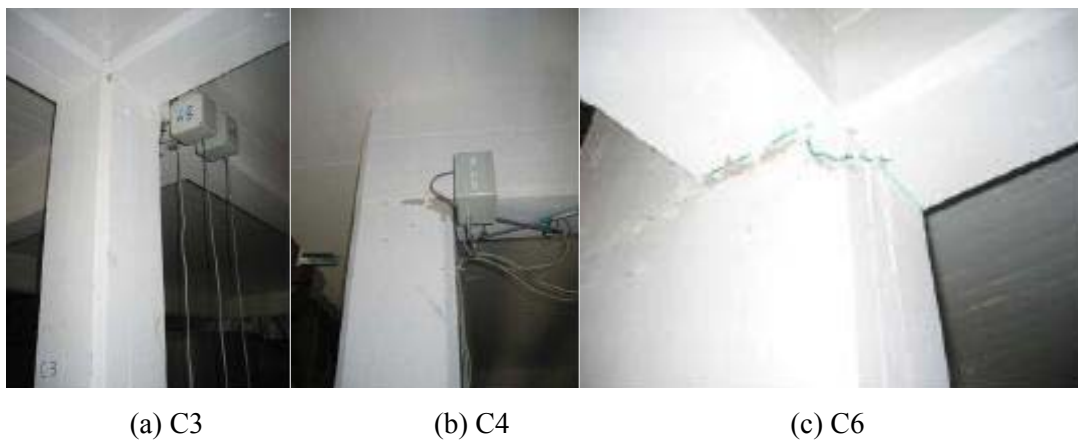
Figure 3.6 Damage observed at the second story columns after the 0.15 PGA test (Adapted from Jeong and Elnashai, 2004)

| (d) C7 | (e) C9 |

Figure 3.7 Damage observed at the second story columns after the 0.15 PGA test (Adapted from Jeong and Elnashai, 2004)

3.5   ANALYTICAL MODEL

NTHA of the SPEAR test building were carried out with the commercially available finite element analysis program-Perform 3D (Ram International, 2005). For modeling, distributed plasticity was employed through fiber analysis approach.

Different nonlinear modeling approaches have been proposed in the literature. These models can be divided into two groups as lumped and distributed plasticity models. In lumped plasticity models, nonlinear behavior is concentrated typically at the element ends. In distributed plasticity models, nonlinear behavior is considered through entire element by integration of the constitutive behavior at a finite number of sections. Nonlinear behavior at these sections is derived by using moment-curvature relations, classical plasticity theory for force-deformation resultants or subdivision of the elements into fiber segments and integration of the uniaxial fiber stress-strain relation. Although the computational burden of the fiber models is high, they are the only rational choice for cases with significant interaction between bending moment and axial force (Spacone et al. 1996). Besides, these frame models are also economical solutions for nonlinear dynamic analysis of structures with up to several hundred members (Spacone et al., 1996).

In the analytical model, beam sections use the fiber properties for axial force and in plane bending only and are elastic for out-of-plane bending. Column sections use the fiber properties for bending about both axes, and account for N-M-M interaction. Beam and column sections are both assumed to be elastic for shear and torsion. Input for the fiber sections are the geometrical and material properties of the steel and concrete by means of stress-strain. The output can be obtained in any terms such as stress-strain, moment-curvature and moment-rotation etc.

Structural dimensions were considered through the section centerlines. Masses were assumed as concentrated at the mass center of each floor. Three DOFs–two translational and one rotational around vertical axis were considered at each floor. Rigid end offsets were not taken into account to reflect the slip effect and unconfined joint behavior in the model. Following customary practice, T sections were utilized for beam sections and the effective flange width was assumed to be the beam width plus 7 percent of the clear span of the beam on both side of the web. Since the structure was a bare frame, it had no source of energy dissipation except hysteretic damping (Jeong and Elnashai 2004). Viscous damping was not implemented in the PsD test, so the post-test simulation was kept consistent with the experimental study. Other assumptions about material and loading employed in the analytical modeling are summarized in Table 3.1

Table 3.1 Assumptions for the analytical model

Material	Reinforcement Steel	E_s=206000 MPa
	Concrete	f_{ck}=25 MPa E_c=23750 MPa (ACI 318, 2008)
	Stress-strain relationship	Reinforcement Steel: Bilinear Model Concrete: Mander et al. (1988) (Unconfined)
Loading	Seismic dead load for mass calculation	DL+0.3LL
	Centre of mass	Floor 1&2 X=4.58 m Y=5.35 m Floor 3 X=4.65 m Y=5.44 m
	Mass	Floor 1&2 67.26 t Floor 3 62.08 t
	Mass moment of inertia	Floor 1&2 1500 tm^2 Floor 3 1363 tm^2

3.5.1 ELASTIC PERIODS AND MODE SHAPES

The elastic fundamental periods and mode shapes obtained from 3D eigenvalue analysis are presented in Figure 3.8. Torsional mode shapes are significant and coupling between the flexural and torsional behaviors are apparent starting from the very first modes. The period values are 0.59, 0.51 and 0.42 sec for the first, second and third modes, respectively

(a) T_1 = 0.59 sec   (b) T_2 = 0.51 sec   (c) T_3 = 0.42 sec
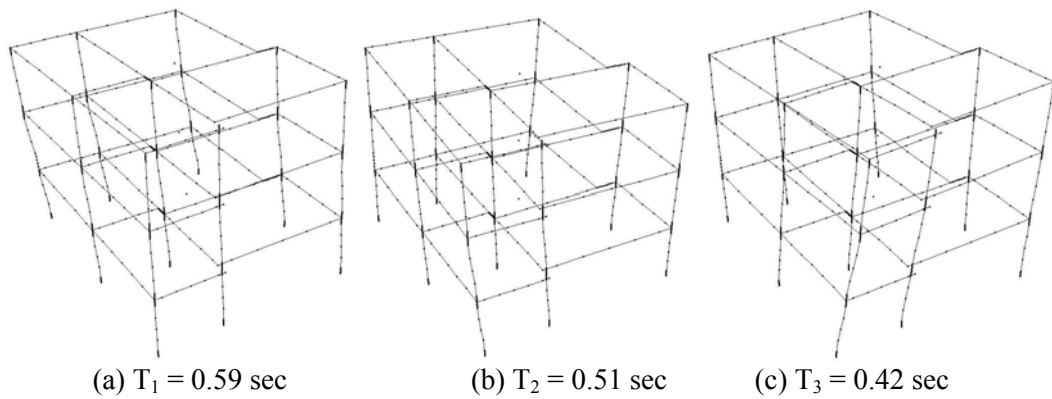
Figure 3.8 Elastic periods and mode shapes of 3D eigenvalue analysis

3.5.2 Comparison of Identified Periods from the Low Intensity (0.02g PGA) PsD Test and Calculated from the NTHA

The initial stiffness matrix and mode shapes of the structure with their frequencies were obtained through low-intensity-0.02 PGA test (Negro et al. 2004).

Table 3.2 Comparison of fundamental period values identified from the 0.02g–PGA test and the dynamic analysis of the analytical model

Mode #	Period Values Identified from the 0.02g PGA Test (Experiment)	Fourier Transformation of the Dynamic Analysis-0.02g PGA (Analytical Model)	Error (%)
1	0.85	0.89	4.5
2	0.78	0.76	2.1
3	0.66	0.63	3.5

To compare the frequencies identified from the test, Fourier Transformation of the results regarding the NTHA of the analytical model were carried out and shown in Table 3.2. The calculated values are very close to these identified from the experiment.

3.6   VERIFICATION OF THE ANALYTICAL MODEL: 0.15 PGA TEST

In order to validate the analytical model, top story displacement (Figure 3.9) and base shear response history (Figure 3.10) results regarding the bi-directional NTHA were obtained for both orthogonal directions. Then the test results were compared quantitatively with those of the analytical model as shown in Tables 3.3 and 3.4. The analytical results demonstrate 5.38 % and 13.8 % discrepancy for the deformation and 3.7% and 3.2 % errors for the base shear in the X and Y direction respectively. The model is quite successful in predicting the test results.
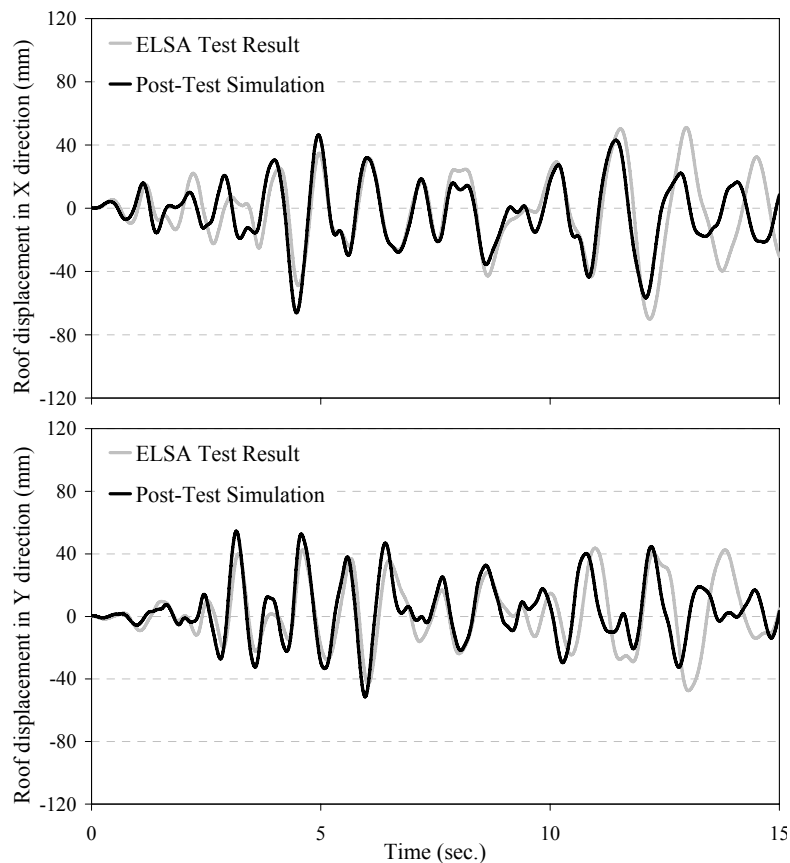
Figure 3.9 Top story displacements in X and Y directions (0.15 PGA Test)

41

Table 3.3 Comparison of the analytical and experimental results: Maximum Roof Disp. in the orthogonal directions of the building (0.15 PGA Test)

	Max. Roof Displacement (mm)	
	X	Y
Test Result	70	48
Post-Test Simulation Result	66	54
% difference	-5.38	13.80
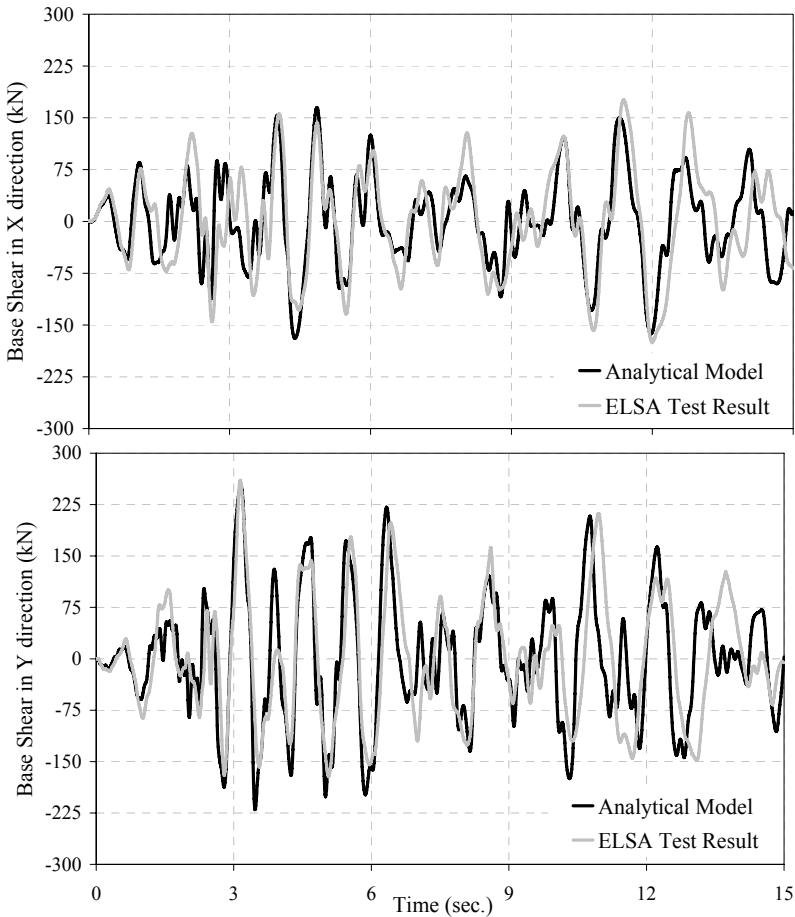
Figure 3.10 Base shear response histories in the orthogonal directions of the test structure for the 0.15g PGA Test

Table 3.4 Comparison of the analytical and experimental results: Maximum Base Shear values in the orthogonal directions of the building (0.15 PGA Test)

	Max. Base Shear (kN)	
	X	Y
Test Result	175.9	260.5
Post-Test Simulation Result	169.4	252.2
% difference	3.7	3.2

3.7   PERFORMANCE ASSESSMENT OF THE TEST STRUCUTRE: 0.15 PGA TEST

The performance assessment of the SPEAR test building under 0.15 PGA test was employed according to the nonlinear procedures of ASCE/SEI-41 (2007), Supplement-1 (2008) and TEC (2007). Since the experimental and analytical results indicated that the beams remained within the elastic range, no plastic demand could be calculated for beam elements. Only the second story columns were assessed where the cracking was observed during the 0.15 PGA test. As the stirrup configuration was inadequate and confinement effect was almost non-existent due to the following reasons, acceptance limit values of the codes corresponding to the condition of "non-conforming transverse reinforcement" were considered.

- Inadequate transverse reinforcement configuration: the stirrups had been closed with 90° angle hooks instead of 135° angle of those specified in the standards and codes (ASCE/SEI-41, TEC)
- Insufficient amount of stirrups: no confinement zone exists and no transverse reinforcement in the beam-column joints

3.7.1   Performance Assessment of the Columns According to ASCE/SEI-41 (2007) and its Supplement-1 (2008)

Evaluation process of the second story columns was employed according to the nonlinear procedures of ASCE/SEI-41. Plastic rotation demands obtained by the NTHA results were compared with the acceptance limit values specified in the guidelines. Plastic rotations of the elements were calculated by using their curvature demands (Figure 3.11) and assumed plastic hinge length. Various researchers (Baker 1956; Mattock 1967; Corley 1966; Park et al. 1982; Priestley and Park 1987; Paulay and Priestley 1992) have proposed expressions to estimate the plastic hinge length of concrete members. These expressions give different values (Bae and Bayrak 2008). Here, the Eqn. 3.1 suggested by Paulay and Priestley (1992) and the plastic rotation definition that is given by Eqn. 3.2 was used. As a note,

determination of plastic length under bi-directional dynamic effects is still an issue to be resolved.

$$l_p = 0.08l + 0.022d_b f_y \qquad 3.1$$

$$\theta_p = (\phi_u - \phi_y)l_p \qquad 3.2$$

where l_p is the plastic hinge length, l is the length of the cantilever or the distance between the inflection point and the member end, d_b is the bar diameter, f_y is the yield strength of steel, θ_p is the plastic rotation, Φ_u is the ultimate curvature and Φ_y is the yield curvature (Figure 3.11).
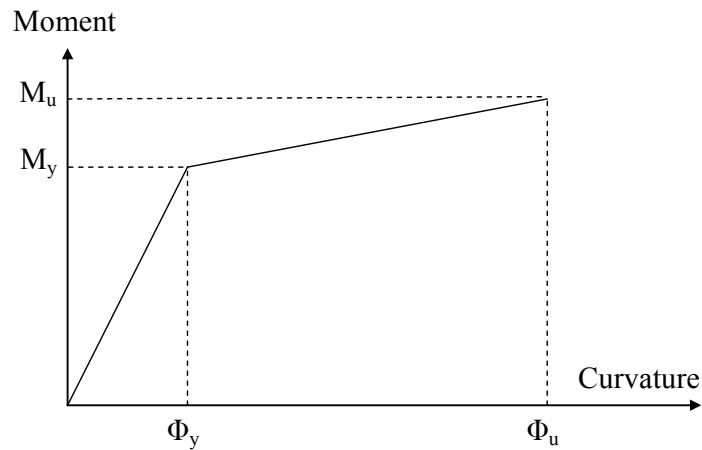
Figure 3.11 Representation of ultimate and yield curvatures on the moment curvature diagram of any cross-section

Performance assessment results in the most critical direction are shown comparatively in Table 3.5. Plastic rotation limits of the column members corresponding to different performance levels were calculated. The difference in the acceptance limit values between the previous (2007) and updated (2008) versions of ASCE/SEI-41 and corresponding performance levels are obvious in Table 3.5. The columns are in CP performance level according to the previous version while they are in LS performance level according to the current document except for the column C6. This indicates that the old version of ASCE/SEI-41 gives more

conservative results compared to the current one when the columns with nonconforming conditions are of concern. However, these results are still conservative compared to the observed damage; since light damage was observed in the second story columns after the test.

Table 3.5 Performance assessment results of the second story columns according to ASCE/SEI-41 (2007) and Supplement-1 (2008). The values are shown as "old/current" values in each cell

Member	$\theta_{capacity}$ (Acceptance limits)			θ_{demand}	Performance Level
	IO (old/current values)	LS (old/current values)	CP (old/current values)		
	(rad)	(rad)	(rad)	(rad.)	(old/current)
C1	0.005/0.005	0.005/0.009	0.006/0.010	0.0061	CP / LS
C2	0.005/0.005	0.005/0.009	0.006/0.010	0.0051	CP / LS
C3	0.0043/0.0046	0.0043/0.0081	0.0053/0.009	0.0081	CP / LS
C4	0.0048/0.0049	0.0048/0.0088	0.0058/0.0097	0.0059	CP / LS
C5	0.005/0.005	0.005/0.009	0.006/0.010	0.0052	CP / LS
C6	0.005/0.005	0.005/0.009	0.006/0.010	0.0101	CP / CP
C7	0.005/0.005	0.005/0.009	0.006/0.010	0.0056	CP / LS
C8	0.005/0.005	0.005/0.009	0.006/0.010	0.0051	CP / LS
C9	0.005/0.005	0.005/0.009	0.006/0.010	0.0065	CP / LS

LS: Life safety, CP: Collapse prevention

3.7.2 Performance Assessment of the Columns According to TEC (2007)

Evaluation of the columns according to TEC (2007) was employed in two steps. First, the acceptability limit values of strain regarding different performance levels were calculated considering the Eqs. through 2.9-2.11 The corresponding values for concrete and strain fibers are as follows:

$$(\varepsilon_{cu})_{IO}=0.0035 \qquad (\varepsilon_s)_{IO}=0.01$$

$$(\varepsilon_{cu})_{LS}=0.0035 \qquad (\varepsilon_s)_{LS}=0.04$$

$$(\varepsilon_{cu})_{CP}=0.0040 \qquad (\varepsilon_s)_{CP}=0.06$$

It should be kept in mind that nonconforming transverse reinforcement was considered in the calculations due to the reasons expressed in section 3.7.

Second, the strain demands obtained by the NTHA were compared with these acceptance limit values. Since the calculated strain values of concrete fibers were below the specified limits, only the strain values of the steel fibers were considered here. The capacity and demand values are comparatively depicted in Table 3.6.

Table 3.6 Performance levels of the second story columns according to TEC (2007)

Member	$(\varepsilon_s)_{capacity}$			$(\varepsilon_s)_{demand}$	Performance Level
	IO	LS	CP		
C1	0.01	0.04	0.06	0.0134	LS
C2	0.01	0.04	0.06	0.0124	LS
C3	0.01	0.04	0.06	0.0172	LS
C4	0.01	0.04	0.06	0.0122	LS
C5	0.01	0.04	0.06	0.0139	LS
C6	0.01	0.04	0.06	0.0218	LS
C7	0.01	0.04	0.06	0.0157	LS
C8	0.01	0.04	0.06	0.0140	LS
C9	0.01	0.04	0.06	0.0169	LS

LS: Life safety

Table 3.6 indicates that the calculated performance level overestimate the observed damage level similar to that of ASCE/SEI-41 Supplement-1 (2008).

3.8 COMPARISON BETWEEN ANALYTICAL AND EXPERIMENTAL RESULTS

Damage pattern identified through visual inspections after the 0.15g PGA test showed that only light damage occurred at the top ends of the second story columns as depicted before in Figs. 3.6 and 3.7. Thus, these columns were judged to be in IO performance level. The acceptance limits of ASCE/SEI-41 (2007) were found to be very conservative since the columns were calculated in CP performance level (Table 3.5).

After the acceptance limits have been revised in Supplement-1 (2008), the columns were calculated to be in LS performance level that is more consistent with the observed damage. TEC (2007) gave similar performance level results with those of revised ASCE/SEI-41 that the columns were calculated to be in LS performance level.

Those similar results obtained from ASCE/SEI-41 and TEC may be related to the high safety provisions considered in the guidelines and codes that are particular to the existence of nonconforming transverse reinforcement condition.

Table 3.7 Comparison of assessment and experimental results of the second story columns

	Performance Levels				
Member	TEC2007	ASCE/SEI-41 (2007)	ASCE/SEI-41 (2008)	Measured Colum Drift Ratio (%)	Observed Damage
C1	LS	CP	LS	1.13	Light
C2	LS	CP	LS	1.13	Light
C3	LS	CP	LS	0.78	Light
C4	LS	CP	LS	0.83	Light
C5	LS	CP	LS	1.13	Light
C6	LS	CP	CP	0.75	Light
C7	LS	CP	LS	0.83	Light
C8	LS	CP	LS	0.75	Light
C9	LS	CP	LS	0.80	Light

3.9   CONCLUDING REMARKS

This benchmark study indicates that the main difference between the procedures arises from the difference of definitions in the acceptance limit values, even in the case of a specimen with well known properties tested under tightly controlled circumstances. In addition, comparison of calculated and observed damage levels showed that high safety provision of the codes for structural members with nonconforming transverse reinforcement result in conservative results.

The variability under field conditions is likely to be much higher because actual properties of existing buildings and precise ground motions to which they have been subjected are typically known only approximately. In this concept, laboratory tests provide valuable data to understand the behavior of buildings under seismic actions. Besides, the structures that are well instrumented to measure the input motion and damage are of importance to understand how successful the current codes are in making accurate predictions.

CHAPTER 4

A RECONSTRUCTION OF THE SEISMIC RESPONSE

4.1   INTRODUCTION

Once modeling capabilities of the software have been verified by comparing the measured response of a 3D RC structure tested in the laboratory with the calculated response of the analytical model, the approaches employed in representation of the analytical model are now used to investigate the response of the MPWR buildings that were subjected to near-field strong ground motions in different regions of Turkey at different times.

Figure 4.1 Epicenters of the earthquakes (adapted from http://www.google.com) Magnitudes are obtained from HRV-Harvard Centroid Moment Tensor solutions

The case-study building, the main office building of MPWR is a ground-plus-four-story RC frame building that was constructed in the 1980s in many different regions of Turkey. The three that are reported here suffered damage to varying degrees of severity during the March 13th, 1992 Erzincan, November 12th, 1999 Düzce, and May 1st, 2003 Bingöl earthquakes (Figure 4.1).
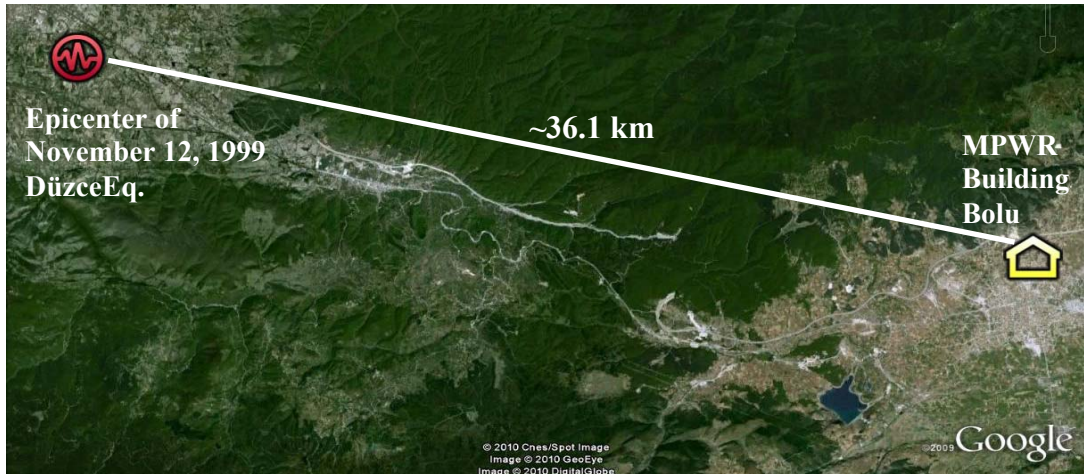
Figure 4.2 Epicenter of the 1999 Düzce earthquake and location of the MPWR building in Bolu (adapted from http://www.google.com)
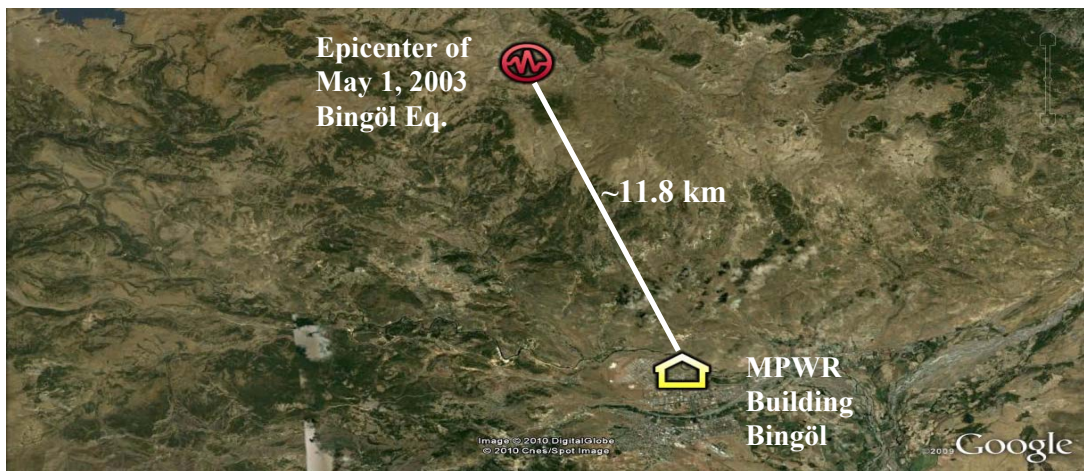
Figure 4.3 Epicenter of the 2003 Bingöl earthquake and location of the MPWR building in Bingöl (adapted from http://www.google.com)

During these events, three-component strong ground motion data were recorded in a one-story building adjacent to the case-study building in Bolu (Figure 4.2) and Bingöl (Figure 4.3) and in a one-story meteorological services building about two kilometers away from the case study building in Erzincan (Figure 4.4).
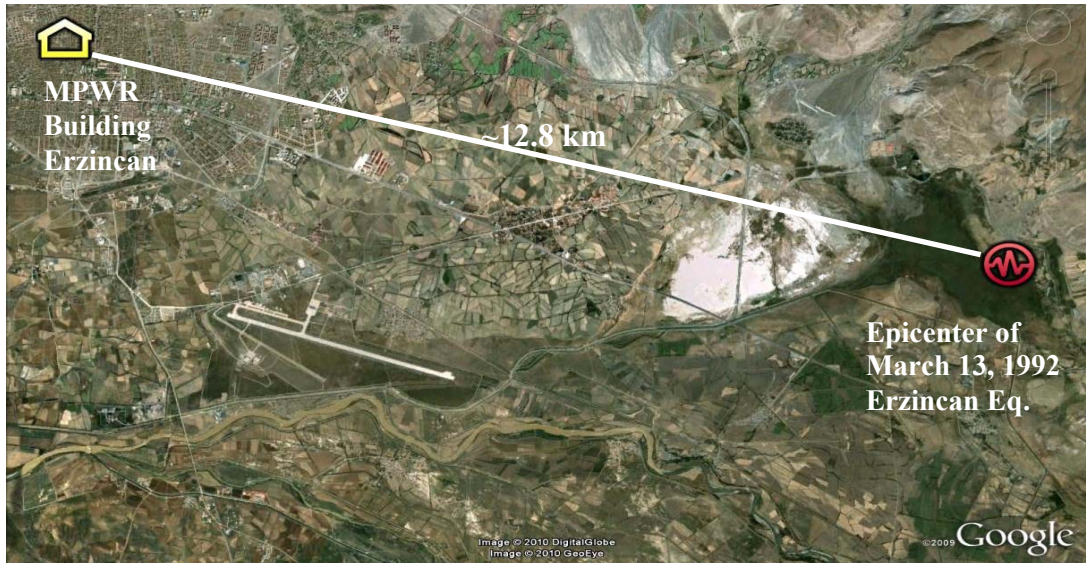
Figure 4.4 Epicenter of the 1992 Erzincan earthquake and location of the MPWR building (http://www.google.com)

Figure 4.5 Location of the record station and MPWR building in Erzincan (http://www.google.com)

That the ground motions are known for two of the three buildings is a uniquely fortuitous occurrence. The exception was that, the motion in Erzincan was recorded by a station situated about two km from the building (Figure 4.5). However, the ground composition between the sites is very similar and no tall buildings existed in the vicinity of the recording station to modify the ground

motions significantly. Thus, in the absence of a better theory it will be assumed here that the record represents the input motion to the building.

After the Düzce earthquake, a careful examination of the damage state was performed for the building in Bolu. A similar exercise was conducted in Bingöl four years later. The Erzincan building was not subjected to an investigation in 1992 as the other two because it seemed practically intact following the earthquake and served as an important critical facility for attending to the needs of the homeless citizens. The Erzincan Building was judged to be in "immediate occupancy" status by its users that included engineers and damage assessors employed by the ministry. The intervening period of eighteen years has not been helpful in retrieval of evidence to the contrary, so the initial damage assessment of "negligible" (a few inconsequential partition wall cracks; the phrase "immediate occupancy" had not been invented yet) is probably correct.

The known input motions for the buildings, their design drawings, material properties and structural damage information provided an opportunity to evaluate the current performance assessment methods. Here, the answer to the question of whether we could predict the seismic damage in RC buildings at the site well by proper modeling will be investigated. The comparisons that will be made between the models and the real buildings are expected to provide a test of the concepts embodied in structural performance assessment procedures in the light of empirical evidence.

4.2   DESCRIPTION OF THE MPWR BUILDING

The case study building is main part of the typical branch office of the MPWR building which is a five-building complex designed and constructed in the 1970s and 1980s, respectively. In all branch office complexes, there are four service buildings in addition to the main building. All buildings are separated by seismic joints in the same compound at all locations (Figure 4.6a). Here, particular emphasis will be placed on the case-study building that is shown in Figure 4.6b and will be called for short the "MPWR Building" in this study.
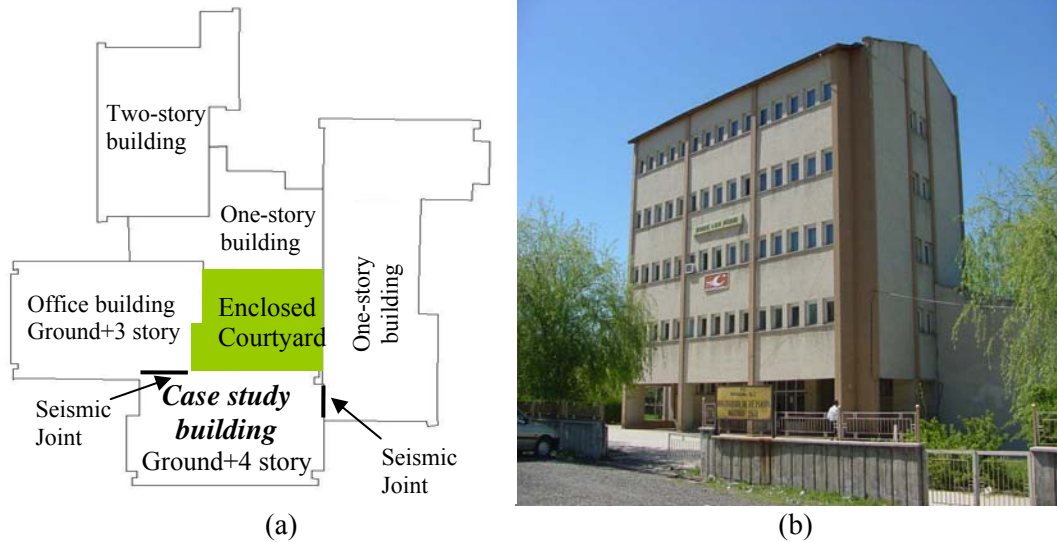
Figure 4.6 a) Plan of the building complex b) General view of the case study building

4.2.1 Physical Description of the MPWR Building

The building is a ground-plus-four-story RC structure where the story height is 3.8 m in the ground floor and 3.2 m in the rest (Figure 4.7). The building is rectangular in shape with three bays in both orthogonal directions. The plan dimensions are about 20 m and 13 m in the longitudinal and transverse directions, respectively (Figure 4.8).
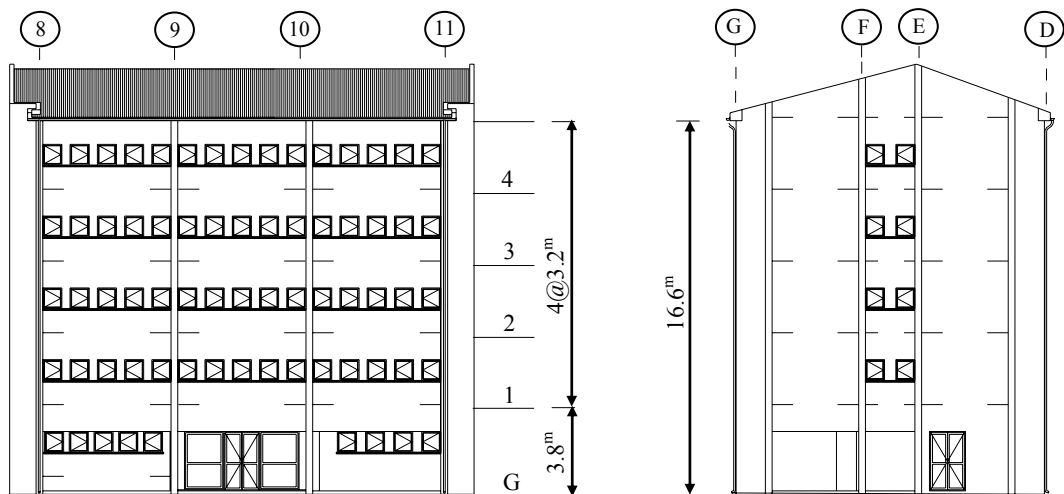
Figure 4.7 Front and lateral elevation views of the MPWR building (adapted from Çağnan, 2001)

The building consists of columns, beams and slabs for carrying the vertical load. To resist the main portion of lateral load three L-shaped columns (Figure 4.8) exist on the corners which are continuous from the ground floor to the roof. These columns are connected with peripheral deep-beams.
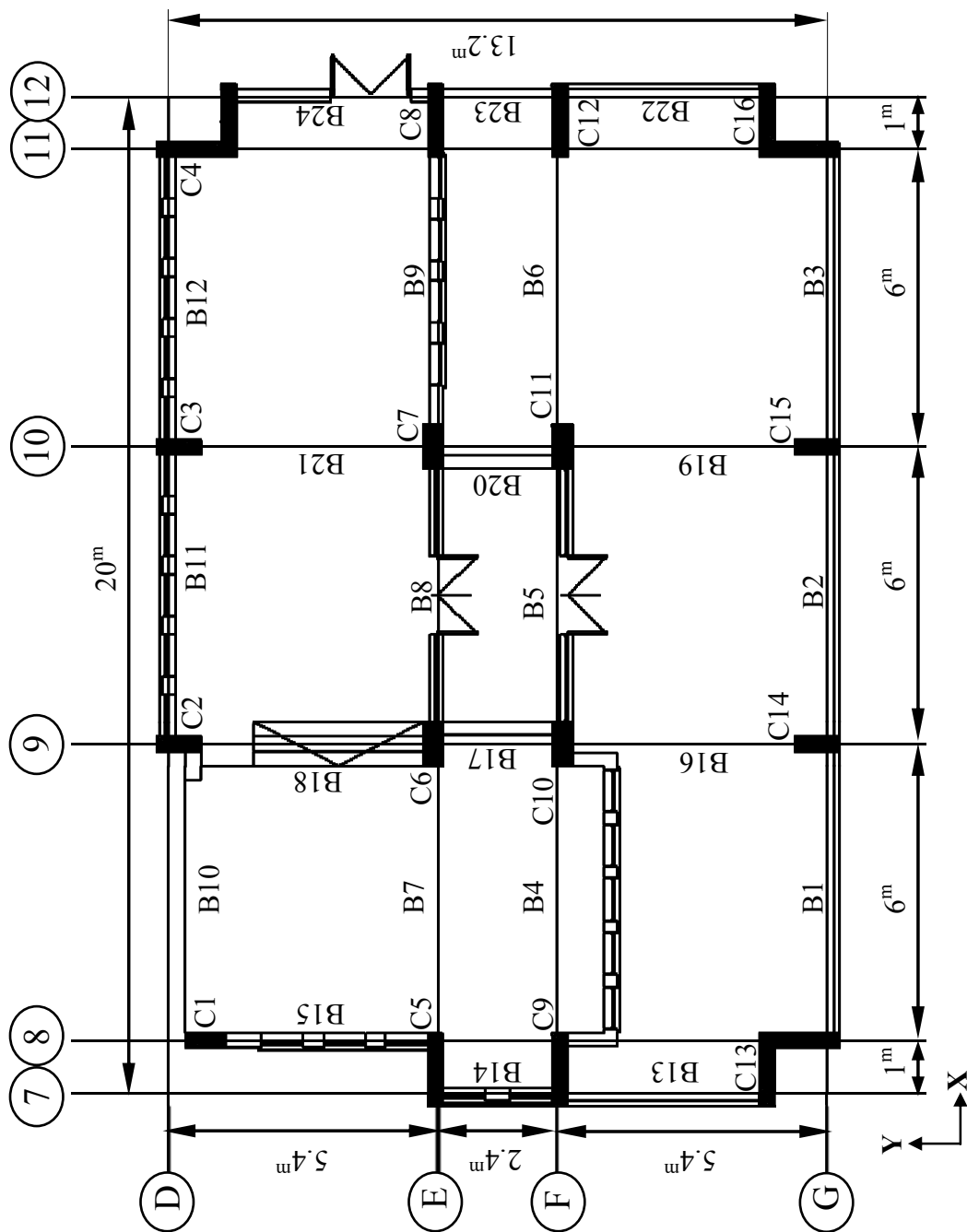
Figure 4.8 Typical floor plan of the MPWR building (adapted from Çağnan, 2001)

4.2.1.1 Beam Details

Beams in the exterior frames have an unusual depth of 1.2 m with 0.3 m width. Dimensions of the beams in the interior frames are 0.3 m by 0.7 m in the longitudinal direction and 0.3 m by 0.6 m in the transverse direction (Figure 4.9).

Peripheral Beams
30^{cm} x 120^{cm}
3Φ14+2Φ14+2Φ12
Φ8/200

Interior Beams – Long. Dir.
30^{cm} x 70^{cm}
2Φ14+2Φ14+2Φ12
Φ8/200

Interior Beams – Trans. Dir.
30^{cm} x 60^{cm}
2Φ14+2Φ12+2Φ12
Φ8/200

ρ_s =0.16 % ρ_s =0.18 % ρ_s =0.21 %
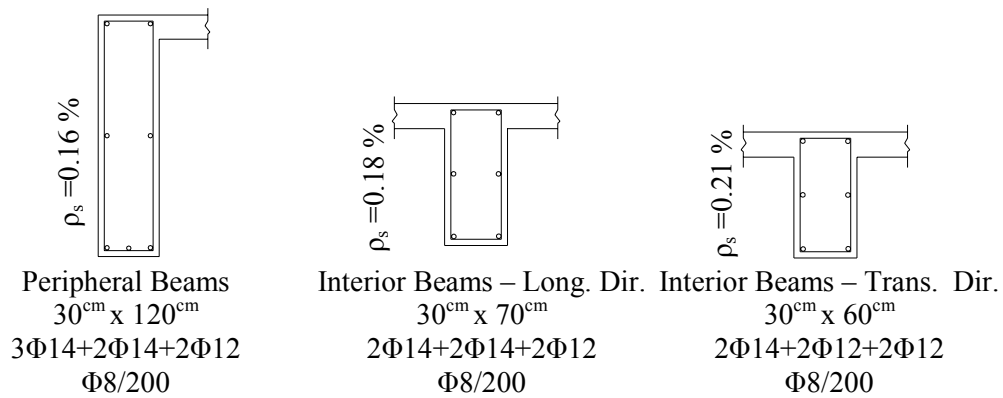
Figure 4.9 Cross-section dimensions, longitudinal and transverse reinforcement of the (a) peripheral beams, (b) interior beams in the longitudinal direction and (c) interior beams in the transverse direction of the building

The longitudinal reinforcement ratio of the beams ranges from 0.16 to 0.21 percent and the transverse reinforcement ratio is 0.17 percent. All beams contain sparsely spaced ties (Φ8 bars at 200 mm). In the confinement regions and joints no transverse bars exists. Dimensions of the beams and amount of the longitudinal reinforcement remain constant with the height of the building.

4.2.1.2 Column Details

Eight rectangular columns have their strong axis oriented in the longitudinal direction and five rectangular columns in the transverse direction of the building (Figure 4.8). Except for the L-shaped corner columns, sizes and longitudinal reinforcement in these members decrease progressively from lower to the upper stories. The longitudinal reinforcement ratio of the columns range from 0.58 to 2.49 percent and the transverse reinforcement ratio ranges from 0.06 to 0.17 percent

(Figure 4.10). All columns contain sparsely spaced ties (2Φ8 bars at 200 mm) even in the confinement zones.

$\rho_l = 0.86\text{-}1.90\ \%$

$\rho_l = 0.6\text{-}1.97\ \%$

$\rho_l = 0.59\ \%$

C1
30^{cm} x 80^{cm}
12Φ22
2Φ8/200

C2-C3-C14-C15
30^{cm} x 90^{cm}
14Φ20
2Φ8/200

C4-C13-C16
30^{cm} x 147^{cm} x 165^{cm}
3x4Φ20+2x3Φ16+2x4Φ16
4Φ8/200

$\rho_l = 0.58\text{-}2.49\ \%$

$\rho_l = 0.73\text{-}1.69\ \%$

C5-C8-C9-C12
147^{cm} x 30^{cm}
2x6Φ14+2x12Φ22
2Φ8/200

C6-C7-C10-C11
80^{cm}x40^{cm}
16Φ20
2Φ8/200
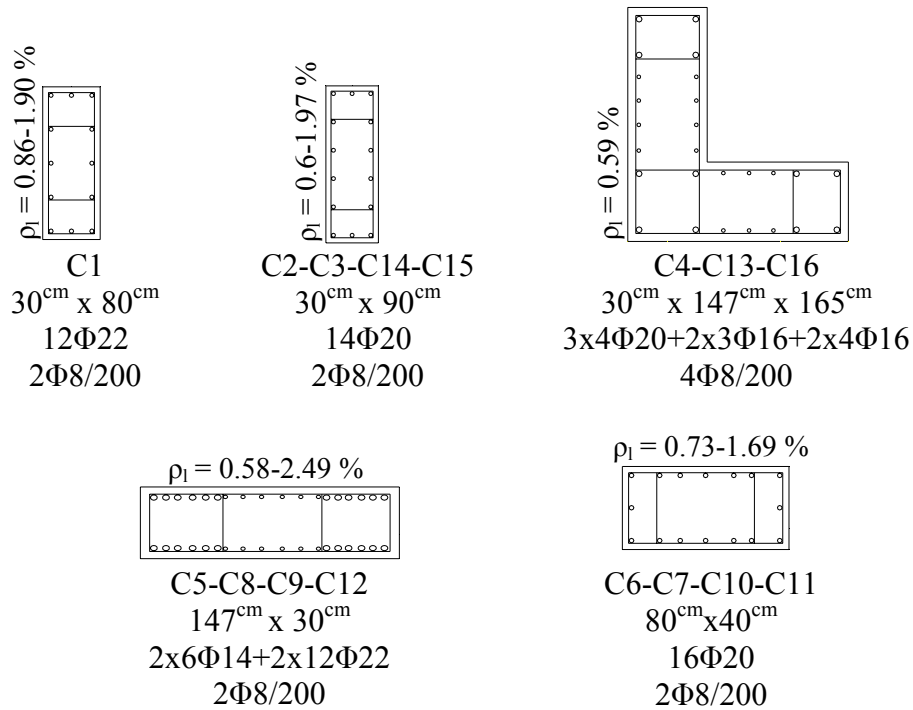
Figure 4.10 Cross-section dimensions, longitudinal and transverse reinforcement of typical column sections at the ground level (adapted from Çağnan, 2001)

4.2.1.3 Seismic Joint, Foundation and Slabs

The seismic joints (50 mm) between the adjacent buildings in the complex were aimed to allow the main building to vibrate as a 5-story structure. The foundation system consists of mat foundation with 50 cm thickness. The slab thickness is 15 cm at each floor.

4.2.1.4 Masonry Infill Wall Details

The peripheral hollow clay brick infill walls are 26 cm in thickness. The infill walls separating office rooms from corridors are 19 cm thick and those separating office rooms from each other are made up of 9 cm masonry units. The amount of masonry walls at the ground and top floor is less than that of the other

56

floors. The ground story is used as the reception area for citizens who sought to do business in the buildings while the top level is used as an archival repository.

4.2.2 Design Criteria

The MPWR Building was designed according to the provisions of TS500 (1975)–The Turkish Building Code Requirements for Design and Construction of RC Structures, and the Turkish Seismic Code (1975). In this time period, design method for concrete was the allowable stress method and structural members were designed for both gravity and seismic loading. Following subsections provide a succinct description of that code because the MPWR Provincial Building was designed according to it.

4.2.2.1 Column Design Criteria

The inter-story drift ratio was allowed to be 0.25 percent. Minimum column dimensions were not allowed to be smaller than 25 cm and 1/20 of the story height. Height/width ratio of the columns should not be smaller than 3. Minimum longitudinal reinforcement ratio could not be less than 1 percent and higher than 3 percent for B160 (28-day cylindrical compressive strength of 14 MPa) concrete. For the lap spliced regions, this ratio was allowed to be 4 percent. The columns were divided into three regions along their height by means of transverse bars;
- Confined region
- Mid region
- Column-beam connection region

The confined region was not allowed to be smaller than 1/6 of column height or 45 cm. Minimum volumetric ratio of the transverse bar was required not to be less than 1 percent. Minimum bar diameter to be used was 8 mm. Spacing of stirrups should not be less than 5 cm and higher than 10 cm in the confined region. The hooks of the stirrups should be bent 135 degrees. In the mid-region the stirrup spacing could not be less than the half of the column height, 20 cm and 12 times the smallest bar diameter. The transverse bar in the joints should be calculated considering the

maximum shear force occurring in the connection zone and stirrup spacing could not be less than that of confinement zone.

4.2.2.2 Beam Design Criteria

Minimum dimensions for the beams were 200 mm by 300 mm. For steel-type-I (a yield strength of 220 MPa) minimum longitudinal reinforcement ratio was 0.005. Minimum transverse reinforcement bar diameter could not be less than 8 mm. Stirrup spacing was not allowed to exceed the half width or height of the beam. In the confinement regions which are assigned as twice the depth of beam at both ends, stirrup spacing should not exceed 1/4 of the beam depth. The first stirrup should be at most 50 mm far from the column surface.

4.2.2.3 Infill Wall Design Criteria

The infill walls should be thin and light as could be constructed. Any infill wall contributing to the mass or stiffness of the structural system should be taken into consideration.

4.2.2.4 Seismic Loads

In determination of seismic design forces, code used the formulation given below;

$$F = CW \tag{4.1}$$

where F is the design base shear to be applied to the building and W is the total weight of the structure as defined below;

$$W = \sum_{i=1}^{n} W_i \tag{4.2}$$

$$W_i = G_i + nP_i \tag{4.3}$$

G_i and P_i are the total dead and live loads regarding the story i, respectively; n is the live load factor that could be taken as 0.3 for the office buildings. C is the seismic coefficient that is calculated according to the formula below;

$$C = C_o \times K \times S \times I \qquad (4.4)$$

where Co is the seismic region coefficient, K is building type coefficient that could take values in the range of 0.60~1.20 according to ductility level of the framing system, S is spectral coefficient and I is building importance factor. C_o was taken as 0.1 and 0.08 for the seismic zones 1 and 2, respectively. K was taken as 1.0 for office buildings. Spectrum coefficient was calculated according to the formulation given below;

$$S = \frac{1}{|0.8 + T - T_o|} \qquad (4.5)$$

where T is the fundamental period of the structure and T_o is the soil effective period T could be assumed from one of the following equations given below in order to be on the safe side;

$$T = \frac{0.09H}{\sqrt{D}} \qquad (4.6)$$

or

$$T = (0.07 \sim 0.10)N \qquad (4.7)$$

Here, H (m) is the total height of the structure, D (m) is the dimension of the building parallel to the direction of the lateral force and N is the story number above the ground level. T_o can be calculated according to the equation given below;

$$T = \frac{4H_z}{V_S} \qquad (4.8)$$

where H_z is soil layer thickness and V_s is shear wave velocity.

4.2.3 Material Properties of the Buildings

The quality of materials and their conformance with the design specifications are of great importance in assessing the structural performance of the buildings. Here, the material properties of the concrete and reinforcing steel used in the construction of the buildings are described.

4.2.3.1 Concrete

After the 1999 Düzce earthquake, engineers from MPWR took concrete samples from the Bolu building. The average characteristic compressive strength of the concrete was calculated as 20 MPa as shown in Table 4.1. The corresponding values for the buildings in Erzincan and Bingöl were obtained from the technical report prepared by the engineers of MPWR (MPWR, 2004). They reported that measured average characteristic compressive strength of both buildings was 9 MPa. Hence, they applied the same retrofit project to both buildings after the 2003 Bingöl earthquake.

Table 4.1 Compressive strength test results regarding the MPWR building in Bolu (Adapted from Çağnan, 2001)

Core No.	Sample taken from	Compressive Strength (MPa)
1	Ground Floor – C7	16.7
2	Ground Floor - C8	28.9
3	Ground Floor – C11	19.9
4	Ground Floor – C12	17.6
5	Ground Floor – C14	18.4
6	Ground Floor – C15	27.1
7	Ground Floor – C16	22.9
8	Ground Floor – Adjacent Building	15.9
9	First Floor – Adjacent Building	20.6
10	First Floor – Adjacent Building	16.8
11	Second Floor – Adjacent Building	20.1
Average		**20**

4.2.3.2 Reinforcing Steel

All cities where the MPWR buildings existed were seated in the highest seismic hazard zones of the country designated as Zone 1, so it was assumed that there could not have been any difference in the reinforcement areas. Smooth longitudinal and transverse bars with yield strength of 220 MPa made from medium grade steel were used in all buildings which was standard practice during the period when the buildings were constructed.

4.2.4 Conformance of Design Specifications with the Construction Quality

The 1975 seismic code included more stringent requirements for geometry and detailing of components in comparison with the preceding ones (1940-1968). However, difficulties in transmitting a new code and the weakness in control mechanism still caused severe damage to the buildings and life losses during the earthquakes. Thus, in order to determine if any differences between the design specifications and the construction quality existed in the MPWR buildings, investigations were made at the sites and following results were obtained. The concrete type was specified as B160 in the structural drawings corresponding to a characteristic compressive strength (cylindrical specimen) of 14 MPa (C14). Compressive strength of the concrete samples taken from the Bolu building surprisingly resulted in an average value of 20 MPa. However, those values were reported (MPWR 2004) as 9 MPa for Erzincan and Bingöl buildings that is much lower than it should be. A note of caution is necessary here because standards for removing concrete samples from existing RC buildings did not exist, or may well not have been fully observed during these tests.

After the 1999 Düzce earthquake, engineers of MPWR checked the amount of longitudinal reinforcement in some of the columns. It was concluded that the required area of reinforcement was provided in almost all columns (Table 4.2).

61

Table 4.2 As-built data regarding the MPWR Building in Bolu

	Design Dimensions (mm)	Measured Dimensions (mm)	Design	Measured
Ground Floor–C3	300/900	300/900	14Φ22	16Φ20
Ground Floor–C8	300/1470	300/1470	24Φ22+12Φ14	24Φ20
Ground Floor–C15	300/900	300/900	14Φ22	14Φ20
Second Floor–C10	300/800	300/800	10Φ18	12Φ20

4.3 DESCRIPTION OF THE STRONG GROUND MOTIONS

In this section, important seismological features of the three major earthquakes and their strong ground motions will be examined. However, before that, general seismicity of Turkey is briefly described.

4.3.1 Introduction

Turkey is located on a highly active Eurasian Geological Plate which has caused numerous large magnitude earthquakes in history. The relative movements of Eurasian, African and Arabian plates are the cause of these events. The Arabian/African and Eurasian plates move north and south towards each other and as a result Turkey is being squeezed out westwards. The main sources of seismic activity in Turkey are as follows:

- *North Anatolian Fault (NAF)*

The North Anatolian Fault (Figure 4.11) extends in the east-west direction for over 1600 km across Turkey extending from Bingöl-Karlıova in the east to the Northern Aegean in the west. It is one of the world's major fast-moving continents. The Anatolia block moves west about 24 mm/year relative to the Asian plate to the north. It is a morphologically distinct and seismically right-lateral strike-slip fault. (Barka and Reilinger, 1997).

- East Anatolian Fault (EAF)

The East Anatolian Fault (Figure 4.11) is an active left-lateral strike-slip fault which extends from Antakya on the south to Bingöl-Karlıova on the east. It is a fault zone which is about 2-3 km wide in most places, and links into the Dead Sea Fault System.

- Western Turkey Graben Complex

This is an area of intense seismic activity which is related to the east-west trending graben complexes in the Aegean region (Figure 4.11).
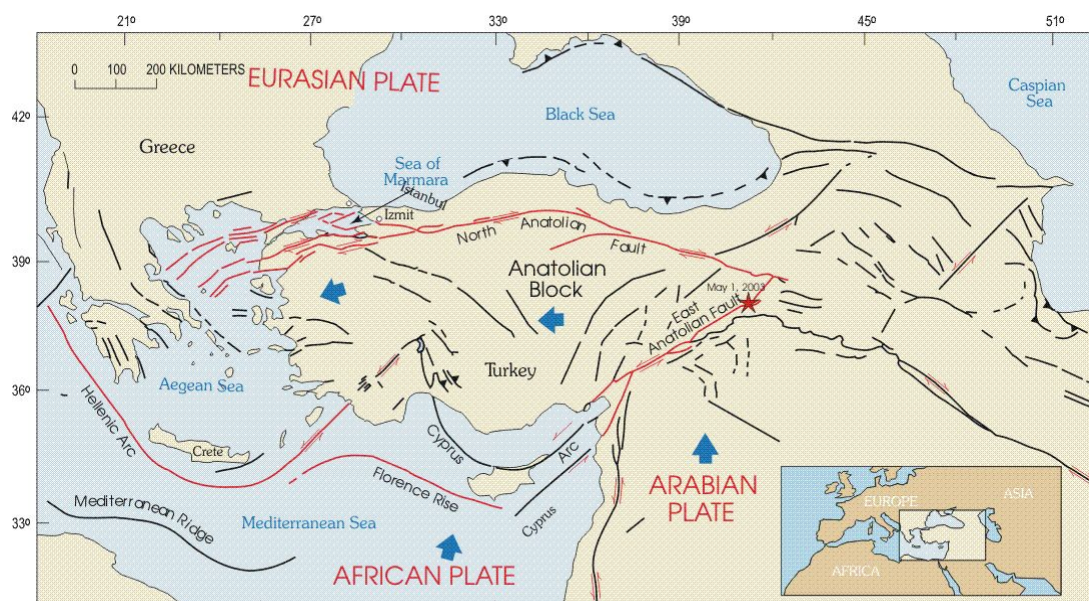
Figure 4.11 The tectonic map of Turkey. Adapted from http://neic.usgs.gov/neis 2003/eq_030501/neic_tgac_maps.html

4.3.2 Seismological Features of the Earthquakes and their Ground Motions

The strong ground motions regarding the three major earthquakes were recorded by the stations of the Turkish National Strong-motion Network that are operated by the Engineering Research Department of General Directorate of Disaster Affairs. The processed data and seismological features of the motions have been obtained from the METU strong motion repository (Tübitak, 2009) which is

the first systematic compilation and uniform processing on strong motion data recorded by the Turkish national strong motion network with detailed geophysical and geotechnical site measurements for all stations. The station information and important seismological features of the ground motion data are summarized in Table 4.3.

Table 4.3 Seismological features of the ground motions

Earthquake	March 13,1992 *Erzincan*	November 12, 1999 *Düzce*	May 1, 2003 *Bingöl*
Station Location	Meteorology Building, *Erzincan*	MPWR Building *Bolu*	MPWR Building, *Bingöl*
Epicenter Latitude	39.716	40.806	38.999
Epicenter Longitude	39.629	31.187	40.463
Station Latitude	39.752	40.746	38.897
Station Longitude	39.487	31.607	40.503
Depth (km)	22.6	10.4	10.0
R_{jb} (km)	3.3	8.0	2.2
Fault Type	Strike-slip	Strike-slip	Strike-slip
M (HRV)	6.6	7.1	6.3
Soil Type (*Kalkan and Gülkan.2004*)	Soil	Soil	Stiff Soil
Longitudinal PGA (g)	0.413	0.754	0.556
Transverse PGA (g)	0.480	0.821	0.282
Longitudinal PGV(cm/s)	108	56.6	34.5
Transverse PGV(cm/s)	78.2	66.9	21.9
Longitudinal PGD (cm)	34.4	25.2	10.2
Transverse PGD (cm)	29.5	12.8	5.1

M: Moment magnitude, HRV: Harvard Centroid Moment Tensor, R_{jb}: Joyner-Boore distance

4.3.3   The March 13th, 1992 Erzincan Earthquake

The city of Erzincan was struck by the M6.6 (HRV) earthquake on March 13th, 1992 at local time 17:18:39.40. Its epicenter was located at 39.72° North,

39.63° East with a focal depth of 22.6 km (ISC-International Seismological Centre). The strong motion considered here was recorded at the Meteorology Station Building that is located at 12.8 km west of the epicenter. Maximum ground acceleration of 0.48g and a maximum ground velocity of 108.4 cm/s in the horizontal direction were recorded at this station.

4.3.3.1 Seismological Background of Erzincan City

The Erzincan area is one of the most seismically active regions of Turkey. Erzincan city was devastated by a catastrophic earthquake (M8.0) that occurred in 1939 and resulted in a death toll of 32,000 people. This earthquake caused a surface break that extended from the Erzincan basin westward for a distance of 350 km, the right-lateral displacement reaching 3.7m in places (Barka et al. 1987). After this earthquake, Erzincan was relocated a few kilometers north of its old location (Akıncı et. al., 2001), physically closer to the fault line.

Although the 1992 earthquake was not as destructive as the 1939 event, 653 people died and it also caused much damage in the city and rural settlements close to the epicentral region.
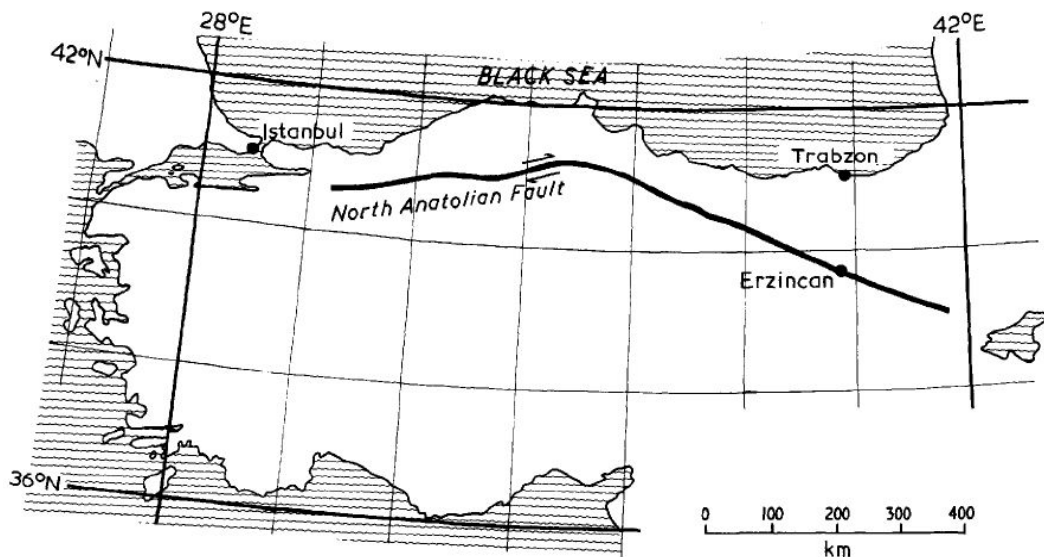
Figure 4.12 Location of Erzincan with respect to the North Anatolian Fault (NAF) (adapted from Hencher and Acar, 1995)
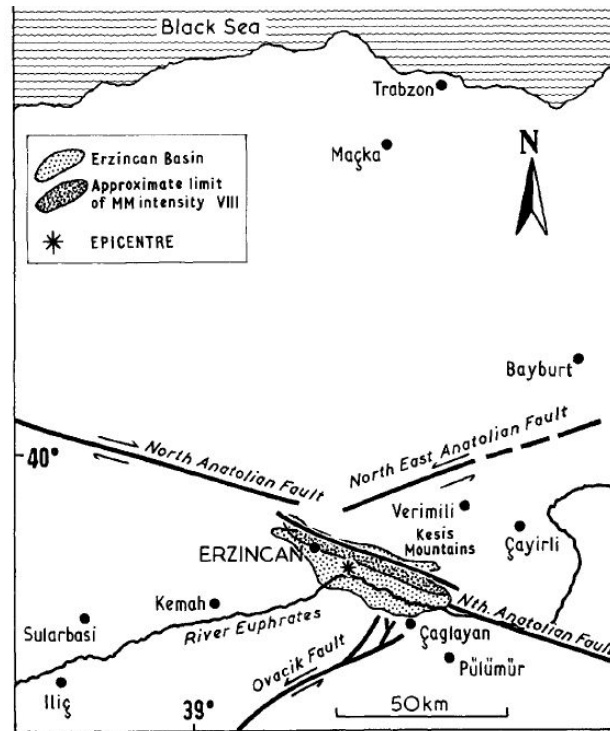
Figure 4.13 Erzincan basin, major faults and location of the earthquake epicenter (adapted from Hencher and Acar, 1995)

4.3.3.2 *Site Conditions of Erzincan City*

The Erzincan basin, with dimensions 50 km by 15 km (Barka and Gülen, 1989) is the largest part of the NAF (Figure 4.12). It is also located between three conjugate fault segments (Figure 4.13) that are one of right lateral strike-slip motion (the NAF), two of left-lateral strike-slip motion the Ovacık Fault and the Northeast Anatolian Fault (Akıncı et al., 2001). Erzincan is located towards the northern edge of the alluvial plain of the River Euphrates. The basin is infilled with hundreds of meters of sediments and surrounded by the mountains which rise to more than 3000 m. to the north and south (Hencher and Acar, 1995).

4.3.3.3 *Local Site Conditions of the Record Station and the MPWR Building in Erzincan*

The building was located at 2.3 km east of the record station and was constructed on "Soil" (Kalkan and Gülkan 2004) that is similar to that of the station.

66

4.3.4 The November 12th, 1999 Düzce Earthquake

In 1999, two destructive earthquakes with magnitudes larger than 7.0 occurred on the western part of NAF zone. These two earthquakes were among the largest seismic events that have occurred in the eastern Mediterranean Basin during the last 100 year (Akkar and Gülkan, 2002). They are also considered to be part of a westward migrating earthquake sequence that formed following the 1939 Erzincan earthquake (Akyüz et al., 2002)

The first one was the August 17th, 1999 Marmara earthquake that struck the Kocaeli and Sakarya provinces in the northwestern Turkey. This earthquake had a magnitude of M7.6 (HRV) and its epicenter was located at 40.7 North and 29.99 East at about 10 km east of the town of Gölcük with a focal depth of 15 km.

The November 12th, 1999 Düzce earthquake (M7.1) occurred three months later than the Marmara earthquake. The epicenter of this earthquake was located at 40.79 North and 31.11 East with a focal depth of 10.4 km near the city of Düzce. The strong motion considered here was recorded at about 36 km east of the epicenter. Maximum ground acceleration of 0.82g and a maximum ground velocity of 66 cm/s in the horizontal direction were recorded at this station. One significant feature of this record is that contains strong pulse fling which is a characteristic of near-field ground motion (Akkar and Gülkan, 2002).

Figure 4.14 Offset (4.5m) garden fences around Çınarlı village (Akyüz et al., 2002)

After the earthquake a 40 km-long surface break was observed along the east-west Düzce fault and the maximum right-lateral surface offset was about 5m (Akyüz et al., 2002). A 4.5 m offset measured around the village of Çınarlı is shown in Figure 4.14.

4.3.4.1 Seismological Background of the Vicinity of Bolu City

Between 1939 and 1967 six large earthquakes occurred along the NAF zone in a westward migrating sequence from Erzincan to the western end of Mudurnu Valley (Figure 4.15). These are 1939 Erzincan ($M_s7.8$), 1942 Erbaa-Niksar ($M_s7.1$), 1943 Tosya ($M_s7.3$), 1944 Bolu-Gerede ($M_s7.3$), 1957 Bolu-Abant ($M_s7.0$), and 1967 Mudurnu Valley ($M_s7.1$), earthquakes. The last three earthquakes were along the southern branch of the Anatolian Fault Zone that occurred in Düzce-Bolu area.
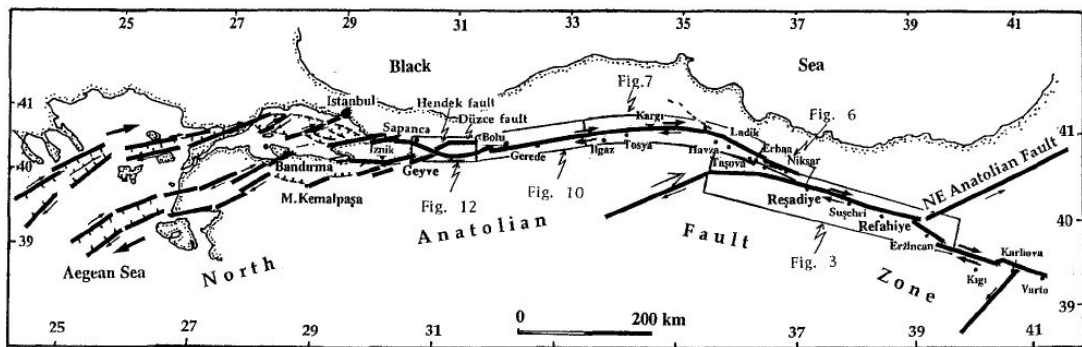
Figure 4.15 Location of the major earthquakes on the NAF zone that occurred between 1939 and 1967 (Barka, 1996)

During the February 1, 1944 Bolu-Gerede ($M_s7.3$) earthquake 9422 buildings collapsed, 8206 buildings suffered severed damage, 2552 people died and 1182 people were injured. Three aftershocks (Ambraseys et al., 1968) with magnitudes larger than M_s5 occurred following this main shock. Those aftershocks were February 15th, 1944 Düzce ($M_s5.8$), March 11th, Gerede ($M_s5.8$) and April 5th, Mudurnu ($M_s5.6$) earthquakes. In those aftershocks, 3000 house collapsed, more than 6000 houses suffered low to severe damage and more than 800 people died. Three years later, the May 26th, 1957 ($M_s7.0$) Abant earthquake caused severe

damage in more than 5000 houses, a death toll of 52 people and injury of 101 people. The July 22nd, 1967 Mudurnu Valley earthquake (M_s7.1) or so-called Adapazarı earthquake caused 13000 houses damage from low to severe damage. 89 people died and 235 people were injured (Özmen B., 2000)

4.3.4.2 Site Conditions of Düzce and Bolu Cities

Düzce and Bolu basins are mainly formed of alluvial soils. Results of the investigations through drilled boreholes indicated that soil conditions consisted principally of silts and clays with inter-beds of sands and gravels No liquefaction was observed during the field surveys and it was observed that many building had basements and that many open excavations were not filled with water which indicates that the ground water table must be at least 3 m deep. This may be the reason of the absence of liquefaction during this earthquake (Rathje et al., 2006).

4.3.4.3 Local Site Conditions of the Record Station and the MPWR Building in Bolu

Soil at the surface was silt-clay. The recording station was on the softest, deepest sediments in the Bolu valley. The soil type was classified as "Soil" according to Kalkan and Gülkan (2004). As a separate note, the recording station and so the building were situated in a localized pocket of the worst damage in Bolu (Akkar and Gülkan 2002).

4.3.5 The May 1st, 2003 Bingöl Earthquake

The city of Bingöl was shaken by a M6.3 (HRV) earthquake on May 1st, 2003 at local time 03:27 am. The epicenter of the earthquake was located at 38.94° North, 40.51° East with a focal depth of 6 km. The strong motion considered here was recorded at one-story building adjacent to the MPWR building that is located at 11.8 km south of the epicenter. Maximum ground acceleration of 0.56g and a maximum ground velocity of 34.5 cm/s in the horizontal direction were recorded at this station.

4.3.5.1 Seismological Background of Bingöl

Bingöl area is located within the Bingöl-Karlıova-Erzincan triangle where two major strike-slip faults, NAF and EAF, intersect. There are also a number of conjugate active faults causing destructive earthquakes in this region. The 1784 Yedisu and 1866 Göynük-Karlıova earthquakes were the most devastating earthquakes that occurred in Bingöl area (Ambraseys, 1988). The most recent earthquake that occurred after these earthquakes was May 22nd, 1971 earthquake with magnitude M6.8 resulted in a death toll of 875. Almost 9000 units suffered medium to severe damage during this earthquake (Özcebe et al., 2004)
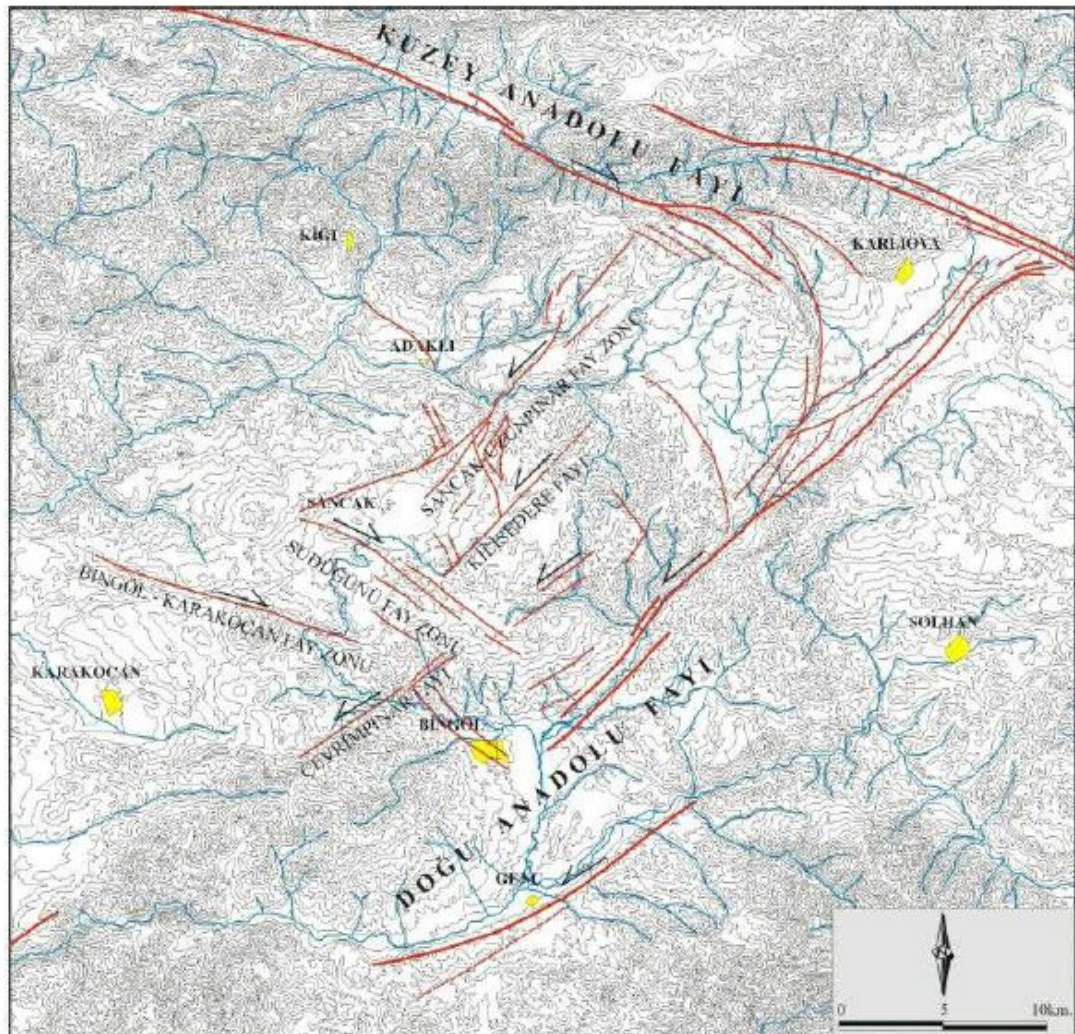
Figure 4.16 The active faults in the vicinity of Bingöl (Emre et. al, 2003)

4.3.5.2 Site Conditions of Bingöl City

Bingöl is surrounded by volcanic formations and most of the city is built on top of an alluvial deposit. The south part of Bingöl is built on a terrace at the same elevation as the north. In this terrace most of the subsurface materials are similar to those in the north. On the south-west, the buildings are founded on moderately weathered bedrock or on stiff, colluvial deposits, which locally can be several meters thick. The colluvial deposits can be classified as clay, brown stiff clay, with variable percentages of sand or gravel which many cases can be described as sandy or gravelly clay (Bobet and Çetin, 2004)

4.3.5.3 Local Site Conditions of the Record Station and the MPWR Building in Bingöl

The recording station was placed in the one–story building that is adjacent to the MPWR building. The station and the building were located in the north of the city on an estimated 5 m high alluvial terrace between on two streams (Bobet and Çetin, 2004). The terrace material is dense formations composed of predominantly uniform granular alluvial deposits. The soil type was classified as "stiff soil" by Kalkan and Gülkan (2004).

4.4 STRUCTURAL DAMAGE

Following the earthquakes, each building was examined thoroughly, and in accordance with ministerial procedures, reports (MPWR 1993, 2004) were prepared to indicate the usability and facility of the buildings. The building in Bolu sustained severe damage that was judged to represent a "life safety" performance level while those in Erzincan and Bingöl sustained lighter damage levels corresponding to "immediate occupancy" and "immediate occupancy-life safety" levels, respectively. In terms of occupancy, the Erzincan building was judged to have performed best of all, thus it was populated immediately following the earthquake in 1992, and served as a prime public service facility for citizens who had lost their homes or had

damages in them. On the other hand, the building in Bolu has since been demolished following a protracted court ruling because it was initially judged as unsafe for occupancy. The dispute with the contractor was probably meaningless because no construction flaws as such existed.

In the following sections, a general description of damage in vicinity of the MPWR buildings and detailed structural damage to them will be given. Damage to be described here is based on the observations made by the author, by Çağnan (2001), by Bayülke (1993) and the engineers of MPWR (2004). The damage will be rated using the following descriptions of ASCE/SEI-41 (2007) and Gür et. al, (2009):

Columns and Beams:

    - *Light Damage*: Minor hairline cracking. No crushing

    - *Moderate Damage*: Shear and/or flexural cracks on beams. Spalling of concrete cover and shear cracking in columns

    - *Severe Damage*: Extensive cracking and hinge formation in the elements, concrete crushing and failure of captive columns

Infill Walls:

    - *Llight Damage*: Hairline cracks in plaster and perimeter

    - *Moderate Damage*: Extensive cracking, some crushing but wall remains in place

    - *Severe Damage*: Extensive cracking and crushing; loss of crushing portions

4.4.1 Damage in Vicinity of the MPWR Building in Erzincan

The March 13th, 1992 (M6.6) earthquake was the most devastating earthquake that occurred after the 1939 earthquake (M8.0) in Erzincan. 7007 units sustained heavy damage or collapsed. 9227 units sustained moderate damage that was judged as repairable and 15042 units sustained light damage (Çelebi, 1993). Many RC frame buildings with more than four stories were severely damaged

(Gülkan, 1992) where the masonry structures and 1-2 story RC buildings sustained almost no damage. Those severely damaged structures included many municipals such as schools, public housing and hospitals (Bayülke, 1993).

The building stock in Erzincan prior to the 1992 earthquake consisted of (i) one-story brick masonry with RC tie-beams and ceilings, (ii) two-story RC frame buildings with infill walls, (iii) three-story RC frames with infill walls and RC shear walls and (iv) four-story RC tunnel formed shear wall buildings. The reasons causing damage in those structures are stated below (Bayülke, 1993);

- *Use of low-quality concrete*: In those years the highest quality concrete used in the structures had a maximum compressive strength of 7-8 MPa.
- *Lack of seismic design calculation*: Although 1975 seismic code was introduced, still only gravity load was being considered in design calculations due to old habits.
- *Lack of control mechanism*

As a note; the structures that were built prior to 1960 and buildings that were designed according to the Turkish Seismic Code of 1975 sustained less damage than the structures that were built between the years 1960-1975 and private buildings that were built later than 1975 (Bayülke, 1993).

4.4.2 Damage to the MPWR Building in Erzincan

The main building in Erzincan continued to serve the public immediately after the 1992 earthquake. There was light damage in the building, thus, it was judged to be in the "immediate occupancy" level. After the earthquake, minor cracks that occurred in the building were repaired and covered with plaster. No detailed investigation was needed to be done by the engineers of MPWR until the identical MPWR building in Bingöl suffered more severe damage during the 2003 Bingöl earthquake. As the damage in the Bingöl building after the 2003 earthquake was more severe than that of Erzincan, it was decided to prepare a retrofit project for the Bingöl building in 2003. Following this, the officials of MPWR in Erzincan

agreed to make a technical investigation on the Erzincan building since it is located in an earthquake region with active faults. At the end of the investigation it was concluded that

- Both buildings had the same design project and as-built properties
- The average compressive strength of concrete measured from the tests was the same for both buildings

Thus, it was decided to apply the same retrofit project to the Erzincan building with a few additional applications (MPWR, 2004).

Damage in the Erzincan building consisted of minor hairline cracks in the ground and first story L-shaped corner columns. Hairline cracks in the ground and first story beams were observed. Minor shear cracks were noticed in first story masonry infill walls. In upper stories hairline cracks in the beams and infill walls and L-shaped corner columns at the window level were observed. The most significant damage that occurred in the Erzincan building was the minor shear cracks observed in the first story captive column-C14. Thus, different from the Bingöl building, an additional retrofit was conducted for the column-C14 in the Erzincan building as shown in Figs. 4.17 and 4.18.
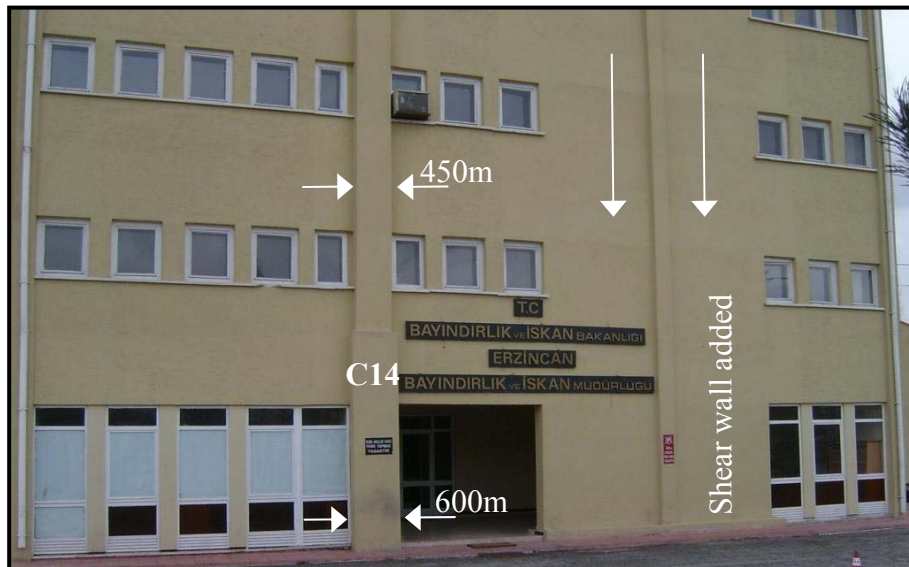
Figure 4.17 The front view of the Erzincan building after the retrofit. Shear walls added at the exterior frame. Jacketed column-C14 at the ground and upper floors; the initial width of the column was 300 mm.
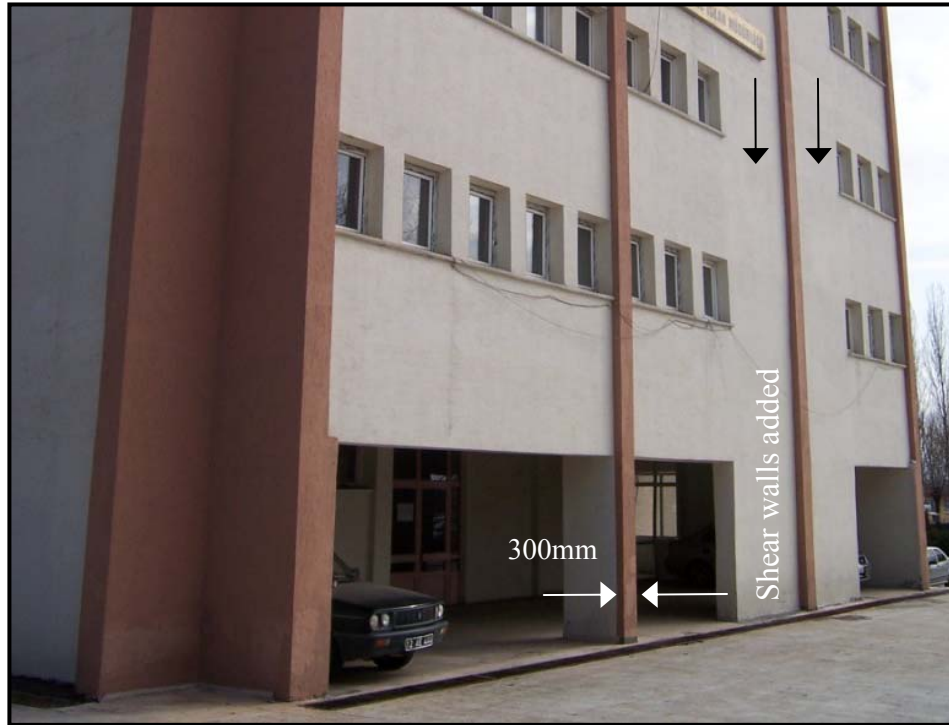
Figure 4.18 The front view of the Bingöl building after the retrofit. Shear walls added in the exterior frame.

4.4.3 Damage in Vicinity of the MPWR Building in Bolu

In the 1999 Düzce earthquake 26704 buildings suffered severe damage, 37825 sustained moderate damage and 40944 structures suffered light damage (Özmen and Bağcı, 2000). The buildings in Düzce consisted of 4-5 story RC buildings and 2-3 story buildings of timber construction with brick infill walls. Many of these buildings had already been damaged during the 1999 Marmara earthquake. Mid-rise buildings, typically 4-5 stories tall, sustained greater damage compared to low-rise buildings. This could be related to the construction standards of the 1970s and sediment amplification of intermediate-to-long period ground motions; however, recorded ground motions indicate that large spectral accelerations in the T=0.4-0.8 range tend to match the period of those kind of structures (Rathje et al. 2006).

4.4.4 Damage to the MPWR Building in Bolu

After the Düzce earthquake, a careful recording of the damage distribution was performed for the building in Bolu. The structural and nonstructural damage was concentrated in the bottom three stories. Damage in the upper two stories consisted of cracking in partition walls and nonstructural damage.

The front, rear and lateral views of the building after the earthquake are shown in Figs. 4.19-4.21. In these figures, damage to the exterior frames of the building is depicted. The damage consisted of:

- Shear failures in infill walls

- Shear failure in captive columns

- Shear cracks in the columns

- Cracking and collapse of roof supporting infill walls at the roof

- Structural damage due to impact

Figure 4.19 (a) Front view of the Bolu building: Shear failures in masonry infills between the narrow windows

Figure 4.20 Rear view of the Bolu building: Infill failures at the bottom three stories and shear failures of the captive columns at the ground and first story

Figure 4.21 Lateral views from the Bolu building: Damage in infill walls, shear cracks in the ground story column-C16 and first story column-C12

4.4.4.1 Seismic Joint and Foundation

The building had been initially separated with the adjacent structures by a 50 mm seismic joint. However, it was evident that an impact had occurred with the adjacent building during the earthquake due to insufficient separation provided by the seismic joints. After the earthquake, column-C1 at the ground floor was in close contact with the adjacent building and the gap was closed at the bottom (Figure 4.22).

(a)   (b)
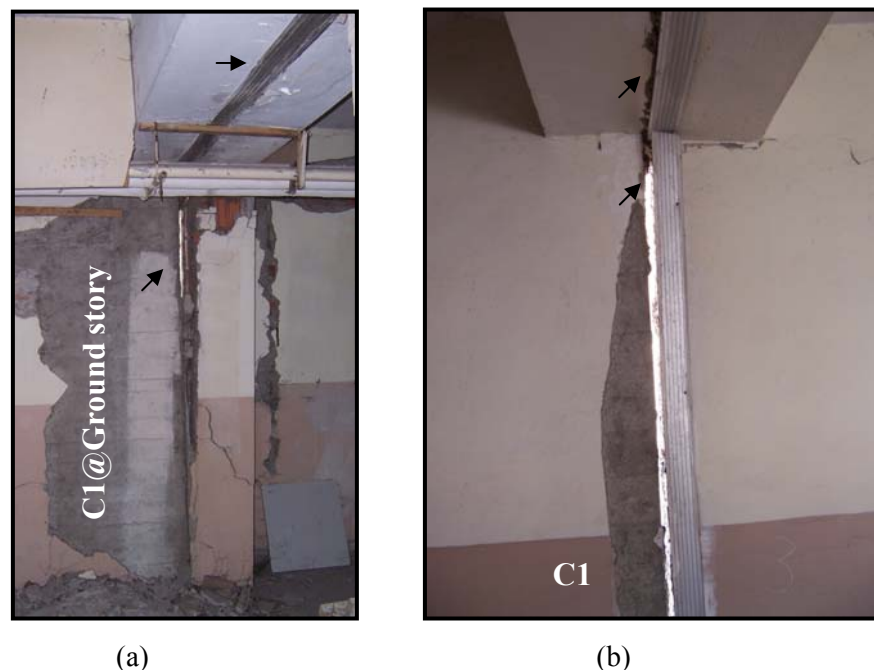
Figure 4.22 Seismic joints between the case-study building and ground-plus-three story building at the (a) ground and (b) third floor levels in Bolu

The foundation system performed well that there was no evidence for failure of substructure or the supporting soil.

4.4.4.2 Columns

At the ground floor, column damage consisted essentially of shear cracks (Figs.4.23-4.33). Most of the columns sustained shear damage due to insufficient lateral reinforcement.

Figure 4.23 Shear cracks in the ground story column-C5 (Bolu)

Figure 4.24 Shear cracks in the ground story column-C6 (Bolu)
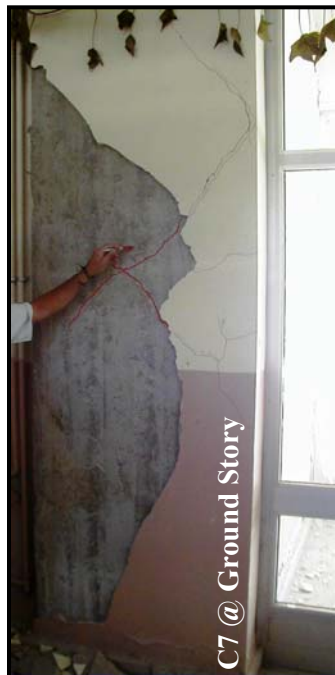
Figure 4.25 Shear cracks in the ground story column-C7 (Bolu)

Figure 4.26 Shear cracks in the ground story column-C8 (Bolu)

Figure 4.27 Shear cracks in the ground story column-C9 (Bolu)
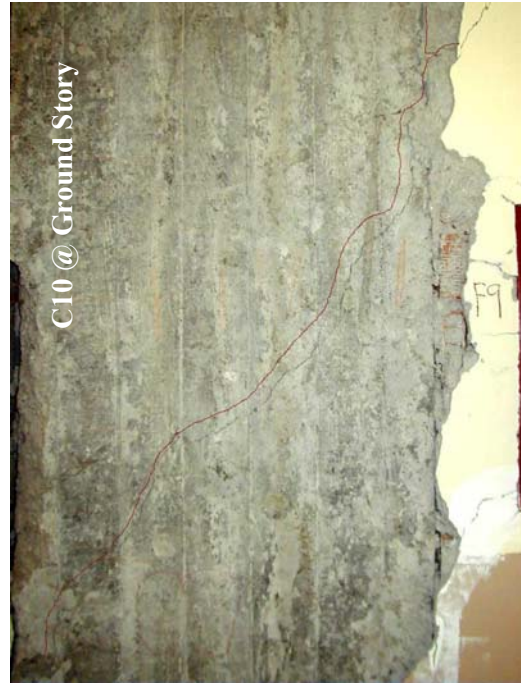
Figure 4.28 Shear cracks in the ground story column-C10 (Bolu)

Figure 4.29 Shear cracks in the ground story column-C13 (Bolu)

Figure 4.30 Shear cracks in the ground story column-C15 (Bolu)

Figure 4.31 Shear cracks in the ground story column-C16 (Bolu)

Figs. 4.32 and 4.33 show damaged C3-column due to captive column condition. The clear height of the column is reduced with the narrow windows and this caused an increase in shear demand that the column could not resist.

Figure 4.32 Damage to the ground story captive column-C3 (outside view)

Figure 4.33 Damage to the ground story captive column-C3 (inside view)

Damage in the first and second story was also extensive but number of damaged elements was less than that of the ground story. Figs. 4.34 and 4.35 indicate shear cracks in the first story L-shaped corner column-C4 and first story column-C6.

Figure 4.34 Shear cracks in the first story L-shaped corner column–C4 (Bolu)

Figure 4.35 Shear cracks in the first floor column-C6 (Bolu)

Figs 4.36 and 4.37 indicate extensive shear damage in the first story captive column-C12 and first story captive column-C3.

Figure 4.36 Shear cracks in the first story column–C12 (Bolu)

| (a) | (b) |

Figure 4.37 Damage to the first story captive column-C3 (a) inside and (b) outside view (Bolu)

In the second story columns, damage was lighter than that of the first story. It consisted of shear (Figure 4.38) or combined flexural and shear cracks (Figs. 4.39 and 4.40).

Figure 4.38 Shear cracks in the second story column-C11 (Bolu)

Figure 4.39 Shear and flexural cracks in the second story column-C12 (Bolu)

Figure 4.40 Shear and flexural cracks in the second story L-shaped corner column-C16

Overall detailing of the columns was insufficient to achieve a ductile behavior for the following reasons: (i) inadequate stirrup spacing, (ii) insufficient transverse reinforcement area (iii) non-existing confinement zones (iv) 90° hooks of the horizontal hoops and probably poor workmanship. These were observed through shear damage in captive columns and incipient shear cracking in bottom three story columns.

4.4.4.3   Beams

Beams in the bottom three floors suffered flexural cracking in different intensities (Hairline cracks-extensive flexural cracks). Damage was the most severe in the ground floor beams (Figs. 4.41-4.44) and they were judged to be in a performance level between "immediate occupancy" and "life-safety". Spalling of concrete was rarely noticed.

Figure 4.41 Flexural cracks in the ground floor beam-B8 (Bolu)

Figure 4.42 Flexural cracks in the ground floor beam-B12 (Bolu)
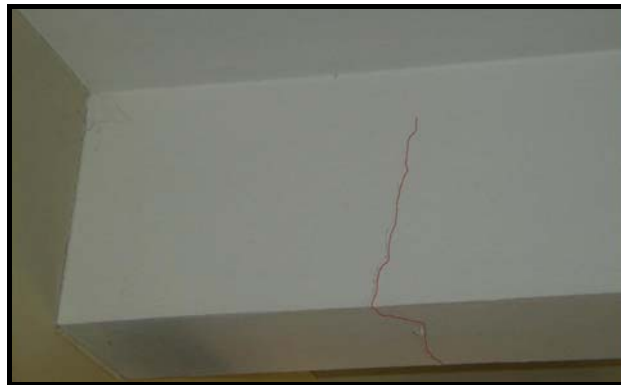
Figure 4.43 Flexural crack in the ground floor beam-B18 (Bolu)
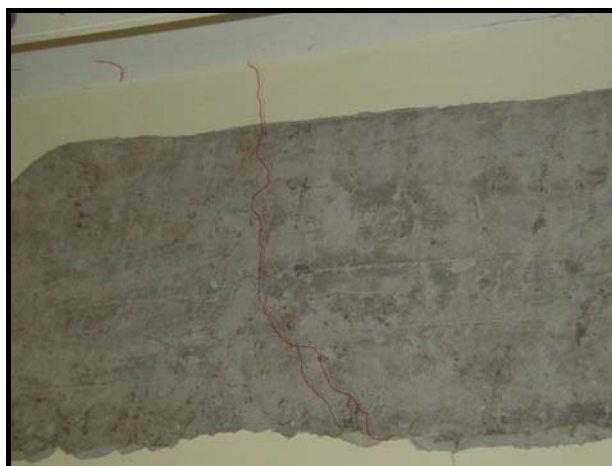
Figure 4.44 Flexural crack in the ground floor beam B24 (Bolu)

4.4.4.4 Beam-Column Connections

Although no transverse reinforcement was used, no distress was observed in the interior and exterior beam-column joints (Figs. 4.45-4.50). Critical shear stress might have not been reached.

Figure 4.45 Interior joint between the ground story column-C6 and beams B7-B8-B17-B18 (Bolu)

Figure 4.46 Interior joint between the ground story column-C7 and beams B8-B9-B20-B21 (Bolu)

Figure 4.47 Exterior joint between the ground story column-C12 and beams B6-B22-B23 (Bolu)

Figure 4.48 Corner joint between the ground story L-shaped column-C13 and beams B1-B13 (Bolu)

Figure 4.49 Exterior joint between the ground story column-C14 and beams B1-B2-B16 (Bolu)

Figure 4.50 Exterior joint between the ground story column-C15 and beams B2-B3-B19 (Bolu)

4.4.4.5 Masonry Infill Walls

Damage to the masonry infill partitions and architectural components was of particular concern. The collapse of those elements posed a serious hazard to the occupants. The masonry infill walls of the building were not intended to contribute to the lateral force resisting system of the building; however, they contributed to the system since a gap was not provided at the perimeter of these walls. Thus, the walls were able to resist lateral forces. Figs. 4.51-4.54 show infill wall damage at the ground and first story of the Bolu building.

Figure 4.51 Severe damage to the infill wall between the ground floor columns-C6 and C10 (Bolu)

Figure 4.52 Severe damage to the infill wall between the first floor columns-C12 and C16 (Bolu)

Figure 4.53 Severe damage to the infill wall between the first floor columns-C11 and C15 (Bolu)

Figure 4.54 Severe damage to the infill wall in the first story (Bolu)

4.4.4.6 *Nonstructural Damage*

Nonstructural damage in the portions of bottom three stories was significant; partial or complete collapse was observed in the partitions, ceiling panels, lighting fixtures, heating, ventilation, air-conditions equipment and windows (Figs 4.55 and 4.56)

Figure 4.55 Nonstructural damage: The broken windows (Bolu)

Figure 4.56 Nonstructural damage to the heating system and partition walls (Bolu)

4.4.4.7 Damage in the Upper Stories

Structural damage observed in the upper two stories was relatively minor. Nonstructural damage was noticeable in these stories. Crackings in the plaster were observed. The damage in the roof consisted of cracking and collapse of the support walls (Figure 4.57). The fallen parts posed threat to the safety of the people outside the building.

Figure 4.57 Damage to the roofs of the main and the adjacent building (Bolu)

4.4.4.8 Deficiencies Observed in the Construction

Poor workmanship was noted considering the damage to the ground story column-C3 (Figure 4.58) and first story column-C4 (Figure 4.59). Transverse and longitudinal bars were improperly placed in those columns during the construction.

Figure 4.58 Disengagement of ties (Bolu)

Figure 4.59 Longitudinal reinforcement in the first story L-shaped corner column-C4

4.4.5 Damage in Vicinity of the MPWR Building in Bingöl

5-6 story RC buildings, timber framed structures with adobe infills and unreinforced masonry buildings were the typical structure types in the city after the 2003 earthquake. The structures, which suffered significant damage, were the governmental buildings such as schools, dormitories and office buildings. 15 total collapses occurred and the number of buildings to be repaired was in the range of 3000 (Gülkan, 2004). One tragic consequence of this event was the death of 84 students and a teacher as a result of the collapse of a dormitory block (Doğangün, 2004). This collapse triggered an intensive program of school safety (Gülkan, 2004).

4.4.6 Damage to the MPWR Building in Bingöl

The building in Bingöl sustained moderate damage that corresponds to a level between "immediate occupancy-life safety" after the earthquake (Figure 4.60).

Figure 4.60 Side views of the MPWR building in Bingöl after the 2003 earthquake (a) the case study building, (b) the case study building and the adjacent four-story facility

The structural and nonstructural damage was concentrated in the ground and first stories. There was almost no structural damage in the upper stories except for the masonry infill supports at the roof.

Similar to the Erzincan and Bolu buildings, the Bingöl building had been initially separated from the ground-plus-three story adjacent building by a 50 mm seismic joint. However, it was evident that pounding had occurred between the mid-rise facility and the case-study building (Figure 4.61).

Figure 4.61 Impact was observed at the roof with the adjacent mid-rise building (Bingöl)

Similar to the other MPWR buildings the foundation system of the Bingöl building performed well and there was no evidence for the failure of footing and supporting soil.

4.4.6.1 Columns

Damage to the columns consisted of hairline shear cracks. Damage was concentrated in the exterior frame of the ground floor. The most significant shear crack occurred in the ground story captive column-C3. Figure 4.62 shows extensive crack in the column-C3 and shear failure of infill walls between the narrow windows.
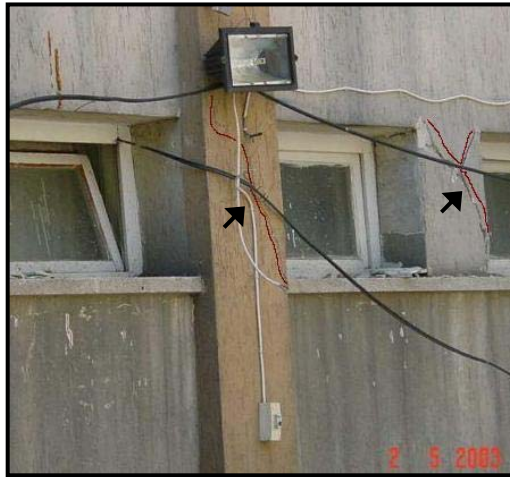
Figure 4.62 Damage to the ground story captive column-C3 and infill wall between the windows (Bingöl)

Another significant damage occurred in the ground story column-C12 (Figure 4.63) and L-shaped corner column-C16 (Figure 4.64). The column-C12 was adjacent to the one-story facility building at the ground floor and a partial spalling of concrete cover was observed at its contact surface with the adjacent structure.
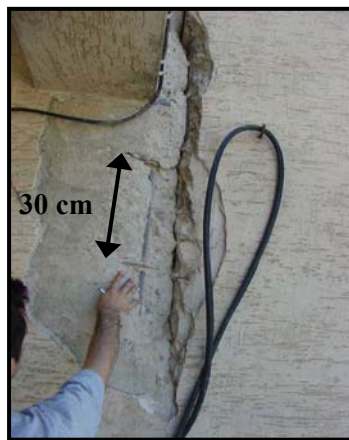
Figure 4.63 Damage to the ground floor column-C12 and sparsely spaced ties

Figure 4.64 Extensive shear crack in the ground floor L-shaped column-C16

4.4.6.2 Beams

Beams in the ground and first floors suffered minor flexural cracking (Figure 4.65). Spalling of concrete cover was rarely noticed. No distress was observed in the beam-column joints.

Figure 4.65 Light damage to the beams (Bingöl)

4.4.6.3 Masonry Infill Walls and Nonstructural Damage

Nonstructural damage consisted of cracking in masonry infills and broken windows of the ground floor (Figure 4.66)

Figure 4.66 Structural damage to the ground story infill wall and broken windows (Bingöl)

4.4.6.4 Deficiencies Observed in the Construction

The existence of inadequate lateral reinforcement was observed in the ground story column-C12 (Figure 4.63). Distance between the transverse bars was measured as 30 cm, even more than what it should be in design (20 cm). The transverse reinforcement which consisted of $\Phi 8$ ties spaced at 30 cm intervals was insufficient in the existence of columns with 30 and/or 40 cm width.

Similar to the Bolu building, poor workmanship was noticed in the Bingöl building. Figure 4.67 indicates the disengagement of reinforcement bars in columns.

Figure 4.67 Disengagement of reinforcement bars in the columns (Bingöl)

4.5   CONCLUDING REMARKS

The three identical MPWR buildings that will be analyzed in the next chapter have been introduced. First, detailed description of the buildings was provided. Second, seismological features of the earthquakes and their ground motions were described. Lastly, structural damage to the buildings was depicted.

The building is an older type structure lacking adequate transverse reinforcement especially in confinement zones and beam-column joints. Use of smooth bars with low yield strength is typical at that era. The drawbacks regarding the buildings are the captive columns, use of hand made concrete and poor workmanship. The low compressive concrete strength measured in the Erzincan and Bingöl buildings are not surprising but the higher value obtained from the Bolu building is an unexpected event. Despite having these drawbacks, the building is a well designed structure in Turkish circumstances of 1970s and 1980s.

The strong ground motions were all near-field records that in every single case, the closest distance from the recording site to the surface projection of the fault rupture was less than 10 km. Since the recording stations were in one-story buildings adjacent to the case-study buildings in Bolu and Bingöl, it was assumed that the input motions are known for these buildings. The input motion for the Erzincan building may be subject to speculation as it was recorded in a one-story building two km away from the building, however, the ground composition between the sites is very similar and no tall buildings existed in the vicinity of the recording station to modify the ground motions significantly.

The severity of structural damage to the buildings was in different intensities. The Bolu building sustained the most and the Erzincan building sustained the least severe damage. The most surprising was the minor damage to the Erzincan building. The Erzincan and Bingöl buildings were assumed to be the same related to their same material properties and the Erzincan ground motion was considered to be the most severe demand a near-source ground motion imposes on structural frames since it contains a large acceleration pulse that may increase the ground story drift demands (Akkar and Gülkan, 2002). However, damage to the Bingöl building was between light and moderate. This will be discussed in the next chapter.

CHAPTER 5

SEISMIC RESPONSE ANALYSES

5.1   INTRODUCTION

In this chapter, the dynamic properties and responses of the three MPWR buildings are examined thoroughly. 3D nonlinear time history analyses (NTHA) are conducted under bi-directional ground motion excitations. The analytical instrument employed for the 3D nonlinear studies including all structural member-level characterizations is Perform 3D (Ram International, 2005).

In the following sections, modeling of the buildings is described first. Second, the eigenvalue analyses are performed to determine the modal properties of the buildings. Finally, once the NTHA of the buildings are conducted, their calculated response indicators are compared with the observed damage after the earthquakes.

5.2   SOFTWARE FEATURES

Perform3D is a structural analysis program with its origin dating to Drain-3DX developed at UC Berkeley in the 1990s (Powell and Campbell., 1994). It enables both linear and nonlinear analysis of 3D frame and wall buildings subjected to both static and dynamic loadings. Hence, the user can develop both linear and nonlinear force-deformation relationships to represent component behavior. One of the key features included in this program is the nonlinear force-deformation relationship that can be assigned to fiber sections, moment-rotation and curvature

relationships and plastic hinge properties. Definition of nonlinear behavior is performed by means of a generic trilinear backbone curve where strength loss is optional. Users can also employ available bilinear and elastic-perfectly-plastic relationships already included in the software with proper modifications.

Fiber beam and column elements are the powerful features of the program that allow modeling both 2D and 3D elements including N-M and N-M-M interactions. Each element is divided into segments and fiber cross-sections are defined at the center of each segment where its behavior is monitored. Nonlinear stress-strain relationship of concrete or steel material is assigned to each fiber. Thus, the element model within its length is distributed plasticity type accounting for the spread of inelastic behavior both over the cross sections and along the member length. Shear deformations of the elastic elements are included based on their specified shear modulus and effective shear area and nonlinear shear force-deformation relationship is modeled with rigid-plastic biaxial shear hinges.

Another feature of Perform 3D is that P-delta effects, which may be of concern under large deformations, can be considered if desired. For this purpose, a geometric stiffness matrix is added to the stiffness matrix of each element accounting for P-delta effects in resisting force computation. Geometric stiffness matrix is updated at each incremental time step throughout the analysis.

Both horizontal components of ground motions can be applied to 3D models simultaneously in arbitrary directions with respect to the orientation of the structural models. Any demand quantity regarding the analyses can be obtained such as forces, deformations, rotations, curvatures and strains.

5.3   ANALYTICAL MODELS OF THE MPWR BUILDINGS

In this section, the modeling aspects considered for 3D analytical models of the MPWR buildings are discussed. To set frame of the structures, beams, columns and struts were used. Since all of the three buildings studied here are identical in design, an analytical model with the same geometrical but different material

properties was used for all buildings. Figure 5.1 indicates front, side and 3D views of the analytical model.

<div align="center">(a)   (b)   (c)</div>
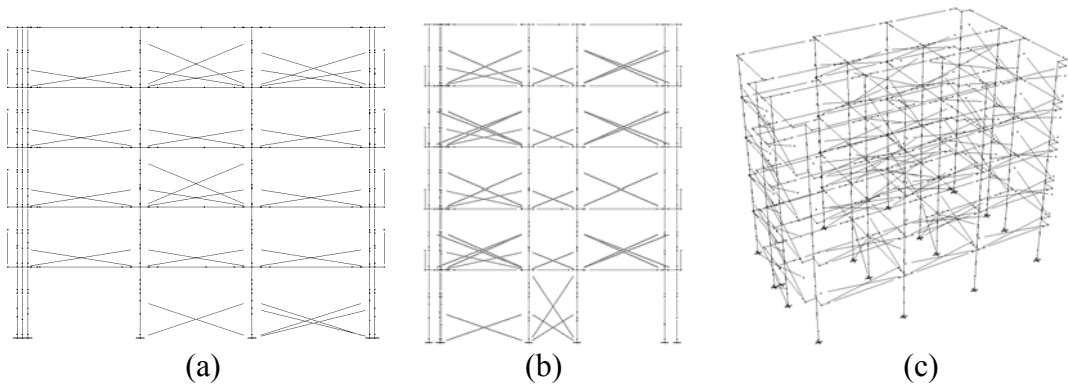
Figure 5.1 (a) Front elevation (b) Side elevation and (c) 3D views of the analytical models

The mass and mass moment of inertia of each story was calculated and assigned to the mass center of each floor. The horizontal floor diaphragms were rigid in their own plane and three DOFs; two-lateral and one-torsional DOF were introduced for horizontal displacements. The mass of each floor is the same with the exception of ground and top story levels. Except for the ground floor and roof, the mass of the remaining floors was assumed to be the same. Both mass and mass moment of inertia of each floor level are given in Table 5.1.

Table 5.1 The mass and mass moment of inertia of the floors

Floor	Mass (t)	Mass Moment of Inertia (t.m^2)
4	219	12300
1-2-3	332	19100
Ground	406	23000

The material properties assumed in the analytical modeling are the average values obtained from the sample tests and other investigations done by the MPWR engineers as discussed in the previous chapter. Following the geometrical

definition, assignment of material, section and mass properties, three-dimensional mode shapes and natural frequencies of the models were computed. Detailed information about modeling is given in the proceeding sections.

5.3.1 Modeling Beams and Columns

The beam members were introduced as elastic elements with reduced effective stiffness $(0.3E_cI_g)$ as per ASCE/SEI 41, Sup.1, 2008. Elastic-perfectly-plastic moment-curvature relationship was assigned at both ends of the beams. The values constituting that relationship for all beams are shown in Table 5.2.

Table 5.2 The properties of moment-curvature hinges defined at the end of the beams

Beam ID	0.3I (m^4)	My+ (kNm)	My- (kNm)	Ky+ (rad/m)	Ky- (rad/m)	Ku+ (rad/m)	Ku- (rad/m)
B1-B2-B3-B11-B12	0.024	93.7	229.0	2.77E-04	6.78E-04	1.75E-01	1.77E-01
B4-B5-B6-B7-B8-B9	0.006	51.1	112.0	5.97E-04	1.31E-03	3.08E-01	3.19E-01
B10	0.003	43.9	70.4	9.52E-04	1.53E-03	3.63E-01	3.71E-01
B13-B22	0.022	111.0	184.0	3.58E-04	5.93E-04	1.75E-01	1.76E-01
B14-B23	0.018	114.0	140.0	4.39E-04	5.39E-04	1.76E-01	1.76E-01
B15-B24	0.022	114.0	209.0	3.66E-04	6.71E-04	1.75E-01	1.76E-01
B16-B18-B19-B21	0.004	32.5	69.7	6.45E-04	1.38E-03	3.63E-01	3.19E-01
B17-B20	0.003	42.6	51.3	1.02E-03	1.23E-03	3.62E-01	3.77E-01

I: moment of inertia; My+: Positive yield moment; My-: Negative yield moment; Ky: yield curvature; Ku: Ultimate curvature

Table 5.3 The effective flange widths regarding the items (ii), (iii) and (iv)

| Beam Id | Effective flange width (m) | | |
| | (ii) | (iii) | (iv) |
	$8t_f$ (m)	$1/2*d_{(next web)}$ (m)	$l_n/5$ (m)
B1-B2-B3-B11-B12	1.20	2.85	*1.14*
B4-B5-B6-B7-B8-B9	1.20	1.10	*1.10*
B16-B18-B19-B21	1.20	2.85	*0.90*
B17-B20	1.20	2.85	*0.42*
B10	1.20	2.55	*1.14*
B14-B23	1.20	3.35	*0.44*
B13-B22	1.20	3.35	*0.90*
B15-B24	1.20	2.85	*0.90*

An effective flange width on each side of the web equal to the smallest of the following values was taken into consideration in calculating the inertia of beam elements: (i) the provided flange width (ii) eight times the flange thickness (iii) half the distance to the next web and (iv) one fifth of the span (ASCE/SEI-41, 2007). The values corresponding to items (ii), (iii), (iv) are shown in Table 5.3. The item (i) stands for precast/prestressed beams so it is not of concern here. The smallest values were obtained for item (iv).

Distributed plasticity was used through fiber analysis approach (Perform 3D, Ram International 2005) in order to simulate the nonlinear, biaxial flexure behavior of the columns. In addition, the columns were investigated for their shear capacities associated with shear and flexural-type failures for orthogonal directions. The shear capacities associated with flexural-type failure for the columns were calculated by assuming flexural hinges at the top and bottom of each element. The shear-type failure capacities were calculated based on the equation in ASCE/SEI-41 (2007).

$$V_n = V_s + V_c = k\frac{A_v f_y d}{s} + \lambda k \frac{0.5\sqrt{f_c^{'}}}{M/Vd}\sqrt{1 + \frac{P}{0.5\sqrt{f_c^{'}}A_g}}0.8A_g \qquad (5.1)$$

where A_v is the area of shear reinforcement within a distance s, f_y is the yield strength of reinforcement, d is the distance from extreme compression fiber to the centroid of longitudinal tension reinforcement, $f_c^{'}$ is the compressive strength of concrete and, λ is taken as 1.0 for normal weight concrete, k is assumed 0.7 in regions of high ductility demand, M/Vd is the largest ratio of moment to shear times effective depth under design loadings and shall not be taken greater than 4 nor less than 2, P is the axial compressive force and A_g is the gross sectional area of the column.

Experimental research indicates that flexural deformability may be reduced as co-existing shear forces increase. As flexural ductility demands increase, shear capacity decreases which may result in a shear failure before flexural deformation

capacities are reached (ASCE, 2008).When the flexural deformations increase, cracks open and strength of concrete in the plastic hinge zone degrades: the shear strength is reduced below the flexural strength and shear behavior dominates. Hence, shear capacities corresponding to the shear-type failure of the columns were calculated by Eq. 5.1 and compared with the shear demand associated with the flexural-type failure. The comparison for the ground story columns is given in Figs 5.2 and 5.3. These figures indicate that the shear capacities associated with shear failure are lower than those associated with flexural failure. Therefore, shear failure of the columns is expected to develop before flexural failure occurs.
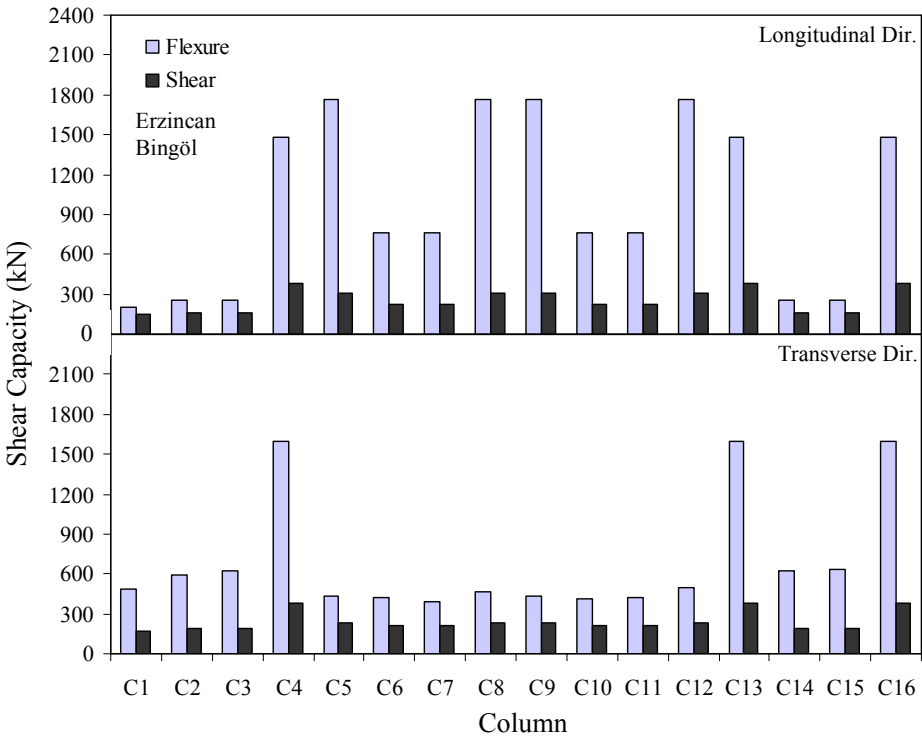
Figure 5.2 The shear capacities of the ground story columns associated with the flexural–type failure and shear-type failure in the Erzincan and Bingöl buildings
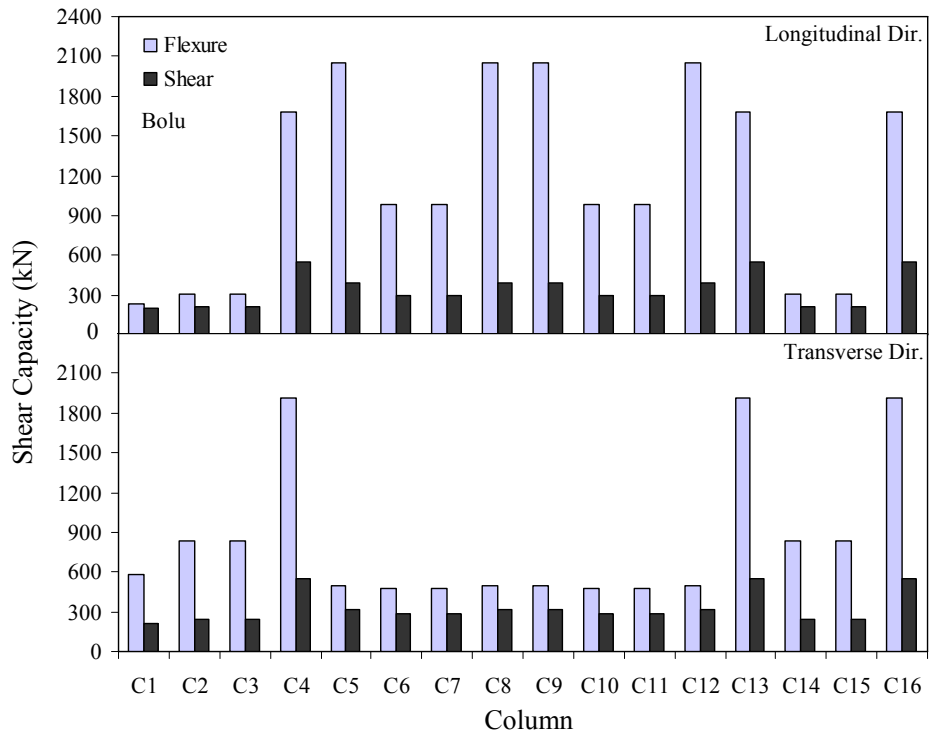
Figure 5.3 The shear capacities of the ground story columns associated with the flexural–type failure and shear-type failure in the Bolu building

Next step for the construction of model is assignment of rigid-plastic shear hinges at both ends of the shear-critical columns without strength degradation. Since the analytical models are three-dimensional, bi-directional shear relationship based on the following expression was introduced to each shear hinge at the top and bottom of the columns. This relationship has been implemented in Perform 3D by means of the following equation:

$$\left(\frac{V_X}{V_{nX}}\right)^{\alpha} + \left(\frac{V_Y}{V_{nY}}\right)^{\alpha} = 1 \tag{5.2}$$

where V_X and V_Y are instantaneous shear demands occurring during the analyses. V_{nX} and V_{nY} are the shear capacity of the columns calculated by Eqn. 5.1 and α is equal to 2 in order to sustain an elliptical force path considering both orthogonal horizontal directions.

5.3.2 Modeling Masonry Infill Walls

Existence of masonry infill walls in RC frames may lead to an increase in the base shear capacity, change the stiffness of the system, and load distribution through the frame members. These variations may even change the response of a structure compared to cases where the lateral load carrying capacity of infill walls are ignored.

The initial research on infill walls go back to the 1960s. The studies were intended to develop an effective method to estimate the strength of infill walls under monotonic lateral loading. Holmes (1961) proposed the diagonal strut model that should have a width equal to the one-third of the infill's diagonal length. Smith (1966, 1967) found out that the contact length between frame and infill panel may influence the width of the strut or the behavior of the frame. They calculated the width of equivalent strut and this proposal is still used with success for evaluating the elastic stiffness of the infilled frame. Mainstone (1971,1974) also proposed methods for estimation of the diagonal strut based on test results. According to Mainstone (1971) the equivalent strut width, a, was calculated by the following empirical formulation in terms of λ_l, a dimensionless stiffness parameter proposed by Smith (1966).

$$\lambda_l = \left[\frac{E_{me} t_{inf} \sin 2\theta}{4 E_{fe} I_{col} h_{inf}} \right]^{\frac{1}{4}} \quad (5.3)$$

$$a = 0.175 (\lambda_l h_{col})^{-0.4} r_{inf} \quad (5.4)$$

were a is the equivalent strut width (Figure 5.4) for a masonry infill wall, which is characteristically between 1/10 and 1/4 length of the infill diagonal, r_{inf}. λ_l is a coefficient used to determine the equivalent width of infill strut and h_{col} is the column height between centerlines of beams. h_{inf} is the height of infill panel. E_{me} and E_{fe} are the expected modulus of elasticity of the infill material and frame, respectively. t_{inf} is the thickness of infill. I_{col} is the moment of inertia of the column.

θ is the angle whose tangent is equal to the infill height-to-length aspect ratio. Equations (5.3) and (5.4) have been derived for purposes of reflecting the stiffness enhancing properties of infill walls. While they are known to be qualitatively accurate these expressions have been used in many applications by the research community.
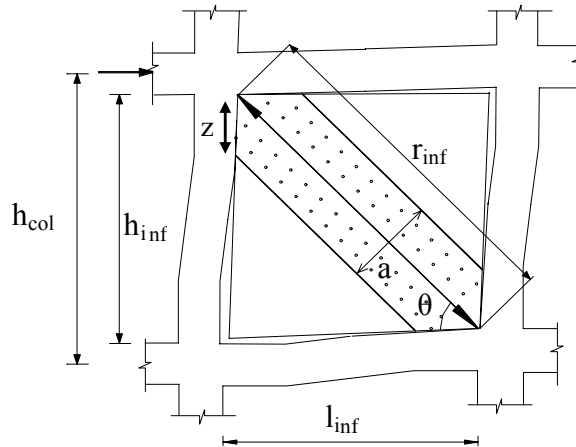
Figure 5.4 Representative diagonal compression strut of masonry infill (Adapted from Çağnan, 2001)

Klingner and Bertero (1976) proposed the first hysteretic diagonal strut that simulates the stiffness degradation under cyclic loading. However, their model was not successful in estimating the experimental results, especially in cases of cycles with large displacements.

Several researchers (Liauw and Lee, 1977; Thiruvengadam, 1985; Hamburger R.O. and Chakradeo A.S., 1993; Asteris, 2003) conducted analytical and experimental studies on infill frames with openings; however, proposed models included large number of variables and uncertainties or the experimental studies were performed on single-story specimens under monotonic loading that an agreement on this subject has not been reached. The research conducted on steel frames, on purpose of retrofit and infilled frames with concrete infill panels are out of interest, here.

A remarkable study is the analytical model of Crisafulli (1997) that was implemented in software program SeismoStruct (Seismosoft, 2006) by Blandon (2005). The prominent side of the model is that its accuracy was assessed through comparisons with experimental results of PsD tests of full-scale frame models and the parameters regarding the model were calibrated. However, it is not practical to implement this model to different software.

In this thesis, hollow clay brick infilled frames without openings were modeled as compression-only equivalent diagonal struts based on simple equations through 5.3-5.7. Out-of-plane behavior was not considered due to software limitations. Typical failure modes of infill walls are sliding shear and compression of diagonal strut.. The diagonal compression (R_c) and sliding shear (R_s) failure forces were calculated according to the following equations proposed by Paulay and Priestley (1992);

$$R_c = \frac{2}{3} z.t_{inf}.f'_m.sec\,\theta \tag{5.5}$$

$$z = \frac{\pi}{2}\frac{1}{\lambda_l} \tag{5.6}$$

$$R_s = \frac{\tau_o}{1 - \mu(h_{inf}/l_{inf})}d_m.t_{inf} \tag{5.7}$$

where f'_m and τ_o are the compressive and bond shear strengths of the infill wall, respectively. l_{inf} is the infill horizontal length, d_m is the diagonal length and μ is the coefficient of friction. z is the vertical contact length between the representative diagonal compression strut and column (Figure 5.4). The elasticity modulus E_I and the compressive strength f_c of the masonry were taken as 1100 MPa and 2 MPa, respectively. The bond shear strength was assumed as three percent of its compressive strength as proposed by Paulay and Priestley (1992). The lowest limit value of compression and sliding shear strength was assigned to each equivalent diagonal strut in the model. Force-controlled model was used.

All other assumptions about material and loading employed in the analytical models are summarized in Table 5.4. The yield strength of the reinforcement steel is 220 MPa for all buildings. The compressive strength of concrete was measured from cored concrete samples as 20 MPa in the case of Bolu and 9 MPa for the cases of Erzincan and Bingöl.

Table 5.4 Summary of the parameters for the analytical models of the MPWR buildings

	Parameter	Bolu	Erzincan	Bingöl
Material	Concrete	f_c=20 MPa $\qquad\qquad$ f_c =9 MPa E_c=21170 MPa $\quad$ E_c=14200 MPa *(ACI318, 2008)*		
	Reinforcement Steel	f_y=220 MPa, E_s=200000 MPa		
Loading	Gravity	DL + 0.3 LL		
	Seismic dead load for mass calculation	DL + 0.3 LL		
Modeling	P-delta effect	Yes		
	Rayleigh Damping	5 percent damping ratio		

5.4   THREE-DIMENSIONAL ANALYSES

5.4.1   Eigenvalue Analyses and Modal Properties of the Analytical Models

The buildings were analyzed for their first five mode shapes, periods and participation factors. For the building in Bolu, the first mode is in its longitudinal (X) direction with a period of 0.39 sec., the second mode is in its transverse (Y) direction with a period of 0.35 sec. The third mode is torsional with a period of 0.28 sec (Figure 5.5).
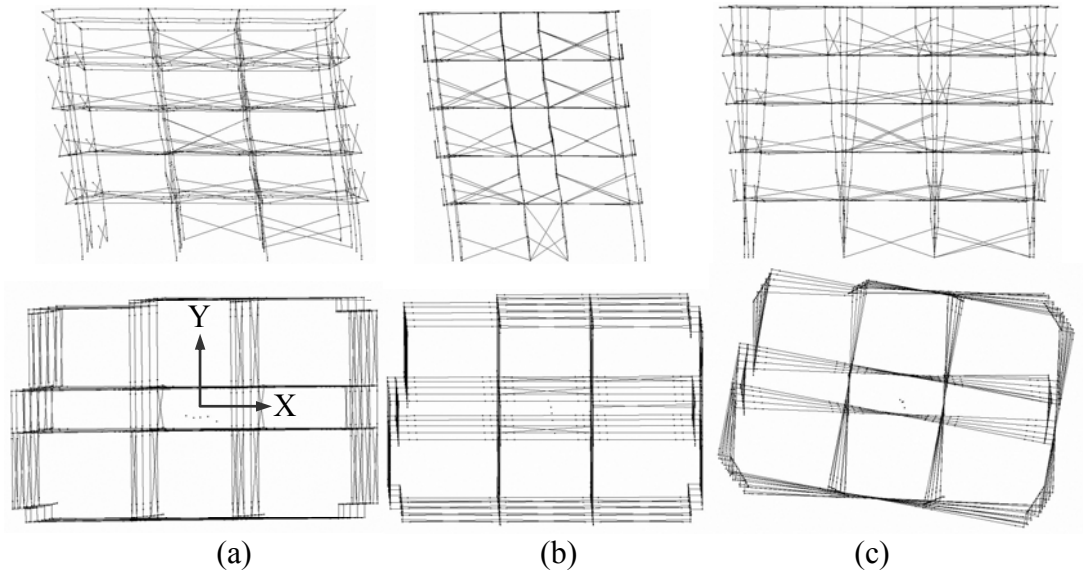
Figure 5.5 (a) 1st Mode: Translational-X (b) 2nd Mode: Translational-Y (c) 3rd Mode: Torsional

In addition to having the same geometrical properties, material properties are the same for the buildings in Erzincan and Bingöl as stated before; hence, they have the same modal properties. For the Erzincan and Bingöl buildings, the first mode is in the longitudinal direction with a period of 0.45 sec., the second mode is in the transverse direction with a period of 0.40 sec. The third mode is torsional with a period of 0.32 sec. The free vibration analysis results of the three buildings are listed in Table **5.5**. It shows that more than 75 percent of the total mass participates in the fundamental mode in the direction under consideration.

Table 5.5 Eigenvalue analysis results of the analytical models of the buildings

Mode	*Bolu*			*Erzincan and Bingöl*		
	Period	MPR* (%)	MPR (%)	Period	MPR (%)	MPR (%)
	(sec)	Long. (X) Dir.	Trans. (Y) Dir.	(sec)	Long. (X) Dir.	Trans. (Y) Dir.
1	0.39	78.4	0.8	0.45	78.3	0.4
2	0.35	0.7	79.2	0.40	0.3	78.6
3	0.28	0.2	0.1	0.32	0.2	0.3
4	0.12	1.3	12.9	0.14	1.5	13.1
5	0.11	12.5	1.7	0.13	12.5	1.9

*Mass participation ratio

5.4.2 The Measured Period of the Building in Bingöl

Following the 2003 Bingöl earthquake, strong motion sensors were located temporarily at the fourth (top) floor of the Bingöl building to record the aftershocks. Gülkan and Akkar (2004) conducted Fourier analysis on 59 sets of aftershock time series that were recorded at both the fourth and ground story levels. The results indicate that the periods are in the range between 0.5 and 0.6 sec.
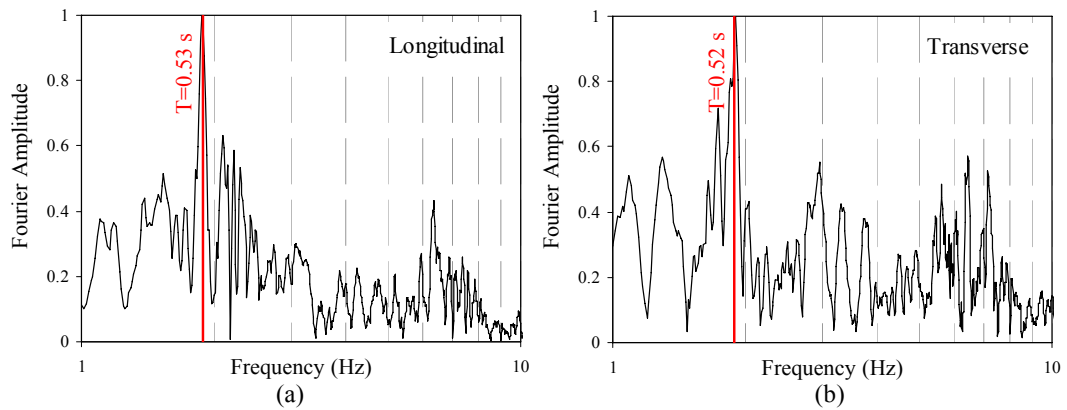
Figure 5.6 Normalized Fourier amplitudes for horizontal components of the roof acceleration data. The dominant frequency is 1.89 Hz (T=0.53 s) for the longitudinal and 1.90 Hz (T=0.52 s) for the transverse direction shown in parts (a) and (b).

To verify the analytical model with the results described above, fast Fourier analyses were conducted using the roof acceleration data obtained from the dynamic response. The fundamental vibration period of the building was calculated to be 0.53 and 0.52 s for the longitudinal and transverse direction of the building, respectively which is consistent with the previous research (Figure 5.6).

5.5 NONLINEAR TIME HISTORY ANALYSES (NTHA)

Nonlinear time history analyses (NTHA) of the buildings were performed using 3D nonlinear models. Since the strong motion sensors had been located at an angle relative to the orthogonal axes of the buildings, horizontal components of the ground motions were applied at an angle to the analytical models to provide

consistency. The input motions with their acceleration response spectra (5% damping) and orientations of the sensors with respect to the buildings are shown in Figs. 5.7 and 5.8 respectively.
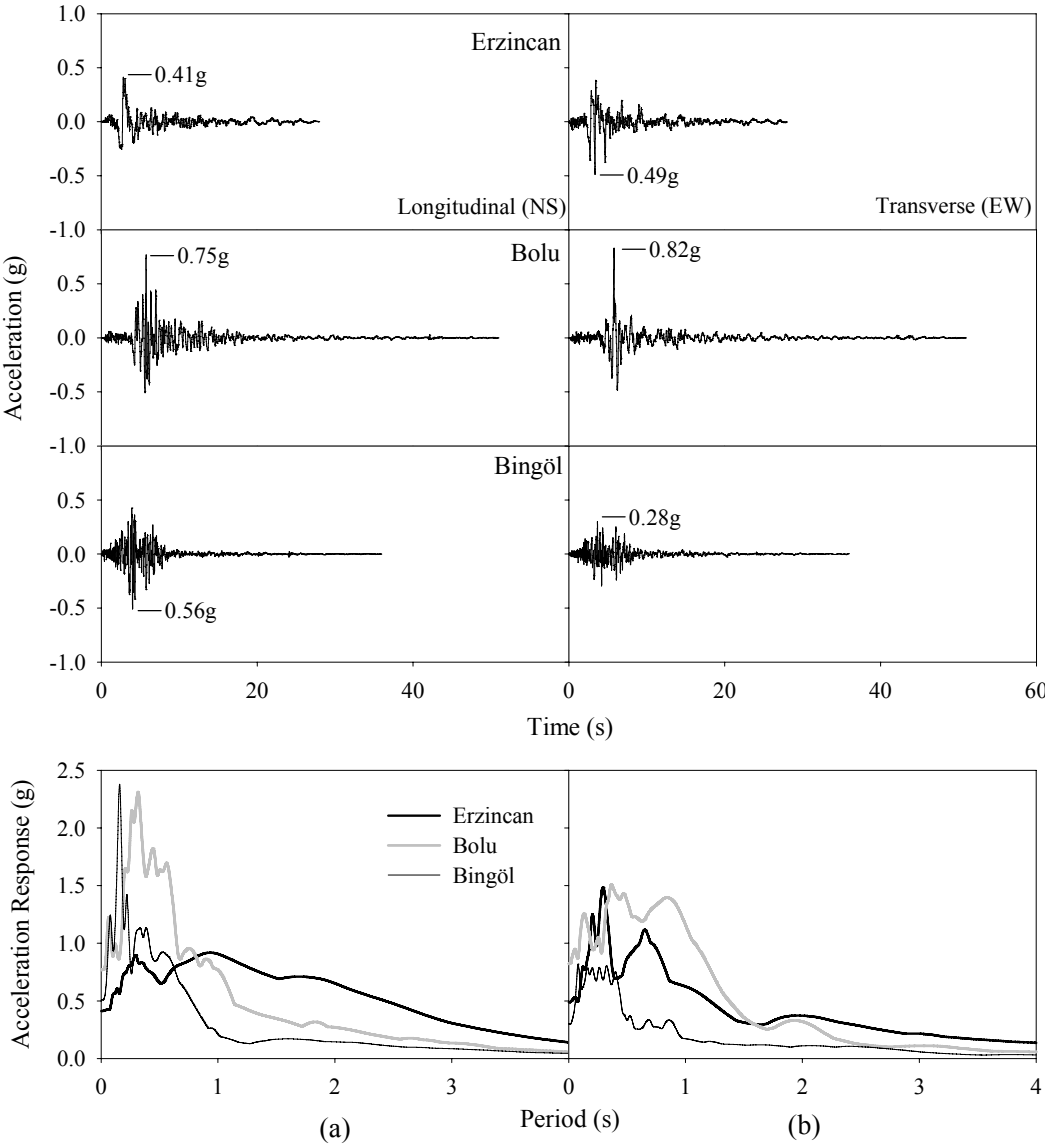
Figure 5.7. Horizontal ground acceleration history and acceleration response spectra (5% damping) graphs of the ground motions for (a) longitudinal and (b) transverse components of the earthquakes
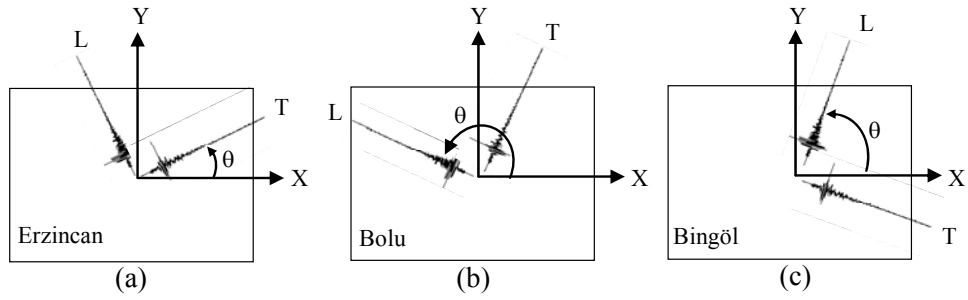
Figure 5.8 Orthogonal components of the ground motions applied to the buildings a) Erzincan, θ=26° b) Bolu, θ=165° c) Bingöl, θ=70°. L for longitudinal and T for the transverse component of the ground motion
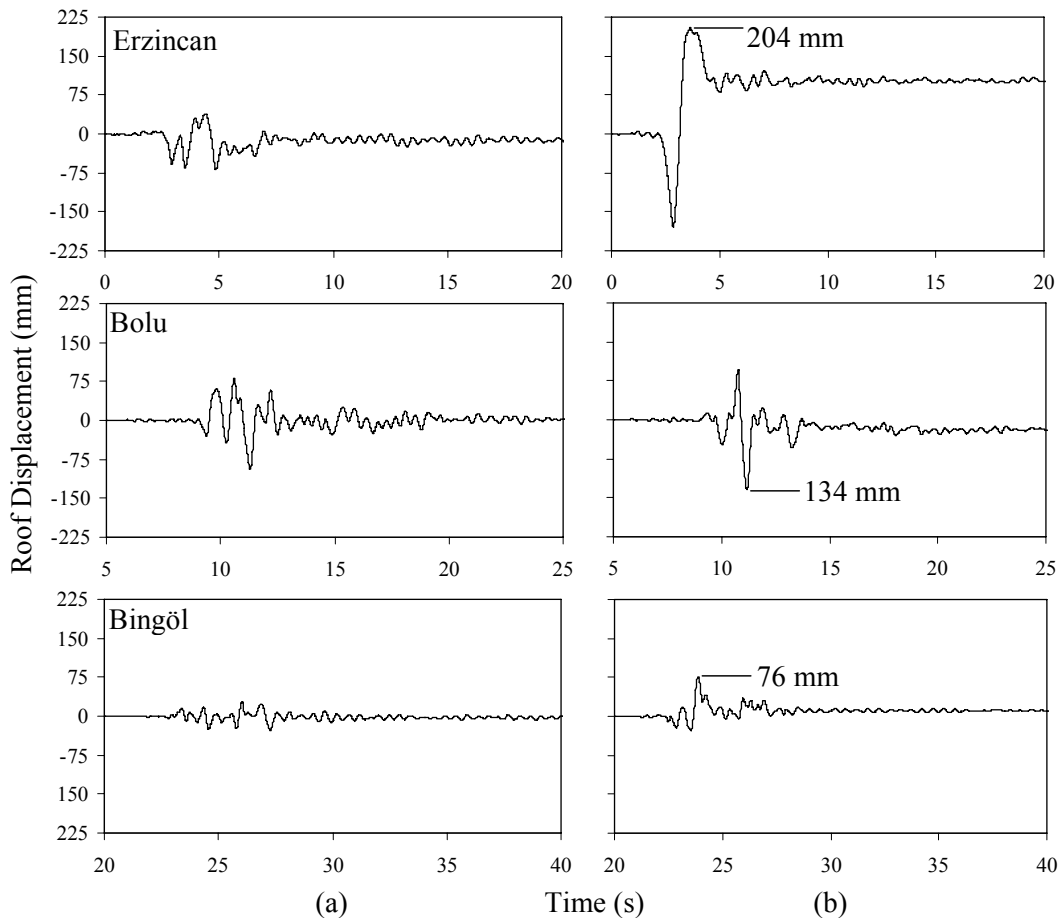
Figure 5.9 Roof displacement response history of the buildings in Erzincan, Bolu and Bingöl in the (a) longitudinal and (b) transverse directions of the buildings

After determination of the sensor orientation, bi-directional NTHA were performed for all buildings. Shear response of the brittle columns, plastic rotation and strain demand of beam elements and inter-story drift ratios (ISDRs) were primarily of concern. The roof displacement response histories obtained from those analyses are given in Figure 5.9. The calculated maximum values are 204, 134 and 76 mm corresponding to global drift ratio (GDR, roof displacement divided by the height of the building) values of %1.23, 0.81 and 0.46 percent for the buildings in Erzincan, Bolu and Bingöl, respectively. The maximum values were obtained for the transverse directions of the buildings.
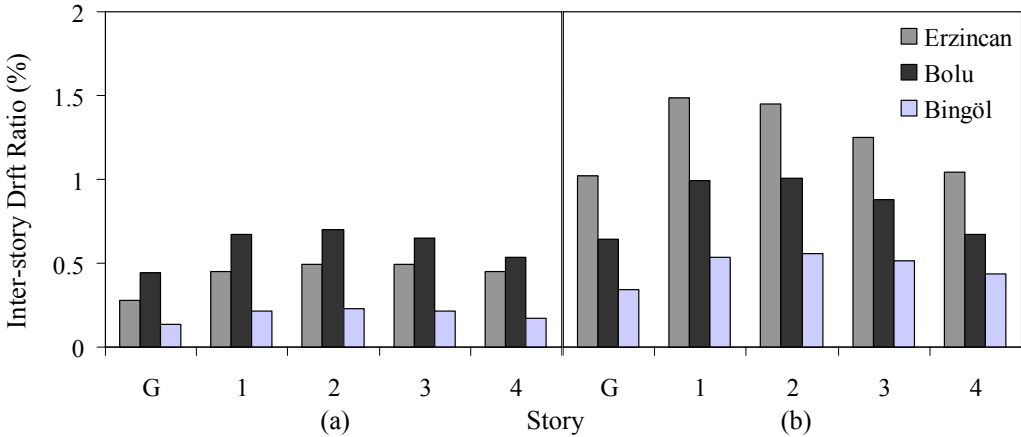
Figure 5.10 The ISDR results of bi-directional NTHA in the (a) Longitudinal and (b) Transverse directions of the buildings

The ISDR results obtained from the bi-directional NTHA are shown in Figure 5.10. It indicates that the Erzincan building has the highest whereas the building in Bingöl has the lowest relative drift value. For all buildings, the minimum ISDRs are observed in the ground story levels while the maximum response is obtained at the first and second story levels. Actually, the relative displacement of the ground floor is the same as that of the second floor and greater than that of the fourth floor but it should be kept in mind that the story height of the ground floor is 1.2 times more than those of the upper floors so the ISDR values are smaller.
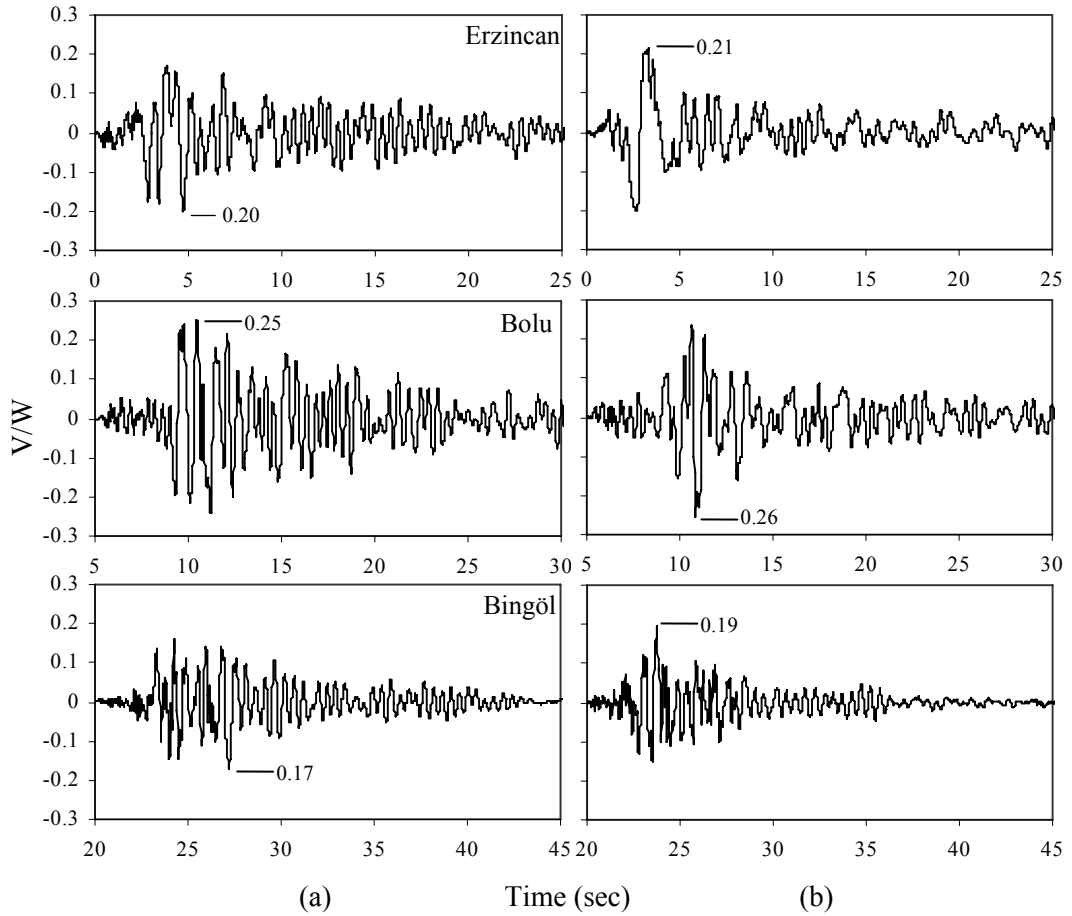
Figure 5.11 Base shear/Weight response histories of the buildings in Erzincan, Bolu and Bingöl for the (a) longitudinal and (b) transverse directions

If the structural damage is related to ISDRs, the most severe damage would be expected at the first and second floors. However, the observations following the earthquakes indicate that the structural damage diminishes from the lower to upper stories.

In Figure 5.11, the base shear response histories in the orthogonal directions of the buildings are depicted. The demand values are given in the form of base shear divided by the weight (W) of the structure. The maximum values are 0.21W, 0.26W and 0.19W for the buildings in Erzincan, Bolu and Bingöl, respectively. When this figure is investigated with the Figs. 5.2 and 5.3, it is obvious that almost all columns that were assigned shear capacity by Eq. 5.1 in the analytical model, fail in shear at

the end of the analyses. Thus, it is concluded that the shear capacities of the columns are underestimated by Eq. 5.1 in the evidence of observed structural damage.

5.6   NONLINEAR STATIC ANALYSES

NTHA is considered to be the most reliable way to estimate the inelastic seismic demand of structures. However, in the interest of applying more practical and less time consuming procedures, current civil engineering practice recommends use of NSPs (ATC-40, 1996, FEMA-356, 2000, ASCE/SEI-41, 2007, TEC 2007).
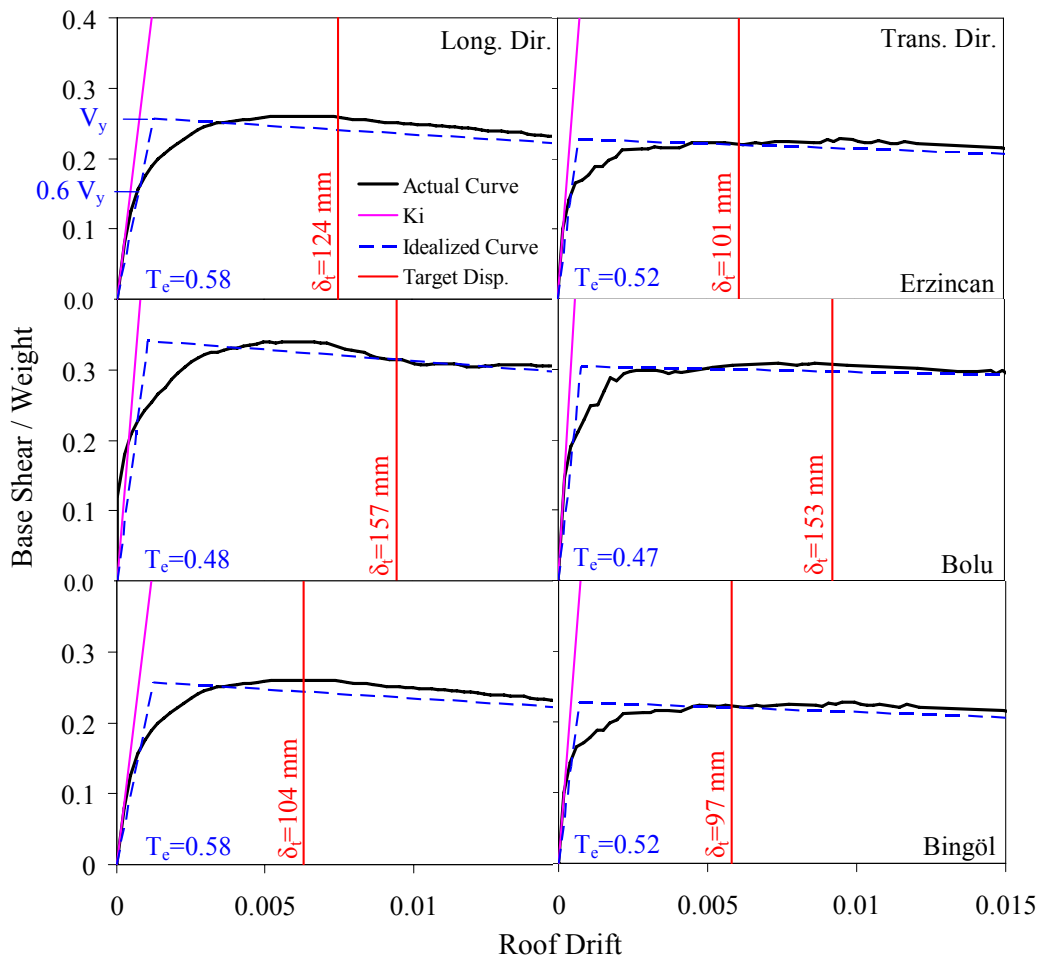
Figure 5.12 Pushover Curves of the buildings in the longitudinal and transverse directions of the Erzincan, Bolu and Bingöl building; the effective periods, T_e and target displacement values, δ_t are depicted

The displacement coefficient method (CM) of ASCE/SEI-41 (2007) described in Chapter 2 is one of these methods. Based on this method, first, a vertical distribution of lateral load proportional to the fundamental mode shape in the direction under consideration was applied to each model in order to construct the nonlinear force-deformation (pushover) curve of the system. The pushover curves obtained in both orthogonal horizontal directions are then used to calculate the effective fundamental period, T_e as defined in Section 2.3.2.1 (Figure 5.12). The effective fundamental period, T_e in the direction under consideration is calculated from that idealized curve. Then, the target displacement, δ_t is calculated in accordance with the Equations 2.5 and 2.6 (Table 5.6). Here, the purpose of the nonlinear static analyses is to calculate the ISDRs corresponding to those target displacement values, making a comparison with NTHA results and to determine the performance levels of those buildings based on ISDR limits of ATC-40 (1996).

The target displacement values based on each component of the ground motions and their comparison with the NTHA results are presented in Table 5.6. Calculation of the modification factors and target displacements of the SDOF systems have been explained in Chapter 2. Hence, only the values are given here.

Table 5.6 The modification factors, target displacement values calculated form NSP and their comparison with NTHA results in the longitudinal and transverse directions of the buildings

		Coefficients			Spectral Disp.	Target Disp. (NSP)	Roof Disp. (NTHA)	Roof Drift (NSP)	Roof Drift (NTHA)
		C_0	C_1	C_2	S_d (mm)	δ_t (mm)	δ_t (mm)	δ_t/H	δ_t/H
Long. Dir. of the building	**Erzincan**	1.43	1.06	1.01	81	124	68	0.75	0.41
	Bolu	1.43	1.17	1.03	91	157	94	0.95	0.57
	Bingöl	1.43	1.00	1.00	73	104	28	0.63	0.17
Trans. Dir. of the building	**Erzincan**	1.53	1.08	1.01	61	101	204	0.61	1.23
	Bolu	1.50	1.21	1.04	81	153	134	0.92	0.81
	Bingöl	1.53	1.02	1.00	62	97	76	0.58	0.46

The maximum target displacement values obtained by the CM are 124, 157, 104 mm for the buildings in Erzincan, Bolu and Bingöl corresponding to GDR values of 0.75%, 0.95%, and 0.63% respectively. These values are smaller than 1 percent that corresponds to a level of light damage according to current codes. However, as explained before, the observed damage is very different from this outcome.

5.7 PERFORMANCE ASSESSMENT OF THE BUILDINGS AND COMPARISON WITH THE OBSERVED STRUCTURAL DAMAGE

In this section, the performance assessment of the MPWR buildings is employed in two steps:

(i) First, the ISDRs obtained both from the NTHA and NSP are compared and evaluated according to the ATC-40 limitations

(ii) Second, structural members of the bottom three stories of all buildings that sustained varying levels of damage during the earthquakes are investigated with respect to the following parameters:

   (i) Plastic rotations

   (ii) Strains

   (iii) Shear capacities for brittle members

5.7.1 Evaluation on the Basis of Inter-story Drift Ratio (ISDR) Limits

The maximum ISDRs obtained from the NTHA and NSP are compared for the longitudinal and transverse directions of the buildings as depicted in Figure 5.13. The discrepancy between two analyses is due to divergent maximum displacement values shown in Table 5.6. This discrepancy can be observed in Figure 5.14 where maximum story displacements regarding the NTHA and NSP are shown.

The ISDRs of Figure 5.13 indicates that the Erzincan building falls to IO level according to CM method and determined to be in IO-LS according to NTHA results while it was judged to have a performance level of IO after the earthquake.

The building in Bolu is at IO level according to the NTHA result while it is slightly higher than IO level according to CM method. The building was judged to be in LS-CP performance level just after the earthquake. The Bingöl building had a performance level of IO for both analyses while it was judged to be in IO-LS after the earthquake.
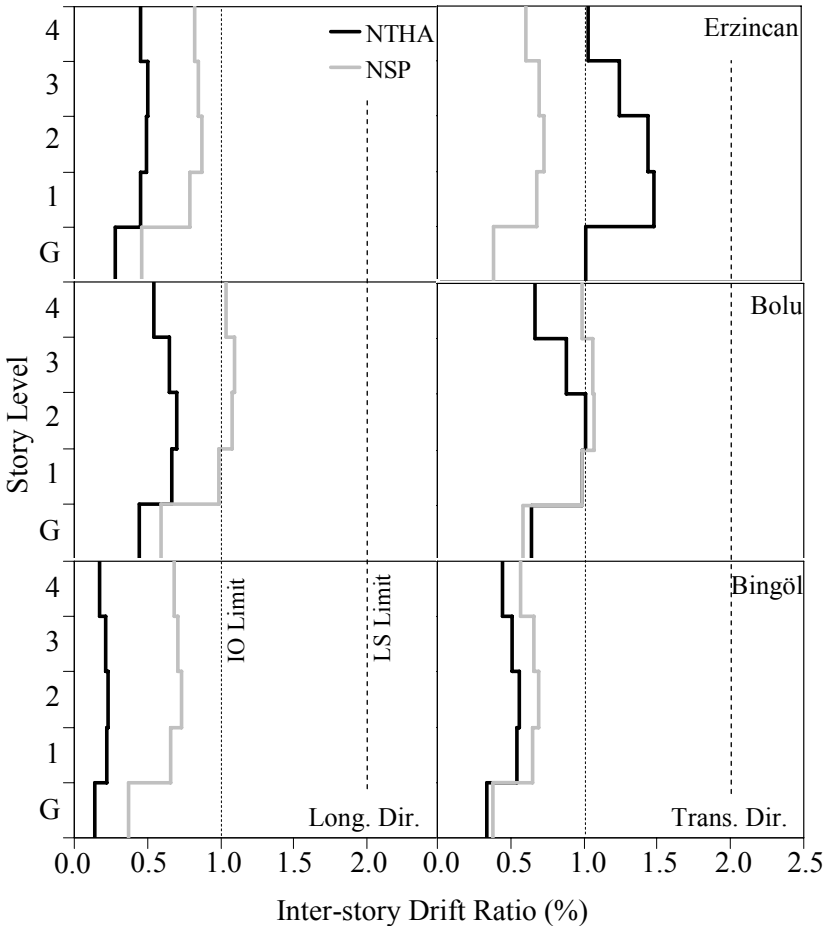
Figure 5.13. Comparison of ISDRs according to the NTHA and nonlinear static analysis results in the longitudinal and transverse directions of the buildings
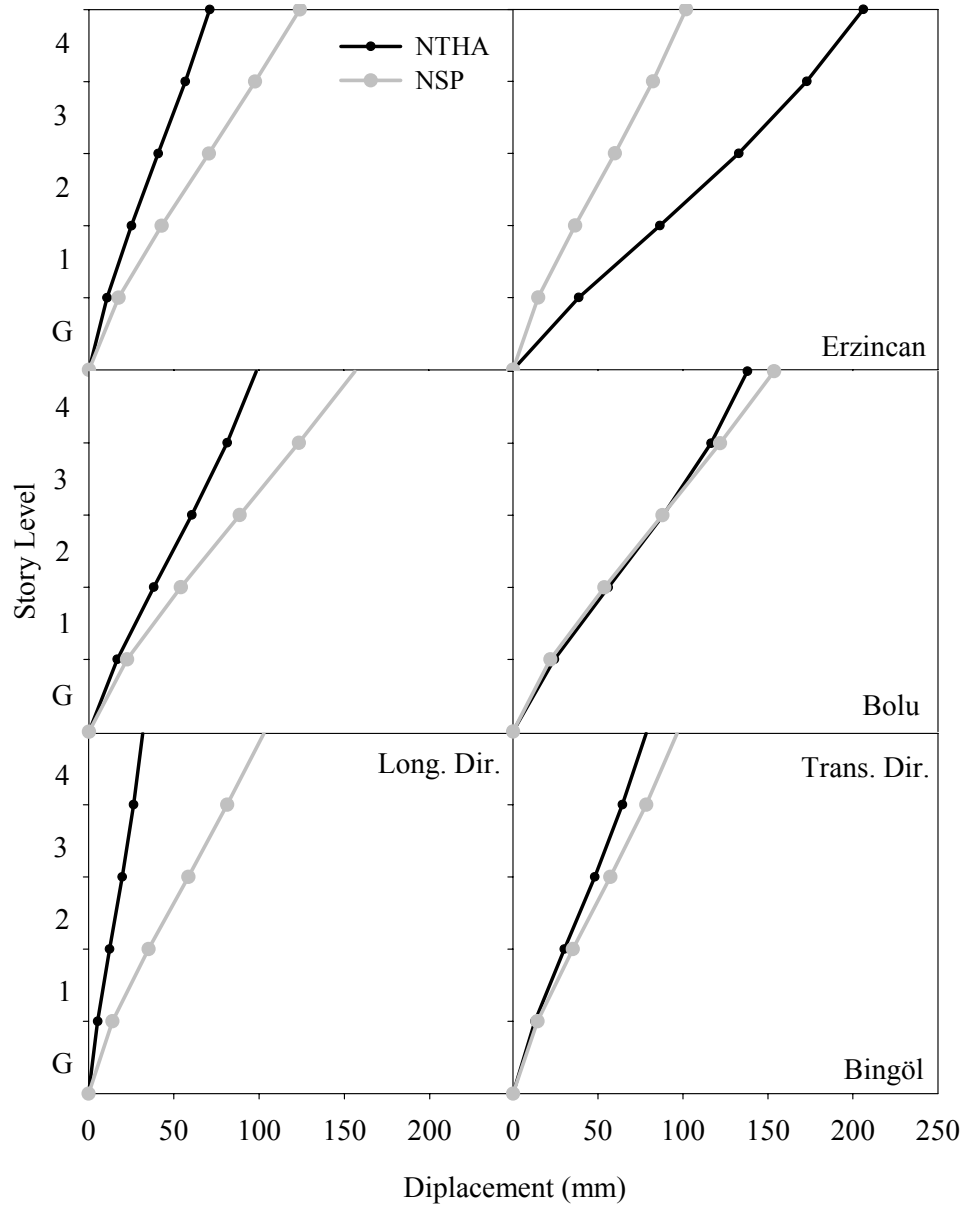
Figure 5.14. Comparison of maximum displacements calculated from the nonlinear time history and nonlinear static analyses of the buildings in longitudinal and transverse directions

In this circumstance, it is impossible to discuss the superiority of one method over another considering such divergent results (Figure 5.14) with the observed behavior. The performance assessment results (Table 5.7) based on the ISDR criterion and ATC-40 acceptance limits give variable estimates for these buildings and the applied ground motions.

Table 5.7 The comparison of calculated and observed performance levels of the buildings

	NTHA			NSP		
	Erzincan	Bolu	Bingöl	Erzincan	Bolu	Bingöl
Max. Inter-story drift (%)	1.49	1.01	0.56	0.87	1.09	0.73
Calculated Performance Level	IO-LS	Slightly higher than IO	IO	IO	Slightly higher than IO	IO
Observed Damage Level	Light Damage	Severe Damage	Moderate Damage	Light Damage	Severe Damage	Moderate Damage

5.7.2 Assessment at Member Level: Evaluation of Columns According to ASCE/SEI-41 Requirements

All columns were evaluated according to the NDP requirements of ASCE/SEI-41 as described in Section 2.3.3. In addition, in Section 5.3.1 it was shown that all column members are shear-critical. Since bi-directional analysis was conducted, the biaxial shear strength relationship introduced by Eq. 5.1 was used in the analytical models. As shown in Figs. 5.13-5.15, shear capacity of a column which is calculated by Eqn. 5.1, is represented by an elliptical orbit. On the other hand, demand from the NTHA is represented by a solid black line. These figures indicate that when the shear demand of a column reaches the shear capacity, the column is assigned to be in CP level.

In Figs 5.13-5.15, shear demand and capacity of the columns at the ground story levels of the buildings in Erzincan, Bolu and Bingöl are compared, respectively. Similar comparisons for the columns at the first and second story levels are also presented in Appendix B. The purpose of these comparisons is to determine the performance levels of the columns.
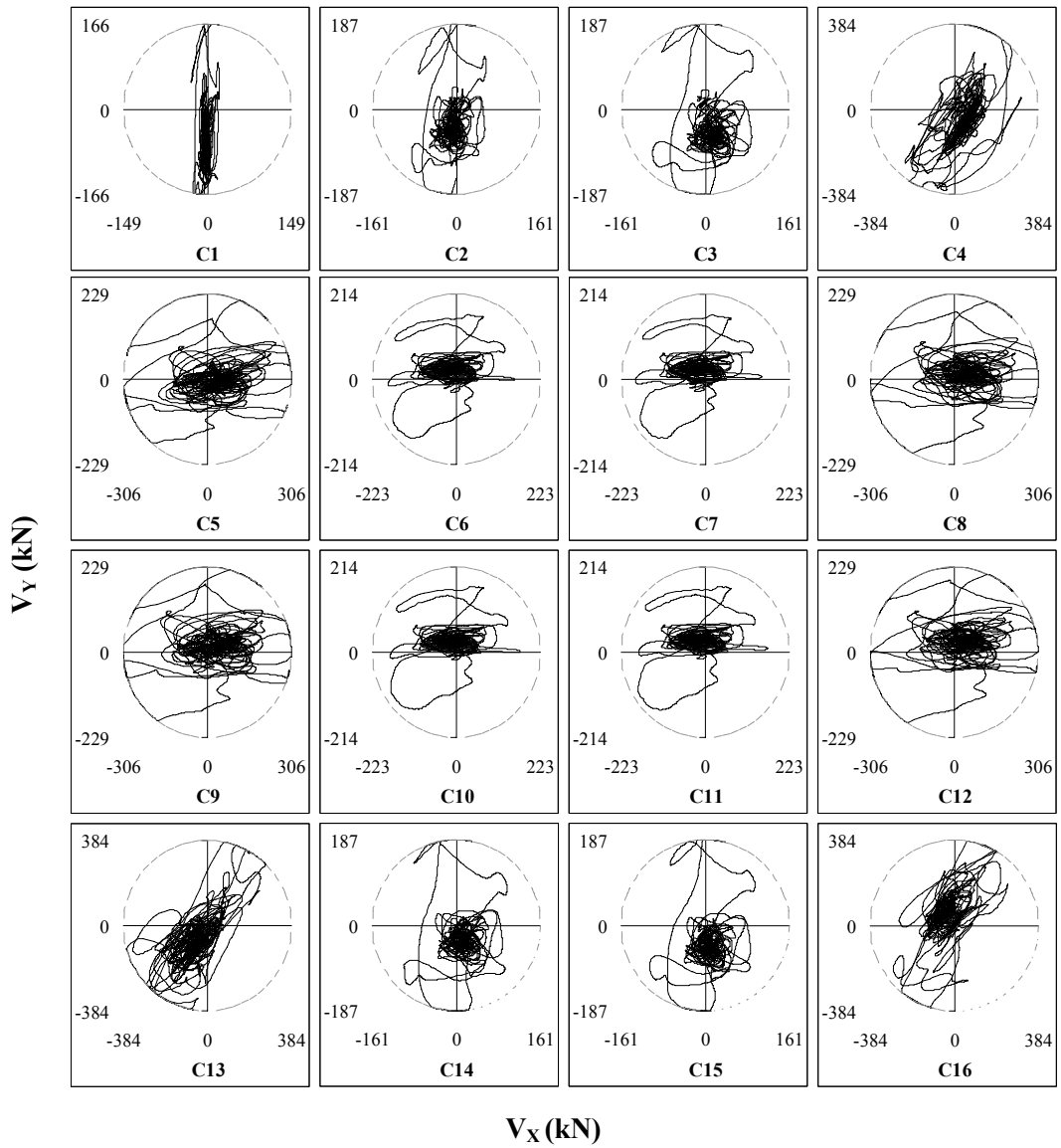
Figure 5.15 Bi-directional shear response history of the ground story columns in the Erzincan building. Dashed lines represent the shear strength calculated by the Eq. 5.1. The values are in the longitudinal (X) and transverse (Y) directions of the buildings. The column orientations are depicted in Figure 4.8

Figs. 5.13, B.1 and B.2 indicate that except for the interior columns-C6,C7,C10 and C11, all ground, first and second story columns of the Erzincan building reach their shear force capacities that corresponds to CP performance level. However, the technical report prepared by the MPWR engineers (Technical Report on Retrofit of the MPWR buildings in Erzincan and Bingöl, 2004) indicates that

only minor hairline shear cracks were observed at the L-shaped corner columns of the ground story in the Erzincan building.
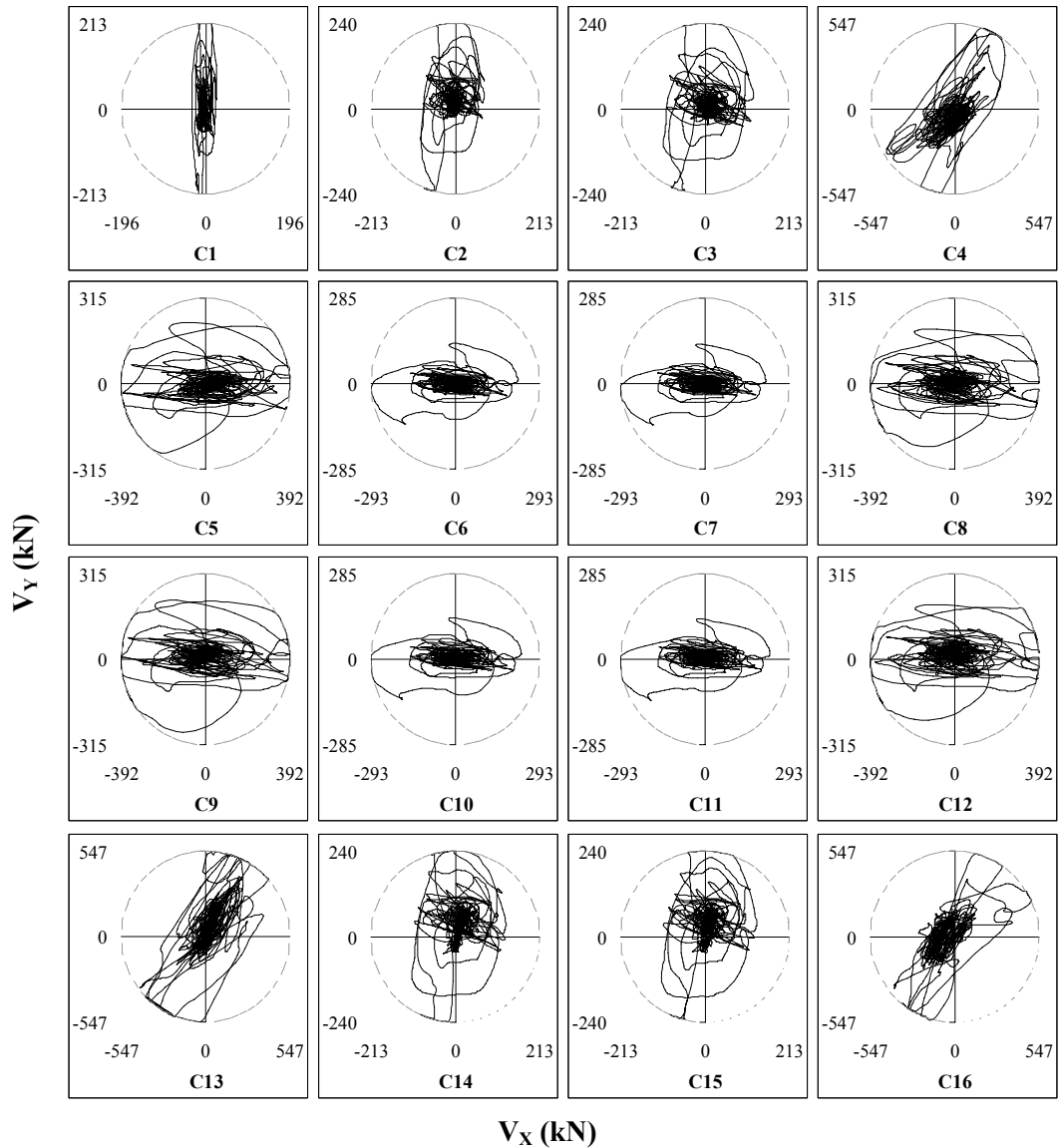
Figure 5.16 Bi-directional shear response history of the ground story columns in the Bolu building. The dashed lines represent the shear strength calculated by the Eq. 5.1. The values are in the longitudinal (X) and transverse (Y) directions of the building

Figure 5.14 indicates that all ground story columns of the Bolu building reach their shear capacities corresponding to a CP level. In the first and second stories, shear demand of the interior columns and the columns C2 and C13 are lower than their shear capacities (Figs. B.3-B.4) but the rest are also in CP level.
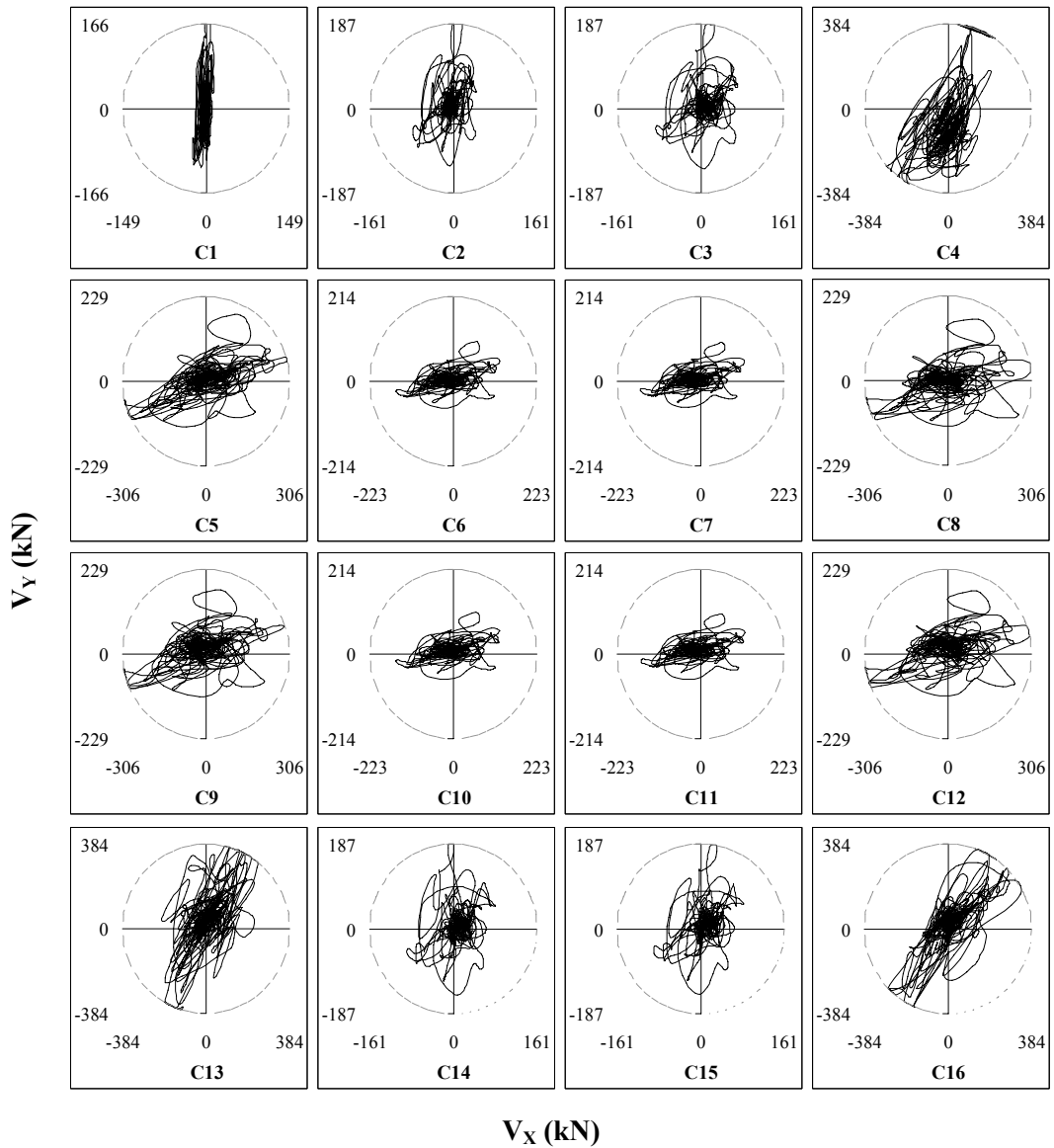
Figure 5.17 Bi-directional shear response history of the ground story columns in Bingöl building. The dashed lines represent the shear strength calculated by the Eq. 5.1. The values are in the longitudinal (X) and transverse (Y) directions of the building

The investigations following the earthquake indicate that severe shear damage was observed at the ground story columns of the Bolu building. The first and second story columns also sustained shear damage but the shear crack width was smaller than those occurred at the ground story columns. Shear failure was observed only in the captive column-C3 of the ground and first stories.

121

In the Bingöl building, the computational results show that except for the four interior columns, all ground story columns reach their shear capacities corresponding to a CP performance level (Figure 5.17). The columns C2, C6-C12 of the first story (Figure B.5) and C1 and C4 of the second story (Figure B.6) are also in CP level. However, the observed damage in the columns of the Bingöl building consisted of only minor shear cracks at the exterior frame and severe shear damage in the captive column-C3, but no shear failure was noticed.

In the light of performed analyses, it is obvious that the computed damage for the columns overestimates the observed damage for all buildings. The reason why it is overestimated may be due to the limitation of the shear strength assigned to the columns with nonconforming condition, in accordance with the prescriptions of ASCE/SEI-41. This guideline assures that for such columns *"where the longitudinal spacing of transverse reinforcement exceeds half the component effective depth, the transverse reinforcement shall be assumed not more than 50 percent effective in resisting shear"*. Hence, during the calculation of shear capacities of columns by means of Eqn. 5.1, only half of the term corresponding to the contribution of transverse reinforcement was taken into consideration. Moreover, in the presence of low quality concrete, the effect of this limitation in calculating the shear capacity of a column becomes significant that this provision should be reexamined.

5.7.3 Assessment at Member Level: Evaluation of Girders According to the ASCE/SEI-41 and TEC Requirements

ASCE/SEI-41 and current Turkish Earthquake Code (TEC, 2007) are taken into consideration for assessing the beams of bottom three stories of all buildings. The evaluating criteria concerning the nonlinear procedures of ASCE/SEI-41 are based on plastic rotations while in TEC, strain values at the extreme concrete and steel fibers of any section are of concern. For both methods, the acceptance limits related to the "nonconforming" transverse reinforcement were considered due to existence of the following conditions:

- o Inadequate transverse reinforcement configuration : The stirrups are closed with 90° angle hooks instead of 135° angle that are not adequately anchored in the concrete core

- o Amount of stirrups is insufficient: no confinement zone and no transverse reinforcement exist in the beam-column joints

The "nonconforming" acceptance limits are lower than those of "conforming". This difference is made clear by the acceptance values given in Tables 5.8 and Table 5.9

Table 5.8 Comparison of the acceptance limits regarding the "conforming" and "nonconforming" transverse reinforcement – The nonlinear procedure of ASCE/SEI-41 RC Beams

ASCE/SEI-41					
Condition: Beam controlled by flexure			**Acceptance Criteria**		
$\dfrac{\rho - \rho^{'}}{\rho_{bal}}$	*Transverse Reinforcement*	$\dfrac{V}{b_w d \sqrt{f_c^{'}}}$	**Plastic Rotation Angle, radians**		
			Performance Level		
			IO	**LS**	**CP**
≤ 0.0	Conforming	≤ 0.25	0.010	0.020	0.025
≤ 0.0	*NonConforming*	≤ 0.25	*0.005*	*0.010*	*0.020*

Table 5.9 Comparison of the acceptance limits regarding the "conforming" and "nonconforming" transverse reinforcement – The nonlinear procedure of TEC 2007–RC Beams

TEC 2007						
	IO		**LS**		**CP**	
	ε_{cu}	ε_{s}	ε_{cu}	ε_{s}	ε_{cu}	ε_{s}
Conforming	0.0035	0.01	$0.0035+0.01(\rho_s/\rho_{sm})$	0.04	$0.004+0.014(\rho_s/\rho_{sm})$	0.06
Nonconforming	*0.0035*	*0.01*	*0.0035*	*0.04*	*0.004*	*0.06*
ρ_s is volumetric ratio of transverse reinforcement and ρ_{sm} is minimum design volumetric ratio of transverse reinforcement						

The performance assessment results of the beams are shown in Figs. 5.16-5.18 for the ground stories of all buildings. Those regarding the first and second stories are given in Figs. C.1-C.6. The numerical values and performance levels computed are presented for each member in such a way that it is easier to compare

the results from the two procedures. The strain values are directly obtained from the fiber sections and the plastic rotations are calculated by Eq. 3.2. These figures indicate that for all buildings, the beams in the longitudinal direction have a performance level of IO according to the ASCE/SEI-41 procedure. When the beams in the transverse direction are considered, the most severe damage occurs in Erzincan (LS), followed by Bolu (IO-LS) and Bingöl (IO) building, in that order. That occurrence of more severe damage in the beams parallel to the transverse direction is due to occurrence of maximum inter-story drift in this direction.

TEC and ASCE/SEI-41 give varying degrees of damage level for evaluation of the beams. Figs. 5.16-5.18 assure that the damage level estimation based on TEC are more conservative than ASCE/SEI-41 in some beams. This is clearly evident from Figure 5.20 that the beams in the transverse direction of the Bingöl building are in IO level according to ASCE/SEI-41 while most of them are in LS level according to TEC. This difference is related to the different acceptance criteria and limit values that were described in the preceding paragraphs. As a footnote related to TEC, following rationalization may be offered: critical criterion in determining the performance level of the nonconforming beams is the steel strain. That is because the longitudinal reinforcement ratio of the beams is very low (0.16-0.21%) compared to that of most other typical beams. Thus, while high strain values occur in the tension steel, compressive strain in the extreme fiber of the concrete section is still at a very low value which is the typical behavior in an under-reinforced section.

In conclusion, similar to the assessment results of columns in the Erzincan building, the performance assessment of beams in Erzincan building is far from matching the observed damage. The beams of the Bolu building were calculated to be in IO-LS performance level as per ASCE/SEI-41 where they sustained moderate damage during the earthquake. The beams in the Bingöl building were calculated to be in IO level as per ASCE/SEI-41 where they sustained light damage during the excitation. Thus, these estimations are consistent with the observed damage. The outcomes regarding TEC are similar; however, TEC may overestimate the damage level in some beams as depicted in the Bingöl building.

124

Figure 5.18. Comparative assessment of the ground floor beams in the Erzincan building as per ASCE/SEI-41 and TEC

125

Figure 5.19. Comparative assessment of the ground floor beams in the Bolu building as per ASCE/SEI-41 and TEC

Figure 5.20. Comparative assessment of the ground floor beams in the Bingöl building as per ASCE/SEI-41 and TEC

5.7.4 Assessment at Member Level: Evaluation of Infill Walls

The performance assessment of the hollow clay brick infill walls regarding the bottom three stories of all buildings are conducted based on prescriptions discussed in Section 5.3.2. The sliding shear strength and diagonal compression strength of the infills were calculated by Eqs. 5.5 and 5.7. Then the critical values were assigned to the analytical models. All calculations and performance assessment results are given quantitatively in Tables D.1-D.3. The representative evaluation of the infill walls at ground stories of the buildings are depicted in Figure 5.21. For the first and second stories of the buildings, the comparative damage data are depicted in Figs D.1-D.3.

Figure 5.21. Comparison of the observed and calculated damage of the ground story infill walls regarding the (a) Erzincan and (b) Bolu buildings. (Observed Damage/Calculated Damage) IO : Immediate Occupancy C: Collapse
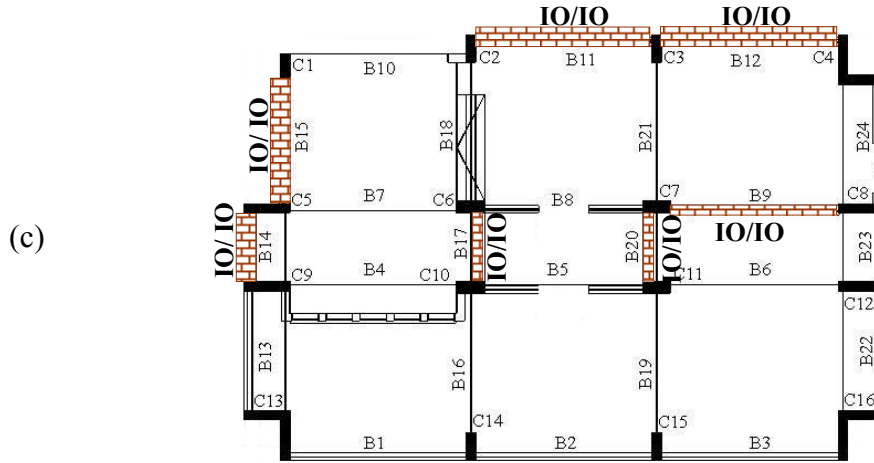
Figure 5.19 Cont'd Comparison of the observed and calculated damage of the ground story infill walls regarding the Bingöl building. (Observed Damage/Calculated Damage) IO : Immediate Occupancy C: Collapse

In Figure 5.21, "observed damage/calculated damage" is given through qualitative comparison for each in-filled frame. The infill walls were assumed to collapse when they reached their calculated critical strength. Since, infill walls are so brittle with negligible deformation capacity, behavior of the infill walls are limited by their strength values. In the evaluation process, the critical value of shear or compressive strength of the representative strut was taken into account. If the force demand reached the capacity, the infill wall was assumed to fail; otherwise it was assumed to be in immediate occupancy level. The assessment results indicate that the calculated damage in the Erzincan building matches the observed damage at the 43, 36, and 54 percent of the infill walls for the ground, first and second story, respectively. In the Bolu building, those values are 86, 93, 69 and in the Bingöl building, the agreement is 100, 79 and 69. The consistency between the calculated and observed damage is more obvious for the infill frames in the longitudinal direction of the buildings (Figure 5.18) but the assessment results overestimate the damage levels for those in the transverse direction in which the calculated ISDRs are much higher.

129

5.8 DISCUSSION OF CONTROVERSIAL RESULTS REGARDING THE ERZİNCAN BUILDING

Although the performance assessment of the Bolu and Bingöl buildings gives reasonably accurate estimations, there is much divergence between the observed and estimated damage levels for the building in Erzincan. It is decided that the best way to understand this discrepancy is to investigate the ground motion of Erzincan because the analytical models of the Bingöl and Erzincan buildings have been assumed to be exactly the same due to their same template designs and material properties. Hence, the different variable may be the characteristics of the Erzincan record.

Different from the Bingöl record, the ground motion record for Erzincan has pulse-like waveform, and the corresponding PGV and PGD values are relatively large (Table 4.3). Anderson and Naeim (1984) Anderson and Bertero (1987) Uang and Bertero(1988) have shown that earthquake ground motion parameters such as velocity, displacement, incremental velocity and incremental displacement may have greater influence on the structural response than the PGA, particularly in the inelastic range.

Anderson and Bertero (1987) suggested the use of maximum incremental velocity that represents the area under the acceleration pulse or/and maximum incremental displacement that represents the area under the velocity pulse for characterizing the damage potential of earthquake motion. In this circumstance higher damage potential would be expected for the Erzincan building than the Bingöl building which had the same concrete material quality (f_c=9 MPa) with the Bingöl building but sustained a ground motion with a large acceleration pulse.

Akkar and Gülkan (1999) stated that, for linear shear buildings major contribution to drift is due to ground velocity v(t), confirming that large velocity pulses constitutes the damage potential of near-field ground motions. They also stated that PGAs of most near-field records are not high as expected and become saturated for increasing magnitudes but their PGVs and corresponding drift demands are significant and confirmed by observed structural damage

Akkar and Gülkan (2002) investigated different characteristics of near-field and far-field ground motions from the following two randomly chosen records of earthquakes with similar magnitudes and PGAs that one of those records was from the Erzincan earthquake (M6.6) and the other was from a station that was triggered during the Northridge earthquake (M6.7). The influence of the coherent large acceleration pulse in the Erzincan record is shown through greatly enhanced ground story drift ratio demands it causes (Figure 5.22). According to Akkar and Gülkan (2002) this is the most severe demand a near-source ground motion imposes on structural frames.
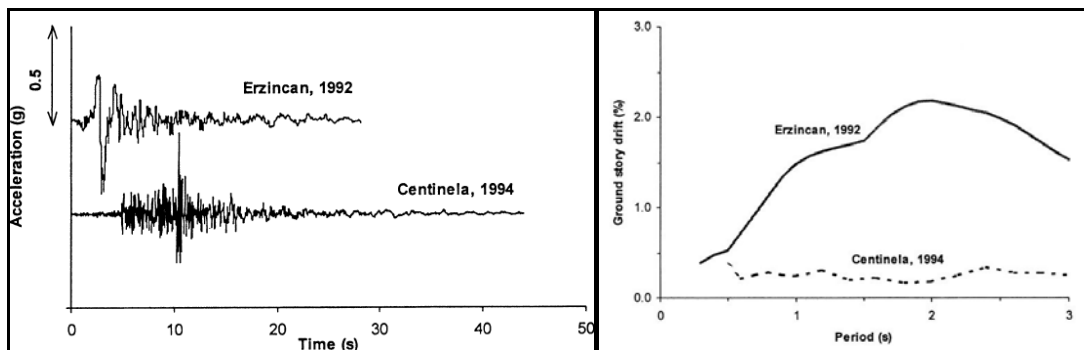
Figure 5.22 Comparison of the ground story drift spectra for near-field (Erzincan) and far-field (Northridge) earthquakes. NS component of the N6.6 Erzincan earthquake has a PGA of 0.402 and was recorded at 2km Its PGV was 107.5 cm/sec. The McBride school at Centinela Street S25E component was recorded during the M6.7 Northridge earthquake at 25.3 km and had a PGA of 0.442g and a PGV of 19.9 cm/sec (Akkar and Gulkan, 2002)

Table 5.10 Comparison of the maximum drift spectrum intensities for the 1992 Erzincan and 1999 Düzce (Bolu record) near-field earthquakes (structural damping of 5%) (Modified from Akkar and Gülkan, 2002)

		Maximum Drift Spectrum Intensities (%)		PGV (cm/s)	
Earthquake	**Record**	**EW**	**NS**	**EW**	**NS**
1992 Erzincan	Erzincan	3	4.1	78.2	108.4
1999 Düzce	Bolu	2.6	2.5	66	52.3

The comparison of drift spectrum intensities regarding the 1992 Erzincan and 1999 Düzce (Bolu record) earthquake were also compared in Akkar and Gülkan

131

(2002). The authors developed a drift spectrum that is defined as the plot of drift equation based on shear beam model as a function of period and damping. The maximum drift spectrum intensities calculated by the authors for the structures with 5% damping are shown in Table 5.10. Based on this table they concluded that "*If we accept the premise that drift spectrum intensity is a measure of destructiveness, then we can say that maximum ground velocity occurs in the direction where the drift spectrum intensity is also maximum*". Moreover, it is inferred from Table 5.10 that the Erzincan record with larger PGV values yields larger drift spectrum intensities than those of Bolu. This indicates that the Erzincan earthquake is more destructive than the Düzce earthquake which also shows parallelism with the outcomes of this study.

More recent research has shown that there is a correlation between structural deformation demands and PGV. Küçükdoğan (2007) showed that PGV exposes a good correlation with the global deformation demands such as maximum ISDR of mid-period RC frames. Maximum deformation demand obtained in the dynamic response of the Erzincan building is due to a large displacement excursion rather than numerous oscillations which supports this statement.

To sum up, NTHA and performance assessment results regarding the Erzincan building are in agreement with the outcomes obtained from the previous research described in the preceding paragraphs. More severe damage might be expected for Erzincan building than the Bingöl building due to being subjected to the ground motion with a large acceleration pulse. However, as stated before, the Erzincan building performed the best during the earthquake and was used for occupancy.

5.9   CONCLUDING REMARKS

This chapter indicates that the current performance assessment methods and established guidelines provide reasonable estimates for the performance of the MPWR buildings except for the Erzincan case; however, there is still much

uncertainty in estimation of their dynamic responses. The author states these uncertainties as follows;

- *Precise Input Motion*: Due to the fact that the strong ground motion sensors were located in one-story building structures adjacent to the case-study buildings in Bingöl and Bolu and in a one-story building two kilometers away from the Erzincan building, the "exact" input motions to the buildings have been assumed known. Although this is a reasonable assumption, SSI effects may alter this exactness.

- *Quality of Materials*: Local deficiencies in strength of materials are not included in as-built projects where these projects are used in establishing analytical models and evaluation of the structural response. A large variation in properties of the structural materials can be observed especially in old-type structures such as those MPWR buildings where the concrete was placed by hand.

- *Quality of Workmanship*: Local deficiencies related to poor workmanship may cause local failures. Nonconforming detailing requirements in ductile moment-resisting frames result in damage concentrations in local regions. For example; improperly tied transverse bars are disturbed during placing of concrete and amass at the same region. Thus, specified spacing and amount of transverse bars are no more provided along the column. Hence, local shear cracks may occur due to lack of necessary transverse reinforcement. This was observed in the Bolu building where the structural damage was the most severe.

- *Seismic Joints and Pounding:* Although seismic joints were provided between the adjacent buildings, it was evident that an impact had occurred between the adjacent buildings during the earthquake due to insufficient separation especially in Bolu and Bingöl. However, it is quite impossible

to predict the "degree of severity" regarding this impact on the structural response and apply to the analytical model.

In addition to these statements, it is difficult to simulate and evaluate the actual behavior of the structure as constructed, especially for the buildings sustained distinct pulse-like behavior such as the Erzincan ground motion. It is obvious that better estimations will be performed as number of large magnitude ground motions with that kind of behavior increase and their effect on real buildings is observed. In this circumstance, the analytical model, analyses and performance assessment methods do not provide a definite prediction. To make better estimates,

 (i) Demand and capacity predictions must be understood better under dynamic loading effects,

 (ii) Performance limits and criteria must be refined through further systematic research before they are incorporated into routine engineering practice

 (iii) Software used to establish the three-dimensional analytical models of the structures shall be developed to obtain more realistic results

CHAPTER 6

CONCLUSIONS AND RECOMMENDATIONS

6.1   SUMMARY

It is an obvious truth that every theory must pass the test provided by nature before serving engineering as a reliable instrument. While performance assessment procedures are being developed and refined, their corroboration with field observations is necessary. Earthquakes are seldom events, and there is as yet little empirical evidence for existing RC building performance well in the nonlinear range except under infrequently occurring conditions or in the lab. Building stock elements are less perfectly known so there is more uncertainty in modeling them. This research answers the rhetorical question of "do we have the means of forecasting building performance under actual earthquakes of real buildings, given their blue prints and their input motion?"

Prior to this study, to our best knowledge, no cast-in-place RC building has ever been subjected to near-field strong ground motions from three major earthquakes. This happened in an indirect way in Turkey over a time span of eleven years. Three identical buildings belonging to MPWR that had been built to the same design templates experienced 1992 Erzincan earthquake in Erzincan, 1999 Düzce earthquake in Bolu and 2003 Bingöl earthquake in Bingöl, respectively. The ground motion sensor stations were fortuitously nearby in an adjacent single story building in Bolu and Bingöl. The station in Erzincan was about 2 km away from the case study building but we assume that the record applies to the building there.

The buildings sustained varying degrees of damage during the earthquakes. After the Düzce earthquake a careful examination of the damage distribution was performed for the building in Bolu. A similar exercise was conducted for the building in Bingöl four years later. The Erzincan building seemed to be intact following the earthquake and served as an important facility for processing applications from homeless citizens seeking re-housing.

Given that the damage information, input motions, design drawings and material properties of the buildings are all known, the following question comes to mind: Could we have predicted the structural damage that occurred in these buildings by proper modeling using the tools of current computational performance assessment procedures? Hence, the main purpose of this dissertation has been to find an answer to this challenging question. For any procedure to qualify as a scientific instrument, it needs to be reasonably able to predict events.

Before investigating the three MPWR buildings that constitute the main objective of this dissertation, first, nonlinear analysis methods and performance assessment procedures were validated through a 3D full scale RC frame building (the SPEAR test structure that had been tested at the ELSA facility in Ispra, Italy) subjected to bi-directional pseudo-dynamic (PsD) test in the laboratory. The displacement and force variables obtained from the analyses were in good agreement with the experimental results. Furthermore, the observed and calculated damage was compared according to ASCE/SEI-41 (2007, 2008) and the Turkish Earthquake Code (TEC, 2007). After this benchmark study was conducted, the MPWR buildings were analyzed. The description of the buildings, input ground motions and observed structural damage were described in detail. Then, the analytical models were employed to perform nonlinear analyses. The principal purpose of these nonlinear analyses was to assess whether the analytical model of the buildings could indicate framing damage consistent with that observed at the sites after the earthquakes using the current performance procedures.

6.2   DISCUSSION OF RESULTS AND CONCLUSIONS

The results presented so far are summarized for the SPEAR test structure, MPWR buildings, performance assessment procedures, software and analytical modeling individually in the following subsections.

6.2.1   The SPEAR Test Structure

- Although the acceptance limit values for nonconforming columns have been revised in the current version of ASCE/SEI-41 (2008), performance assessment results overestimate the damage level compared to that observed.

- Performance assessment of the nonconforming columns based on TEC results in the same damage level with those of ASCE/SEI-41. Hence, evaluation according to TEC also overestimates the damage level compared to that observed.

6.2.2   The MPWR Buildings

- Despite having deficiencies such as short columns, unconfined joints and nonconforming transverse reinforcement, the structural system of the MPWR building is an example of good design in Turkish circumstances of 1970s and 1980s. Its outline indicates that the structural engineer perceived the exterior frames as the principal lateral resisting system of the structure. This is a sound strategy that reaped many benefits.

- The design concrete strength of B160 corresponding to C14 (14 MPa) was specified in the design of the buildings. The as-built concrete quality is higher (20 MPa) than the specified in design template for the Bolu building and lower (9 MPa) for the buildings in Erzincan and Bingöl based on the measured average values.

137

- The building in Bolu sustained severe damage that was judged to represent a "life safety-collapse prevention" performance level while those in Erzincan and Bingöl sustained lighter damage levels corresponding to "immediate occupancy" and "immediate occupancy-life safety" levels, respectively.

- The structural damage was concentrated in the bottom three stories. The common types of damage in the buildings that occurred in varying degrees were shear cracks in the captive columns, flexural cracks in the beams and diagonal cracks in infill walls of the bottom three stories.

- In order to simulate the seismic response of the buildings, analytical models of the structures were employed. In an effort to verify the accuracy of these models, fast Fourier analysis results regarding the NTHA of the Bingöl building were compared with those obtained from the aftershocks recorded at the top floor of the building. The fundamental period values regarding the analytical model were in good agreement with the measured period of the building in its damaged state.

- The Erzincan and Bingöl buildings were assumed to be the same due to having the same geometrical and material properties. Hence, they have the same modal properties. The Bolu building is different from these two only with regard to its higher quality concrete.

- The shear capacities of the columns associated with shear failure were calculated to be lower than those associated with flexural failure. The NTHA results indicate that the columns reach their shear capacity prior to flexural failure.

- The NTHA results indicate that the peak roof displacements are 204, 134 and 76 mm corresponding to global drift ratio (GDR, roof displacement

divided by the height of the building) values of %1.23, 0.81 and 0.46 percent for the Erzincan, Bolu and Bingöl buildings.

- The target displacement values calculated by the NSP of ASCE/SEI-41 are 124, 157 and 104 mm corresponding to global drift ratio (GDR, roof displacement divided by the height of the building) values of %0.75, 0.95 and 0.63 percent for the Erzincan, Bolu and Bingöl buildings.

- The NTHA results indicate that the maximum ISDR values (1.49, 1.01, and 0.56 percent) were obtained for the buildings in Erzincan, Bolu and Bingöl, in descending order. Peak values were obtained for the first and second floors. The ground level ISDR was lower comparatively due to its higher story height.

- The nonlinear static analysis results indicate that the maximum ISDR values (0.87, 1.09, and 0.73 percent) were obtained for the buildings in Erzincan, Bolu and Bingöl, respectively.

- If the structural damage is related to ISDR results of both NTHA and nonlinear static analyses, damage levels of "slightly higher than immediate occupancy" and "immediate occupancy" would be calculated for the Bolu and Bingöl buildings, respectively. However, the observed damage was "severe" and "moderate" for these buildings in the same order. The Erzincan building was calculated to be in "immediate occupancy-life safety" level according to the NTHA result and in "immediate occupancy" level for nonlinear static analysis result, whereas "light damage" was observed after the earthquake. Hence, it is impossible to discuss the superiority of one method over another considering such divergent results with the observed behavior. In conclusion, the performance assessment results based on the ISDR criterion and ATC-40 acceptance limits give

variable estimates for the buildings that were subjected to different near-field ground motions.

- If the structural damage is related to ISDR results of NTHA and nonlinear static analysis, the most severe damage would be expected at the first and second floors compared to the others. However, the observations following the earthquakes indicate that the structural damage was concentrated in the bottom three stories diminishing from the lower to the upper.

- The performance assessment of shear-critical columns based on Eqn. 5.1of ASCE/SEI-41 overestimates the observed damage for all buildings. The reason for this overestimation may be the limitation of the shear strength assigned to the columns with nonconforming transverse reinforcement, in accordance with the prescriptions of ASCE/SEI-41. Hence, during the calculation of shear capacities of columns, half of the term corresponding to contribution of transverse reinforcement was taken into consideration. Moreover, in the presence of low quality concrete, the effect of this limitation on calculation of shear capacity becomes more significant.

- The beams of the Bolu building were calculated to be in IO-LS performance level as per ASCE/SEI-41 where they sustained "moderate damage" during the earthquake. The beams in the Bingöl building were calculated to be in IO level as per ASCE/SEI-41 where they sustained "light damage" during the excitation. Thus, these estimations are consistent with the observed damage. The assessment results of TEC are similar to that of ASCE/SEI-41; however, TEC overestimates the damage level in some beams. This difference may be related to the different acceptance criteria and limit values suggested by the codes.

- Calculated damage in the hollow clay brick infill walls are in agreement with the observed damage except for the Erzincan case.

- More severe damage might be expected for the Erzincan building than the Bingöl building due to being subjected to the ground motion with a large acceleration pulse. However, as stated before, the Erzincan building performed the best and was used for business just after the earthquake.

- This study indicates that the current performance assessment methods and established guidelines provide reasonable estimates for the performance of the structures; however, there is still much uncertainty in estimation of dynamic response of the RC structures subjected to a suite of differing strong ground motions. These uncertainties are grouped under these headings:
  - *Precise Input Motion,*
  - *Quality of Materials*
  - *Quality of Workmanship,*
  - *Seismic Joints and Pounding*

- It is difficult to simulate and evaluate the actual behavior of the structure as constructed, especially for the buildings sustained distinct pulse-like behavior such as the Erzincan ground motion. In this circumstance, the analytical model, analyses and performance assessment methods do not provide a definite prediction. To make better estimates, the following criteria must be fulfilled:
  - Demand and capacity predictions must be understood better under dynamic loading effects,
  - Performance limits and criteria must be refined through further systematic research before they are incorporated into routine engineering practice and

141

o Software used to establish the analytical models of the structures should be developed with contribution of necessary elements to obtain more realistic outcomes.

6.2.3 The Performance Assessment Procedures

- The columns of RC buildings constructed in the1980s in Turkey are prone to shear failure due to existence of insufficient and inadequate transverse reinforcement. However, the performance assessment of these members may overestimate the damage level due to high safety provisions of the current codes.

- The strain limits specified in TEC are likely to be extremely variable in actual circumstances. Thus, in place of individual strains, rotations should be preferred (SPEAR Test building)

- The critical criterion in determining the performance level of the under-reinforced nonconforming beams is the steel strain. Thus, while high strain values occur in the tension steel, compressive strain in the extreme fiber of the concrete section is still at a very low value which is the typical behavior in an under-reinforced section.

- The 2007 version of ASCE/SEI-41 gives more conservative results compared to updated one (2008) when the performance of columns with nonconforming transverse reinforcement are assessed. Evaluation based on the new version is more consistent with the observed damage (SPEAR Test building).

- The main difference between the procedures arises from the difference of definitions in the acceptance limit values, even in the case of a specimen with well known properties tested under tightly controlled circumstances

- The nominal shear strength formulation of ASCE/SEI-41 (Eq. 5.1) tends to underestimate the shear capacity of nonconforming columns due to high safety provisions.

- The demand and capacity predictions must be understood better under dynamic loading effect and performance limits-criteria must be refined through further systematic research before they are incorporated into routine engineering practice.

- Loss estimation procedures are likely to be no more than simplified ways of modeling structural response on the basis of more detailed experimental and analytical evidence. It is not encouraging that far more detailed analyses that have been conducted in this study have failed to arrive at correct damage quantities. We do not know of average damage estimation can be made to match with field experience. This leads to the obvious recommendation for caution in making definite loss estimates for they may turn out to be incorrect by very large margins.

6.2.4   The Software and Analytical Modeling

- Typical computational tools on which engineers base their judgment are flawed under the current state-of-the-knowledge.

.

- A 3D joint model accounting for beam-column connections should be developed. Thus, experimental evidence is needed.

- Element models considering the axial-flexure-shear interaction should be implemented to the analysis program.

6.3   RECOMMENDATIONS FOR FUTURE STUDIES

- Variability under field conditions is likely to be much higher because properties of existing buildings and precise ground motions to which they have been subjected are typically known only approximately, if at all. In this concept, laboratory tests provide valuable data to understand the behavior of buildings under seismic actions. In spite of their high cost and time demand, pseudo-dynamic and shaking table tests should be performed to understand bi-directional dynamic response of RC structures and elements.

- Structures that are well instrumented to measure the input motion and inelastic response are of importance to understand how successful the current codes are in making accurate predictions. Ideally in different seismic regions, identical buildings with same design and architectural properties should be instrumented for this purpose.

REFERENCES

Akıncı A., Malagnini L., Hermann R.B., Pino A.N., Scognamiglio L., Eyidoğan H., 2001, "High-Frequency Ground Motion in the Erzincan Region, Turkey: Inferences from Small Earthquakes", Bulletin of the Seismological Society of America, Volume 91, No.6, pp. 1446-1455.

Akkar S. and Gülkan P., 1999, "Effect of Record Processing Schemes on Damage Potential of Near field Earthquakes," Fourth European Conference on Structural Dynamics, Prague, Czech Republic, pp. 1101-1106.

Akkar S. and Gülkan P., 2002, "A Critical Examination of Near-Field Accelerograms from the Sea of Marmara Region Earthquakes", Bulletin of the Seismological Society of America, Volume 92, No.1, pp. 428-447.

Akkar S., Boore D.M., Gülkan P., 2005. "An Evaluation of the Strong Ground Motion Recorded During the May 1, 2003 Bingöl Turkey, Earthquake", Journal of Earthquake Engineering, Volume 9, No.2, pp. 173-197.

Akkar S., Yazgan U. and Gülkan P., 2005, "Drift Estimates in Frame Buildings Subjected to Near-Fault Ground Motions", Journal of Structural Engineering, ASCE, Volume 131, No.7, pp. 1014-1024.

Akyüz H.S., Hartleb R., Barka A., Altunel E., Sunal G., Meyer B. and Armijo R., 2002, "Surface Rupture and Slip Distribuiton of The 12 November Düzce Earthquake (M7.1), North Anatolian Fault, Bolu, Turkey", Bulletin of the Seismological Society of America, Volume 92, No.1, pp.61-66.

Alavi B. and Krawinkler H., 2001, "Effects of Near-Fault Ground Motions on Frame Structures", Report No. 138, The John A. Blume Earthquake Engineering Center, Department of Civil and Environmental Engineering, Stanford, CA.

Ambraseys N.N., A. Zatopek, M. Taşdemiroğlu, and A. Aytun, 1968, "The Mudurnu Valley (West Anatolia) Earthquake of 22 July 1967", UNESCO Publications, Paris, No.622, 135 pp.

Ambraseys N.N., and Jackson J.A., 1998, "Faulting Associated with Historical and Recent Earthquakes in the Eastern Mediterranean Region", Journal of International Geophysics, Volume 33, pp. 390-406.

American Concrete Institute, 2008, "ACI Committee 318 Building Code Requirements for Structural Concrete (ACI 318–08) and Commentary (ACI 318R-088)", Farmington Hills, Michigan.

American Society of Civil Engineers (ASCE), 2007, "Seismic Rehabilitation of Existing Buildings", Reston, Virginia.

American Society of Civil Engineers (ASCE), 2008, "Seismic Rehabilitation of Existing Buildings", ASCE/SEI 41-06 Supplement 1, Reston, Virginia.

Anderson J. C. and Bertero, V. V., 1987, "Uncertainties in Establishing Design Earthquakes", Journal of Structural Engineering, ASCE , Volume 11, No.8, 1709-1724.

Anderson J.C. and Naeim F., 1984, "Design Criteria and Ground Motion Effects In the Seismic Response of Multi-storey Buildings", Proc. Applied Technology Council, AT*C* 10-1, Seminar on Earthquake Ground Motion and Building Damage Potential, San Francisco.

Antoniou S., Rovithakis A., Pinho R., 2002, "Development and Verification of a Fully Adaptive Pushover Procedure", Proceedings of the Twelfth European Conference on Earthquake Engineering, London, UK, Paper No. 822.

Applied Technology Council, 1996, "Seismic Evaluation and Retrofit of Concrete Buildings", ATC-40 Report, Redwood City, California.

Applied Technology Council, 2005, "Improvement of Nonlinear Static Seismic Analysis Procedures", Report Federal Emergency Management Agency-FEMA 440, Washington, DC.

Applied Technology Council, ATC-55, 2003. "Improvement of Inelastic Seismic Analysis Procedures: Draft Report for ATC55 Project", Redwood City, CA.

Aschheim M.A., Moehle J.P. and Lynn A., 1998, "Progress in Structural Engineering and Materials", Volume 1, No.4, pp. 370-377.

Asteris P.G, 2003, "Lateral Stiffness of Brick Masonry Infilled Frame Planes", Journal of Structural Engineering, Volume 129, No.8, pp. 1071-1079.

Aydınoğlu M.N., 2003, "An Incremental Response Spectrum Analysis Procedure Based On Inelastic Spectral Deformation for Multi-mode Seismic Performance Evaluation", Bulletin of Earthquake Engineering, Volume 1, 3-36.

Aziz T.S., 1976, "Inelastic Dynamic Analysis of Building Frames", Publication No. R76-37, Department of Civil Engineering, Massachusetts Institute of Technology, Cambridge.

Bae S. and Bayrak O., 2008, "Plastic Hinge Length of Reinforced Concrete Columns", ACI Structural Journal, Volume 105, No.3, pp. 290-300.
Baker A.L.L., 1956, "Ultimate Load Theory Applied to the Design of Reinforced and Prestressed Concrete Frames", Concrete Publications Ltd., London, UK, pp. 91.

Barka A., 1996, "Slip Distribution Along the North Anatolian Fault Associated with Large Earthquakes of the Period 1939–1967, Bulletin of the Seismological Society of America, Volume 59**,** pp. 521–589.

Barka A., Reilinger R., 1997, "Active Tectonics of the Eastern Mediterranean Region, Deduced from GPS, Neotectonic, and Seismicity Data", Annali Geofisica, Volume 40, pp. 587-610.

Barka A.A., Toksöz M.N., Kandisky-Cade K., and Gülen L., 1987, "Segmentation, Seismicity and Earthquake Potential of the Eastern Part of the North Anatolian Fault Zone", Yerbilimleri, Volume 14, pp. 275–283.

Barka, A., and Gülen L., 1989, "Complex Evolution of the Erzincan Basin (eastern Turkey)", Journal of Structural Geology, Volume 11, pp. 275–283.

Bathe K.J., 1982, "Finite Element Procedures in Engineering Analysis", Prentice-Hall Inc.

Bayülke N., 1993, "Report on March 13, 1992 Erzincan Earthquake", Earthquake Research Department of General Directorate of Disaster Affairs, Ministry of Public Works and Resettlement, Ankara.

Blandon C.A., 2005, "Implementation of an Infill Masonry Model for Seismic Assessment of Existing Buildings", Individual Study, European School for Advanced Studies in Reduction of Seismic Risk (ROSE School), Pavia, Italy

Bobet A. and Çetin K.Ö., 2004. 1 May 2003 Bingöl Earthquake Engineering Report, Publication No: 2004/1, Editors:Özcebe, G., Ramirez, J., Wasti T.S., Yakut A, Tübitak-METU, Ankara.

Boore M.D. and Zoback D.M., 1974, "Two-Dimensional Kinematic Fault Modeling Of The Pacoima Dam Strong-Motion Recordings of the February 9, 1971, San Fernando Earthquake", Bulletin of the Seismological Society of America, Volume 64, No.3, pp. 555-570.

Bracci J.M., Kunnath S.K., and Reinhorn A.M., 1997, "Seismic Performance and Retrofit Evaluation of Reinforced Concrete Structures", Journal of Structural Engineering, ASCE, Volume 123, No.1, pp. 3-10.

Browning J.P., 2001, "Proportioning of Earthquake-Resistant RC Building Structures", Journal of Structural Engineering, ASCE, Volume 127, pp. 145-151.

Çağnan, Z., 2001, "Three Dimensional Nonlinear Dynamic Analysis of a Reinforced Concrete Frame Building in Bolu", MS Thesis, Middle East Technical University, Ankara.

Çelebi M., 1993, The Reconstruction of Erzincan, Turkey, EERI Special Earthquake Report.

Chopra A.K. and Goel R.K., 1999, "Evaluation of NSP to Estimate Seismic Deformation: SDF Systems", Journal of Structural Engineering, ASCE, Volume 126, No.4, pp. 482–490.

Chopra A.K. and Goel R.K., 2002, "A Modal Pushover Analysis Procedure for Estimating Seismic Demands of Buildings", Earthquake Engineering and Structural Dynamics, Volume 31, pp.561-582.

Corley W.G., 1966, "Rotational Capacity of Reinforced Concrete Beams", Journal of the Structural Division, ASCE, Volume 92, (ST5), pp. 121-146.

Crisafulli F.J., 1997, "Seismic Behaviour of Reinforced Concrete Structures with Masonry Infills," University of Canterbury, PhD Thesis.

Cuesta I., Ascheim M.A., Fajfar P., 2003, "Simplified R-Factor Relationships for Strong Ground Motions", Earthquake Spectra, Volume 19, No.1, pp. 25-45.

Doğangün A., 2004. "Performance of Reinforced Concrete Buildings during the May 1, 2003 Bingöl Earhquakes in Turkey, Engineering Structures; Volume 26, pp. 841-856.

Elnashai A.S., 2001, "Advanced Inelastic Static (pushover) Analysis for Earthquake Applications, Structural Engineering and Mechanics, Volume 12, No.1, pp. 51-69.

Emre O., Herece E., Doğan A., Parlak O., Ozaksoy V., Çıplak R ve Özalp S., 2003, "1 Mayıs 2003 Bingöl Depremi", http://www.mta.gov.tr/Bingöl/Bingöl.asp, pp.17. (unpublished report in Turkish), 18/05/2005.

Fajfar P. and Fischinger M., 1988, "N2–A Method for Nonlinear Seismic Analysis of Regular Structures", Proceedings of 9th World Conference on Earthquake Engineering, Tokyo-Kyoto, Japan.

Fajfar P., 1999, "Capacity Spectrum Method Based On Inelastic Demand Spectra", Earthquake Engineering and Structural Dynamics, Volume 28, pp. 979-993.

Fajfar P., 2000, "A Nonlinear Analysis Method for Performance Based Seismic Design", Earthquake Spectra, Volume 16, No.3, pp. 573-592.

Federal Emergency Management Agency, 1988, FEMA 310. "Handbook for the Seismic Evaluation of Buildings", American Society of Civil Engineers for the Federal Emergency Management Agency, Washington D.C.

Federal Emergency Management Agency, 1988. Rapid Visual Screening of Building for Potential Seismic Hazards: A Handbook FEMA 154 Earthquake Hazards Reduction Series 41". July.

Federal Emergency Management Agency, 1997, "NEHRP Guidelines for the Seismic Rehabilitation of Buildings", FEMA-273, Applied Technology Council (ATC-33 Project), Redwood City, CA.

Federal Emergency Management Agency, 2000, "Prestandard and Commentary for the Seismic Rehabilitation of Buildings", FEMA-356, American Society of Civil Engineers, Reston, Virginia.

Freeman S.A, 1978, "Prediction of Response of Concrete Buildings to Severe Earthquake Motion", Douglas McHenry International Symposium on Concrete and Concrete Structures, American Concrete Institute, Detroit, sp 55, pp. 589-605.

Goel R.K., 2003, "Evaluation of Nonlinear Static Procedures Using Strong-Motion Records of Buildings", CSMIP Data Utilization Report, California Strong Motion Instrumentation Program, California Geological Survey, Sacramento, CA.

Goel R.K., 2005, "Evaluation of Modal and FEMA Pushover Procedures Using Strong-Motion Records of Buildings", Earthquake Spectra, Volume 21, No.3, pp. 653-684.

Goel R.K. and Chadwell C., 2007, "Evaluation of Current Nonlinear Static Procedures For Concrete Buildings Using Recorded Strong-Motion Data", Report, Department of Civil and Environmental Engineering, California Polytechnic State University, San Luis Obispo.

Gupta A. and Krawinkler H., 2000, "Estimation of Seismic Drift Demands for Frame Structures", Earthquake Engineering and Structural Dynamics, Volume 29, 1287-1305.

Gupta B. and Kunnath S.K., 2000, "Adaptive Spectra-based Pushover Procedure for Seismic Evaluation of Structures", Earthquake Spectra, Volume 16, No.2, pp. 367-392.

Gülkan P., and Sözen M.A., 1974, "Inelastic Responses of Reinforced Concrete Structures to Earthquake Motions", American Concrete Institute, Volume 71, No.12, pp. 604-610.

Gülkan P., 1993, "Special In-Country Report", Earthquake Spectra, Volume 9, pp. 149-210.

Gülkan P. and Sözen M.A., 1999, "A Procedure for Determining Seismic Vulnerability of Building Structures", ACI Structural Journal, Volume 96, No.3, pp. 336-342.

Gülkan, P. and Akkar, S., 2004, 1 May 2003 Bingöl Earthquake Engineering Report, Publication No: 2004/1, Editors:Özcebe, G., Ramirez, J., Wasti T.S., Yakut A, Tübitak-METU, Ankara.

Gülkan, P., 2004. "Seismic Safety of School Buildings in Turkey: Obstacles Impeding the Achievable?", Ad Hoc Experts Group Meeting on Earthquake Safety in Schools, OECD Programme on Educational Building and GeoHazards International, Paris.

Gür T., Pay A.C., Ramirez J.A., Sözen M.A, Johnson A.M, İrfanoğlu A., Bobet A., 2009, "Performance of School Buildings in Turkey During the 1999 Düzce and the 2003 Bingöl Earthquakes", Earthquake Spectra, Volume 25, No.2, pp. 239-256.

Hamburger R.O. and Chakradeo A.S., 1993, "Methodology For Seismic Capacity Evaluation of Steel-Frame Buildings with Infill Unreinforced Masonry. Proceedings of the 1993 National Earthquake Conference, Earthquake Hazard Reduction in the Central and Eastern United States, Memphis, TN.

Hassan A.F. and Sözen M. A., 1997, "Seismic Vulnerability Assessment of Low-rise Buildings in Regions with Infrequent Earthquakes, ACI Strucutral Journal, Volume 94, pp. 31–39.

Hencher S.R. and Acar I.A, 1995, "The Erzincan Earthquake, Friday, 13 March 1992", Quarterly Journal of Engineering Geology and Hydrogeology, Volume 28, pp. 313-316,

Holmes M., 1961, "Steel Frames with Brickwork and Concrete Infilling", Proceedings of Institute of Civil Engineers, London, England, Part 2, Volume 73, 473-478.

Housner G.W. and Trifunac M.D., 1967, "Analysis of Accelerograms: Parkfield Earthquake", Bulletin of the Seismological Society of America, Volume 57, No.6, pp. 1193-1220.

Iwan, W.D., Huang, C.-T. and Guyader, A.C., 2000, "Important Features of the Response of Inelastic Structures to Near-field Ground Motion", Paper. No. 1740, Proceedings of the 12th World Conference on Earthquake Engineering, Auckland, New Zealand.

Jeong S-H. and Elnashai A.S., 2004, "Analytical Assessment of an Irregular RC Full Scale 3D Test Structure, Mid-America Earthquake Centre", University of Illinois at Urbana-Champaign.

Kalkan E. and Gülkan P., 2004, "Site-dependent Spectra Derived From Ground Motion Records in Turkey", Earthquake Spectra, Volume 20, pp.1111-1138.

Klingner R. E., and Bertero V. V., 1976, "Infilled Frames in Earthquake Resistant Construction", Report No. EERC 76-32, Earthquake Engineering Research Center, University of California, Berkeley, CA.

Krawinkler H., 2005, "Van Nuys Hotel Building Testbed Report: Exercising Seismic Performance Assessment", Peer Report, 2005/11, UC Berkeley, Berkeley, CA.

Krawinkler H. and Seneviratna G.D.P.K, 1998, "Pros and Cons of a Pushover Analysis of Seismic Performance Evaluation", Engineering Structures, Volume 20, 4-6, pp. 452-464.

Kreger M.E, Sözen M.A., 1989, "Seismic Response of Imperial County Services Building in 1979", Journal of Structural Engineering, Volume 115, No.2, pp. 3095-3111.

Küçükdoğan B., 2007, "Investigation of the Effect of Ground-motion Intensity Measures on Seismic Demand Parameters Using Probabilistic Methods", M.Sc. Thesis, Department of Civil Engineering, Middle East Technical University, Ankara, Turkey.

Liauw T.C. and Lee S.W., 1977, "On the Behaviour and Analysis of Multi-story Infilled Frames Subject to Lateral Loading", Proc., Inst. Civ. Eng., Struct. Build., Volume 63, pp. 641–656.

Magliulo G. and Ramasco R., 2007, "Seismic Response of Three-Dimensional R/C Multi-Storey Frame Building Under Uni-and Bi-directional Input Ground Motion", Earthquake Engineering and Structural Dynamics, Volume 36, pp. 1641-1657.

Mahin S.A, Bertero V.V, Chopra A.K, Collins R.G., 1976, "Response of the Olive View Hospital Main Building During the San Fernando Earthquake", Pacific Earthquake Engineering Center, Report No. EERC 76-22, University of California, Berkeley, CA.

Mainstone R.J., 1971, "On the Stiffness and Strength of Infilled Frames", Proceedings of Institute of Civil Engineers, Suppl., London, England, pp. 57-89.

Mainstone R.J., 1974, "Supplementary Note on the Stiffnesses and Strengths of Infilled Frames", Current Paper CP 13/74, Building Research Station, Garston, Watford, United Kingdom.

Mander J.B., Priestley M.J.N., Park R., 1988, "Theoretical Stress-Strain Model for Confined Concrete", Journal of Structural Engineering, ASCE, Volume 114, No.8, pp. 1804-1826.

Makris N., and Black, C. J. 2004, "Dimensional Analysis of Bilinear Oscillators Under Pulse-type Excitations", Journal of Engineering Mechanics, Volume 130, No.9, pp. 1006–1031.

Matsumori T., Otani S., Shiohara H., Kabeyasawa T., 1999, "Earthquake Member Deformation Demands in Reinforced Concrete Frame Structures", Proceedings of the US-Japan Workshop on Performance-Based Earthquake Engineering Methodology for R/C Building Structures, PEER Center Report, UC Berkeley, pp. 79-94, Maui, Hawaii.

Mattock A.H., 1964, "Rotational Capacity of Hinging Regions in Reinforced Concrete Beams," Flexural Mechanics of Reinforced Concrete, SP-12, American Concrete Institute, Farmington Hills, MI, pp. 143-181.

Mattock A. H., 1967, "discussion of Rotational Capacity of Hinging Regions in Reinforced Concrete Beams," Journal of the Structural Division, ASCE, Volume 93, (ST2), pp. 519-522.

Mavroeidis G.P. and A.S. Papageorgiou, 2003, "A Mathematical Representation of Near-Fault Ground Motions", Bulletin of the Seismological Society of America, Volume 93, No.3, pp. 1099–1131.

Medina R.A and Krawinkler H., 2005, "Evaluation of Drift Demands For the Seismic Performance Assessment of Frames", Journal of Structural Engineering, Volume 131, No.7, pp. 1003-1013.

Menun C. and Q. Fu, 2002, "An Analytical Model for Near-fault Ground Motions and the Response of SDOF Systems, Proceedings of 7th U.S. National Conference on Earthquake Engineering, Boston, Massachusetts.

Metin A., 2006, "Inelastic Deformation Demands on Moment-Resisting Frame Structures", MS Thesis, Department of Civil Engineering, Middle East Technical University, Ankara.
Ministry of Public Works and Resettlement (MPWR), 2004, "Technical Report on Retrofit of the MPWR buildings in Erzincan and Bingöl", Ankara.

Miranda E. and Ruiz-Garcia J., 2002. "Evaluation of Approximate Methods to Estimate Maximum Inelastic Displacement Demands", Earthquake Engineering and Structural Dynamics, Volume 31, No.3, pp. 539-560.

Mola E., Negro P., Pinto A.V., 2004, "Evaluation of Current Approaches for the Analysis and Design of Multi-storey Torsionally Unbalanced Frames, Proc. of 13th World Conference on Earthquake Engineering, Vancouver, Paper No. 3304.

Negro P., Mola E., Molina F.J, Magonette G.E., 2004, "Full-scale PSD testing of a Torsionally Unbalanced Three-Storey Non-seismic RC frame. Proceedings of the 13th World Conference on Earthquake Engineering, Vancouver, BC Canada, Paper No. 968.

Özcebe G., Ramirez J., Wasti T.S., Yakut A. (Editors), 2004, "1 May 2003 Bingöl Earthquake Engineering Report", Publication No: 2004/1, Tübitak-METU, Ankara.

Özmen B. and Bağcı G, 2000, "12 November 1999 Düzce Earthquake Report", General Directorate of Disaster Affairs, Earthquake Research Department, Ministry of Public Works and Resettlement (MPWR), Ankara, Turkey.

Özmen, B., 2000, "Düzce-Bolu Bölgesi'nin Jeolojisi, Diri Fayları ve Hasar Yapan Depremleri", 12 Kasım 1999 Düzce Raporu, Afet İşleri Genel Müdürlüğü, Deprem Araştırma Dairesi, Ankara.

Papanikolaou V., 2000, "Development and Verification of Adaptive Pushover Analysis Procedures", MSc dissertation, Engineering Seismology and Earthquake Engineering Section, Imperial College, London, UK.

Park R., Priestley M.J.N. and Gill, W.D., 1982, "Ductility of Square-Confined Concrete Columns," Journal of Structural Division, ASCE, Volume 108, (ST4), pp. 929-950.

Paulay T., Priestley M.J.N, 1992, Seismic Design of Reinforced Concrete and Masonry Buildings, John Wiley and Sons, Inc, New York, New York, pp. 768.

Perform 3D, 2005. Element Descriptions, v2.52, RAM International L.L.C. Chico, CA.

Pique J.R., 1976, "On the Use of Simple Models in Nonlinear Dynamic Analysis", Publication No.R76-43, Department of Civil Engineering, Massachusetts Institute of Technology, Cambridge.

Powell G.H., and Campbell S., 1994, "Drain 3D-X Element Description and User Guide for Element Type-01, Type-04, Type-05, Type-08, Type-09, Type-15 and Type-17", Report No. UCB-SEMM-94-08, UC Berkeley, CA.

Priestley M.J.N., and Park R., 1987, "Strength and Ductility of Concrete Bridge Columns under Seismic Loading", ACI Structural Journal, Volume 84, No.1, pp. 61-76.

Rathje, E.M., Stewart J.P., Baturay M.B., Bray J.D and Bardet J.P., 2006, "Strong Ground Motions and Damage Patterns from the 1999 Düzce Earthquake in Turkey", Journal of Earthquake Engineering, Volume 10, No. 5, pp. 693-724.

Requena M., Ayala G., 2000, "Evaluation of a Simplified Method for the Determination of the Nonlinear Seismic Response of RC Frames", Proceedings of the Twelfth World Conference on Earthquake Engineering, Paper No. 2109, Auckland, New Zealand.

Saiidi M. and Sözen M.A., 1981, "Simple Nonlinear Seismic Analysis of RC Structures", Journal of Structures Division, ASCE, Volume 107, pp. 937-952.

Sasaki K.K., Freeman S.A., Paret T.F., 1998, "Multi-mode Pushover Procedure (MMP)–A method to Identify the Effects of Higher Modes in a Pushover Analysis", Proceedings of the Sixth US National Conference on Earthquake Engineering, Seattle, Washington Earthquake Engineering Research Institute, Oakland, California.

Satyarno I., Carr A.J. and Restrepo J., 1998, "Refined Pushover Analysis for the Assessment of Older Reinforced Concrete Buildings", Proceedings of the New Zealand Society for Earthquake Engineering Technology Conference, Wairakei, New Zealand, pp. 75-82.

SeismoSoft, 2006, "SeismoStruct–A Computer Program for Static and Dynamic Nonlinear Analysis of Framed Structures", (online), available from URL: http://www.seismosoft.com, 12/07/2009.

Smith B.S., 1966, "Behavior of Square Infilled Frames", J.Struct. Div., ASCE, Volume 92, (ST1), pp. 381-403.

Smith B.S., 1967, "Methods for Predicting the Lateral Stiffness and Strength of Multi-story Infilled Frames, Building Science, Volume 2, pp. 247-257.

Somerville P.G., Smith N.F., Graves R.W., Abrahamson N.A., 1997, "Modification Of Empirical Strong Ground Motion Attenuation Relations to Include the Amplitude and Duration Effect of Rupture Directivity", Seismological Research Letters, Volume 68, No.1, pp. 199-222.

Spacone E., Filippou F.C. and Taucer F., 1996, "Fibre Beam-column Model For Nonlinear Analysis of R/C Frames:Part I. Formulation, Earthquake Engineering and Structural Dynamics, Volume 25, pp. 711-725.

Sucuoğlu H. and Yazgan U., 2003, "Simple Survey Procedures for Seismic Risk Assessment in Urban Building Stocks", Seismic Assessment and Rehabilitation of Existing Buildings Nato Science Series: IV: Earth and Environmental Sciences, 29, Editors: Wasti, S.T and Özcebe G., p.546.

Sucuoğlu H., 2006, "The Turkish Seismic Rehabilitation Code", First European Conference on Earthquake Engineering and Seismology, Geneva, Switzerland.

Thiruvengadam V., 1985. "On the Natural Frequencies of Infilled Frames, Earthquake Engineering and Strucutral Dynamics, Volume 13, pp. 401–419.

Tübitak, 2009, "Seismological Features of Re-compiled Turkish Strong-Motion Database (1976-2007)",The Scientific and Technical Council of Turkey, Ankara.

Turkish Earthquake Code (TEC), 1975, "Specifications for the Buildings to be Constructed in Disaster Areas", Ministry of Public Works and Resettlement (MPWR), Ankara, Turkey.

Turkish Earthquake Code (TEC), 2007, "Specifications for the Buildings to be Constructed in Disaster Areas", Ministry of Public Works and Resettlement (MPWR), Ankara, Turkey.

Uang Chia-Ming and V. V. Bertero, 1988, "Implications of Recorded Earthquake Ground Motion on Seismic Design of Building Structures", UCB/EERC-88/13, Earthquake Engineering, Research Center, University of California, Berkeley, CA.

Yakut A., 2004 "Preliminary Seismic Performance Assessment Procedure for Existing RC Buildings", Engineering Structures, Volume 26, No.10, pp. 1447-1461.

APPENDIX A

TABLES AND DRAWINGS OF THE BUILDINGS

Appendix A contains tables that include the geometrical properties and reinforcement data of the beam-column cross sections and the architectural and engineering drawings of the MPWR buildings. Floor plans and elevation views of the buildings are shown in Figures A.1-A.10. Engineering drawings for column, beam, slab reinforcement details are presented in Figs A.11 - A.18.

Table A.1 Dimensions of all story columns, their longitudinal and transverse reinforcement ratios.

	Dimensions of All Story Columns (b/h, cm)					ρ_{sl} (%)					$\rho_{sh\text{-}x}$ (%)	$\rho_{sh\text{-}y}$ (%)
	G	1	2	3	4	G	1	2	3	4		
C1	30/80	30/80	30/60	30/60	30/60	1.90	1.90	0.86	0.86	0.86	0.17	0.13
C2	30/90	30/90	30/90	30/90	30/90	1.97	1.63	1.40	0.94	0.60	0.17	0.11
C3	30/90	30/70	30/70	30/60	30/60	1.97	2.09	1.80	1.75	0.89	0.17	0.11
C4	30/160 /147	30/160 /147	30/160 /147	30/160 /147	30/160 /147	0.64	0.59	0.59	0.59	0.59	0.17	0.06
C5	30/147	30/147	30/147	30/147	30/147	2.49	2.49	1.45	0.91	0.58	0.17	0.07
C6	40/90	40/80	30/80	30/70	30/70	1.69	1.57	1.06	0.96	0.73	0.13	0.11
C7	40/90	40/80	30/80	30/70	30/70	1.69	1.57	1.06	0.96	0.73	0.13	0.11
C8	30/147	30/147	30/147	30/147	30/147	2.49	2.49	1.45	0.91	0.58	0.17	0.07
C9	30/147	30/147	30/147	30/147	30/147	2.49	2.49	1.45	0.91	0.58	0.17	0.07
C10	40/90	40/80	30/80	30/70	30/70	1.69	1.57	1.06	0.96	0.77	0.13	0.11
C11	40/90	40/80	30/80	30/70	30/70	1.69	1.57	1.06	0.96	0.73	0.13	0.11
C12	30/147	30/147	30/147	30/147	30/147	2.49	2.49	1.45	0.91	0.58	0.17	0.07
C13	30/160 /147	30/160 /147	30/160 /147	30/160 /147	30/160 /147	0.71	0.71	0.59	0.59	0.68	0.17	0.06
C14	30/90	30/70	30/70	30/60	30/60	1.97	2.09	1.80	1.75	1.34	0.17	0.11
C15	30/90	30/70	30/70	30/60	30/60	1.97	2.09	1.80	1.75	1.34	0.17	0.11
C16	30/160 /147	30/160 /147	30/160 /147	30/160 /147	30/160 /147	0.64	0.59	0.59	0.59	0.59	0.17	0.06

G: ground story, ρ_{sl}: longitudinal reinforcement ratio, ρ_{sh}: transverse reinforcement ratio

C is for "Column" and C1-C16 represents the sixteen columns as depicted in Figure 4.8 before. The second row represents the story floors: ground, first, second, third and fourth floors. 30/80: 30 cm for the width (b_w) and 80 cm for the height (h) of section. 30/160/147: dimensions of the L shaped columns. ρ_{sl} is the longitudinal reinforcement ratio that is calculated by $A_{sl}/b_w d$. A_{sl}: area of the longitudinal reinforcement in the section. b_w: section width. d: effective depth that is taken as 0.8h. ρ_{sh} is the transverse reinforcement ratio that is calculated by $A_{sv}/ b_w s$. A_{sv}: transverse reinforcement area, s: stirrup spacing

Table A.2 Dimensions of all story beams, their longitudinal and transverse reinforcement ratios.

	b/h (cm)	ρ_{sl} (%)	ρ_{sh} (%)
B1	30/120	0.28	0.17
B2	30/120	0.28	0.17
B3	30/120	0.28	0.17
B4	30/70	0.40	0.17
B5	30/70	0.40	0.17
B6	30/70	0.40	0.17
B7	30/70	0.40	0.17
B8	30/70	0.40	0.17
B9	30/70	0.40	0.17
B10	30/60	0.47	0.17
B11	30/120	0.28	0.17
B12	30/120	0.28	0.17
B13	30/120	0.28	0.17
B14	30/120	0.28	0.17
B15	30/120	0.28	0.17
B16	30/60	0.42	0.17
B17	30/60	0.42	0.17
B18	30/60	0.42	0.17
B19	30/60	0.42	0.17
B20	30/60	0.42	0.17
B21	30/60	0.42	0.17
B22	30/120	0.28	0.17
B23	30/120	0.28	0.17
B24	30/120	0.28	0.17

B is for beam and B1-B24 represents the twenty-four beams as depicted in Figure 4.8 before. ρ_{sl} is the longitudinal reinforcement ratio that is calculated by $A_s/b_w d$. A_s: area of tension reinforcement in the section. b_w: section width. d: effective depth . ρ_{sh} is the transverse reinforcement ratio that is calculated by $A_{sv}/ b_w s$. A_{sv}: transverse reinforcement area, s: stirrup spacing
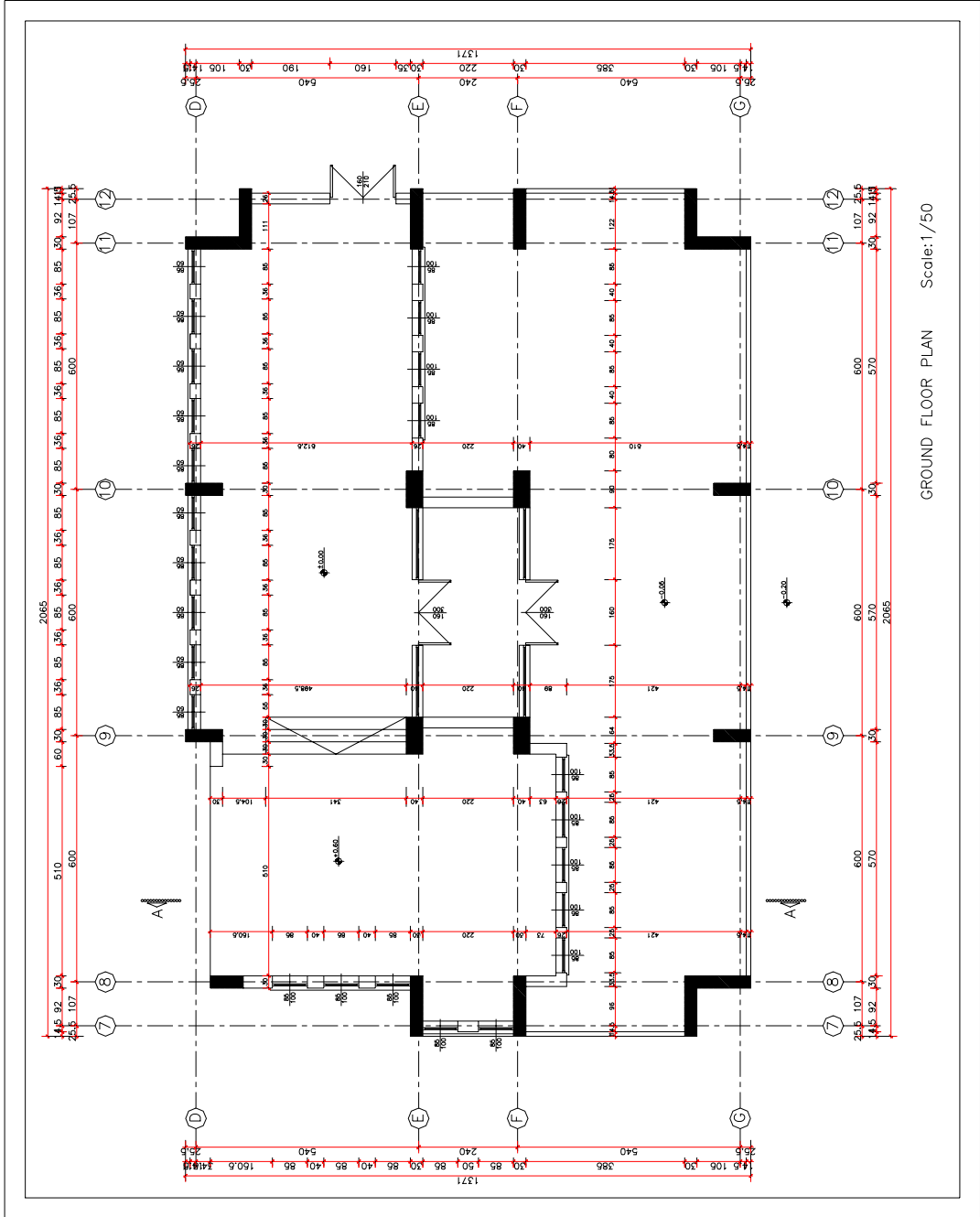
Figure A.1 Ground Floor Plan

158
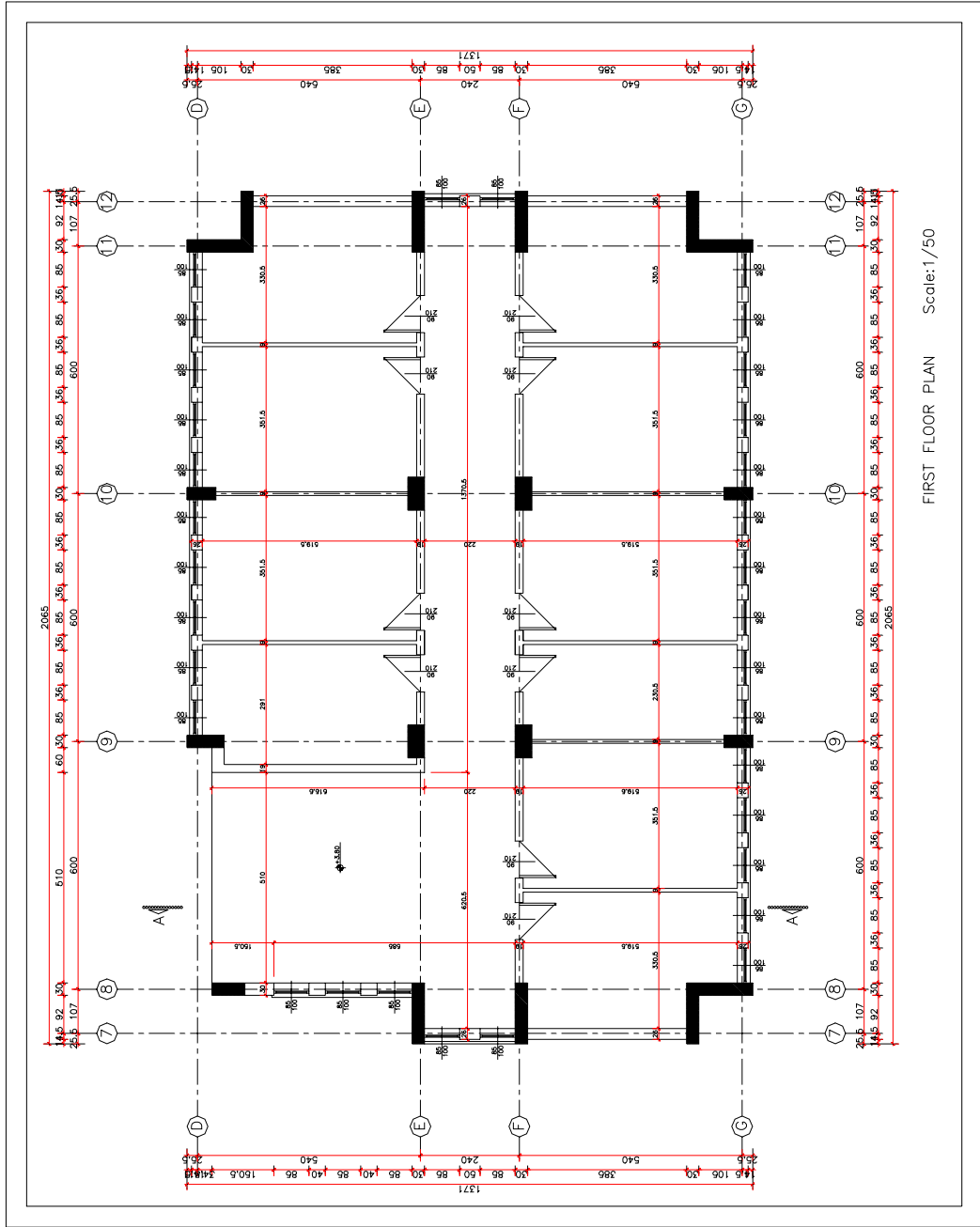
Figure A.2 First Floor Plan

159
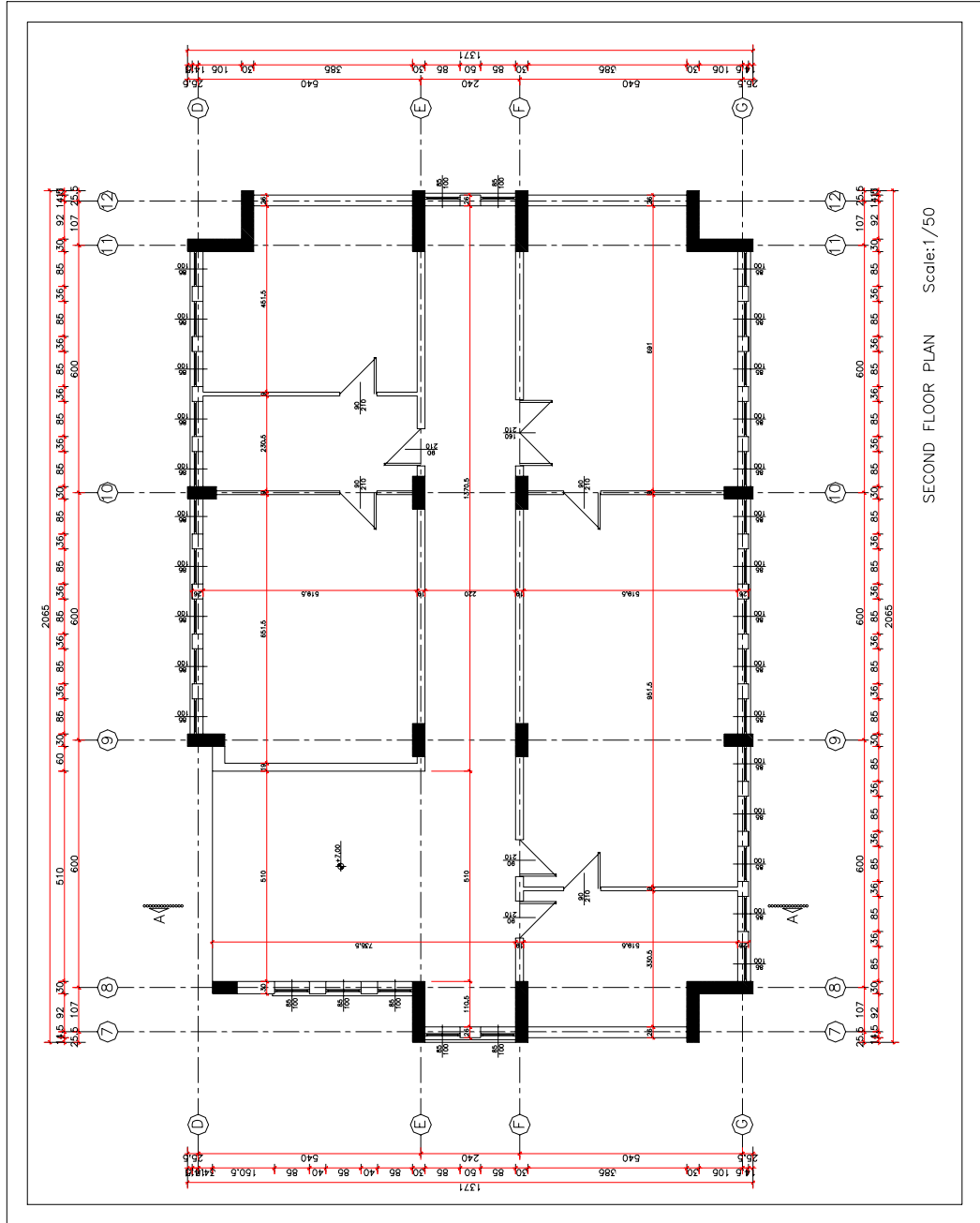
Figure A.3 Second Floor Plan
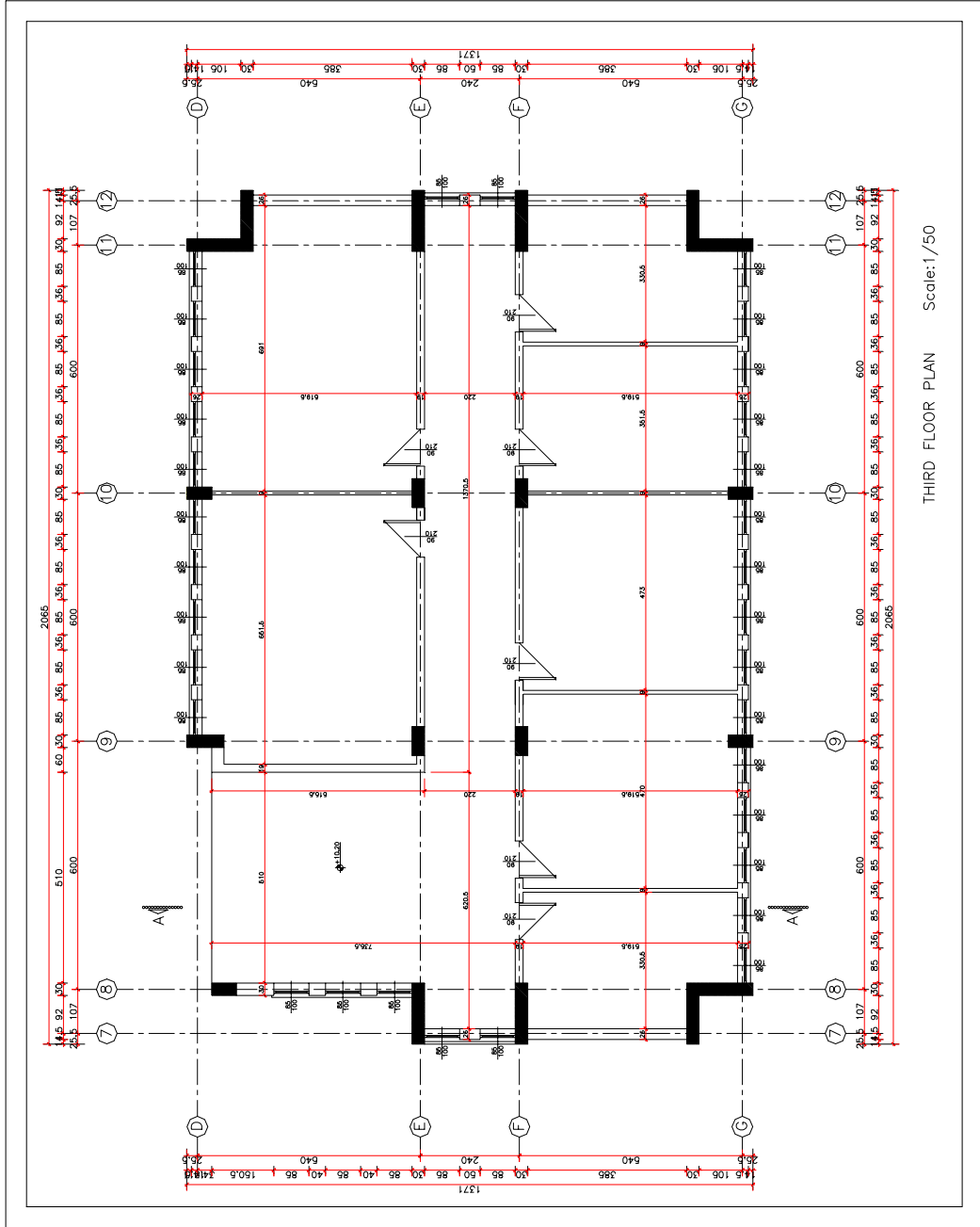
160

Figure A.4 Third Floor Plan

161
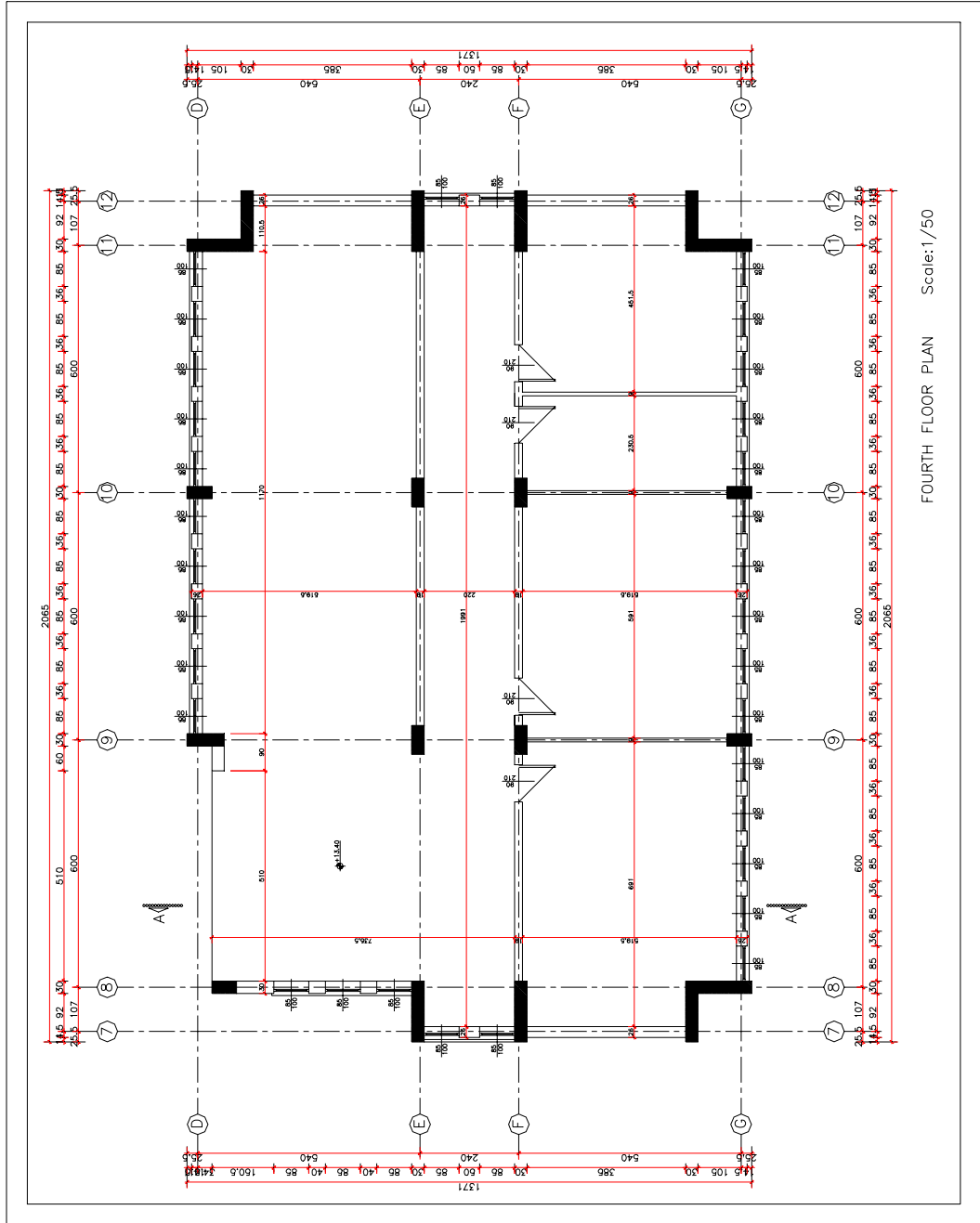
Figure A.5 Fourth Floor Plan
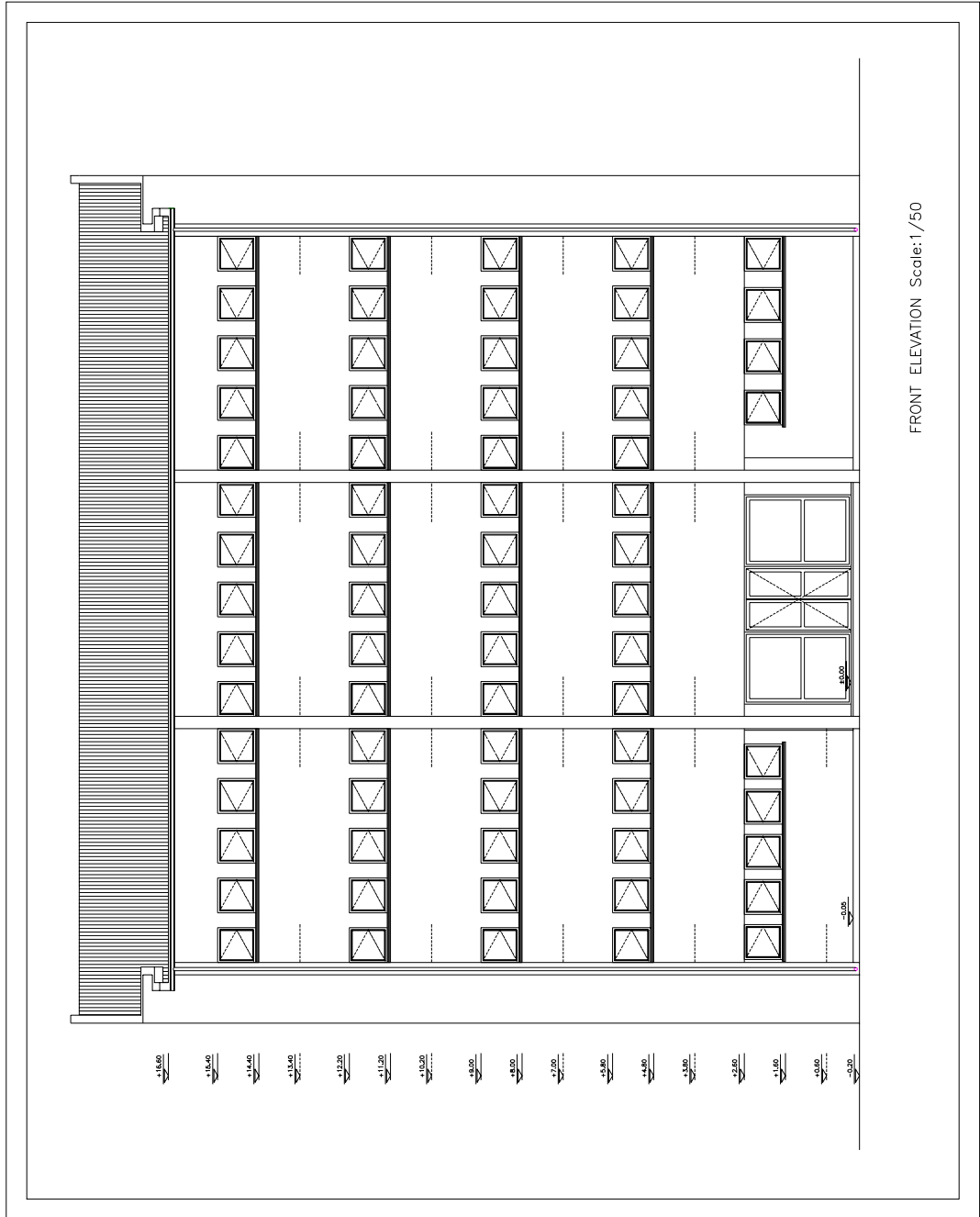
Figure A.6 Front Elevation
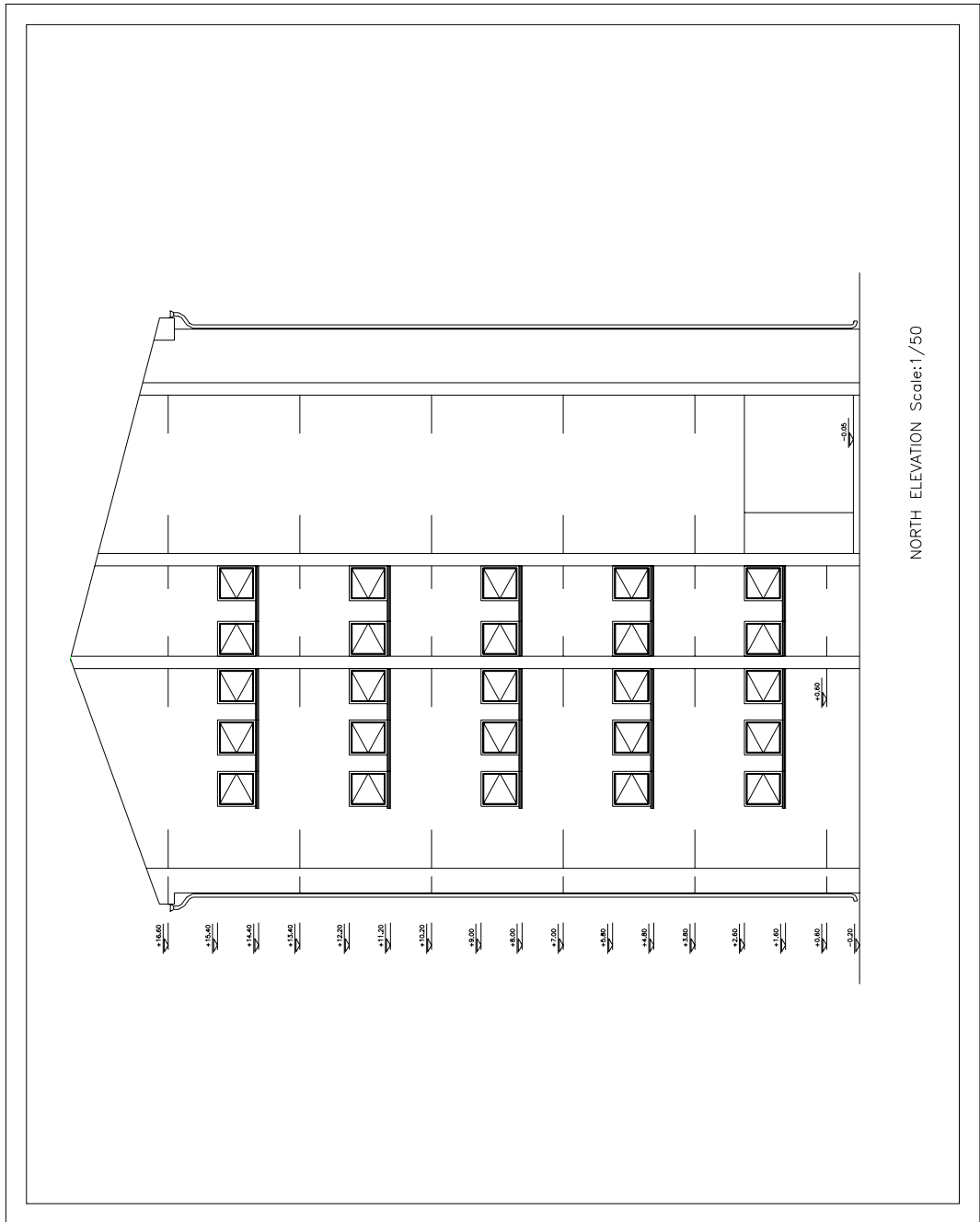
Figure A.7 North Elevation

164
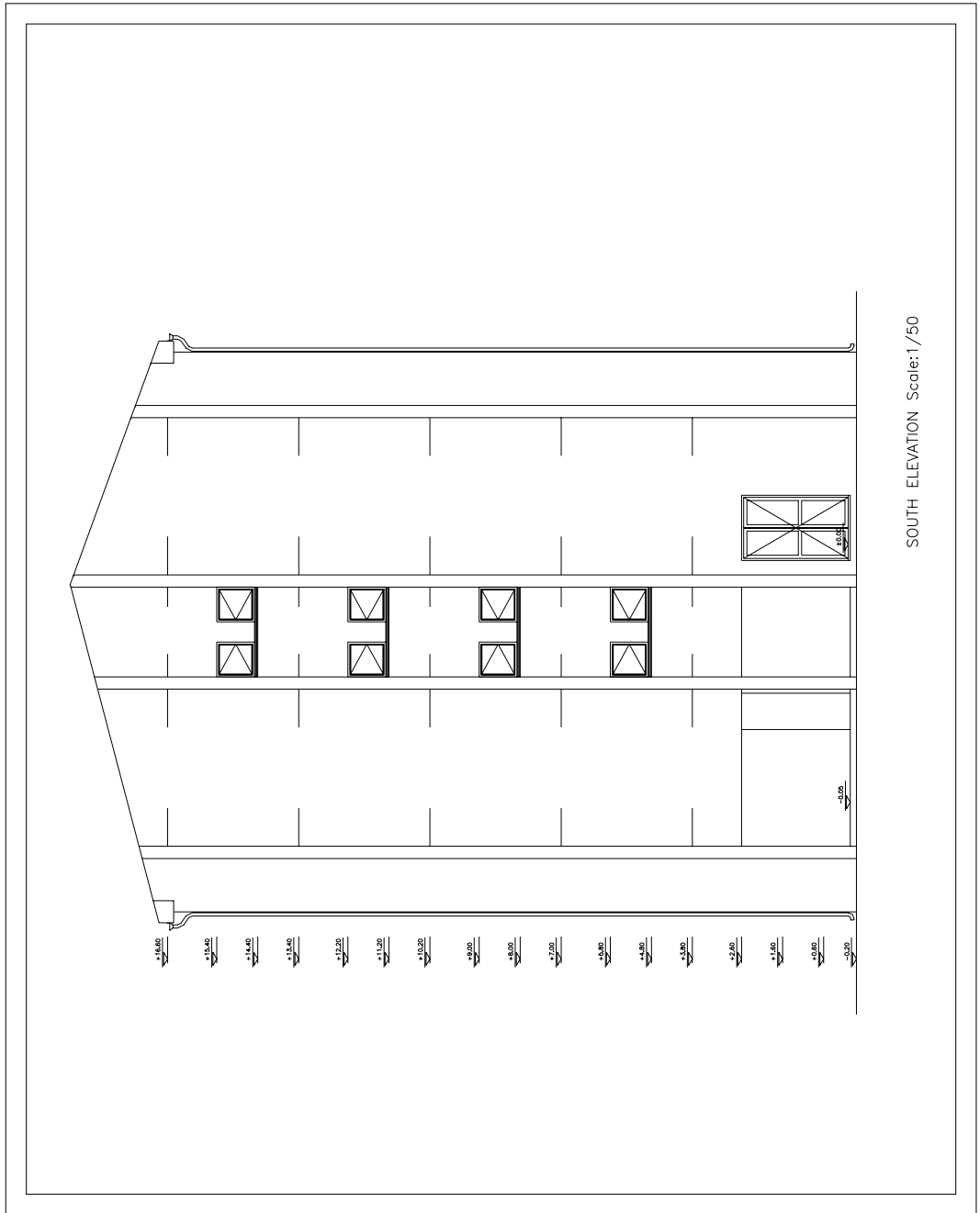
Figure A.8 South Elevation

165
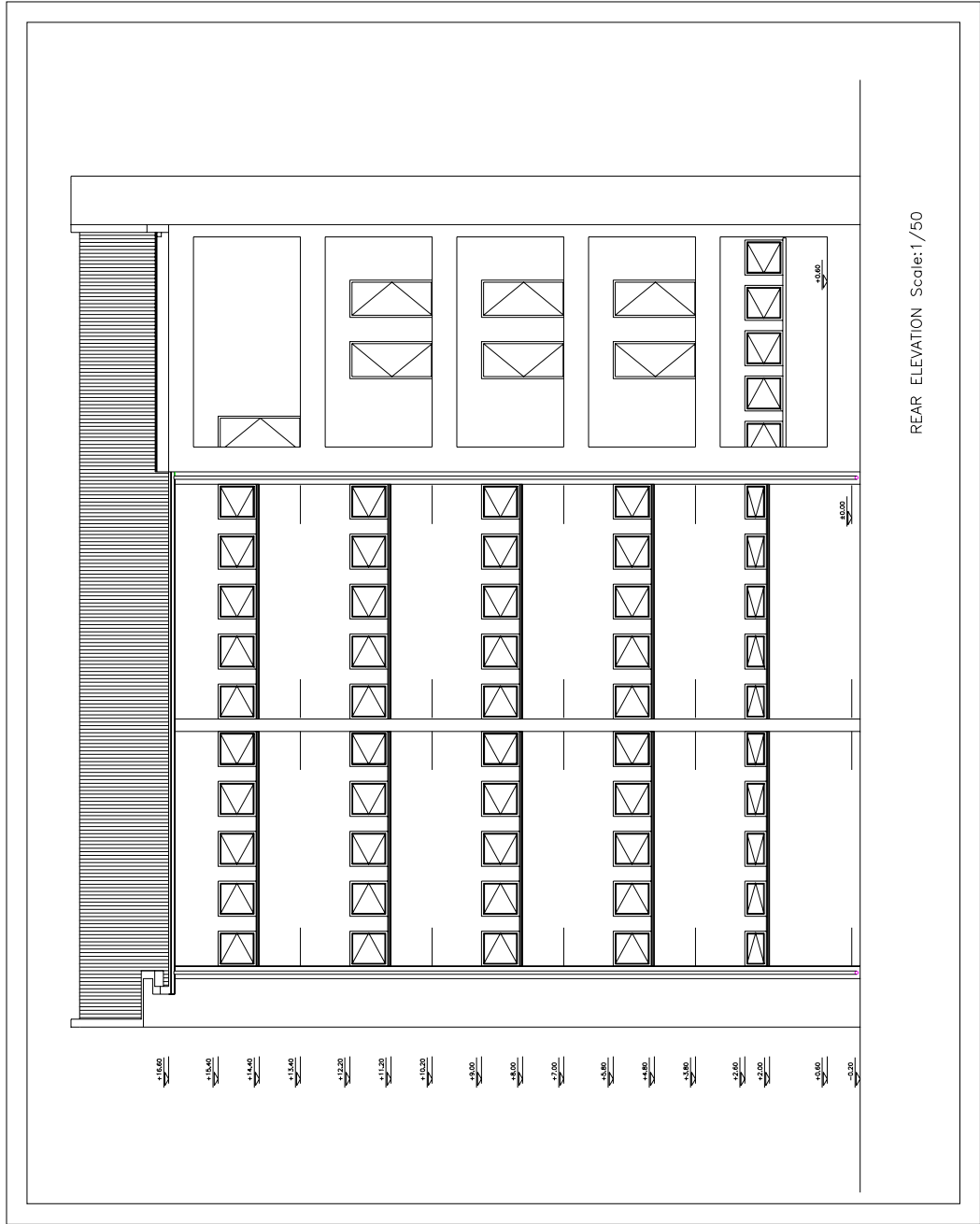
Figure A.9 Rear Elevation
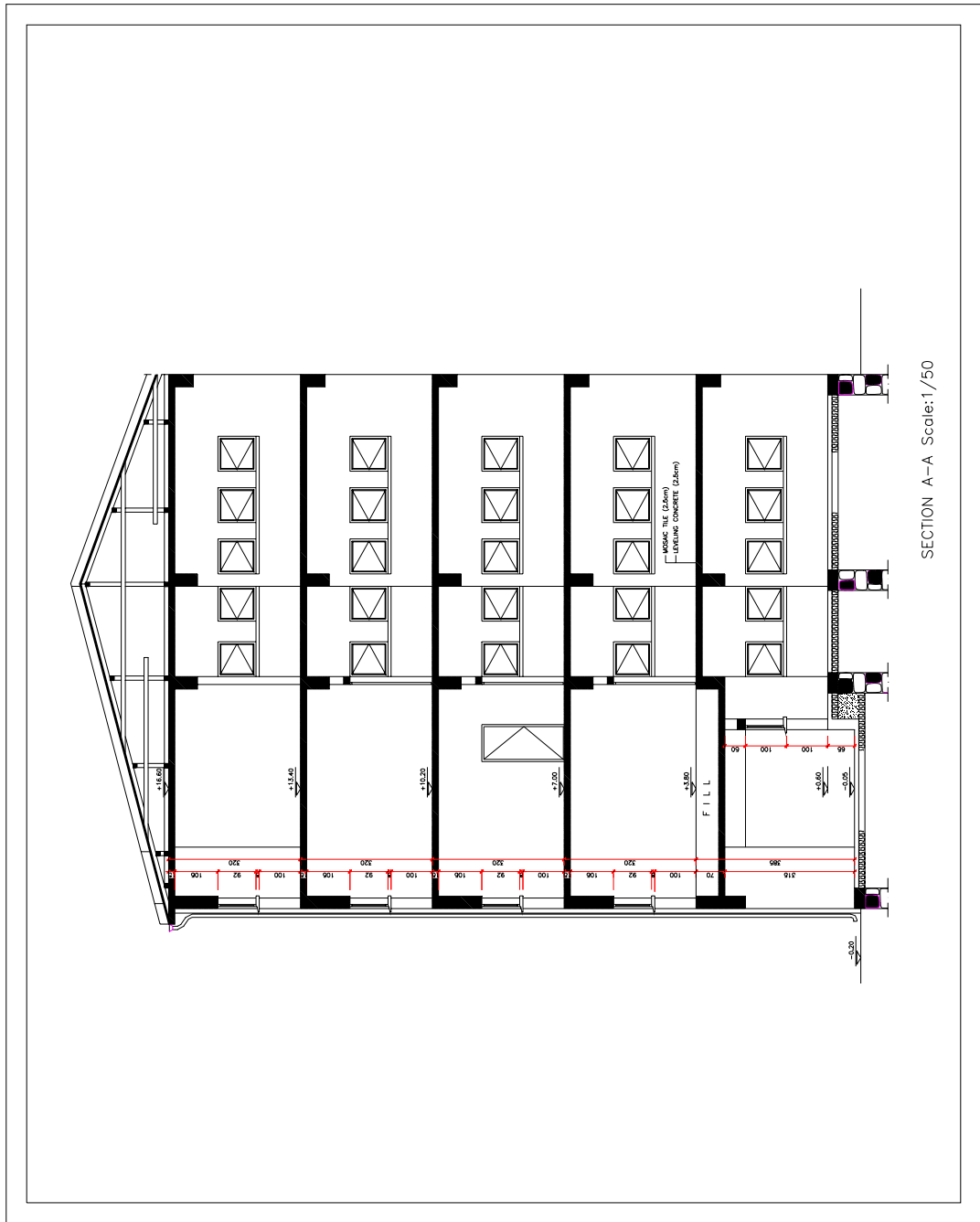
Figure A.10 Section A-A (A-A section has been depicted in Figure A.5)
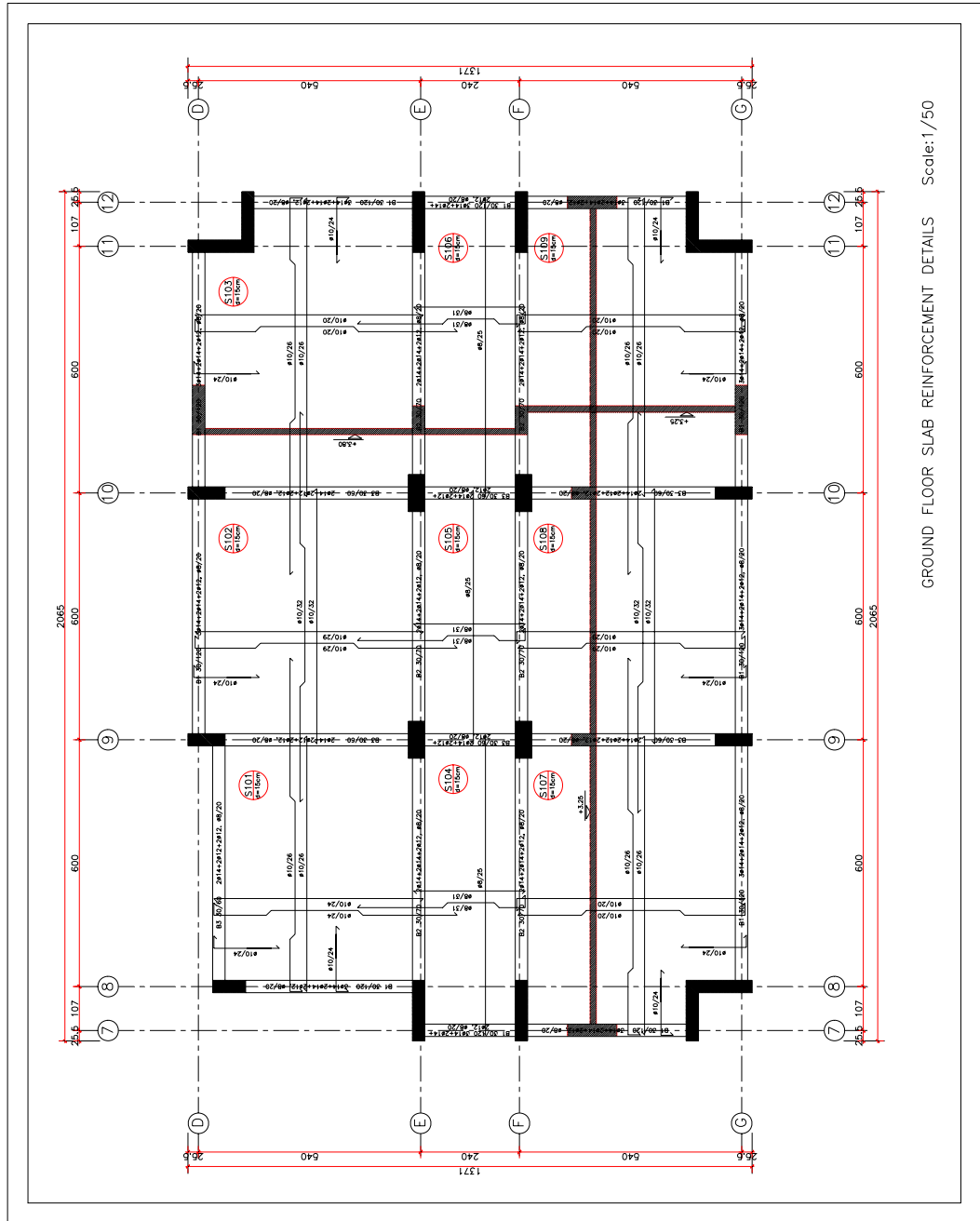
Figure A.11 Ground Floor Slab Reinforcement Details

168
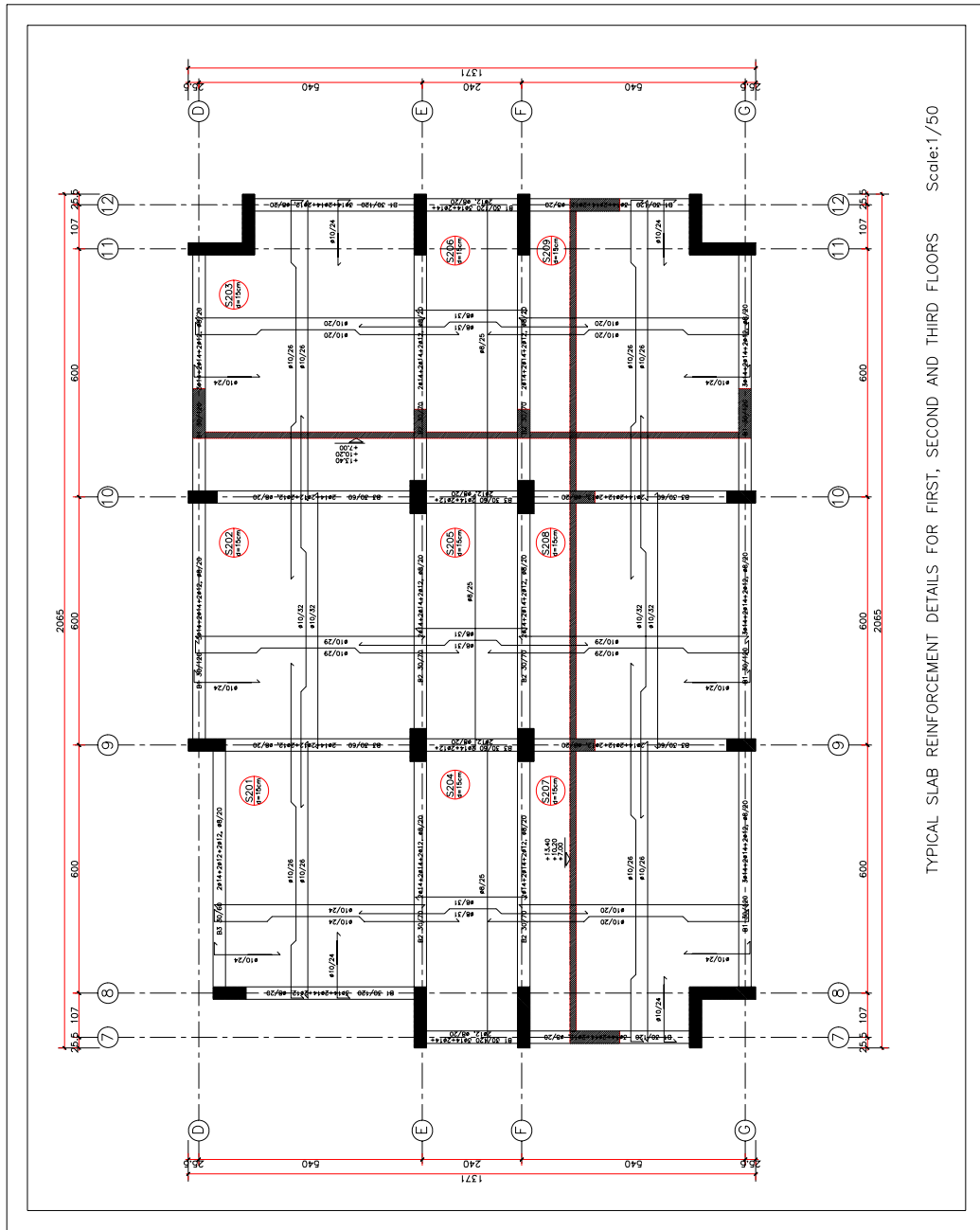
Figure A.12 Typical slab reinforcement details for the first, second and third floor levels

169
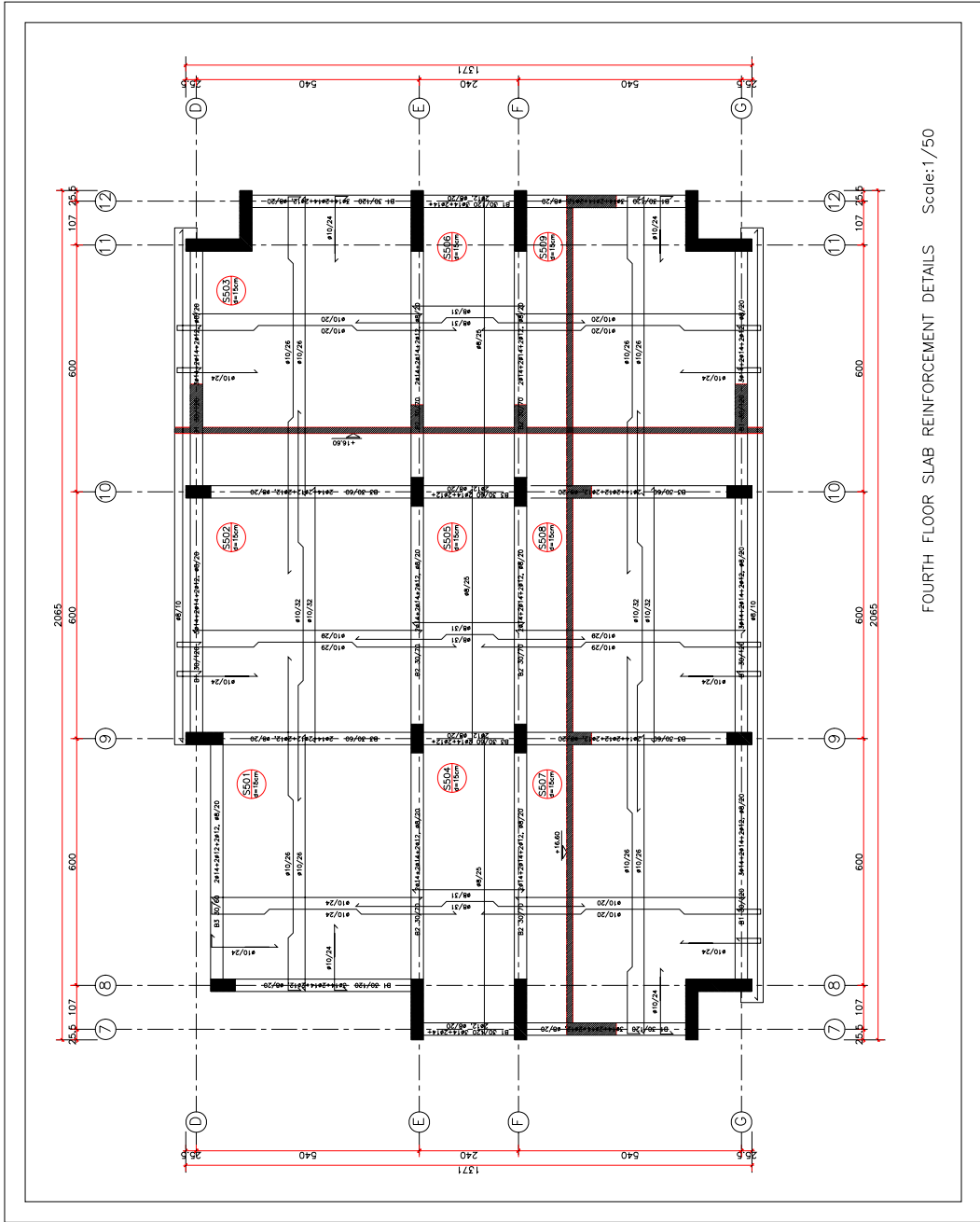
Figure A.13 Fourth floor slab reinforcement retails
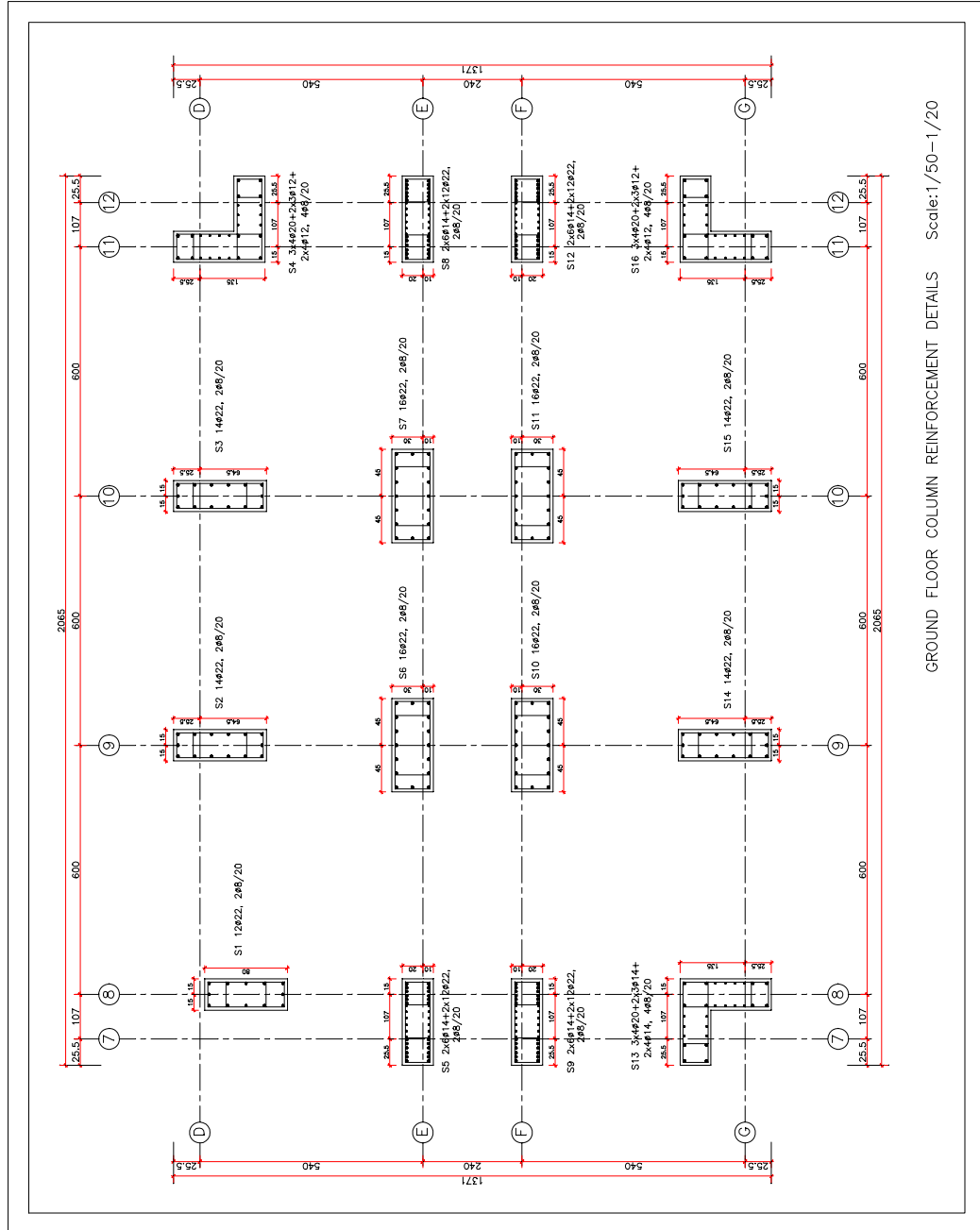
Figure A.14 Ground floor column reinforcement details

171
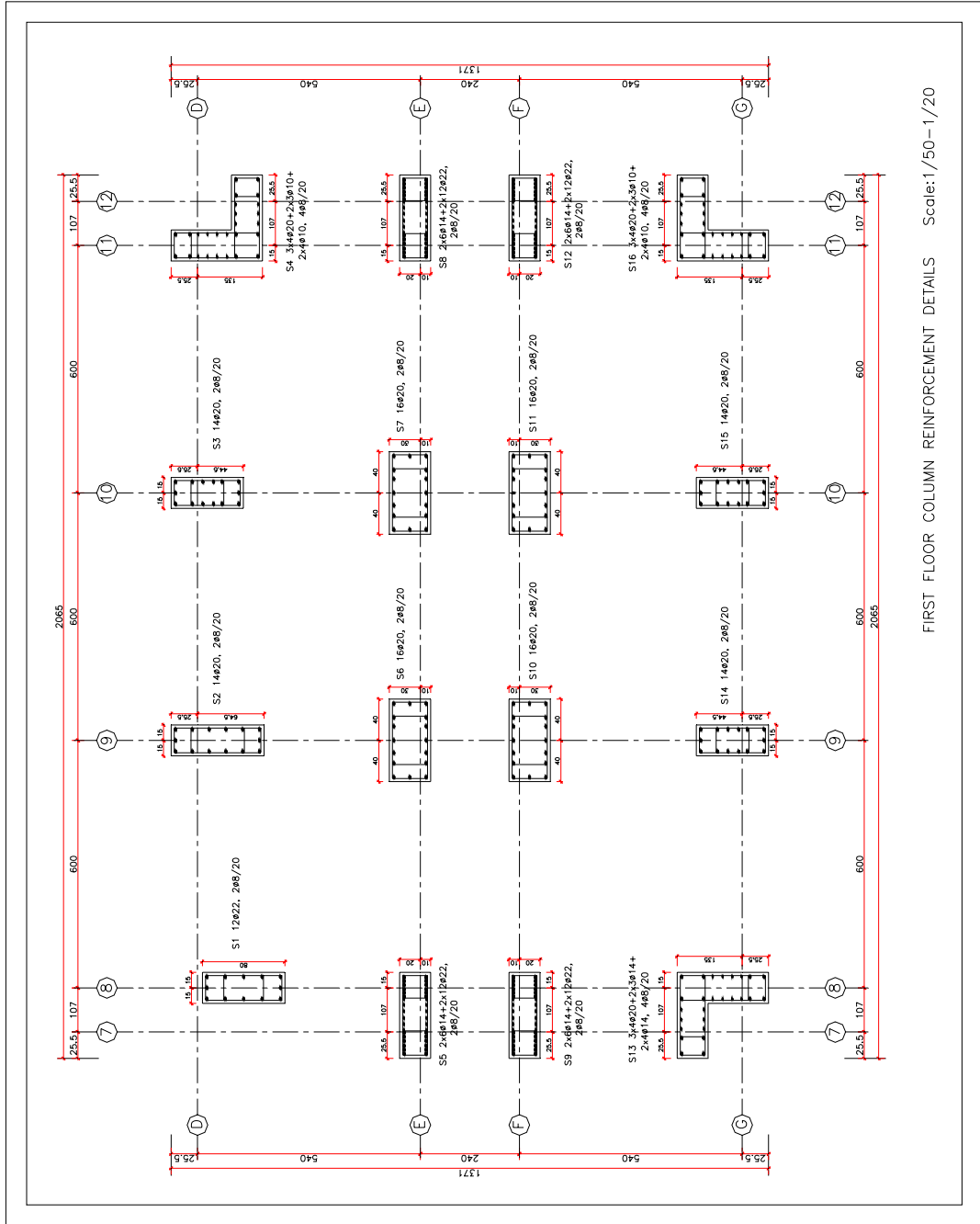
Figure A.15 First floor column reinforcement details

172
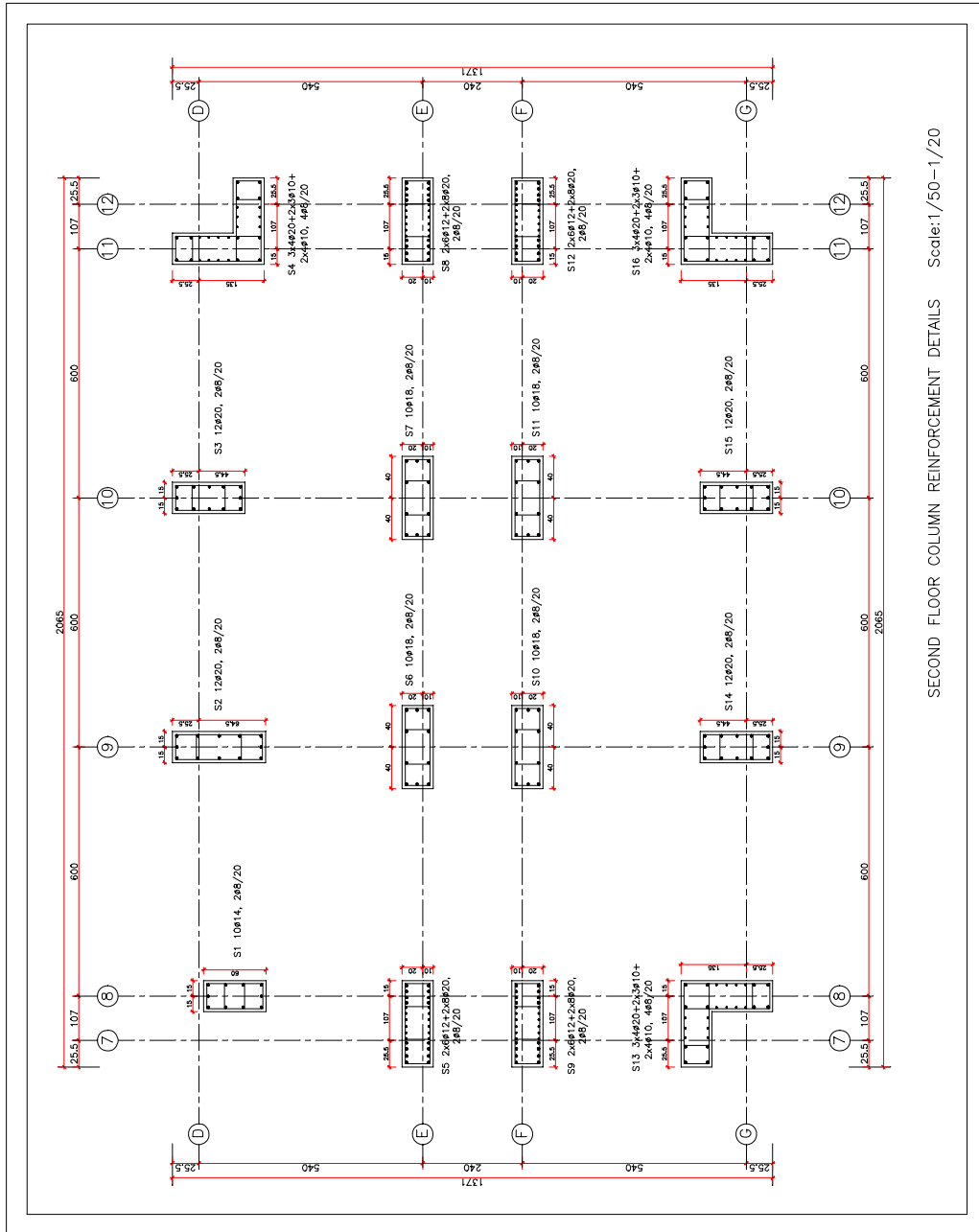
Figure A.16 Second floor column reinforcement details

173
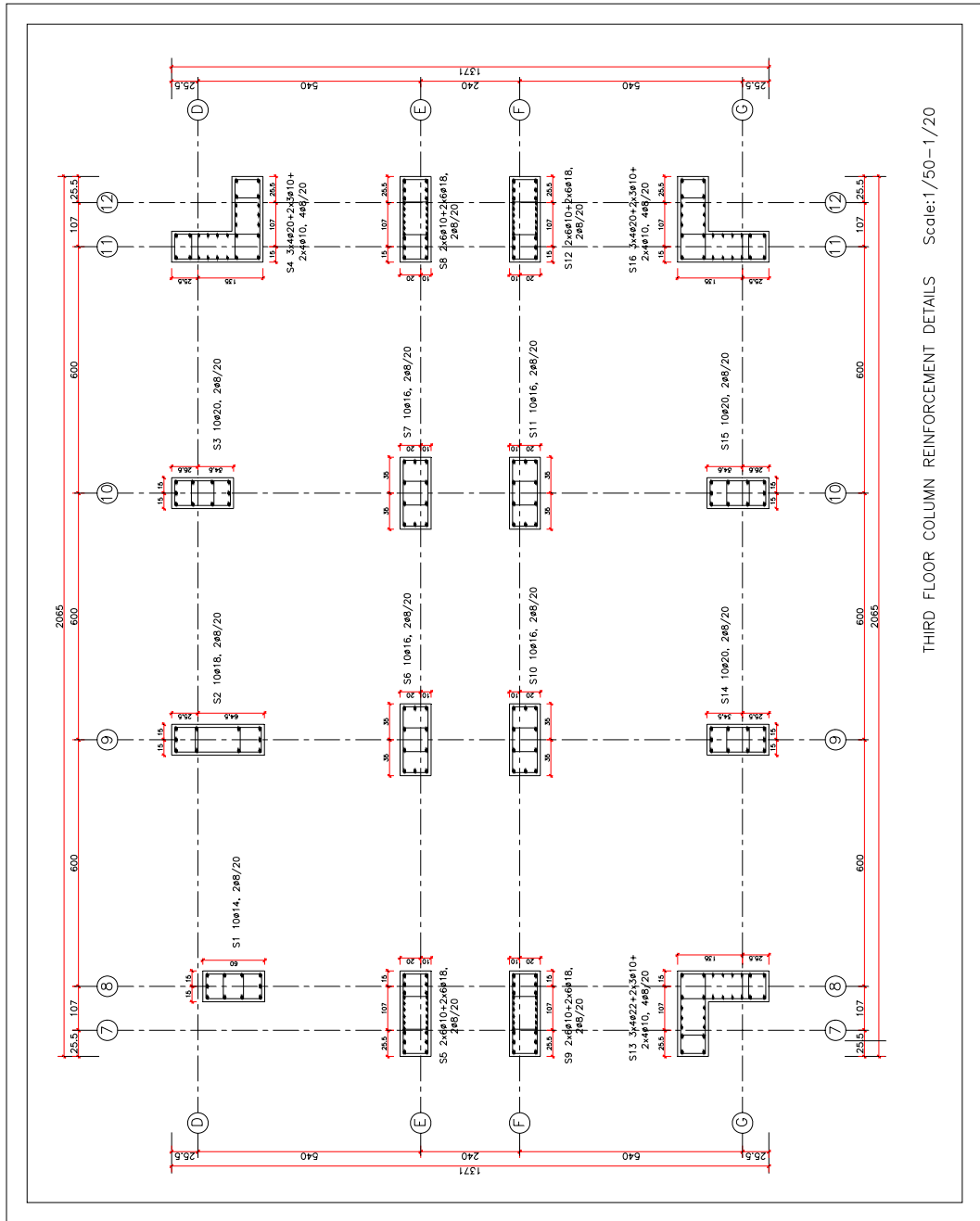
Figure A.17 Third floor column reinforcement details

174
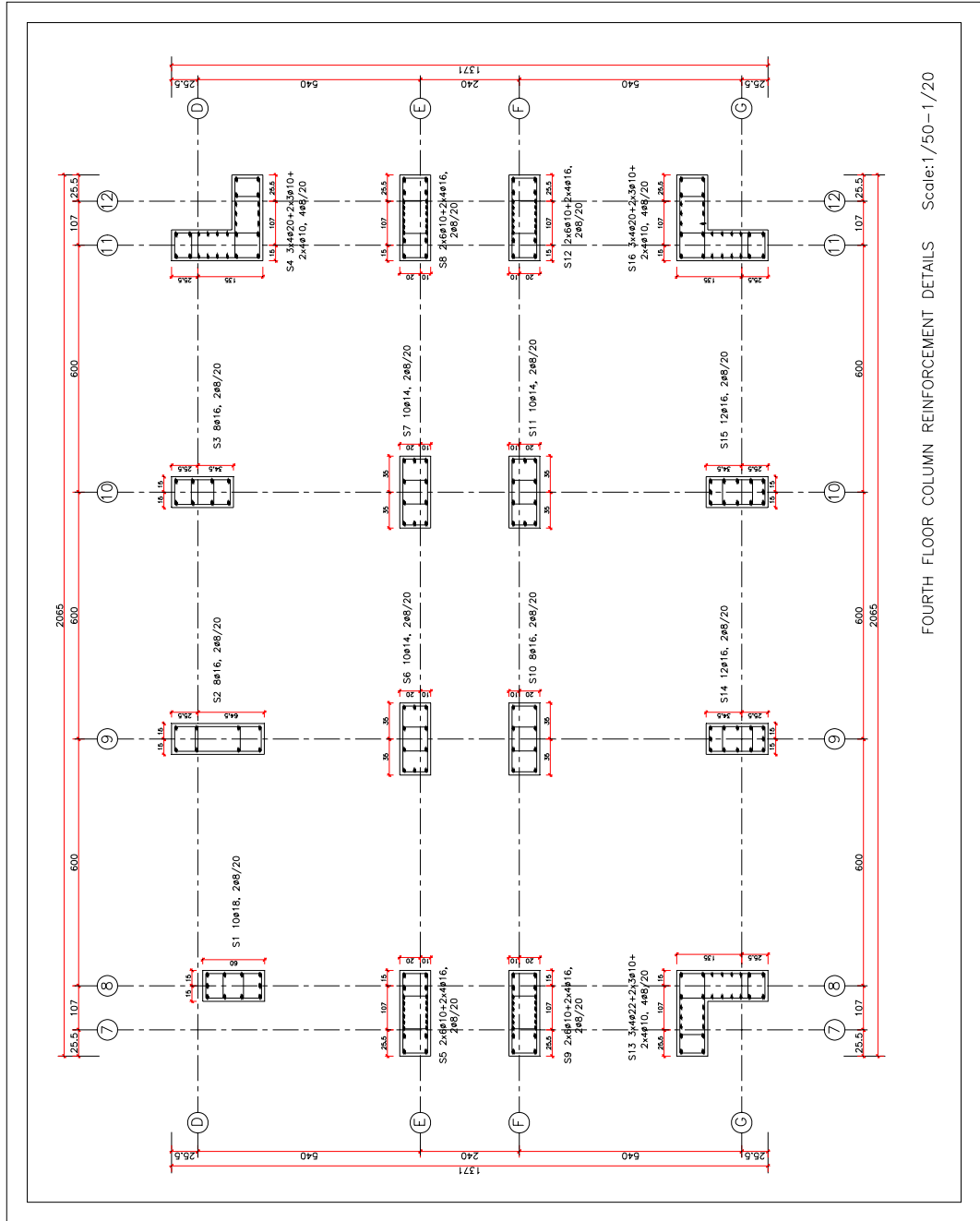
Figure A.18 Fourth floor column reinforcement details

175

APPENDIX B

PERFORMANCE ASSESSMENT RESULTS OF THE FIRST AND SECOND STORY COLUMNS

All columns were evaluated according to the nonlinear procedures of ASCE/SEI-41 as described in Section 2.3.3. In addition, in section 5.3.1 it was shown that all column members are shear-critical. Since bi-directional analysis was conducted, the biaxial shear strength relationship introduced by Eq. 5.1 was used in the analytical models. As shown in Figs. B1-B6, shear capacity of a column which is calculated by Eqn. 5.1, is represented by an elliptical orbit. On the other hand, demand from the nonlinear time history analysis is represented by solid black line. These figures indicate that when the shear demand of a column reaches the shear capacity, the column is assigned to be in CP level
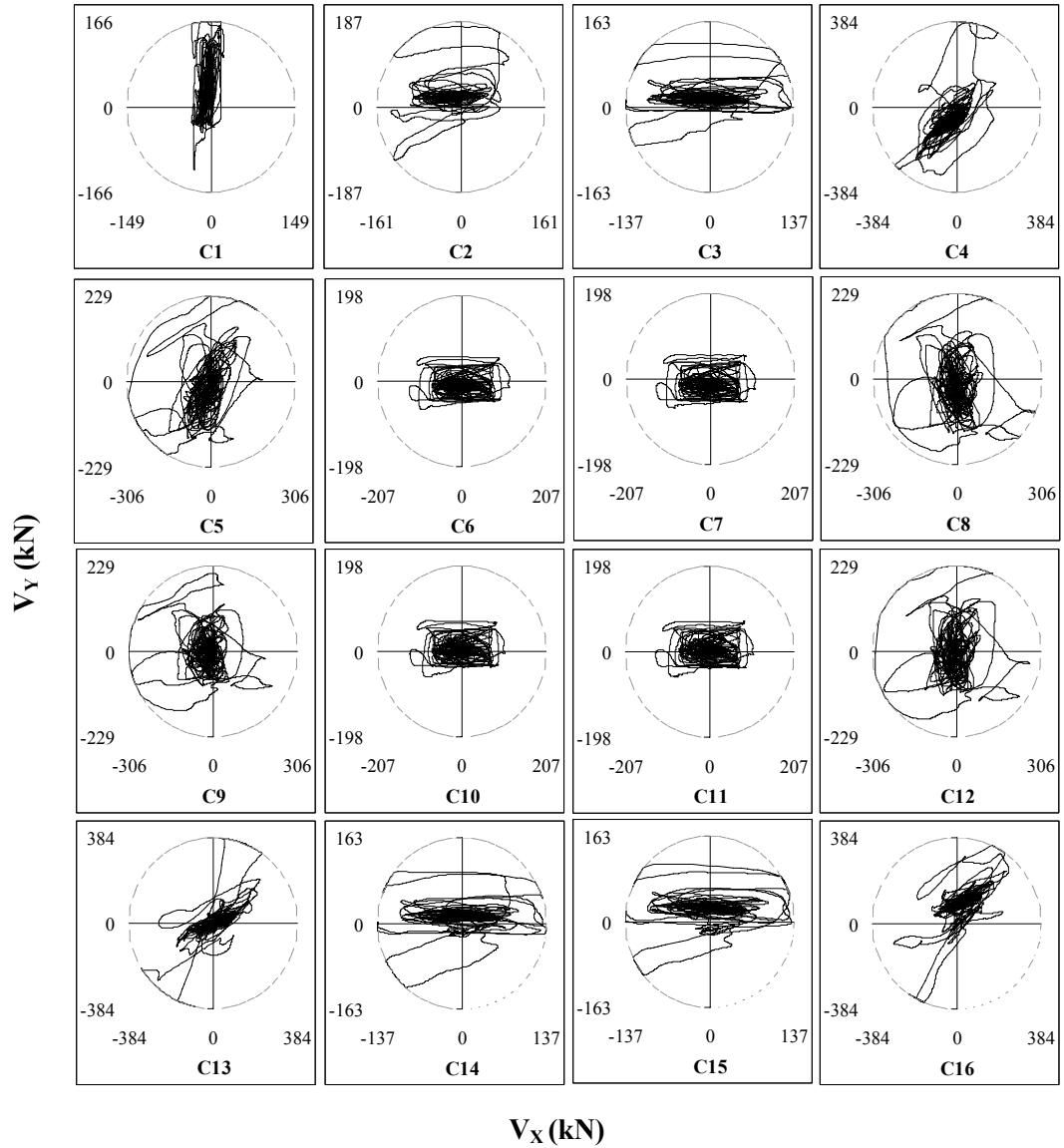
Figure B.1 Bi-directional shear response history of the first story columns in the Erzincan building. The dashed lines represent the shear strength calculated by the equation 5.1 and the values are in the global X and Y axes (longitudinal and transverse directions of the building). The column orientations are depicted in Figure 4.8

177
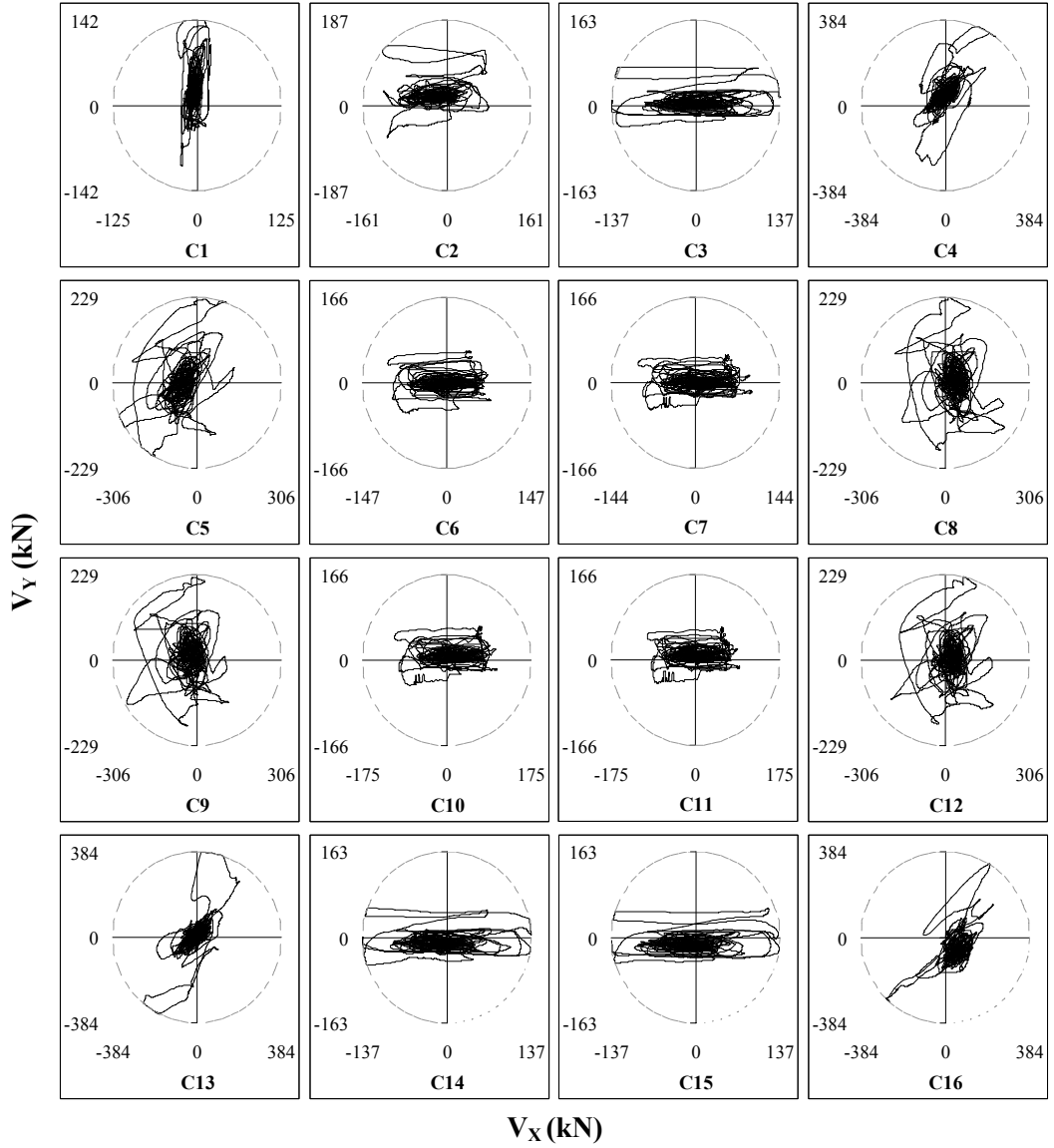
Figure B.2 Bi-directional shear response history of the second story columns in the Erzincan building. The dashed lines represent the shear strength calculated by the equation 5.1 and the values are in the global X and Y axes (longitudinal and transverse directions of the building). The column orientations are depicted in Figure 4.8

178
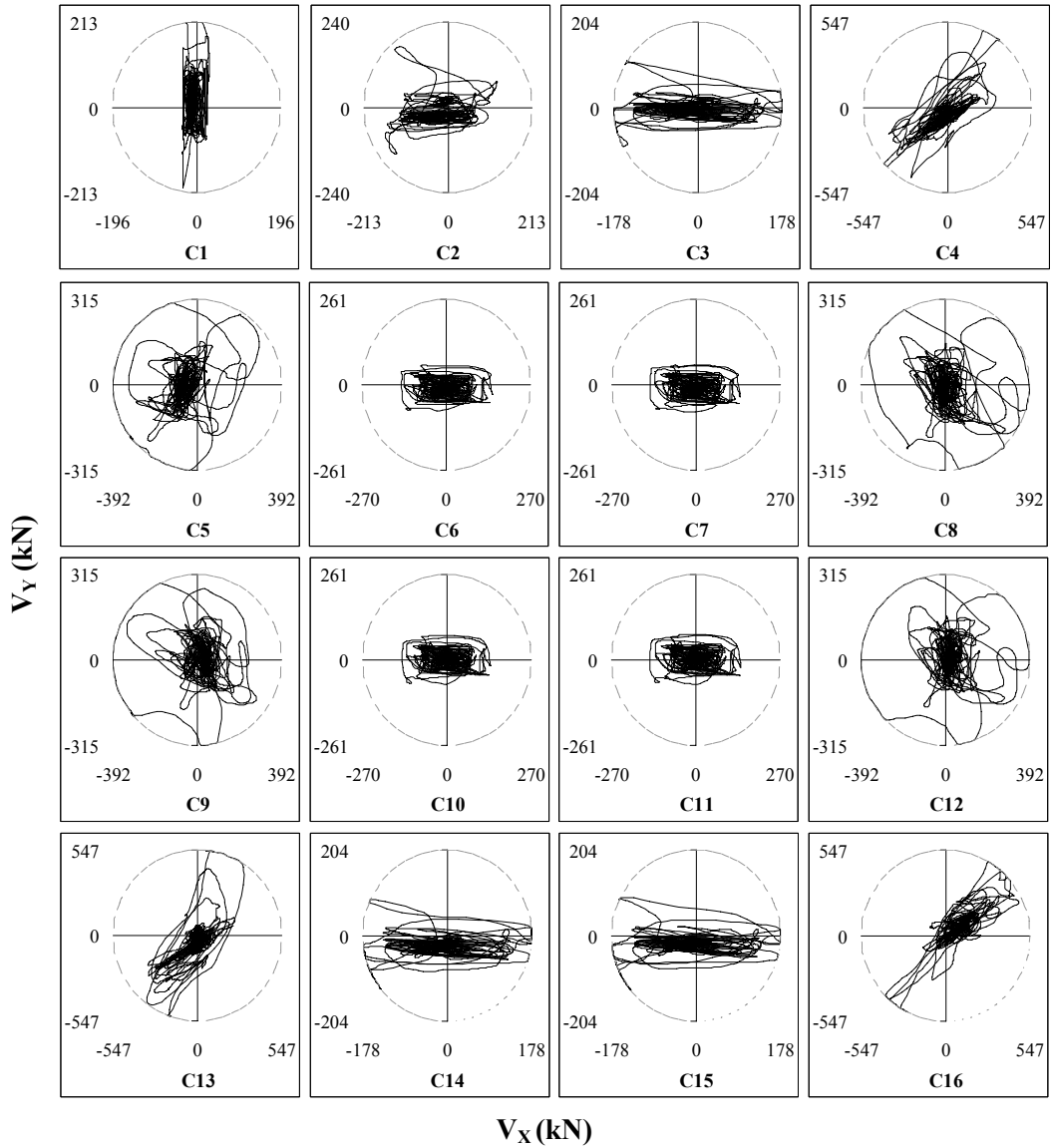
Figure B.3 Bi-directional shear response history of the first story columns in the Bolu building. The dashed lines represent the shear strength calculated by the equation 5.1 and the values are in the global X and Y axes (longitudinal and transverse directions of the building). The column orientations are depicted in Figure 4.8

179
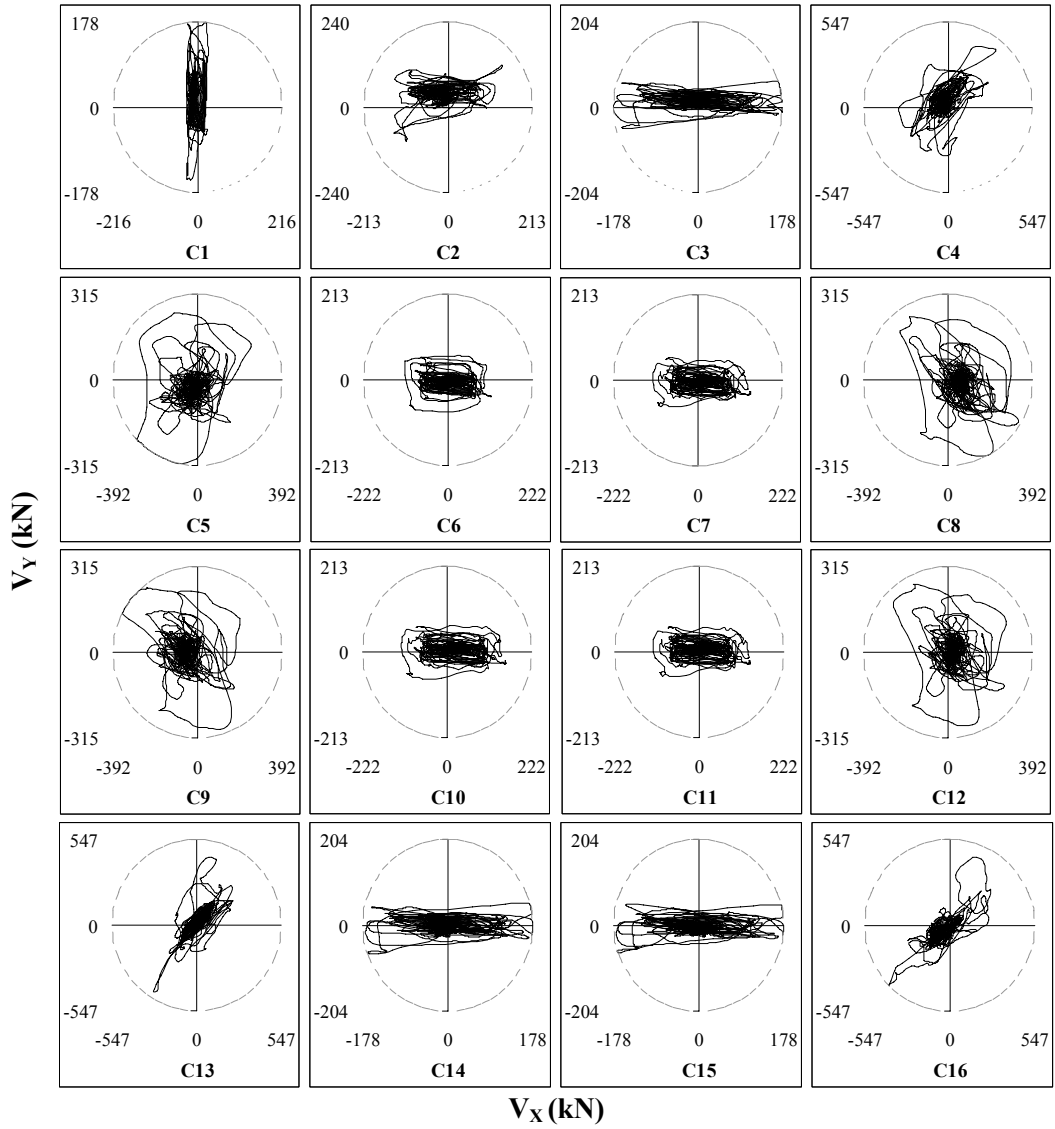
Figure B.4 Bi-directional shear response history of the second story columns in the Bolu building. The dashed lines represent the shear strength calculated by the equation 5.1 and the values are in the global X and Y axes (longitudinal and transverse directions of the building). The column orientations are depicted in Figure 4.8
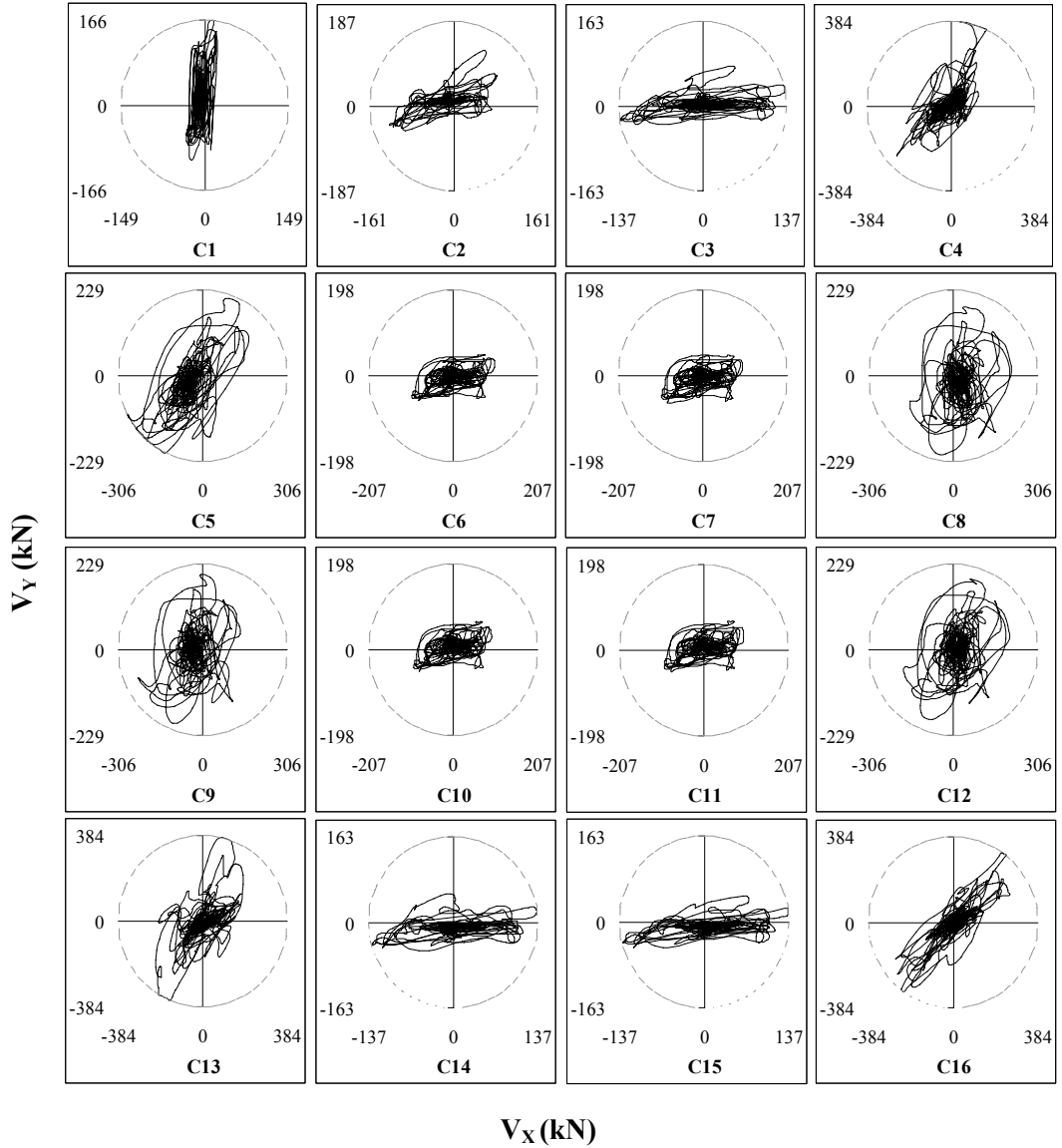
Figure B.5 Bi-directional shear response history of the first story columns in the Bingöl building. The dashed lines represent the shear strength calculated by the equation 5.1 and the values are in the global X and Y axes (longitudinal and transverse directions of the building). The column orientations are depicted in Figure 4.8

181
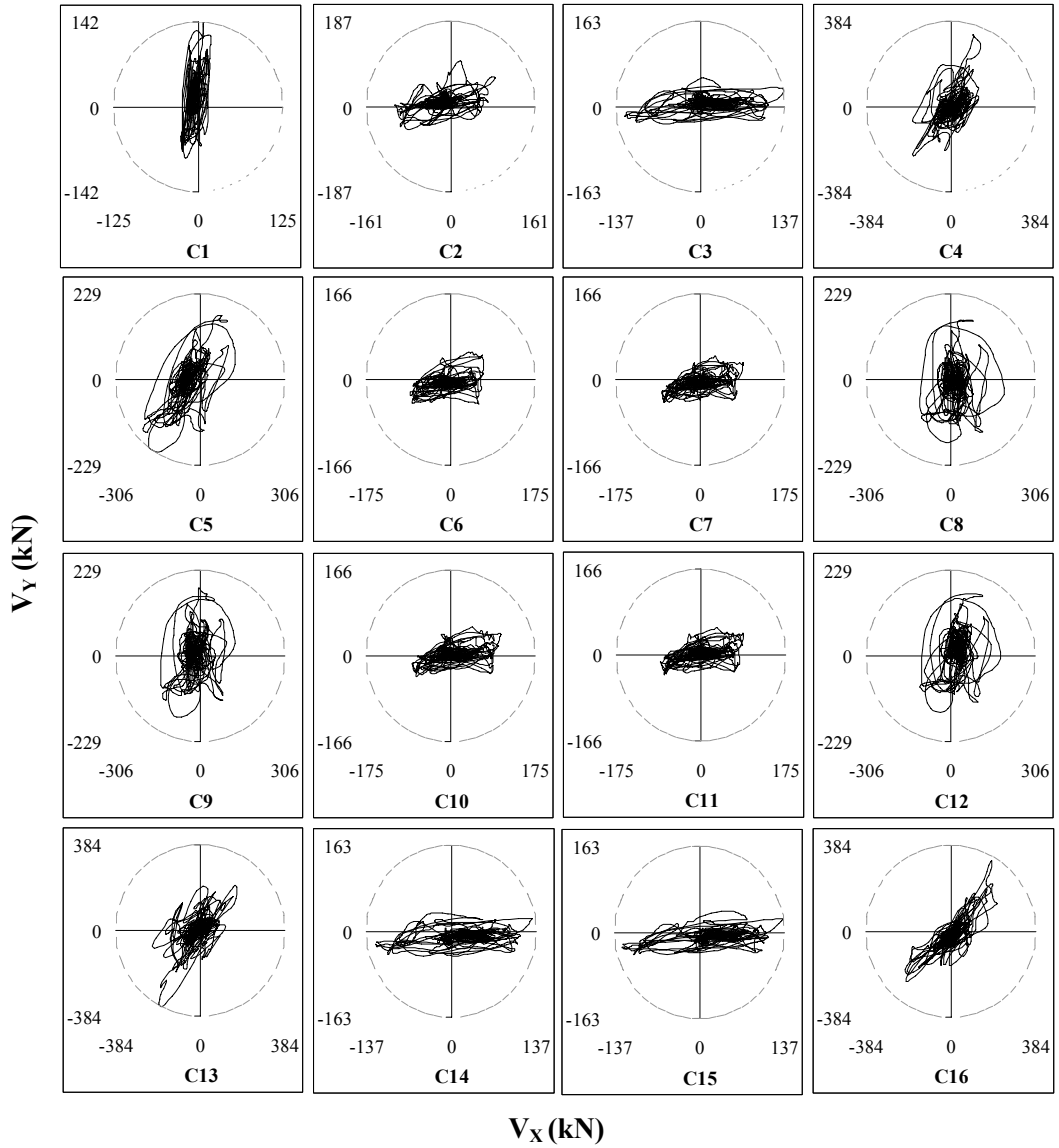
Figure B.6 Bi-directional shear response history of the second story columns in the Bingöl building. The dashed lines represent the shear strength calculated by the equation 5.2 and the values are in the global X and Y axes (longitudinal and transverse directions of the building). The column orientations are depicted in Figure 4.8

APPENDIX C

PERFORMANCE ASSESSMENT RESULTS OF THE FIRST AND SECOND FLOOR BEAMS

The performance assessment results of the beams are performed according to the nonlinear procedures of ASCE/SEI-41 (2007) and TEC (2007). The acceptability criterion of ASCE/SEI-41 is plastic rotation (θ_p). The acceptability criteria of TEC are the strain values in the extreme fibers of concrete (ε_c) and steel (ε_s). Figs. C.1-C.6 illustrates the demand values on each beam and indicates the performance level schematically. The acceptance limits were given in Table 5.8 and 5.9 before.

ε_c=0.0018

ε_c=0.0020 ε_s=0.0341 ε_s=0.0426 ε_c=0.0006 ε_s=0.0263

θ_p=0.0066 θ_p=0.0057 θ_p=0.0051

ε_c=0.0009 ε_s=0.0088 θ_p=0.0021 ε_c=0.0011 ε_s=0.0057 θ_p=0.0024 ε_c=0.0002 ε_s=0.0055 θ_p=0.0025 ε_c=0.0010 ε_s=0.0101 θ_p=0.0025

ε_c=0.0020

ε_c=0.0017 ε_s=0.0194 ε_s=0.0283 ε_c=0.0021 ε_s=0.0250

θ_p=0.0086 θ_p=0.0077 θ_p=0.0092

ε_c=0.0009 ε_s=0.0078 θ_p=0.0021 ε_c=0.0010 ε_s=0.0056 θ_p=0.0024 ε_c=0.0011 ε_s=0.0061 θ_p=0.0026 ε_c=0.0008 ε_s=0.0069 θ_p=0.0016

ε_c=0.0021

ε_c=0.0018 ε_s=0.0203 ε_s=0.0299 ε_c=0.0021 ε_s=0.0259

θ_p=0.0090 θ_p=0.0081 θ_p=0.0096

ε_c=0.0008 ε_s=0.0056 θ_p=0.0027 ε_c=0.0009 ε_s=0.0056 θ_p=0.0025 ε_c=0.0011 ε_s=0.0066 θ_p=0.0029 ε_c=0.0013 ε_s=0.0150 θ_p=0.0037

ε_c=0.0023 ε_s=0.0432

ε_c=0.0019

θ_p=0.0076 ε_s=0.0520 ε_c=0.0019 ε_s=0.0380

θ_p=0.0068 θ_p=0.0073

X
Y

ASCE41: IO LS CP

TEC : IO LS CP

Figure C.1 Comparative assessment of the first floor beams in the Erzincan building as per ASCE/SEI-41 and TEC

184

Figure C.2 Comparative assessment of the second floor beams in the Erzincan building as per ASCE/SEI-41 and TEC

185

ε_c=0.0010

$\varepsilon_c=0.0005$ $\varepsilon_s=0.0245$ ε_c=0.0010 $\varepsilon_s=0.0287$ $\varepsilon_c=0.0012$ $\varepsilon_s=0.0303$

θ_p=0.0047 θ_p=0.0038 θ_p=0.0058

$\varepsilon_c=0.0008$ $\varepsilon_s=0.0137$ θ_p=0.0033 $\varepsilon_c=0.0009$ $\varepsilon_s=0.0096$ θ_p=0.0041 $\varepsilon_c=0.0009$ $\varepsilon_s=0.0096$ θ_p=0.0041 $\varepsilon_c=0.0008$ $\varepsilon_s=0.0137$ θ_p=0.0034

$\varepsilon_c=0.0012$

$\varepsilon_c=0.0010$ $\varepsilon_s=0.0142$ $\varepsilon_s=0.0210$ $\varepsilon_c=0.0012$ $\varepsilon_s=0.0190$

θ_p=0.0061 θ_p=0.0057 θ_p=0.0069

$\varepsilon_c=0.0008$ $\varepsilon_s=0.0129$ θ_p=0.0034 $\varepsilon_c=0.0009$ $\varepsilon_s=0.0089$ θ_p=0.0038 $\varepsilon_c=0.0009$ $\varepsilon_s=0.0089$ θ_p=0.0038 $\varepsilon_c=0.0007$ $\varepsilon_s=0.0106$ θ_p=0.0026

$\varepsilon_c=0.0011$

$\varepsilon_c=0.0010$ $\varepsilon_s=0.0142$ $\varepsilon_s=0.0210$ $\varepsilon_c=0.0012$ $\varepsilon_s=0.0197$

θ_p=0.0061 θ_p=0.0057 θ_p=0.0071

$\varepsilon_c=0.0007$ $\varepsilon_s=0.0071$ θ_p=0.0034 $\varepsilon_c=0.0009$ $\varepsilon_s=0.0090$ θ_p=0.0039 $\varepsilon_c=0.0009$ $\varepsilon_s=0.0089$ θ_p=0.0038 $\varepsilon_c=0.0008$ $\varepsilon_s=0.0129$ θ_p=0.0031

$\varepsilon_c=0.0005$ $\varepsilon_s=0.0293$

$\varepsilon_c=0.0011$

θ_p=0.0051 $\varepsilon_s=0.0325$ $\varepsilon_c=0.0005$ $\varepsilon_s=0.0290$

θ_p=0.0043 θ_p=0.0055

X

Y

ASCE41: IO LS CP

TEC : IO LS CP

Figure C.3 Comparative assessment of the first floor beams in the Bolu building as per ASCE/SEI-41 and TEC

Figure C.4 Comparative assessment of the second floor beams in the Bolu building as per ASCE/SEI-41 and TEC

187

Figure C.5 Comparative assessment of the first floor beams in the Bingöl building as per ASCE/SEI-41 and TEC
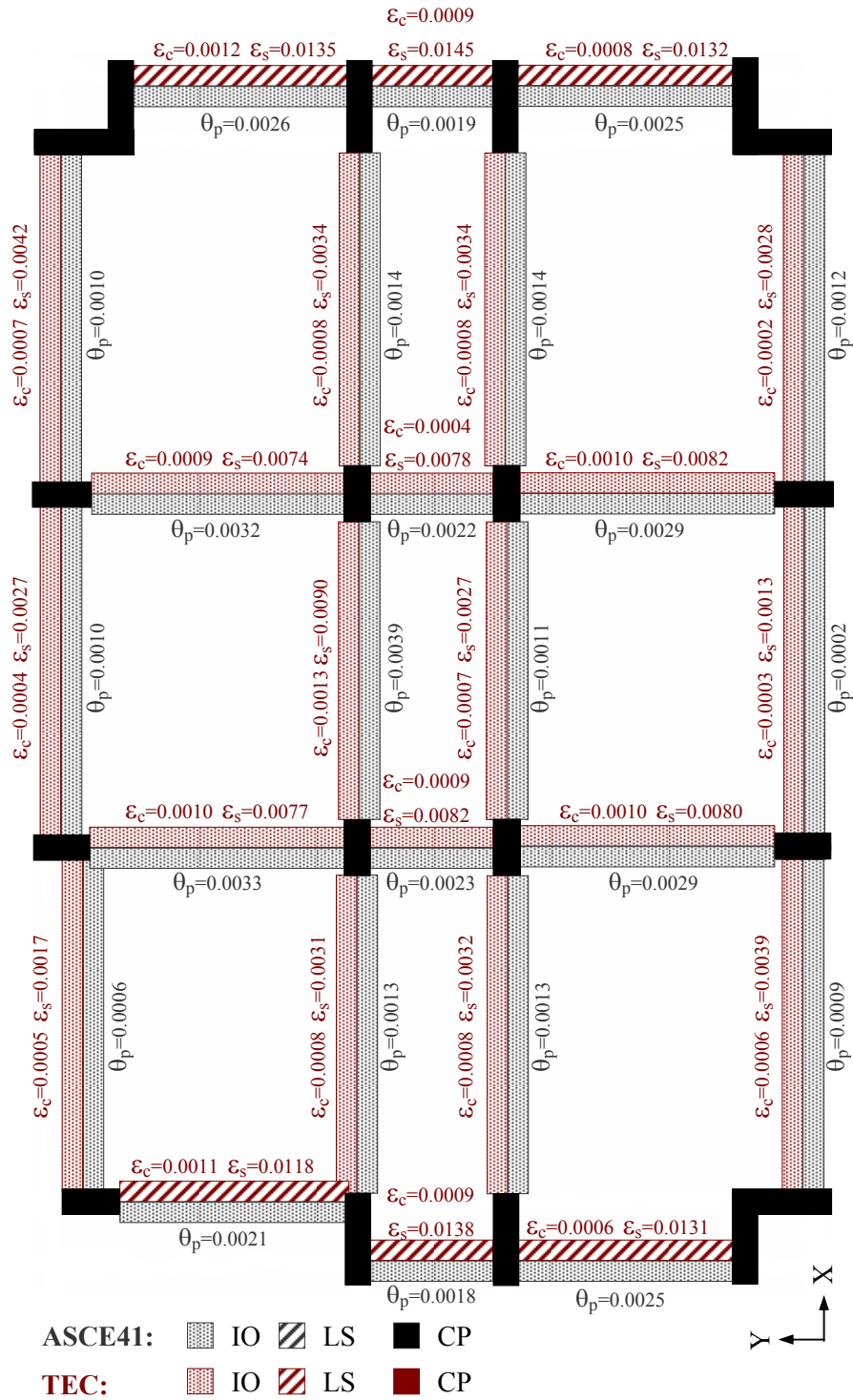
Figure C.6 Comparative assessment of second floor beams in the Bingöl building as per ASCE/SEI-41 and TEC 2007

189

APPENDIX D

PERFORMANCE ASSESSMENT RESULTS OF THE HOLLOW CLAY BRICK INFILL WALLS

Hollow clay brick infilled frames were modeled as equivalent diagonal compression struts based on simple equations through 5.3-5.7. Typical failure modes of infill walls are sliding shear and compression of the diagonal strut. In the analytical model, the lowest value was used among these failure modes. When the force demand from the nonlinear time history analysis equals the diagonal compression (R_c) or sliding shear (R_s) failure forces, the strut element is considered as it collapsed. Other definitions are given in section 5.3.2

Table D.1 Comparison of the observed damage and calculated performance levels of the bottom three-story infill walls regarding the Erzincan building

	Infill Id	t_{inf} (mm)	θ (rad)	I_{col} (mm^4)	h_{inf} (mm)	λ	h_{col} (mm)	r_{inf} (mm)	a (mm)	z (mm)	l_{inf} (mm)	R_s (kN)	R_c (kN)	OD	CPL
Ground Story	B9	260	0.29	2.4E+10	1600	0.0131	3800	5632	753	120	5400	161	55.7	IO	IO
	B11	260	0.34	2E+09	2000	0.0238	3800	6041	636	66	5700	176	31.1	IO	IO
	B12	260	0.34	2E+09	2000	0.0238	3800	6041	636	66	5700	176	31.1	IO	IO
	B14	260	0.63	3.3E+09	1600	0.0248	3800	2720	282	63	2200	90	34.9	IO	C
	B15	260	0.35	3.3E+09	1600	0.0225	3800	4682	505	70	4400	137	33.1	IO	C
	B17	260	0.95	4.8E+09	3100	0.0191	3800	3801	437	82	2200	171	63.3	IO	C
	B20	260	0.95	4.8E+09	3100	0.0191	3800	3801	437	82	2200	171	63.3	IO	C
1st Story	B1	260	0.17	2E+09	1000	0.0244	3200	5787	647	64	5700	159	29.1	IO	IO
	B2	260	0.17	2E+09	1000	0.0244	3200	5787	647	64	5700	159	29.1	IO	IO
	B3	260	0.17	2E+09	1000	0.0244	3200	5787	647	64	5700	159	29.1	IO	IO
	B11	260	0.17	2E+09	1000	0.0244	3200	5787	647	64	5700	159	29.1	IO	IO
	B12	260	0.17	2E+09	1000	0.0244	3200	5787	647	64	5700	159	29.1	IO	IO
	B13	260	0.48	3.3E+09	2000	0.0226	3200	4338	500	70	3850	134	34.9	IO	C
	B14	260	0.43	3.3E+09	1000	0.0263	3200	2417	262	60	2200	73	29.2	IO	C
	B15	260	0.22	3.3E+09	1000	0.0229	3200	4512	517	69	4400	126	31.3	IO	C
	B16	90	0.42	1.8E+10	2000	0.0110	3200	4879	748	142	4450	51	24.0	IO	C
	B19	90	0.42	1.8E+10	2000	0.0110	3200	4879	748	142	4450	51	24.0	IO	C
	B21	90	0.42	1.8E+10	2000	0.0110	3200	4879	748	142	4450	51	24.0	IO	C
	B22	260	0.48	3.3E+09	2000	0.0226	3200	4338	500	70	3850	134	34.9	IO	C
	B23	260	0.43	3.3E+09	1000	0.0263	3200	2417	262	60	2200	73	29.2	IO	C
	B24	260	0.48	3.3E+09	2000	0.0226	3200	4338	500	70	3850	134	34.9	IO	C
2nd Story	B1	260	0.17	2E+09	1000	0.0244	3200	5787	647	64	5700	159	29.1	IO	IO
	B2	260	0.17	2E+09	1000	0.0244	3200	5787	647	64	5700	159	29.1	IO	IO
	B3	260	0.17	2E+09	1000	0.0244	3200	5787	647	64	5700	159	29.1	IO	IO
	B5	190	0.46	2.4E+10	2500	0.0119	3200	5680	846	132	5100	127	47.9	IO	IO
	B8	190	0.46	2.4E+10	2500	0.0119	3200	5680	846	132	5100	127	47.9	IO	IO
	B11	260	0.17	2E+09	1000	0.0244	3200	5787	647	64	5700	159	29.1	IO	IO
	B12	260	0.17	2E+09	1000	0.0244	3200	5787	647	64	5700	159	29.1	IO	IO
	B13	260	0.48	3.3E+09	2000	0.0226	3200	4338	500	70	3850	134	34.9	IO	C
	B14	260	0.43	3.3E+09	1000	0.0263	3200	2417	262	60	2200	73	29.2	IO	C
	B15	260	0.22	3.3E+09	1000	0.0229	3200	4512	517	69	4400	126	31.3	IO	C
	B22	260	0.48	3.3E+09	2000	0.0226	3200	4338	500	70	3850	134	34.9	IO	C
	B23	260	0.43	3.3E+09	1000	0.0263	3200	2417	262	60	2200	73	29.2	IO	C
	B24	260	0.48	3.3E+09	2000	0.0226	3200	4338	500	70	3850	134	34.9	IO	C

R_c: diagonal compression failure force, R_s: sliding shear failure force, OD: observed damage, CPL: calculated performance level, IO: Immediate Occupancy, C: collapse,

Table D.2 Comparison of the observed damage and calculated performance levels of the bottom three-story infill walls regarding the Bolu building

	Infill Id	t_{inf} (mm)	θ (rad)	I_{col} (mm^4)	h_{inf} (mm)	λ	h_{col} (mm)	r_{inf} (mm)	a (mm)	z (mm)	l_{inf} (mm)	R_s (kN)	R_c (kN)	OD	CPL
Ground Story	B9	260	0.29	2.4E+10	1600	0.0118	3800	5632	784	133	5400	161	61.5	IO	IO
	B11	260	0.34	2E+09	2000	0.0216	3800	6041	661	73	5700	176	34.3	IO	IO
	B12	260	0.34	2E+09	2000	0.0216	3800	6041	661	73	5700	176	34.3	IO	IO
	B14	260	0.63	3.3E+09	1600	0.0224	3800	2720	293	70	2200	90	38.6	IO	C
	B15	260	0.35	3.3E+09	1600	0.0203	3800	4682	525	77	4400	137	36.6	IO	IO
	B17	260	0.95	4.8E+09	3100	0.0173	3800	3801	455	91	2200	171	69.9	C	C
	B20	260	0.95	4.8E+09	3100	0.0173	3800	3801	455	91	2200	171	69.9	C	C
1st Story	B1	260	0.17	2E+09	1000	0.0220	3200	5787	673	71	5700	159	32.2	IO	IO
	B2	260	0.17	2E+09	1000	0.0220	3200	5787	673	71	5700	159	32.2	IO	IO
	B3	260	0.17	2E+09	1000	0.0220	3200	5787	673	71	5700	159	32.2	IO	IO
	B11	260	0.17	2E+09	1000	0.0220	3200	5787	673	71	5700	159	32.2	IO	IO
	B12	260	0.17	2E+09	1000	0.0220	3200	5787	673	71	5700	159	32.2	IO	IO
	B13	260	0.48	3.3E+09	2000	0.0204	3200	4338	520	77	3850	134	38.6	C	C
	B14	260	0.43	3.3E+09	1000	0.0238	3200	2417	273	66	2200	73	32.3	C	IO
	B15	260	0.22	3.3E+09	1000	0.0207	3200	4512	538	76	4400	126	34.6	C	C
	B16	90	0.42	1.8E+10	2000	0.0100	3200	4879	779	157	4450	51	26.5	C	C
	B19	90	0.42	1.8E+10	2000	0.0100	3200	4879	779	157	4450	51	26.5	C	C
	B21	90	0.42	1.8E+10	2000	0.0100	3200	4879	779	157	4450	51	26.5	C	C
	B22	260	0.48	3.3E+09	2000	0.0204	3200	4338	520	77	3850	134	38.6	C	C
	B23	260	0.43	3.3E+09	1000	0.0238	3200	2417	273	66	2200	73	32.3	C	C
	B24	260	0.48	3.3E+09	2000	0.0204	3200	4338	520	77	3850	134	38.6	C	C
2nd Story	B1	260	0.17	2E+09	1000	0.0220	3200	5787	673	71	5700	159	32.2	IO	IO
	B2	260	0.17	2E+09	1000	0.0220	3200	5787	673	71	5700	159	32.2	IO	IO
	B3	260	0.17	2E+09	1000	0.0220	3200	5787	673	71	5700	159	32.2	IO	IO
	B5	190	0.46	2.4E+10	2500	0.0108	3200	5680	880	146	5100	127	52.9	C	C
	B8	190	0.46	2.4E+10	2500	0.0108	3200	5680	880	146	5100	127	52.9	C	C
	B11	260	0.17	2E+09	1000	0.0220	3200	5787	673	71	5700	159	32.2	IO	IO
	B12	260	0.17	2E+09	1000	0.0220	3200	5787	673	71	5700	159	32.2	IO	IO
	B13	260	0.48	3.3E+09	2000	0.0204	3200	4338	520	77	3850	134	38.6	C	IO
	B14	260	0.43	3.3E+09	1000	0.0238	3200	2417	273	66	2200	73	32.3	C	IO
	B15	260	0.22	3.3E+09	1000	0.0207	3200	4512	538	76	4400	126	34.6	C	IO
	B22	260	0.48	3.3E+09	2000	0.0204	3200	4338	520	77	3850	134	38.6	C	C
	B23	260	0.43	3.3E+09	1000	0.0238	3200	2417	273	66	2200	73	32.3	C	IO
	B24	260	0.48	3.3E+09	2000	0.0204	3200	4338	520	77	3850	134	38.6	C	C

R_c: diagonal compression failure force, R_s: sliding shear failure force, OD: observed damage, CPL: calculated performance level, IO: Immediate Occupancy, C: collapse,

Table D.3 Comparison of the observed damage and calculated performance levels of the bottom three-story infill walls regarding the Bingöl building

	Infill Id	t_{inf} (mm)	θ (rad)	I_{col} (mm^4)	h_{inf} (mm)	λ	h_{col} (mm)	r_{inf} (mm)	a (mm)	z (mm)	l_{inf} (mm)	R_s (kN)	R_c (kN)	OD	CPL
Ground Story	B9	260	0.29	2.4E+10	1600	0.0131	3800	5632	753	120	5400	161	55.7	IO	IO
	B11	260	0.34	2E+09	2000	0.0238	3800	6041	636	66	5700	176	31.1	IO	IO
	B12	260	0.34	2E+09	2000	0.0238	3800	6041	636	66	5700	176	31.1	IO	IO
	B14	260	0.63	3.3E+09	1600	0.0248	3800	2720	282	63	2200	90	34.9	IO	IO
	B15	260	0.35	3.3E+09	1600	0.0225	3800	4682	505	70	4400	137	33.1	IO	IO
	B17	260	0.95	4.8E+09	3100	0.0191	3800	3801	437	82	2200	171	63.3	IO	IO
	B20	260	0.95	4.8E+09	3100	0.0191	3800	3801	437	82	2200	171	63.3	IO	IO
1st Story	B1	260	0.17	2E+09	1000	0.0244	3200	5787	647	64	5700	159	29.1	IO	IO
	B2	260	0.17	2E+09	1000	0.0244	3200	5787	647	64	5700	159	29.1	IO	IO
	B3	260	0.17	2E+09	1000	0.0244	3200	5787	647	64	5700	159	29.1	IO	IO
	B11	260	0.17	2E+09	1000	0.0244	3200	5787	647	64	5700	159	29.1	IO	IO
	B12	260	0.17	2E+09	1000	0.0244	3200	5787	647	64	5700	159	29.1	IO	IO
	B13	260	0.48	3.3E+09	2000	0.0226	3200	4338	500	70	3850	134	34.9	IO	C
	B14	260	0.43	3.3E+09	1000	0.0263	3200	2417	262	60	2200	73	29.2	IO	C
	B15	260	0.22	3.3E+09	1000	0.0229	3200	4512	517	69	4400	126	31.3	IO	IO
	B16	90	0.42	1.8E+10	2000	0.0110	3200	4879	748	142	4450	51	24.0	IO	IO
	B19	90	0.42	1.8E+10	2000	0.0110	3200	4879	748	142	4450	51	24.0	IO	IO
	B21	90	0.42	1.8E+10	2000	0.0110	3200	4879	748	142	4450	51	24.0	IO	IO
	B22	260	0.48	3.3E+09	2000	0.0226	3200	4338	500	70	3850	134	34.9	IO	IO
	B23	260	0.43	3.3E+09	1000	0.0263	3200	2417	262	60	2200	73	29.2	IO	IO
	B24	260	0.48	3.3E+09	2000	0.0226	3200	4338	500	70	3850	134	34.9	IO	C
2nd Story	B1	260	0.17	2E+09	1000	0.0244	3200	5787	647	64	5700	159	29.1	IO	IO
	B2	260	0.17	2E+09	1000	0.0244	3200	5787	647	64	5700	159	29.1	IO	IO
	B3	260	0.17	2E+09	1000	0.0244	3200	5787	647	64	5700	159	29.1	IO	IO
	B5	190	0.46	2.4E+10	2500	0.0119	3200	5680	846	132	5100	127	47.9	IO	IO
	B8	190	0.46	2.4E+10	2500	0.0119	3200	5680	846	132	5100	127	47.9	IO	IO
	B11	260	0.17	2E+09	1000	0.0244	3200	5787	647	64	5700	159	29.1	IO	IO
	B12	260	0.17	2E+09	1000	0.0244	3200	5787	647	64	5700	159	29.1	IO	IO
	B13	260	0.48	3.3E+09	2000	0.0226	3200	4338	500	70	3850	134	34.9	IO	C
	B14	260	0.43	3.3E+09	1000	0.0263	3200	2417	262	60	2200	73	29.2	IO	C
	B15	260	0.22	3.3E+09	1000	0.0229	3200	4512	517	69	4400	126	31.3	IO	IO
	B22	260	0.48	3.3E+09	2000	0.0226	3200	4338	500	70	3850	134	34.9	IO	IO
	B23	260	0.43	3.3E+09	1000	0.0263	3200	2417	262	60	2200	73	29.2	IO	C
	B24	260	0.48	3.3E+09	2000	0.0226	3200	4338	500	70	3850	134	34.9	IO	C

R_c: diagonal compression failure force, R_s: sliding shear failure force, OD: observed damage, CPL: calculated performance level, IO: Immediate Occupancy, C: collapse,
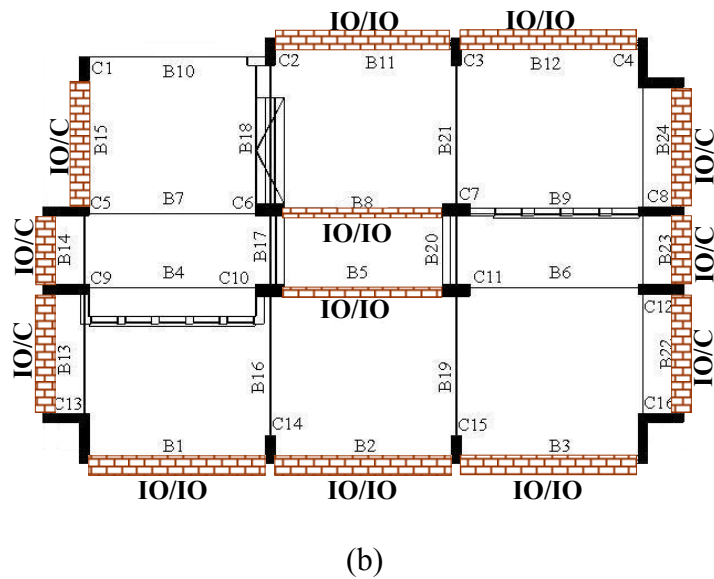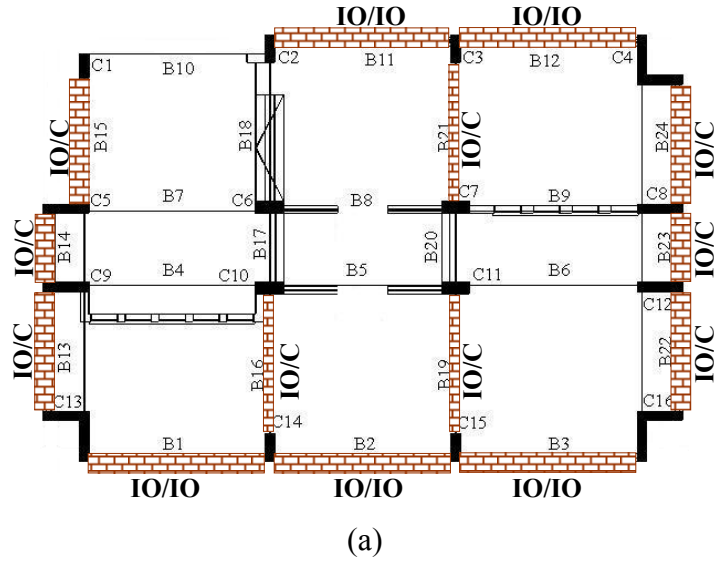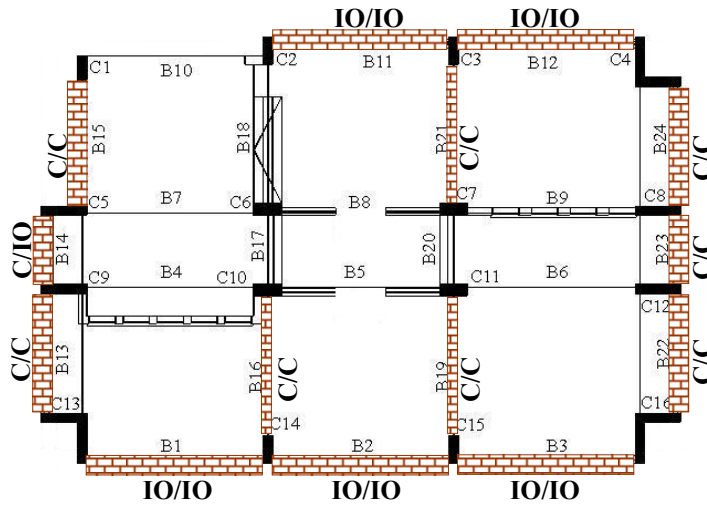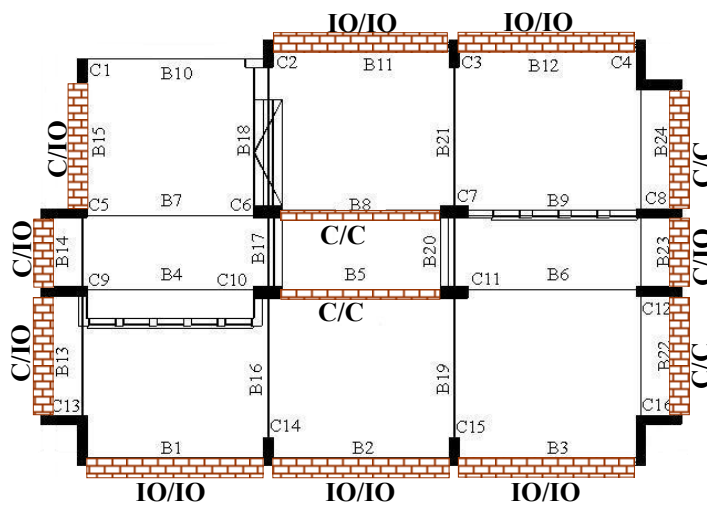
(a)

(b)

Figure D.1 Schematic comparison of the observed and calculated damage of the (a) first and (b) second story infill walls regarding the Erzincan building. (Observed Damage/Calculated Damage) IO : Immediate Occupancy C: Collapse
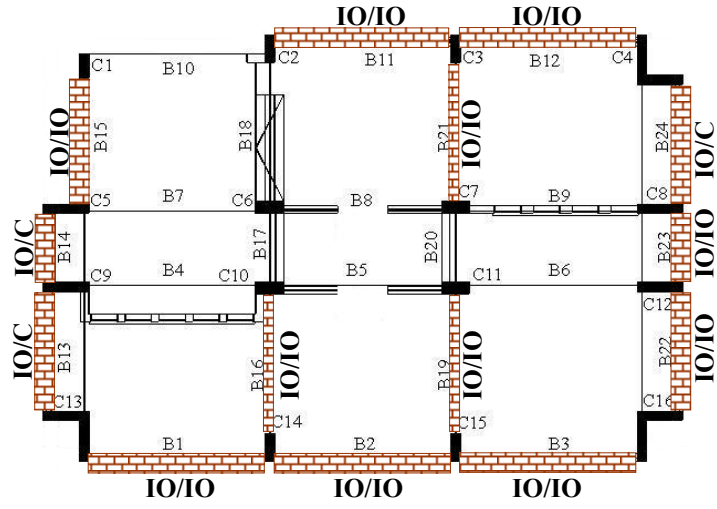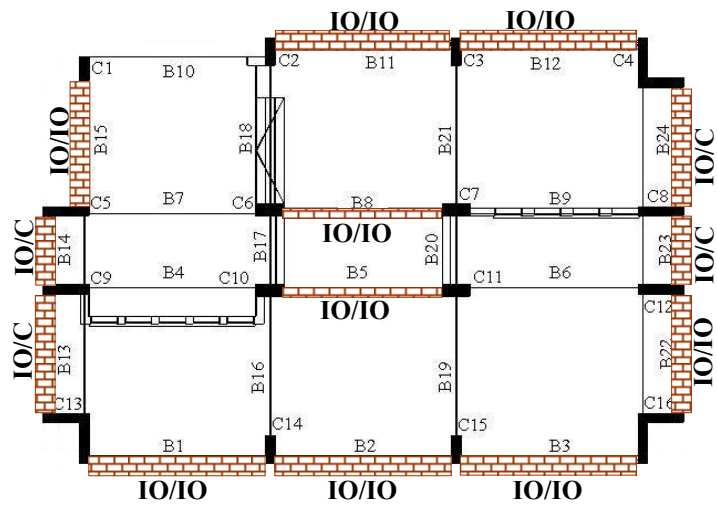
(a)

(b)

Figure D.2 Schematic comparison of the observed and calculated damage of the first and second story infill walls regarding the Bolu building (Observed Damage/Calculated Damage) IO : Immediate Occupancy C: Collapse

195

(a)

(b)

Figure D.3 Schematic comparison of the observed and calculated damage of the first and second story infill walls regarding the Bingöl building (Observed Damage/Calculated Damage) IO : Immediate Occupancy C: Collapse

196

CURRICULUM VITAE

PERSONAL INFORMATION

Surname, Name: Bayhan, Beyhan
Nationality: Turkish (TC)
Date and Place of Birth: 29.04.1978, Diyarbakır
Marital Status: Single
Phone: +90 (312) 210 5465
Fax: +90 (312) 287 8951
Email: bayhan@metu.edu.tr

EDUCATION

2003-2010   Ph.D., Civil Engineering, METU

2008-2009   Research Fellowship at UC Berkeley

2001-2003   MS, Structural Engineering, İstanbul Technical University

1996-2001   BS, Civil Engineering, Gazi University

1993-1996   Gazi Anatolian High School

WORK EXPERIENCE

2004-2010   Research Assistant, Department of Civil Engineering, METU

2002-2003   Civil Engineer, Sistemyapı İnş. ve Tic. A.Ş., İstanbul

PUBLICATIONS

1. **Bayhan B.** and Gülkan P., "Buildings Subjected to Recurring Earthquakes: A Tale of Three Cities", Earthquake Spectra (Under Review)

2. S. Yavari, S-H Lin, K.J Elwood, C-L Wu, S-J Hwang, **B. Bayhan**, and J. P. Moehle, "Shake Table Tests on the Collapse of RC Frames Subjected to Moderate and High Axial Loads", 9th US National and 10th Canadian Conference

on Earthquake Engineering , Paper No. 1628, July 25-29, 2010, Toronto, Canada.

3. **Bayhan B.** and Gülkan P., "A Tale of Three Cities", 9th US National and 10th Canadian Conference on Earthquake Engineering, Paper No. 167, July 25-29, 2010, Toronto, Canada.

4. **Bayhan B.** and Gülkan P., "Seismic Response of a Typical RC Building in Different Regions of Turkey," The 14th European Conference on Earthquake Engineering, Paper No. 1339, September 2010, Ohrid, Macedonia.

5. **Bayhan B.** and Gülkan P., "Is There Disarray in Phrases Describing Performance Requirements", The 14th World Conference on Earthquake Engineering, Paper No. 08-01-0011, October 12-17, 2008, Beijing, China.

6. Avsar O**.**, **Bayhan B.** and Yakut A., "Section Based Determination of Effective Rigidities for RC Beams and Columns", The 8th Pasific Conference on Earthquake Engineering, Paper No. 37, December 2007, Singapore.